SOME STUDIES ON ASPHALTENE STABILISED WATER-IN-OIL EMULSIONS

by

JOHN DAVID SYMONDS, B.Sc., A.R.I.C.

Thesis submitted to the University of Nottingham

for the degree of Doctor of Philosophy

May, 1975

TO MY MOTHER

for her constant encouragement

throughout my education

and

IN MEMORY OF MY FATHER

who died whilst this work was in progress (July 1971)

ABSTRACT

Various workers have shown the asphaltene fraction of crude oil to be responsible for the highly stable W/O emulsions formed after marine oil spillages.

Electron microscope studies on crude oil emulsions using the freeze etching technique showed the oil/water interface to be smooth on the aqueous side but to have a particulate structure on the oil side. In Brega crude oil emulsions, waxy plates were aligned along the interface. Also observed were the coherence of the interfacial film and droplet coalescence.

Allowing a method error of $\pm$ 10%, good agreement was found between computer calculated droplet diameters from the log-normal distribution equation and standard statistical mean diameters. S_c (interfacial area/unit volume oil phase) was larger for salt water emulsions. An equation proposed for S_c as a function of stirring time fitted very well for all three crude oil emulsions. The maximum S_c increased with ϕ (volume fraction) indicating a minimum possible diameter droplet formed by the stirrer. A rate parameter in the equation is probably related to the asphaltene diffusion to the interface. A good fit with the data was obtained when the equation was modified to account for detergent addition delaying emulsion formation. A second rate parameter may reflect the irreversible replacement of detergent at the interface by asphaltenes. Ageing studies showed that once stabilisation was complete, detergent present only slowly affected coalescence.

A heating effect explained the non-linearity of Kuwait and Tia Juana emulsion rheograms. The greater viscosity of Tia Juana stabilised emulsions was explained by a thicker supporting asphaltene layer. The elasticity of the interfacial film accounted for anomalous behaviour in emulsions of asphaltenes dispersed in m-xylene/n-octane. The extrapolated yield point and critical shear rate were used as empirical measures of deformability and attractive forces respectively.

CONTENTS

FOREWORD

This work was carried out over a period of time that saw the changeover to SI units. The guidelines laid down by McGlashan [1] have been mainly adopted here; in cases where literature values were in old units these have been quoted but the SI units have been put in brackets afterwards.

There have been many people helping me in various ways to whom I am very grateful, but in particular I should like to thank the following :

Dr. M.J. Hey and Professor D.D. Eley, my supervisors, for their constant advice, help and suggestions.

Messrs. F. Whetstone and I. Goddard for so cheerfully producing print upon print of emulsion droplets, for more general advice on photographic matters, and for producing the prints in this thesis.

Mr. N. Brown and all the technical staff for their varied expertise at different times.

Dr. J.H.M. Willison for training me in the use of the freeze-etching unit and electron microscope and for many valuable discussions on the interpretation of the results.

Mrs. N. Black who managed to make an excellent job of typing the manuscript without the aid of a Rosetta Stone.

The Ministry of Defence through the Admiralty Oil Laboratory for the grant towards this work.

Finally, all my colleagues in the physical chemistry department at Nottingham and in the research laboratories of International Marine Coatings for serious help infused with liberal lighter moments.

PROLOGUE

The Walrus and the Carpenter
    Were walking close at hand;
They wept like anything to see
    Such oil polluted sand:
'If this were only cleared away,'
    They said, 'it would be grand!'

'If seven maids with seven mops
    Swept it for half a year,
Do you suppose,' the Walrus said,
    'That they should get it clear?'
'I doubt it,' said the Carpenter
    And shed a bitter tear.

(with apologies to Lewis Carroll [2])

1. INTRODUCTION

1.1 The 'Torrey Canyon'

Popular concern for the environment dates quite markedly from the wrecking of the super-tanker 'Torrey Canyon' in 1967. Constant press and television coverage brought home the meaning of large scale pollution to the public at large. Attempts to deal with some of the beached oil sometimes made matters worse. Publicised examples were the sinking of oil directly onto French oyster beds, and the elimination of Cornish rock-pool life by concentrated toxic detergents. With the advent of underwater oil drilling and even larger super-tankers, there was clearly a need for investigation into the problems of oil pollution.

A series of studies were made of various aspects of the 'Torrey Canyon' incident [3,4,5,6] and one outcome was the following observation. After only a few hours on a heavy sea, the crude oil formed a highly stable emulsion containing up to 80% by volume of sea water [3,7]. This emulsion, light brown in colour and highly viscous, was aptly named "chocolate mousse" [8]. Being oil based, very large areas of "mousse" tended to accumulate rather than spread over the ocean as crude oil alone would have done. Pilpel [9,10] has reviewed the fate of crude oil on the sea and he stated that the natural processes of degradation by sunlight and bacteria are considerably retarded by "Mousse" formation. It would clearly be advantageous to know what factors influence the stability of these "mousses".

1.2 Emulsions - Definition and Terminology

Definitions of emulsions are numerous in the literature, but the following is based on that of Becher [11].

An emulsion is a system of one liquid intimately dispersed in a second liquid with which it is immiscible. The size range of the dispersed droplets is between 0.1 and 40 microns (μm). The presence of a third phase which may be either solid or liquid will accentuate the otherwise minimal stability of the system.

Emulsions are usually classified within the general field of colloid science; but one of the definitions of a colloidal system is that at least one dimension lies in the range 1 nm to 1 μm [12]. However, as many of the techniques and theories of colloid science may be applied to emulsions, (despite most droplets observed being larger than 1 μm) it is convenient for them to be considered as colloids. The lower limit of 0.1 μm for emulsions excludes the systems known as microemulsions, but as these require different theories to explain their existence [11], they are considered to be a separate phenomenon. The upper size limit of 40 μm appears arbitrary but is chosen here as being the limit of resolution of the unaided human eye [13].

Most emulsion systems consist of a water phase, W, and an oil phase, O. Ostwald [11] was the first to show the existence of two distinct emulsion types. When water is the "continuous phase" or "dispersion medium", then an "oil-in-water", O/W, system results. When water is the "dispersed phase", then the system is "water-in-oil", W/O.

The third phase has been given a variety of names. The most common is "emulsifying agent" and this is the most convenient to use.

If an emulsion changes, for example, from being oil continuous to water continuous, with the oil becoming the new dispersed phase, then "inversion" has occurred. This is different to "breaking" where the emulsion separates out into the two immiscible phases.

"Creaming" occurs when the coarser droplets either rise to the surface to sink to the bottom, depending on whether the dispersed phase is less or more dense than the continuous phase. The smaller droplets remain intimately dispersed due to Brownian motion and convection currents.

"Coalescence" is the process whereby two individual droplets come together and form a single third droplet. "Flocculation" occurs when droplets come together and stick, due to attractive forces, but can be dispersed again by gentle agitation.

1.3 Water-in-Crude Oil Emulsions

The emulsification of water by crude petroleum in oil fields has been known for many years [14]. Although most papers have dealt with the breaking of such emulsions, some work was carried out on the cause. Briggs [14] suggested that finely divided solids in the petroleum were responsible, whilst Ayres [14], when looking at common features between emulsions of different oils, mentioned the asphaltene fraction of petroleum as having some significance.

In a symposium held in 1931, Abozeid mooted the idea that the asphaltenes form a protective film around the droplets [15]. This suggestion was supported by Fisher [16].

A different problem was that investigated by Lawrence and Killner [17] who looked at the difficulties of pumping naval fuel oil containing three times its own weight of water as an emulsion. They too concluded that the asphaltic fraction of the fuel was responsible for the emulsion and recommended the addition of small quantities of teepol to inhibit emulsion formation.

The 'Torrey Canyon' and subsequent large oil spills resulting in the familiar high water concentration emulsions, prompted further studies. Berridge et al [7] studied the stability of the emulsions formed by seven different crude oils and plotted the stabilities against various properties of the oils. The best correlation was shown by the vanadium content and the asphaltene content. However, no emulsion was formed when the asphaltene fraction of an oil was removed, leaving a high vanadium content. As the vanadium is present in the form of a volatile metallo-porphyrin, it was concluded that this metal is unlikely to be the emulsifying agent, indicating once again the asphaltenes.

A German study [18] initiated after a spill in 1969, involved the addition of detergent to various crudes, observing how long they took to emulsify a given quantity of water and which emulsion type was formed. Their suggestion of adding small quantities of detergent to the crude oil at source as a preventative measure echoes the work of Lawrence and Killner.

Mackay et al [19], investigating a "mousse" from a Canadian spill, isolated a compound X as being the emulsifying agent. However, as this was insignificantly different in composition to the asphaltenes, they concluded that the isolated fraction was also an asphaltenic fraction but with "a more favourable orientation of structure or functional groups".

1.4 Crude Oil

It is well known that crude oil is a highly complex mixture of organic materials ranging from the chemically primitive methane and its homologues to complex giant molecules of high molecular weight.

An oil can be classified according to the percentage of material in given boiling ranges. A pertinent example is the percentage of residue left after heating the oil to $>700^{o}F$ ($\theta_c = 370K$). This value may be used to classify the oil as light, medium or heavy [20]. For the purpose of this study, one oil has been taken from each extreme of the range, together with the oil carried by the 'Torrey Canyon'. These are Brega (from Libya), a light oil with 37.5% residue, Tia Juana (from Venezuela), the heavy oil with 57.7% residue, and Kuwait towards the heavy end, with 51.3% residue, (figures from reference 7).

As the literature indicates that the emulsifying agent is in this heavy fraction, it will be useful to note a few definitions. Abraham [20] defined bitumen as a generic term applied to native substances of varying colour, hardness and volatility. They are composed principally of hydrocarbons and are free of oxygenated bodies. This definition included petroleum, which he went on to define as a species of bitumen of liquid consistency and varying asphaltic nature. Asphalt is also a species of bitumen of varying hardness and as well as naturally occurring material, includes residues from the distillation of petroleum.

The terms residue and asphalt are considered interchangeable for the purposes of this thesis. Nellensteyn proposed over forty years ago that asphalt consists of three parts [20, 21]. The first component is a continuous phase of thick oily substances called the maltenes, in which are dispersed a highly complex series of maltene insoluble molecules called the asphaltenes. The third component is an intermediate range of compounds, similar but much lower in molecular weight than the asphaltenes, called the resins. These peptize the asphaltenes in the maltenes. This theory, although largely unchanged, has been brought up to date by Broome [22]. He concluded that the asphaltene micelles are either discrete or in various stages of flocculation depending on the degree of peptization. This in turn is governed by the aromaticity and activity of intermicellar resins.

1.5 The Nature of Asphaltenes

1.5.1 Separation and Structure

A simple definition of the asphaltene class of compounds is that part of crude oil with the highest molecular weight. There are several methods suggested in the literature for separating this fraction, and indeed, the method of separation is generally used in further classification of the asphaltenes. Abraham [23] has reviewed three such methods.

The first is precipitation from a petroleum naphtha of rigorous specification by boiling range. Increasing the boiling point of the petroleum spirit decreases the asphaltene yield. The second method is precipitation from a solution of the crude in a straight-chained paraffin such as n-pentane or n-heptane. The yield decreases on moving up the homologous series. The third method is the carbon disulphide extract from a solution of the asphalt fraction in diethyl ether.

Two other methods described in the recent literature are those of Nicksic and Jeffries-Harris [24] and Poindexter [25]. The former workers compared the properties of asphaltenes precipitated by n-pentane with those obtained by collecting the residue when crude oil is titrated with perchloric acid in glacial acetic acid. The second author added a ten times excess of acetone to a ten times benzene solution of asphalt.

Girdler [26] has carried out an extensive study on the separation and properties of asphaltenes precipitated by n-paraffins where the carbon numbers range from 3 - 12. He showed that a "hard-core" centre existed in the asphaltene micelle. Paraffins above a carbon number of 6 precipitated asphaltenes which gave essentially the same C/H ratios, relative colour intensities (shown to correlate with aromaticity) and vanadium and nickel contents although the yield fell throughout the homologous series. He concluded that the n-pentane asphaltenes carried with them some of the peptizing resins when they were precipitated and so for that reason he preferred to work with n-heptane precipitated asphaltenes.

Nevertheless, the most common method of extraction when asphaltene properties are studied appears to be precipitation using n-pentane. Erdman [27] has reviewed the literature up to 1965 on the chemical nature of this class of asphaltenes. According to his conclusions, an asphaltene molecule is thought to consist of a skeleton of graphite-like clusters of condensed aromatic rings. Condensed naphthenic rings are linked, but not fused, to the aromatic clusters and contain some short or branched alkyl chains attached to the inner carbon atoms (Fig. 1-1). The main heteroatoms present are oxygen, nitrogen and sulphur; the former is present mainly in the double-bond form whilst the other two appear to be present in chains

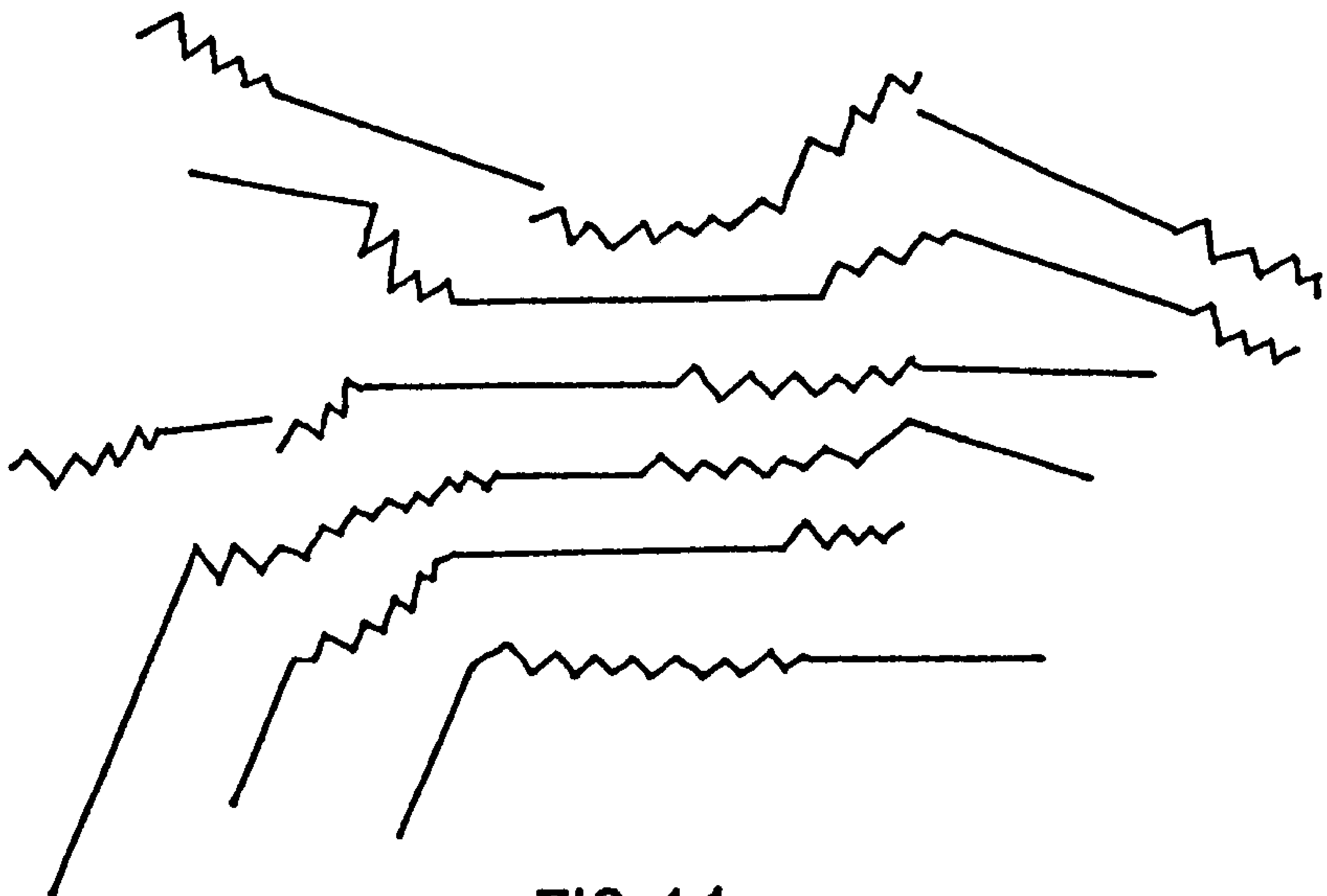

FIG. 1-1

∧∧∧∧ Represents saturated carbon chains or naphthenic rings

—— Represents edges of flat sheets of aromatic rings

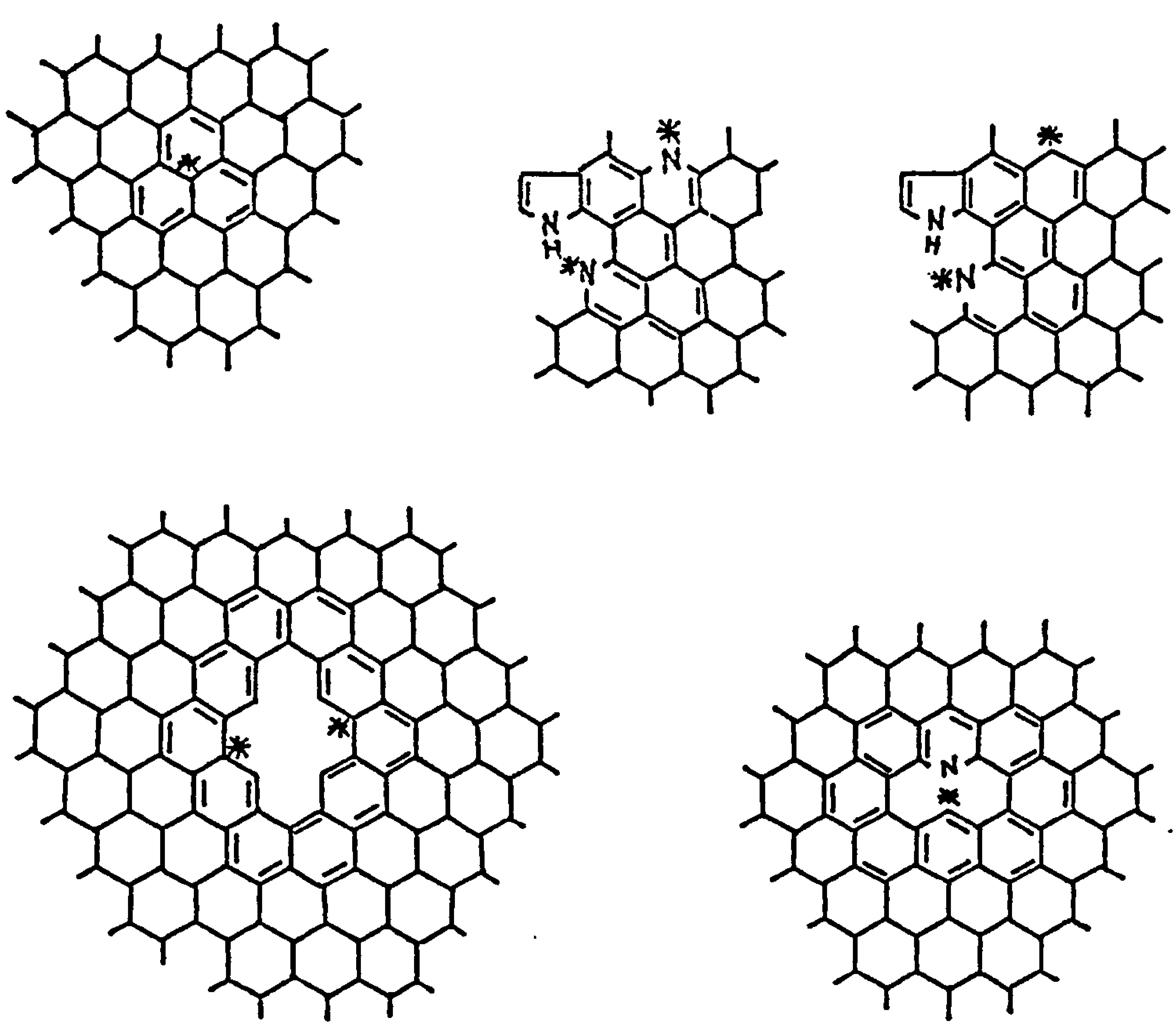

FIG. 1-2

* = Possible sites of free electrons

(Both figures from reference 27)

or rings. Esr studies suggest that free radical sites are present in the aromatic clusters together with sites for complexing nickel (II) and vanadium (IV) (Fig.1-2). The natural concentration of these metals varies greatly; co-ordination with them is generally through nitrogen but also possibly through oxygen or sulphur.

More recently, Nicksic and Jeffries-Harris [24] have proposed structures to explain the behaviour of petroleum in perchloric acid in acetic acid titrations. This procedure is used to determine the "basic nitrogen" and the resulting precipitate, after washing with n-pentane, has been found to be of a very similar nature to n-pentane asphaltenes. The perchlorate asphaltenes, after dispersing in toluene and treating with aqueous potassium hydroxide, are converted to n-pentane asphaltenes. In considering the mechanism of the acid reaction, the authors rejected the explanation of an amine salt being formed. They suggested that the perchloric acid brings the solution to an isoelectric point, which in common with other systems such as amino acids and proteins, is the point of minimum solubility. One of the possible formulae they suggested to support this assertion was a phenazine :

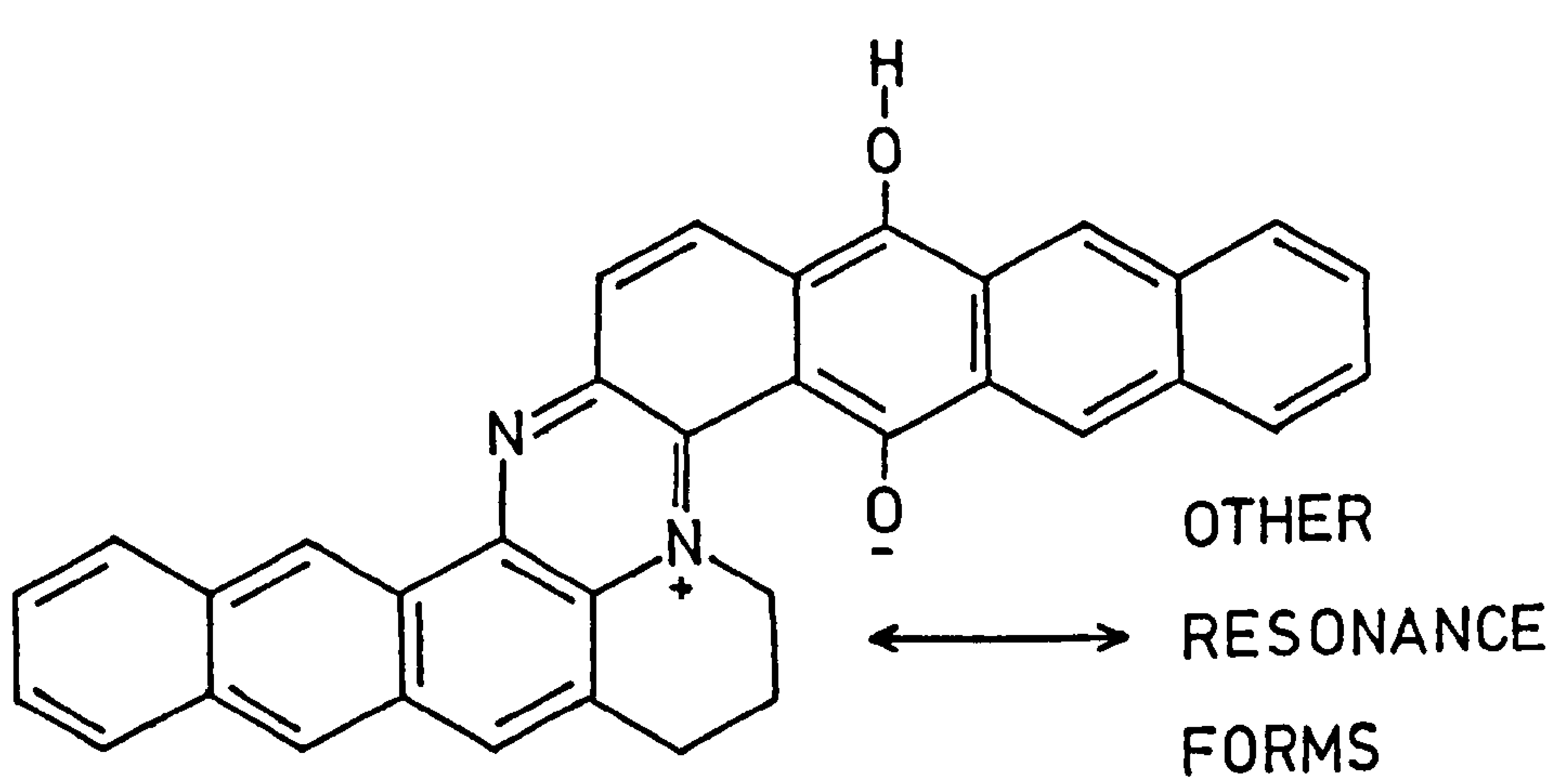

An ion of this precise molecular weight, they added, has been reported to occur in petroleum, in particular in the asphaltene fraction, and furthermore to precipitate in the presence of perchloric acid. Resonance structures of this sort also helped them to explain the shape of the titration curves, the effect of acid on colour and fluorescence and the stability of the perchlorates. However, the contribution of the free radicals was not dealt with.

1.5.2 Environment in Crude Oil

Nellensteyn's updated theory on the asphaltene micelle in crude oil has been outlined in section 1.4. Dickie and Yen [28] have listed various attempts to measure the size of these micelles. More recently, Poindexter [25] has studied asphaltenes (from two sources) colloidally dispersed in many different solvent systems. He used the dynamic nuclear polarization technique (a combination of esr and nmr) which enables the extent of the asphaltene molecular aggregation as a function of solvent species to be determined. The volumes of asphaltene particles were shown to range from 40 nm^3 to 400 nm^3 and higher. This represents a diameter of a spherical particle from approximately 3.4 nm to over 7.4 nm. Poindexter himself noted that the model of asphaltenes presented in these experiments was incomplete and possibly artificial.

Dickie et al [29] have taken electron micrographs of asphaltenes deposited from benzene solutions. These indicated that the structure is spherical rather than laminar, and further indications were that the polar regions of the asphaltene molecules are in the centre of the spheres.

Dickie and Yen [28] have surveyed a variety of physical methods for the determination of the molecular weight of asphaltic materials, (i.e. resins and asphaltenes). The divergent results, with values from 1,000 to 500,000, were explained by an asphalt "molecule" composed of individual sheets (Fig. 1-3). These sheets associate to form unit cells (or particles) and larger associated micelles. Resins have similar structures, but differ in the extent of condensation. The molecular weight of the unit sheets can be obtained from X-ray diffraction and scattering and were shown to vary between 800 and 3,500. Particle molecular weight was obtained from vapour pressure osmometry and electron microscope studies; these gave weights between 3,400 and 5,900. Electron micrographs were used again for micelle size determination which were seen to be 10 - 30 nm in diameter corresponding to 37,000 to 10 million molecular weight range.

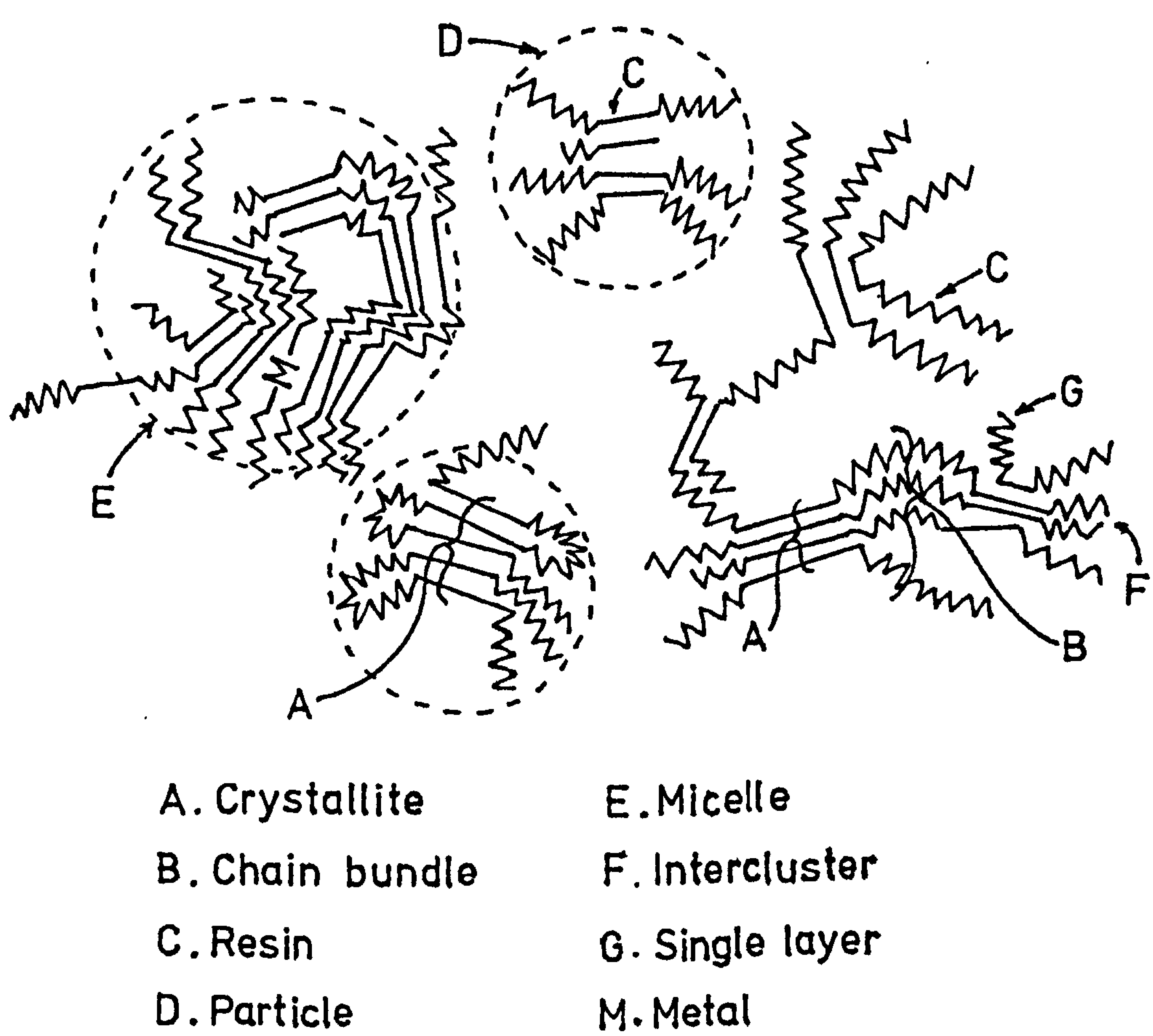

FIG. 1-3 (after ref. 28)

2. THEORY

2.1 Droplet Size Measurement and Analysis

2.1.1 Introduction

Reviews by Davies [30] and Kitchener and Mussellwhite [31] show that most of the quantitative theories of emulsion stability require the mean droplet size. The mean volume diameter is significant in the rheological characterisation of concentrated emulsions [32], whilst a diameter related to surface area may be used in theories of emulsion formation [33]. A comparison of the efficiencies of different emulsifying methods requires not only the mean but also some indication of the spread of the diameters. Detailed knowledge of the droplet size distribution is therefore essential in a physical evaluation of an emulsion system.

2.1.2 Methods of Data Collection

There are three principal methods [34] of collecting size distribution data in emulsions: by the Coulter Counter, by centrifugation devices or by optical techniques. The Coulter Counter is only suitable for O/W emulsions as it depends on a large difference in conductance between the two phases with the highest conductor being the continuous phase. Sherman [34] has described a centrifugation technique using various sucrose solutions but this again is suitable only for O/W emulsions. The centrifugal photosedimentometer described by Groves [35] can be used for both emulsion types. The basic principle is that the rate of sedimentation is measured optically after diluting the emulsion in a medium of known density. A disadvantage with crude oil emulsions is that the nature of the emulsion may change on dilution with a necessarily transparent medium. The opacity of the oil also rules out important optical methods of size distribution determination such as extinction techniques and reflectance measurements. However, use of the optical microscope with a sufficiently thin sample will overcome this problem, although there are still a number of alternative ways in which data from the microscope image can be obtained.

The most convenient method is by use of an electronic scanning analyser of the type developed by Coulter or Imanco. The mode of operation has been described by Fisher [35]. Briefly, an image of the emulsion system either from a microscope slide or a photomicrograph is displayed on a television screen. The instrument scans this image and distinguishes areas of differing light intensity. In this way a dark particle will be picked out from a light background and vice-versa. The areas of "blackness" in the first case are measured either by length or by area. The problem with most emulsions is that they appear on the screen as dark rings with a "light" interior having the same or similar intensity as the continuous phase. One solution would be to use an inert dark dye in the dispersed phase.

Two laborious methods involve analysing the sample whilst on the microscope [34]. The first is the technique known as "double image microscopy" described by Barnett and Timbrell [37]. The microscope is fitted with a beam splitting device between the objective and eyepiece so that two identical images of each droplet are observed. Initially the two images coincide, but a switch with ten size ranges introduces a step-wise increase in separation between then. A droplet is counted when at a particular range, the overlap of its two images becomes a separating gap. (Sherman [34] claims that an experienced operator can grade as many as 600 droplets in twenty minutes with less than a 0.25 μm error). The second method involves the insertion of a calibrated graticule in the eyepiece of the microscope which enables the droplets to be measured directly. Alternatively the image may be displayed on a screen where the measurement may be carried out.

A more convenient procedure is to take a photomicrograph by means of a camera mounted alternately with the microscope eyepiece. The photographs may then be analysed at leisure by a variety of methods. The simplest is by means of a calibrated graticule. A more complicated system utilises a plastic strip with a long metal edged V-shaped cut [38]. The strip is adjusted over the photograph until a droplet image coincides tangentially with each side of the V-cut. A metal nibbed pen, which is connected to a control box, is used to mark the droplet as counted and at the same time is touched on the metal edge to complete a circuit. This registers the size of the droplet on one of a number of counters in the control box.

A more sophisticated system of counting images from photographs has been described by Endter and Gebauer [39] and a similar but simpler system has been developed by Becher [40]. The Endter machine is manufactured by Carl-Zeiss and its use has been fully discussed by Falcon-Uff and Leverington [41] for work on silver halide crystals. The principle of operation is that an illuminated iris diaphragm is imaged by a lens on to the plane of a Plexiglass plate. A photographic print is placed on the plate and the beam of light focussed so that it completely surrounds the droplet. A foot-pedal is then operated so that a hole is punched through the droplet to avoid recounting, whilst the size is simultaneously registered on one of 48 counters.

One advantage of taking photographs in place of direct measurement is that samples are more rapidly dispatched enabling other experiments (e.g. rheological) to be carried out simultaneously. A photographic record can also be kept allowing further investigation should anomalous behaviour be apparent. A disadvantage with all microscope studies is that with the majority of droplets having a diameter in the range 1 - 5 μm, a high magnification is necessary for accurate counting. However, this increase brings with it a corresponding decrease in the depth of field of the sample. This problem is dealt with further in Chapter 5.

2.1.3 Representation of Data

In all the methods of droplet size analysis mentioned so far, the data is obtained as a series of frequencies of occurrence of droplets in certain size ranges. There are three main ways in which such data may be represented [42]: a histogram, a frequency polygon and an ogive or cumulative frequency curve (see Fig. 2-1).

In the histogram, the areas of the rectangles represent the frequency of occurrence at the mid-point of the rectangle along the abcissa. The width of the rectangle along the abcissa is the class interval. In the most desirable case the class widths are equal and the ordinate represents the frequency (else it is just the ratio of frequency to class width). The choice of class width should be such that a clear pattern of frequency distribution may be observed.

FIG. 2-1

If all the classes are of equal width and adjacent points are connected, a frequency polygon is obtained. Distributions of discrete variables (integers) are most commonly represented in this manner. Frequency polygons are better for comparative purposes than histograms [11].

The cumulative frequency graph is obtained directly from the histogram by adding the frequency whilst progressing along the abcissa; but the point is plotted at the end of the class interval. Reading the cumulative frequency at a given value on the abcissa gives to the left the number of droplets with a diameter less than that value. If the total number of results in the histogram is increased indefinitely so that the class widths can be correspondingly decreased, at the limiting case a frequency distribution curve arises. Together with the ogive, the frequency distribution curve is an important feature of the treatment of droplet size analysis in this thesis and is fully discussed after the next section.

2.1.4 Droplet Size Analysis of Crude Oil Emulsions

Although several authors have carried out microscopical investigations of crude oil emulsions, very few appear to have studied the droplet size distribution in any detail. Abozeid [15] gave the droplet diameter range as 0.1 - 200 μm whilst Fisher [16] found a much narrower distribution of 0.2 - 10 μm (both authors dealt with oil field emulsions). Lawrence and Killner [17] mentioned droplet size in a discussion on stability and Berridge et al [7] presented a photomicrograph but gave no data. Blair [43] suggested a range of 10 - 100 μm for his oil field emulsions and included a photomicrograph showing droplets of around 60 μm diameter. Schwarz and

Bezemer [44] used data from water-in-crude oil emulsions to test their equation (discussed later) but did not publish their findings except to say that a good fit was found. Mackay et al [19] published a histogram obtained for their model crude oil emulsion system but did not attempt to analyse it in any detail except to calculate a mean diameter.

2.1.5 Means and Moments

Becher [11] and Sherman [34] have listed several averages or means that can be obtained from droplet size data but they gave little indication of the relation of these to each other or to any sort of distribution. Herdan [45] however, has defined such averages and describes them in terms of their respective distributions. His treatment predominates in the following section.

2.1.5 A Arithmetic Mean

Herdan distinguished between two types of distribution : discontinuous or arithmetic and continuous or geometric. Let there be an arithmetical distribution characterised by the probabilities :

$$w_1(x_1) + w_2(x_2) + \ldots + w_m(x_m) \quad \text{with sizes } x_1,\ x_2 \ldots x_m.$$

Taking a sample of the first N droplets and letting there be n_1 droplets of size x_1, n_2 droplets of size x_2, ... n_m droplets of size x_m, then the average of those N values is given by :

$$\frac{n_1x_1 + n_2x_2 + \ldots + n_mx_m}{N} = \frac{n_1x_1}{N} + \frac{n_2x_2}{N} + \ldots + \frac{n_mx_m}{N} = a \qquad \text{2-1}$$

As N increases, the relative frequencies n_i/N approach the probabilities $w_i(x_i)$ and as N tends to ∞, the average becomes :

$$A = x_1 w_1 + x_2 w_2 + \cdots + x_m . w_m = \Sigma\, x_i . w_i \; (x_i) \qquad 2\text{-}2$$

and A is the Mean Value of the distribution.

2.1.5 B Geometric Mean

Herdan [45] described the geometric mean of a series of values x_1, x_2, ... x_n as being the Nth root of the product of the N values :

$$G = (x_1 . x_2 . \ \ldots\ x_j \ \ldots\ x_N)^{\frac{1}{N}} \qquad 2\text{-}3$$

In terms of logarithms, this becomes :

$$\ln G = \frac{1}{N} . \sum_{j=1}^{N} (\ln x_j) \qquad 2\text{-}4$$

In the experiments described, there will be a set containing n_1 values of equal x_1, another set containing n_2 values of equal x_2 and so on, such that $n_1 + n_2 + \ldots + n_i + \ldots + n_m = N$, where m is the number of classes. Equation 2.4 can be adjusted to :

$$\ln G = \frac{1}{N} . \sum_{i=1}^{m} n_i \ln x_i \qquad 2\text{-}5$$

Herdan [45] gave the proof for the inequality $A \geqslant G$ which increases the greater the dispersion among the number of variables.

2.1.5 C Moments of the Variable

There is no reason why the average of the distribution of the variable should be to the first power in the arithmetical mean [45], thus a is only a particular average. Depending on whether the droplet size is taken to the 1st, 2nd, ... rth power, then the corresponding averages are defined from the 1st, 2nd, ... rth moment distributions as follows :

$$\mu_1' = a_1 = \frac{\Sigma\, n_i x_i}{N} \qquad 2\text{-}6$$

$$\mu_2' = a_2^2 = \frac{\Sigma\, n_i x_i^2}{N} \qquad 2\text{-}7$$

$$\mu_3' = a_3^3 = \frac{\Sigma\, n_i x_i^3}{N} \qquad 2\text{-}8$$

Unless otherwise stated, Σ is understood to mean $\sum_{i=1}^{m}$

2.1.5 D Distribution by Surface and Volume

The total surface area of a number of spherical droplets with a range of diameters $x_1, x_2, \dots x_m$ will be given by :

$$S = \pi \cdot \Sigma\, n_i x_i^2 = N \cdot \pi \cdot \frac{\Sigma\, n_i x_i^2}{\Sigma\, n_i} \qquad 2\text{-}9$$

So the mean surface diameter is :

$$d_s = \left[\frac{\Sigma\, n_i x_i^2}{\Sigma\, n_i}\right]^{\frac{1}{2}} = a_2 \qquad 2\text{-}10$$

The total volume is similarly obtained :

$$V_d = \frac{\pi}{6} \cdot \Sigma n_i x_i^3 = N \cdot \frac{\pi}{6} \cdot \frac{\Sigma\, n_i x_i^3}{\Sigma\, n_i} \qquad 2\text{-}11$$

The mean volume diameter is :

$$d_v = \left(\frac{\Sigma\, n_i x_i^{\,3}}{\Sigma\, n_i}\right)^{\frac{1}{3}} = a_3 \qquad 2\text{-}12$$

In order to describe the mean surface area per unit volume, S/V_d, then :

$$\frac{S}{V_d} = \frac{\pi}{\pi/6} \cdot \frac{\Sigma\, n_i x_i^{\,2}}{\Sigma\, n_i x_i^{\,3}} = 6. \frac{\Sigma\, n_i x_i^{\,2}}{\Sigma\, n_i x_i^{\,3}} \qquad 2\text{-}13$$

To obtain the correct units, the "surface area per unit volume mean diameter" is given as :

$$d_{sv} = \frac{6V_d}{S} = \frac{\Sigma\, n_i x_i^{\,3}}{\Sigma\, n_i x_i^{\,2}} = \frac{a_3}{a_2} \qquad 2\text{-}14$$

2.1.5 E <u>Measures of Dispersion</u>

Consider two sets of numbers, 9, 10, 11 and 1, 10, 19. Both sets have an arithmetic mean of 10 yet the second spreads over a much greater range than the first. A measure of dispersion called the arithmetic standard deviation, with the same units as arithmetic mean, is defined as :

$$\sigma = \sqrt{\frac{\Sigma(x_i - a)^2}{N}} \qquad 2\text{-}15$$

This can be used with the arithmetic mean to provide a unique description for a given distribution.

The logarithmic standard deviation provides a measure of dispersion about the logarithm of the geometric mean [46]:

$$\ln \sigma_g = \sqrt{\frac{\Sigma\, n_i (\ln x_i - \ln G)^2}{N}} \qquad 2\text{-}16$$

2.1.6 Distribution Functions

The treatment so far deals with the data in the non-idealized form of the histogram. It would be of theoretical interest if some sort of mathematical distribution function could be fitted to the data over the histogram. A large number of distribution functions suitable for emulsions have been reviewed by Becher [11], Groves [34] and Sherman [33], but only the following two appear promising from the theoretical viewpoint and from the goodness of fit criteria discussed in the next sub-section.

2.1.6 A The "Amsterdam Distribution Equation" (A.D.E.)

The first is that developed by Schwarz and Bezemer [44]. The numerical distribution, i.e. the percentage of drops in each size range, is given by :

$$\frac{dn}{dx} \cdot \frac{100}{N} = \frac{100}{6} \cdot \frac{\exp\{\alpha/X\}}{\left[1 + \frac{\alpha}{X} + \frac{\alpha^2}{2X^2} + \frac{\alpha^3}{6X^3}\right]} \cdot \frac{\alpha^4}{x^5} \cdot \exp\{-\alpha/x\} \qquad 2\text{-}17$$

The last two parameters of the equation are X and α. X is the diameter of the largest droplet occurring and α is a "characteristic diameter". This is related for example to $x_{n\,-\,max.}$, (the modal or most common value of x with respect to number) by $x_{n\,-\,max.} = \alpha/5$. The two parameters are obtained from the experimental data by plotting $\ln V_x$ versus $1/x$, which gives a straight line, since :

$$\ln V_x = \left[\ln V_d + \frac{\alpha}{X}\right] - \frac{\alpha}{x} \qquad 2\text{-}18$$

V_d is the total volume and V_x is the cumulative volume below diameter x. The authors claim to have applied this equation to many emulsion systems including water-in-crude oil. The same authors have proposed a method of testing the validity of various distribution equations [47]. This involves expressing the parameters of a given equation in terms of various theoretical means (including those described in equations 2-2, 2-10, 2-12 and 2-14) and comparing the values calculated from the parameters with the same means calculated directly from the data. The best fit, and hence the best distribution, is signified by the closest agreement between the greatest number of pairs of means.

2.1.6 B <u>The Logarithmic - Normal Distribution</u>

A distribution that has been found to fit very well in the study of statistics of macroscopic objects is the Normal or Gaussiam frequency distribution. This was originally developed in the treatment of random errors. The standard form of the distribution is given by [45] :

$$\frac{n}{N.dx} = y^{*} = \frac{1}{\sigma\sqrt{2\pi}} \cdot \exp\left[\frac{-(x-a)^2}{2\sigma^2}\right] \qquad 2\text{-}19$$

where y^{*} is the probability density. The curve from this equation is shown in Fig. 2-2-A.

It has been found for a large variety of dispersions (particularly in the 1 - 100 μm range) such as atom bomb fall-out, photographic emulsions and so on, that the logarithmic transformation of the normal distribution applies. Rajogopal [48] has put this on a sound theoretical base for emulsions by considering that the

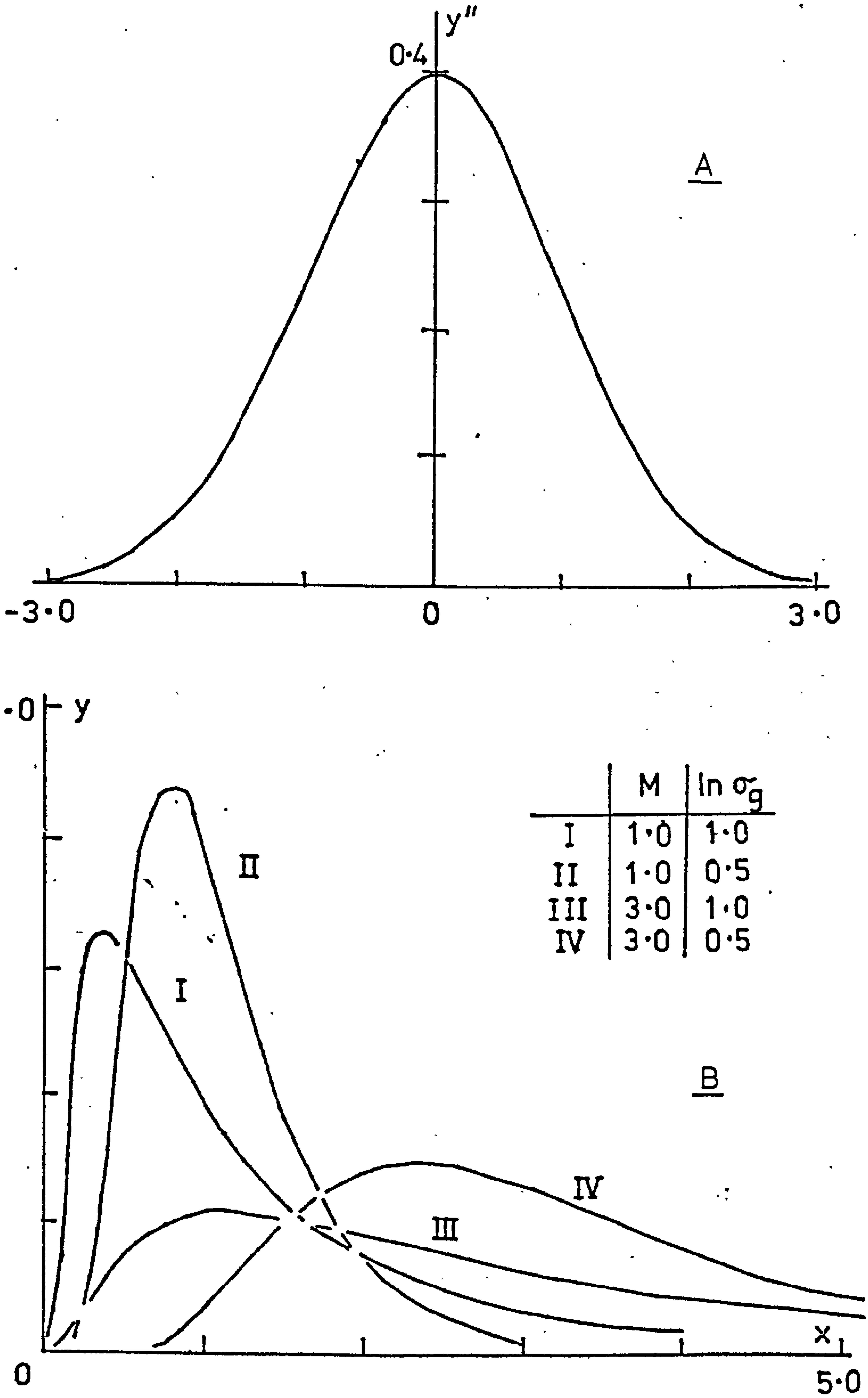
y''
0·4
A
-3·0
0
3·0
1·0
y
M
ln σg
I 1·0 1·0
II 1·0 0·5
III 3·0 1·0
IV 3·0 0·5
II
I
B
IV
III
x
0
5·0

FIG. 2-2

disruption of the interface and the evolution of droplet sizes during emulsification are random turbulent processes. The log-normal distribution is then derived by considering such processes as a Markoff chain. There is some disagreement in the literature as to the general form of the equation, but Herdan [45] and Smith and Jordan [46] quote it as :

$$\frac{n}{Nd(\ln x)} = y' = \frac{1}{\ln \sigma_g \sqrt{2\pi}} \cdot \exp\left[-\frac{(\ln x - \ln M)^2}{2\ln^2 \sigma_g}\right] \qquad 2\text{-}20$$

where M is the geometric mean. The symbol M has been given instead of G so that the two values can be compared to give an indication of the goodness of fit of equation 2-20. M is also the median point on the cumulative frequency curve, i.e. the diameter below or above which half the number of droplets are to be found.

Smith and Jordan [45] have discussed the confusion that surrounds the meaning of y' (the frequency function). However, the more rigorous discussion of this value by Herdan [45] is easier to follow. From equation 2-20, he gives the number of droplets between x_1 and x_2 as :

$$\frac{n_i}{N} = \frac{1}{\ln \sigma_g \sqrt{2\pi}} \cdot \int_{x_1/\ln \sigma_g}^{x_2/\ln \sigma_g} \exp\left[\frac{-(\ln x - \ln M)^2}{2\ln^2 \sigma_g}\right] \cdot d(\ln x) \qquad 2\text{-}21$$

The general expression for the moments of the whole distribution is then given by [45, 49] :

$$\mu_r' = \frac{\Sigma n_i x^r}{N} = \frac{1}{\ln \sigma_g \sqrt{2\pi}} \int_0^{\infty} x^r . \exp \left[\frac{-(\ln x - \ln M)^2}{2 \ln^2 \sigma_g} \right] d(\ln x) \qquad 2\text{-}22$$

$$\therefore \quad \mu_r' = M^r . \exp \left[\frac{r^2 \ln^2 \sigma_g}{2} \right] \qquad 2\text{-}23$$

From the general case of equation 2-23, the various means may be obtained from the log-normal distribution [45] :

$$\ln x_s = \ln \left[\frac{\Sigma n_i x_i^2}{N} \right]^{\frac{1}{2}} = \ln M + 1{\cdot}0 \ln^2 \sigma_g \qquad 2\text{-}24$$

$$\ln x_v = \ln \left[\frac{\Sigma n_i x_i^3}{N} \right]^{1/3} = \ln M + 1{\cdot}5 \ln^2 \sigma_g \qquad 2\text{-}25$$

$$\ln x_{sv} = \ln \left[\frac{\Sigma n_i x_i^3}{\Sigma n_i x_i^2} \right] = \ln M + 2{\cdot}5 \ln^2 \sigma_g \qquad 2\text{-}26$$

The values x_s, x_v and x_{sv} are the mean diameters corresponding to d_s, d_v and d_{sv} respectively with the restraint that they are obtained from the log-normal distribution. If the log-normal distribution is a perfect fit for a given set of data, then the corresponding pairs of values will be identical.

It is important to note that equation 2-20 represents the distribution of the <u>logarithms</u> (base e) of the droplet sizes and if plotted out will appear as a normal curve as shown in Fig. 2-2-A. The distribution for the droplet diameter x itself is given by [45,48] :

$$y = \frac{n}{N.\Delta x} = \frac{1}{x.\ln \sigma_g . \sqrt{2\pi}} \cdot \exp \left[\frac{-(\ln x - \ln M)^2}{2 \ln^2 \sigma_g} \right] \qquad 2\text{-}27$$

The result of plotting out this curve for different values of M and $\ln \sigma_g$ is shown in Fig. 2-2-B.

2.1.6 C <u>Log-normal Treatment of Experimental Data</u>

Rajagopal [48] showed that the substitution of the linear relationship and its derivative :

$$Z = \frac{(\ln x - \ln M)}{\ln \sigma_g} \quad , \quad \frac{dZ}{dx} = \frac{1}{x . \ln \sigma_g} \qquad 2\text{-}28$$

into equation 2-27 gives a standard form of the normal distribution (equation 2-19) :

$$g = \frac{1}{\sqrt{2\pi}} \cdot \exp\left[\frac{-Z^2}{2}\right] = \frac{n}{NdZ} \qquad 2\text{-}29$$

Again from equation 2-27, the probability that the size of a droplet is $\leqslant x_o$, the upper class limit is given by :

$$F_o = \int_o^{x_o} y \, dx \qquad 2\text{-}30$$

F_o may be related to Z in the normal distribution (equation 2-29) through the equation :

$$F_o = \int_{-\infty}^{Z} g \, . \, dZ = \frac{1}{\sqrt{2\pi}} \int_{-\infty}^{Z} \exp\left[\frac{-Z^2}{2}\right] dZ \qquad 2\text{-}31$$

The values of Z corresponding to the values of F_o may be obtained directly from standard probability tables (such as reference 50). Now F_o is simply the cumulative frequency and can either be expressed as a probability (i.e. $\leqslant 1$) or else as a percentage. The log-normal distribution can be linearised in either of two ways. First, by finding each F_o value in terms of Z and plotting the results against ln x_o, where x_o is the <u>upper</u> interval limit. Secondly by plotting F_o directly against ln x_o on probability paper. Both methods are exemplified in Fig. 2-3.

The values of M and σ_g are easy to obtain from the resulting straight line. As M is the median, the value on the ln x_o axis corresponding to F_o = 50% is by definition equal to ln M. Using equation 2-28, when Z = 1 (F_o from the tables = 0·8413) :

$$\ln \sigma_g = \underset{(\text{at } Z=1)}{\ln x_o} - \ln M \qquad 4\text{-}32$$

Rajagopal [47] has emphasised the importance of having a sufficient number of classes in the middle of the linear plot. (If Z is plotted against ln x_o, he calls such a plot a fractile diagram). This is due to the distortion that occurs at either end of the line and this can be demonstrated by supposing that the values of F_o are known to ± 0·5%. At the median point, this will cause a deviation of 0·025 in the value of Z. However, at the 1% and 99% levels, 0·5% represents a difference of 0·406 in the Z values, an error magnification of about 16 times. A deviation of ±1% is indicated in Fig. 2-3 by dotted lines.

It is clear that in using the graphical technique, only a certain intermediate range of x_o values should be used. Drinker and Hatch [48] suggested only using values of x_o between 20% and 80% although Rajagopal [47] considered that the line is sufficiently accurate in the F_o range of 10 - 90%.

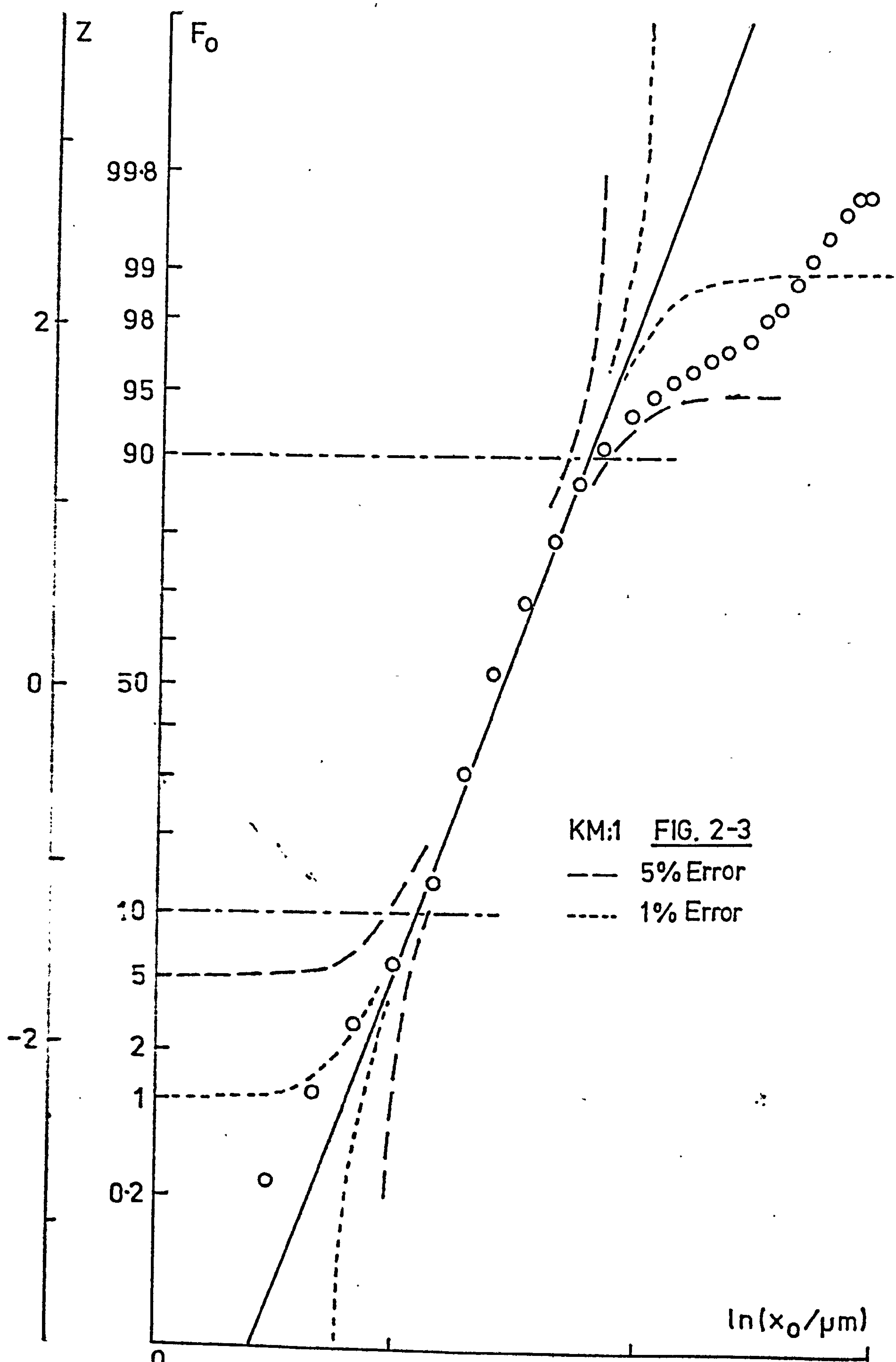

Z
F0
99·8
99
98
95
90
50
10
5
2
1
0·2
2
0
-2
KM:1
5% Error
1% Error
ln(x0/μm)
0
1·0

FIG. 2-3

2.1.6 D Bias in Counting Methods

In any count method there has to be a "largest size" observed. The calculation of any cumulative function is based on this largest size. If such a function is plotted graphically, particularly on probability paper, a curve results that will be asymptotic to such a "largest size". Gwyn et al [51] have discussed this error and proposed a simple method of correcting it. They showed that although such an error is small on the log-normal curve for the number distribution, it becomes much more serious if the area and the volume distribution are represented graphically. This is shown in Fig. 2-4 for a sample set of data.

However it can be seen very clearly that the effect on the normal distribution only takes place above the 90% level suggested by Rajagopal [47] as the upper limit for log-normal graphical representation. Once M and σ_g have been obtained graphically for the normal distribution the rigorous mathematical treatment for finding the corresponding x_s and x_v values discussed earlier may be used.

2.1.7 Statistical Treatment of Experimental Straight Lines

The method of least squares for finding the best straight line to fit a given set of data has two main advantages in the present work. It can be applied using a computer which in turn eliminates subjective "by eye" determinations. The method is based on the assumption that an observed quantity, $\bar{y}$, subject to normal experimental errors is linearly related to a relatively error-free independent variable $\bar{x}$ in the form of the equation $\bar{y} = a' + b'\bar{x}$. The line is found by minimising the sum of the squares of the deviations of the experimental points $\bar{x}_i$ and $\bar{y}_i$ from such a line,

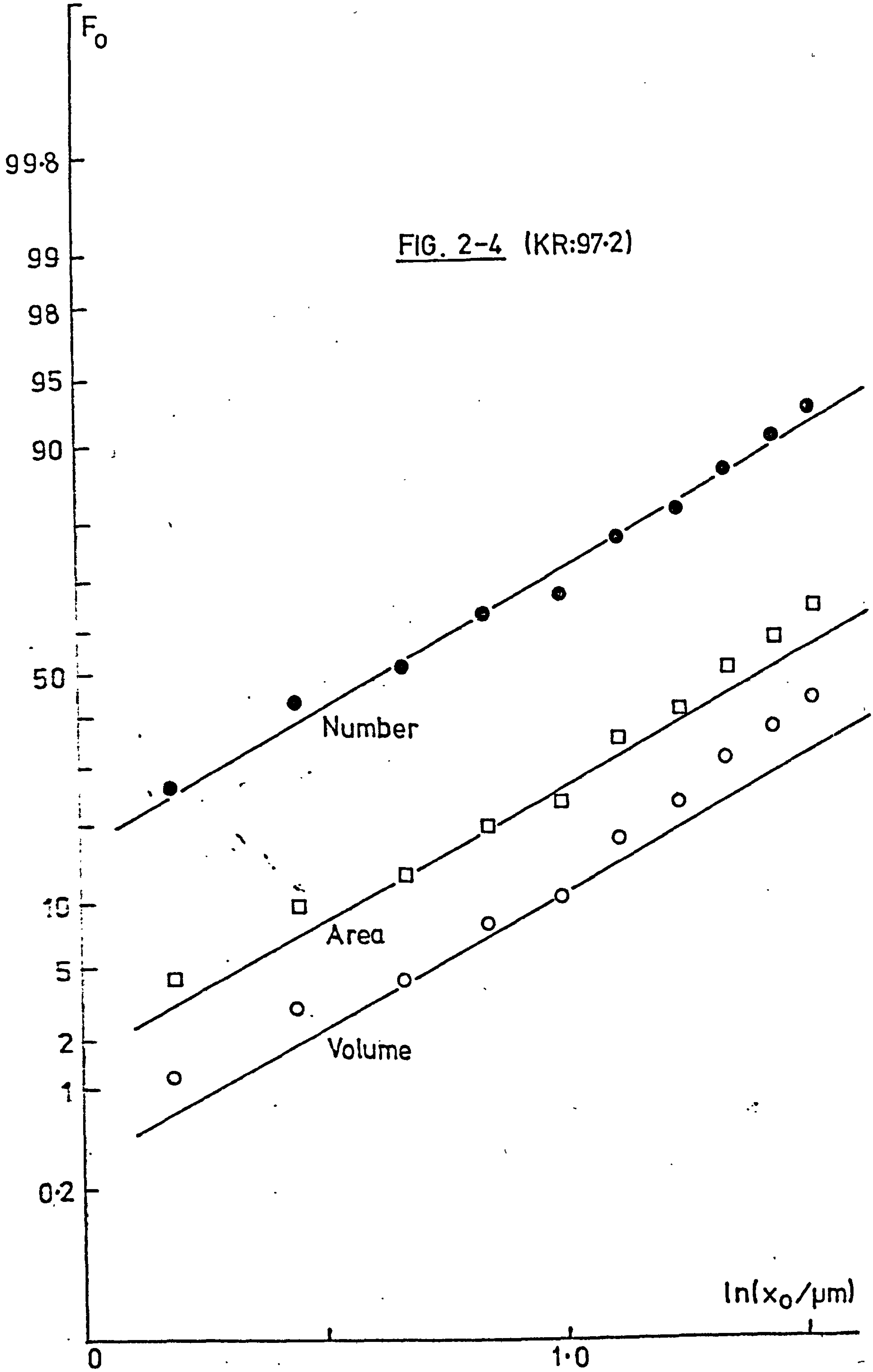
FIG. 2-4 (KR:97·2)
F_o
99·8
99
98
95
90
50
10
5
2
1
0·2
Number
Area
Volume
$\ln(x_o/\mu m)$
0
1·0

i.e. $\Sigma\{\bar{y}_i - (a' + b'\bar{x}_i)\}^2$. The proof of this can be found in most standard statistics books, e.g. Neville and Kennedy [42].
The constants of the line are derived from the experimental data :

$$a' = \frac{\Sigma\bar{x}_i^2 . \Sigma\bar{y}_i - \Sigma\bar{x}_i . \Sigma\bar{x}_i\bar{y}_i}{N.\Sigma\bar{x}_i^2 - (\Sigma\bar{x}_i)^2} \qquad 4\text{-}33$$

$$b' = \frac{N. \Sigma\bar{x}_i\bar{y}_i - \Sigma\bar{x}_i . \Sigma\bar{y}_i}{N.\Sigma\bar{x}_i^2 - (\Sigma x_i)^2} \qquad 4\text{-}34$$

Using these constants, the line is called the linear regression of $\bar{y}$ on $\bar{x}$.

This method is not strictly suitable for the linear treatment of the log-normal equation as the error in $\bar{y}$ should be independent of the level of $\bar{x}$. It has already been shown that the uncertainty of $\bar{y}$ (i.e. Z) at either end of the distribution is greater than at the centre. In addition, the values of $\bar{y}_i$ corresponding to given $\bar{x}_i$ values (i.e. ln x_o) should be normally distributed but in a graph with a $\bar{y}$-axis representing a cumulative function this is doubtful. However, in the absence of a better method and with the "by eye" method the only alternative, the method of least squares seems to be the most reasonable approach. At least a standard method can be defined ensuring identical results from the same data by different operators and a basis of comparison for different data sets, albeit with the limitations that have been emphasised.

2.2 Rheological Phenomena and Measurement

2.2.1 Time Independent Rheological Terms

Many different symbols and more than one description have frequently been attached to certain rheological phenomena. Reiner and Scott-Blair [52] have attempted to standardize terminology and their suggestions are followed here. A full list of symbols appears in Appendix 1.

The four non time dependent types of flow that are found are shown in Fig. 2-5. Newtonian behaviour can best be understood by considering the flow of such a fluid between parallel plates [32]:

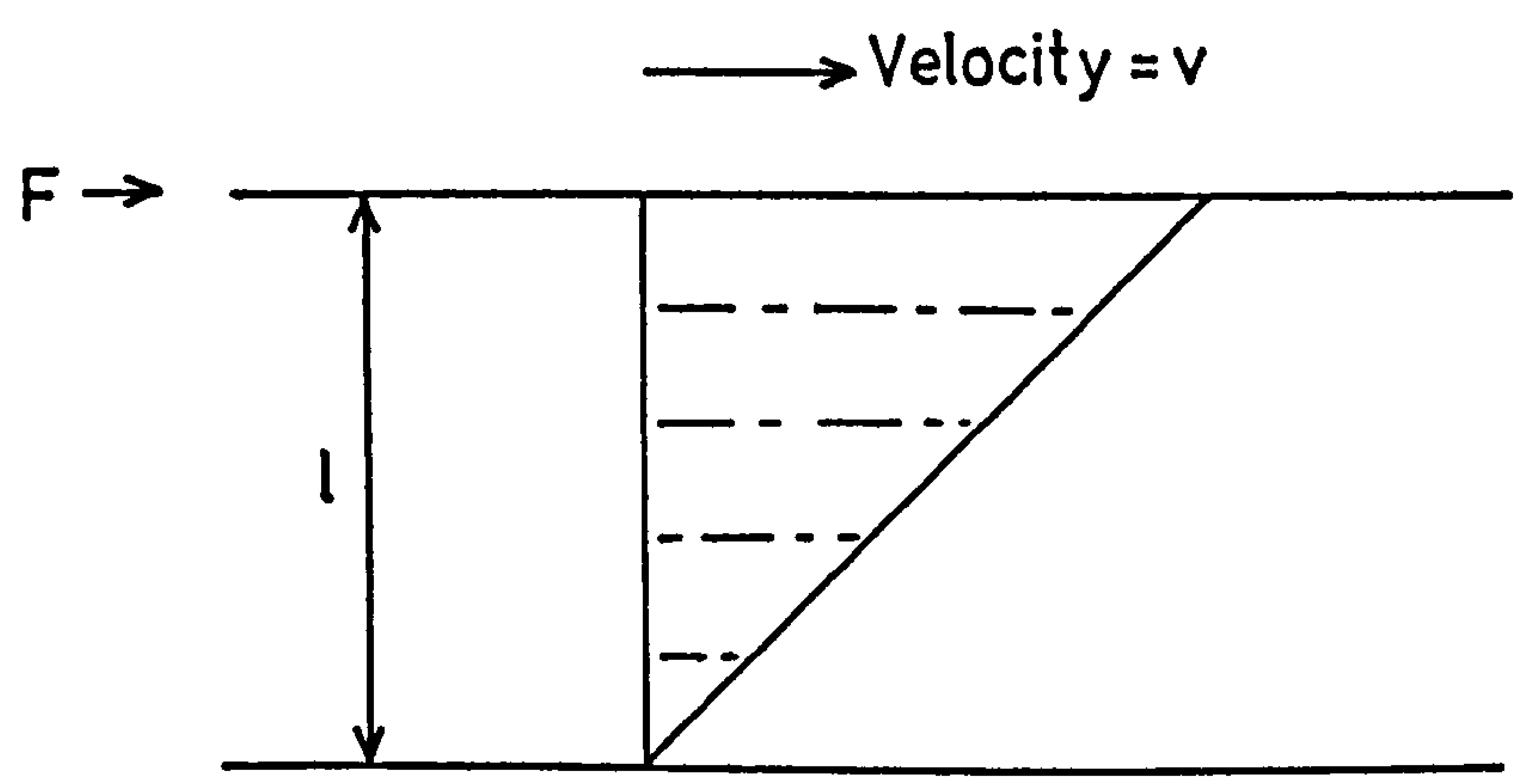

FIG 2-6

When a force, F, is applied to the upper plate so that it moves with a constant velocity v, then if the lower plate is fixed, the liquid between the plates will move with a velocity that varies with its distance from them. The rate of change of fluid velocity is given by dv/dl. As this is linear for Newtonian fluids, the mean rate of shear, $\dot{\gamma}$ is given by v/l. The force per unit area applied to the upper plane, F/L represents the shearing stress, τ (Reiner and Scott-Blair's alternative expression is tangential stress [52]).

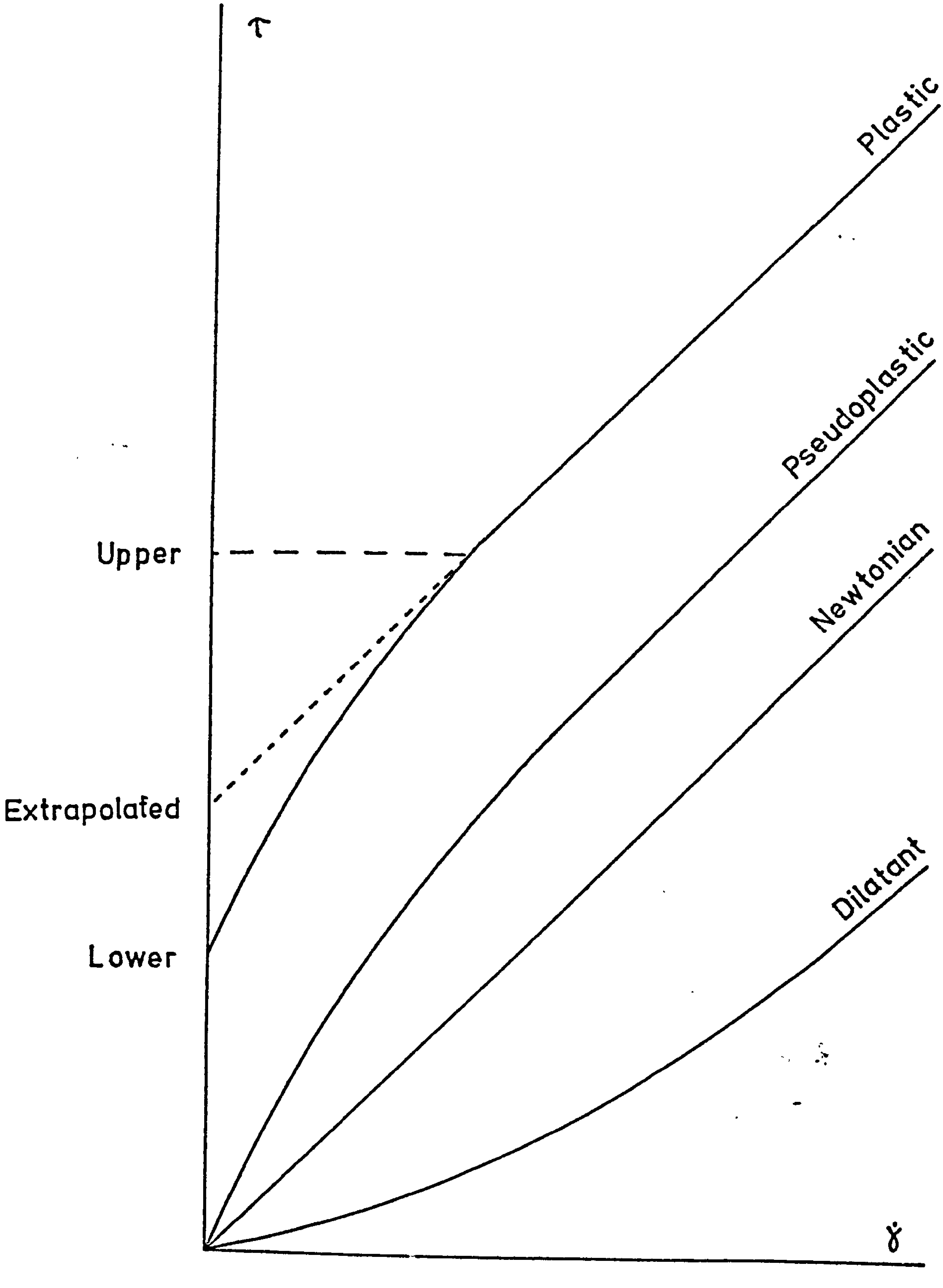
τ
Plastic
Pseudoplastic
Newtonian
Dilatant
Upper
Extrapolated
Lower
γ̇

FIG. 2-5

These authors defined viscosity, η, as "... the resistance to a deformation increasing with the rate of deformation". Thus the following equation can be seen to apply :

$$\tau = \eta \cdot \dot{\gamma} \qquad 4\text{-}35$$

As η is independent of the value of the forces acting in it, it may be determined from single measurements of τ and $\dot{\gamma}$.

In pseudoplastic flow, as $\dot{\gamma}$ increases, the gradient of the $\tau - \dot{\gamma}$ curve, the apparent viscosity (η') falls. After a certain value of $\dot{\gamma}$ is reached η' becomes constant (η_∞) and the resulting straight line can be extrapolated back to a finite intercept on the τ-axis. This type of behaviour in common with all other non-Newtonian flow cannot be determined by single values of τ and $\dot{\gamma}$, so measurements have to be made over a wide range of $\dot{\gamma}$. Reiner and Scott-Blair [52] distinguished between pseudoplasticity and shear thinning. They defined the latter as "... a univalued reduction of the viscosity or consistency with increasing rate of shear". As no profound difference is clear, it is assumed that a system exhibiting shear thinning shows no linear relationship between τ and $\dot{\gamma}$ over a significant range of shear rate.

If a material resists flow until a finite shearing stress has been set up, but then yields and behaves as a pseudoplastic material, plastic flow is being exhibited. The yield point has been labelled in different ways and these are shown in Fig. 2-5. Dilatancy is the term describing substances which on application of a shear rate show an increase in τ accompanied by dilation of the material [52].

2.2.2 Time Dependent Rheological Phenomena

Thixotropy and rheopexy are time dependent forms of shear thinning and shear thickening respectively; the latter will be considered no further. Bauer and Collins [53] have reviewed the work of Freundlich and co-workers who first described thixotropy quantitatively and coined the word. It was originally applied to a "... solid gel which broke down to a liquid sol and then solidified back to the gel state in a time that was reproducible". The concept has been considerably widened and includes certain emulsion systems. Reiner and Scott-Blair [52] defined thixotropy as "... an isothermal and comparatively slow recovery, on standing, of a material, of a consistency lost through shear". Of passing interest is the thixotropy exhibited by waxy crude oils (such as Brega and other Libyan oils) which has been described by Cheng [54]. He explained the structuring as being caused by a series of interlocking crystals. The same behaviour was also observed by this author [55].

Thixotropy can be exhibited in practice in two ways. First, if $\dot{\gamma}$ is kept constant, η' will fall to an equilibrium value. After resting, a certain amount of structure will have recovered which could be seen by applying the same $\dot{\gamma}$ value again. This phenomena is shown in Fig. 2-7. Secondly, if $\dot{\gamma}$ is increased to a maximum without allowing time for an equilibrium situation to arise, and then decreased, a hysteresis loop will result, (Fig. 2-8). A third axis for time is clearly required to fully characterise thixotropy [32].

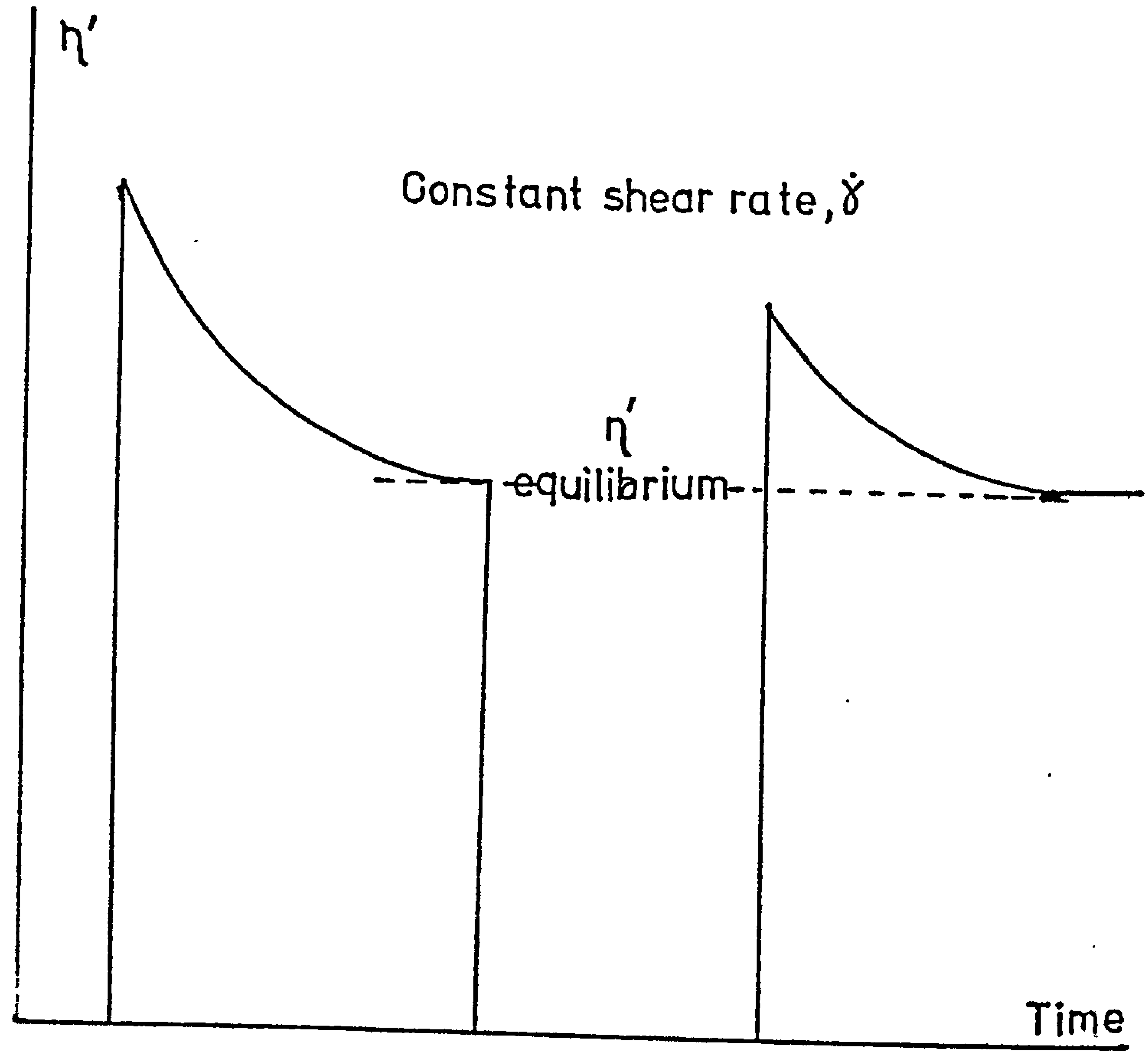

FIG. 2-7

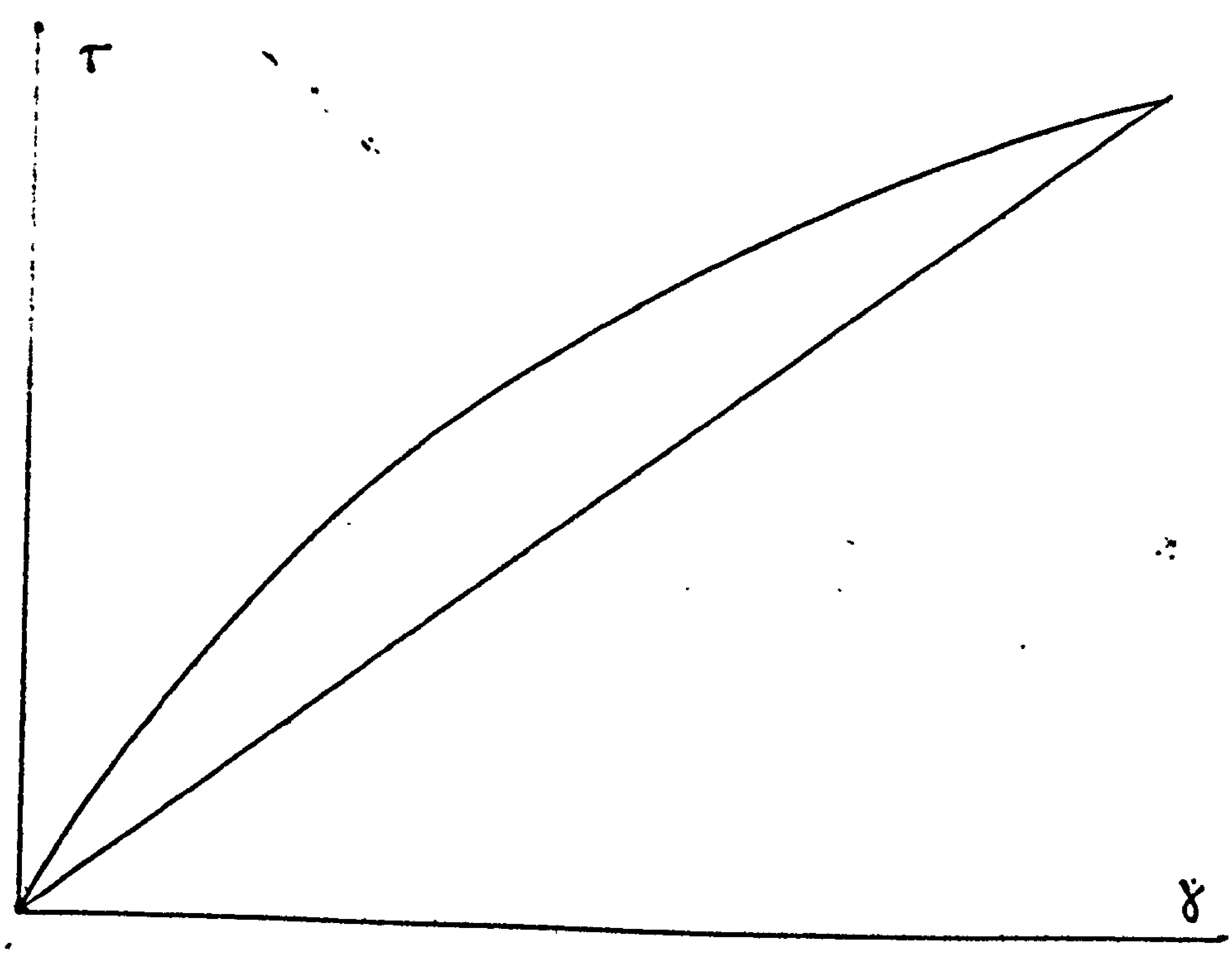

FIG. 2-8

2.2.3 Measurement of Non-Newtonian Behaviour

Sherman [32, 56] has made two comprehensive surveys of the commercial machines available up to 1970. He has also listed equations for calculating the relevant parameters for the four principal classes of viscometer together with any corrections necessary. Two of these, the rolling or falling sphere method and the capillary viscometer, are not convenient for measuring non-Newtonian behaviour.

2.2.3 A Coaxial Cylinder Viscometer

The general principles of the coaxial cylinder (Couette) viscometer are illustrated in Fig. 2-9. In the version shown, the outer cylinder remains stationary whilst the inner cylinder can be rotated at various speeds selected from a gear-box. The viscous drag is obtained by measuring the torque on the spring. Some instruments have a rotating outer cylinder with the spring attached to the inner. One of the main errors in the concentric cylinder viscometer is "end effect". The mode of action is ideally the measurement of the viscous drag between the inner and outer cylinders. However, contact is also made between the bottom of the inner cylinder and the sample; so turbulent flow patterns here can give anomalously high results [56]. This error is eliminated by hollowing the end so that an air bubble is trapped (dotted line in Fig. 2-9). If the inner cylinder is totally immersed by sample, a further end effect results, but this can be avoided by precise sample measurement.

The shear stress at a given radius, R, is related to the torque, G', by [57].

$$G' = 2\pi R^2 h \tau \qquad 4\text{-}36$$

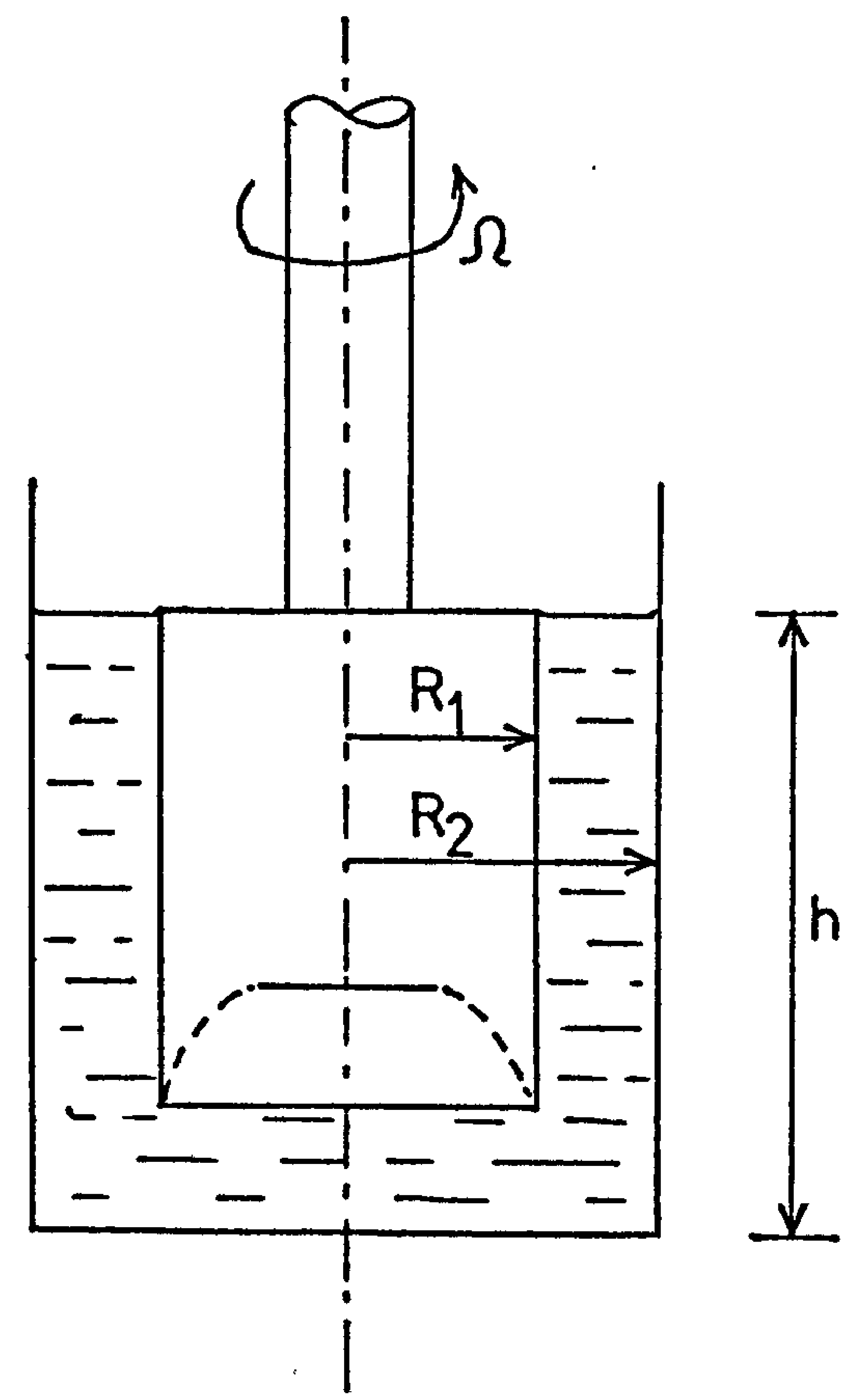

FIG. 2-9

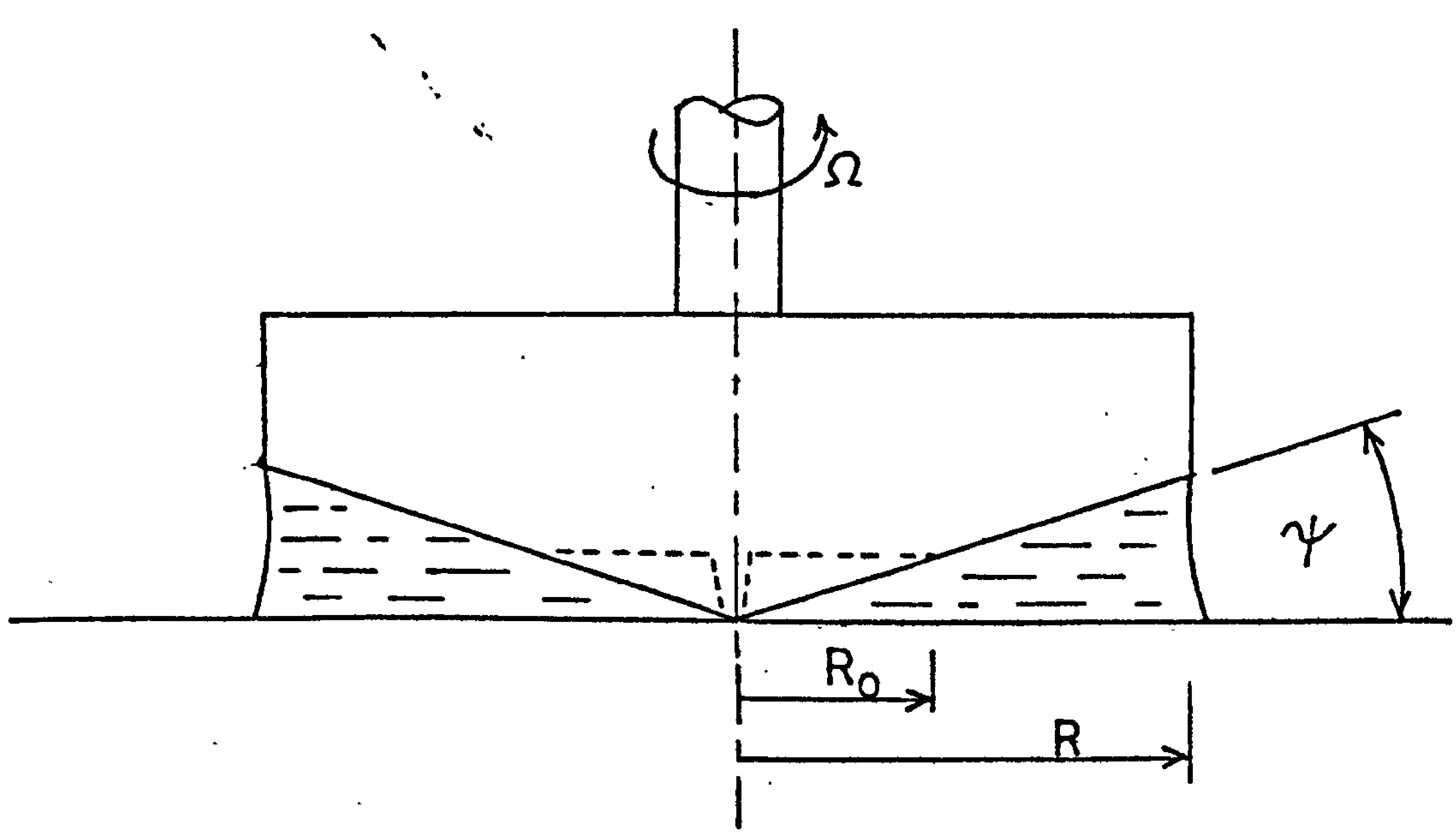

FIG. 2-10

For the shear stress in the sample, the arithmetic mean is taken of the values at the walls of the inner and outer cylinders, so that :

$$\tau = \frac{G'}{4\pi h} \cdot \left[\frac{1}{R_1^2} + \frac{1}{R_2^2} \right] \qquad 4\text{-}37$$

The shear rate is given by :

$$\dot{\gamma} = R \cdot \frac{d\Omega}{dR} \qquad 4\text{-}38$$

where the fluid angular velocity is Ω at R. However, Cheng [54] stated that the shear rate distribution across the annular gap depends on the fluid property. He maintained that a large shear rate variation can result even if the shear stress variation is small. Roscoe [57] suggested the use of an approximate formula obtained from a series expansion. This means that the error can be calculated from the second term in the series. He used Mooney's series and assumed that the arithmetic means of the shear stress and the shear rate occur at the same radius. This gives :

$$\dot{\gamma} = \Omega \cdot \left[\frac{R_2^2 + R_1^2}{R_2^2 - R_1^2} \right] \qquad 4\text{-}39$$

Sherman [56] noted that dispersed systems showed slippage at the cylinder surfaces due to a small amount of phase separation and he suggested roughening the surfaces to overcome this problem. He also discussed the effects of altering the width of the gap $(R_2 - R_1)$ and suggested that this should be 10 - 100 times the size of the largest diameter in the dispersion.

2.2.3 B Cone-Plate Viscometer

The principle of the instrument, shown in Fig. 2-10, is that the sample is put between a flat plate and a cone, the apex of which almost touches the plate. The cone is rotated, and in a similar way to the concentric cylinder apparatus, the shearing stress set up in the sample is obtained from the torque G' measured in the spring [57].

$$\tau = \frac{3G'}{2\pi R^3} \qquad 2\text{-}40$$

This is the only design of viscometer in which the shear rate is uniform throughout the sample [55]. It is also independent of the radius as can be seen from the equation :

$$\dot{\gamma} = \frac{\Omega \cdot R}{\psi \cdot R} = \frac{\Omega}{\psi} \qquad 2\text{-}41$$

One of the disadvantages when investigating dispersed systems is that towards the centre of the cone, the size of the gap gradually reduces until a point is reached where the dispersed phase particle is larger than the gap. By planing down the cone tip, with the exception of a small peg at the centre for alignment, (dotted lines in Fig.2-10) this problem is overcome. The shear rate equation remains unchanged while the shear stress is given by [57] :

$$\tau = \frac{3G'}{2\pi\ (R^3 - R_o^{\ 3})} \qquad 2\text{-}42$$

It is important that the angle ψ is small, and in practice is normally between $0{\cdot}3^o$ and $4{\cdot}0^o$ [57]. The main reasons for this are to give a uniform shear rate and therefore simple formulae, to facilitate keeping the sample in the gap (by surface tension) and to give good temperature control.

2.2.4 Rheology of Emulsions

In his reviews, Sherman[32, 56] has stressed the many factors other than phenomenological effects that must be considered when interpreting rheological data for emulsions. He showed that combinations of properties related to each of the three phases (together with any further additives) influence such data. As he gave very full reviews only the factors of direct reference are outlined.

In his studies he found the volume fraction ϕ (the fraction of the emulsion that is dispersed phase) to be of great importance. At high values ($\phi > 0{\cdot}4$ or lower at very small droplet sizes), he found that pseudoplastic behaviour occurred and so therefore used η_∞ or η_{rel}. He has shown the droplet size to have a marked effect on η_∞, the relationship depending on emulsion type, and he emphasised not only the mean volume diameter, but also the dispersity of the size distribution. A combination of ϕ and d_v gives a useful parameter, the mean distance of separation of droplets. For a reasonably homogeneous emulsion, ϕ_{max} is $0{\cdot}74$ and so :

$$\bar{a} = d_v \left[\sqrt[3]{\frac{0{\cdot}74}{\phi}} - 1 \right] \qquad 2\text{-}43$$

This equation holds only if the droplets behave as rigid spheres which Sherman found to be the case for his W/O emulsions. The relative viscosity, η_{rel} is η_∞ divided by the viscosity of the continuous phase, η_c and is more meaningful than η_∞ for comparing W/O emulsions with different oil phases.

2.2.5 Rheology of Crude Oil Emulsions

Very little quantitative work appears to have been carried out on crude oil emulsions. Lawrence and Killner [17] prepared nujol solutions of soft asphalt from a Venezuelan crude and made emulsions at a ϕ of 0·70. They found that the emulsion viscosities increased with asphalt concentration up to about 22 poise (2·2 Pa s) at a 5% asphalt concentration. Lawrence and Killner [17] also proposed an interesting theory arising from a consideration of mechanical properties of the interfacial film. They suggested that in the laminar flow situation arising from rheological measurements, the "elastic bag" nature of the film required water droplets in emulsions of high water concentration to elongate as they passed their neighbours. This stretching would dissipate work normally employed in driving the system in laminar flow. A further dissipation of work would occur when the droplet returned to its spherical form by means of minute local turbulence. This double dissipation would be manifested by a viscosity increase.

Hellman and Bruns [18] published some graphical information. They showed that the viscosity increased with shaking time for the emulsion formation. As the rate of shear increased, so the viscosity decreased for a given time of shaking. They also plotted the fall in viscosity with shearing stress for two emulsions, one at ϕ = 0·68, the other at ϕ = 0·775. At shear stresses of around 100 dyne/cm^2 (10 N m^{-2}) viscosities of 45·0 and 1150 cp (0·045 and 1·15 Pa s respectively) were observed. These had fallen by half on increasing τ to 200 dyne/cm^2 (20 N m^{-2}). The concentrated emulsion also showed a pronounced hysteresis loop, but this was not discussed in any detail. Various mixing ratios of oil and water showed a viscosity peak at 0·3 (O:W). Tap water gave a more viscous emulsion than sea water. Measuring the viscosity at various ageing times after shaking showed a gradual fall; after 80 minutes it had fallen by more than half in all cases. Throughout their studies, they did not relate mean droplet diameter and viscosity.

2.3 Electron Microscopy using the Freeze Etching Technique

2.3.1 General Introduction

For a direct visual examination of an emulsion system, the optical microscope is sufficient down to a droplet size of around 1 µm [58]. Below this, the droplet edges start to blur, due partly to the direct relationship between the limit of resolution of the microscope and the wavelength of the light used and partly to chromatic aberration, which is related to specimen thickness. In special conditions with light at the ultraviolet end of the spectrum, a resolution of 0·2 µm is possible. In an electron microscope, a high energy beam of electrons is produced with wavelengths well below 0·01 nm which would theoretically allow a resolution of at least 0·05 nm [59]. Factors such as spherical aberration (a lens factor) and diffraction introduced by the specimen restrict the resolution. The electron microscope is limited by the need for a high vacuum to increase the mean free path of the electrons from the beam source to the fluorescent screen, so every sample must have a negligible vapour pressure. In the normal transmission electron microscope, the image is formed on this fluorescent screen. This is a result of the difference in intensity throughout the electron beam as the electrons are deflected into different paths by the sample. In organic systems the atoms do not vary sufficiently in size to give widely differing deflections and so any picture would have a very low contrast. This is overcome by incorporating heavy metal atoms in the specimen as a shadowing device.

Various elaborate techniques have been devised to solidify or to replicate liquid systems and some will be briefly outlined. The most serious question with all of them is whether artifacts are introduced in the sample during the preparation. The first work on replicating a frozen liquid sample was by Hall [60] in 1950. He froze water in vacuo, shadowed the surface with chromium and coated the shadow with silica. Steere [61] extended this method in 1957 to include a cutting device and thus started freeze etching. Four years later Moor et al [62] described a highly sophisticated ultramicrotome and put freeze etching on a much firmer basis. The modern method is only a slightly modified version of the original and is described in section 2.3.2 [63]. Since the work of Moor et al, freeze etching has been used mostly in biological studies, and the interpretation of these water based systems is well understood. Another method similar in principle to that of Moor et al is described by Geymeyer [64] who has looked at the surfaces and cross-sections of colloidal systems. Kolpakov et al [65] have developed their own method of preparing a carbon replica for studying microemulsions.

The first work on emulsions using Moor's method was carried out on both W/O and O/W emulsion ointments by Pajor et al [66]. They discussed the structure of the interfacial film when using pairs of surface active agents. Reed [67] in a more general approach has shown that freeze etching can be used for examining cheese (fat globules in water) and ice cream. A series of papers on milk have been published by Buchheim including two on the structure of the shell of the milk fat globule [68, 69]. Here, the author showed the interface standing up between the oil and water phases. Riegelhuth and Watkins [70] used the technique for an oil based system whilst investigating microdispersed particles in a lubricant. Latex paints and certain pharmaceutical preparations have also been studied [71].

2.3.2 The Freeze Etching Technique [62, 63]

The aim of the freeze etching technique is to make a platinum shadowed, carbon replica of a cut and etched frozen sample. It is necessary to emphasise that the electron micrograph obtained is not of a truly three-dimensional object but rather of a bas-relief type surface. The process is started by placing a small amount of sample on to a gold-nickel alloy mount, 3 mm in diameter. This is plunged into a refrigerant (Freon 12) cooled to 118 K and then stored under liquid nitrogen. Freezing is completed within one second in aqueous systems [71]. The use of a refrigerant is necessary, for if the sample were to be frozen directly in liquid nitrogen, the bubbles of gas forming would insulate the sample against further cooling and thus considerably increase the freezing time ("leidenfrost" phenomena).

The freeze etching unit is shown in Fig. 2-11. The bell jar is lowered and evacuated and the sample table cooled to 123 K. The system is now ready for the samples to be loaded, air is let in and four samples mounted. The bell jar is re-evacuated, the ultra-microtome cooled to 77 K and the table heated to 173 K. When the

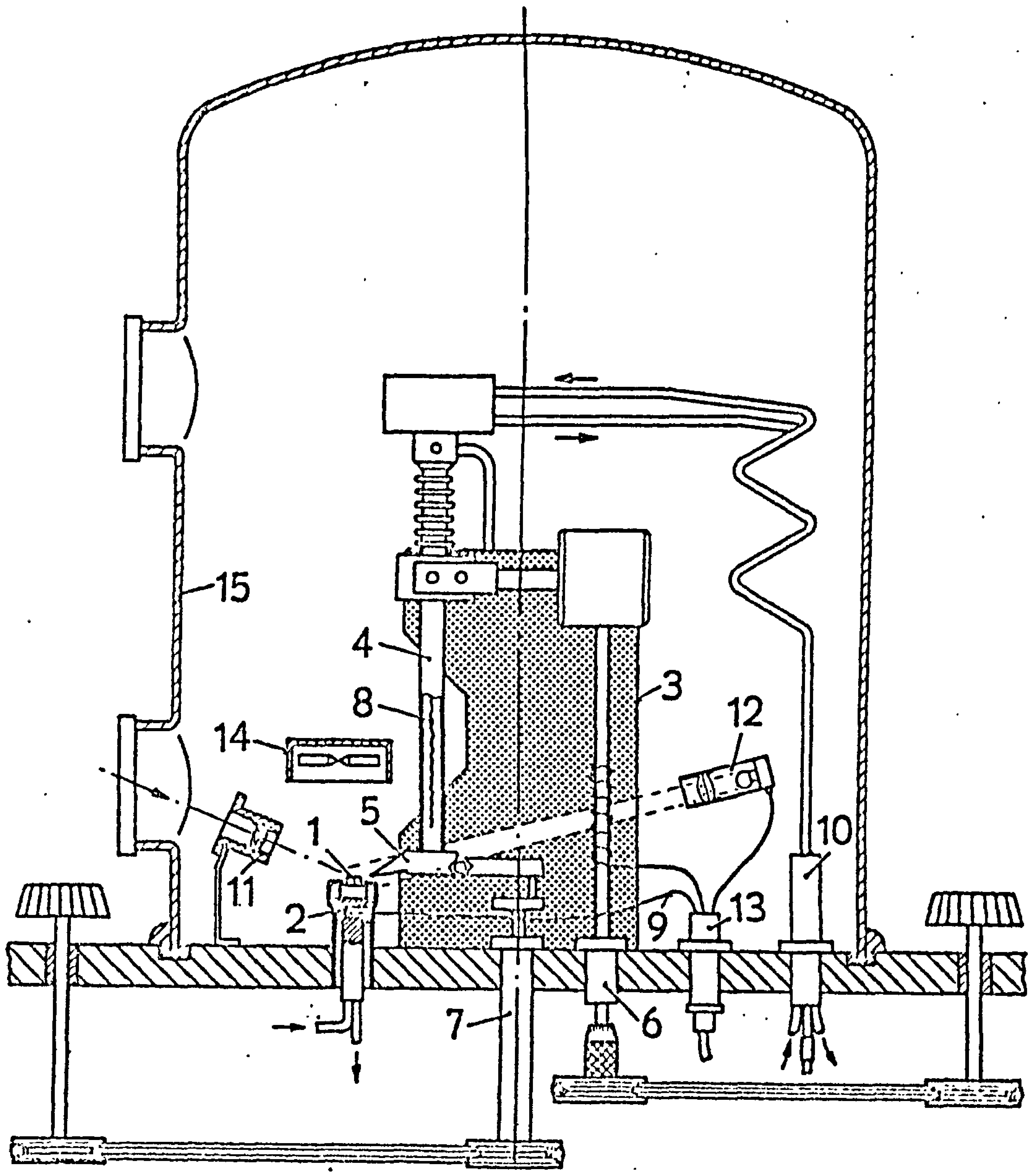

FIG. 2-11

«Freeze-etch» Equipment

according to Mühlethaler and Moor [63]

1 preparation
2 freezing table
3 microtome holder
4 microtome arm
5 knife head
6 microtome setting
7 microtome drive
8 heating device
9 thermo-element
10 coolant feed-through
11 magnifier
12 light
13 measuring current feed-through
14 carbon evaporation device
15 jar bell

pressure is less than 10^{-5} mm. Hg (1·33 mPa) the replicating process is begun. The samples are gradually planed down using the ultramicrotome (a single edged razor blade), the height of which can be finely adjusted. When a good clean face has been achieved, the knife is left directly over the sample for a set time of the order of one minute. This is the etching process, where water and low boiling fractions in the oil sublime from the warmer sample to the cooler knife. The shadow from a platinum/carbon rod is now added by applying a high voltage to a tungsten coil around the rod which is set at the required shadowing angle. Immediately after this, the carbon replica is made by spraying carbon atomically by means of a high voltage arc. The thickness of this carbon film can be controlled by means of a quartz crystal thin film monitor. The process now over, air is let into the system and the samples removed. The replicas are floated free in a suitable solvent system and carefully mounted on "formvar" (polyvinyl formaldehyde) coated grids.

2.3.3 Study of the Oil - Water Interface

Pajor et al [66] found that for their W/O systems the interface revealed from the inside of the droplets was coarser than the interface obtained when the fracture plane followed the outer boundary of the droplet. They attributed this coarseness to a hydrated shell immediately inside the droplet which released the water much slower in the etching process. Buchheim [68, 69] found that the fracture plane followed the course of the interface of a milk fat globule and a double layer membrane was clearly revealed by etching. Fluck et al [73] investigated lipid layers and their technique was sufficiently refined to show the surface patterns on these layers. They found the fracture followed the interface between lipid and water rather than along the centre of the lipid bilayer.

2.3.4 Observation of Sub-micron Droplets

Sherman [32, 34] has emphasised the importance of sub-micron droplets both in their contribution to the total surface area and in their comparatively greater effect on emulsion viscosity. He suggested using weighted mean diameters to compensate for them, but an accurate estimate of their number cannot be made using standard optical microscope techniques. In a review of four counting methods, Groves et al [72] included three that would count sub-micron droplets. The Coulter Counter and the centrifugal photosedimentometer have already been dismissed for this work. The third method was the Craik technique which involves coating emulsion droplets with a heavy metal powder that would render them stable both to removal of the continuous phase and to direct examination in the electron microscope. This is not feasible in this work either.

There is clearly scope for freeze etching as a technique for counting sub-micron droplets. One immediately apparent problem is that droplets would not necessarily be cut through their equator but at some other latitude. However, Herdan [45] has quoted simple expressions to correct the apparent mean diameter of a number of spheres in a thin section provided the position of the spheres is random to the plane of the cut. For example, if the moment of the section diameter is μ'_{x1} and the moment of the true distribution is μ'_{r1}, then :

$$\mu'_{x1} = \frac{\pi}{4} \cdot \mu'_{r1} = 0{\cdot}763\ \mu'_{r1} \qquad 4\text{-}40$$

3. EXPERIMENTAL

3.1 Methods of Emulsion Manufacture

The "Magimix" food liquidiser, manufactured by M.S.E. Ltd., consisted of two parts. The top part was a fluted glass vessel with a four-bladed propeller mounted in the bottom. This rested on top of the second part, a 550 watt motor with a square spindle which fitted into the propeller. Two speeds were possible and were selected by a switch passing from the off position to the middle speed and then the top speed. A constant volume of liquid was always used (250 cm^3).

A stirrer blade was made according to the design published by Berridge et al [7] but scaled down three times. This was fitted into a standard laboratory stirrer with a rheostat speed control. Arrangements were made for water to be added dropwise.

The laboratory shaker used both for making emulsions and for asphaltene separation was the standard type capable of holding four half full 500 cm^3 round bottomed flasks.

Two ultrasonicators were used. The first had a piezoelectric crystal set in the bottom of a water tank so that the ultrasonic vibrations were transmitted through the water to the sample clamped in the tank. The second device was an ultrasonic whistle made by Ultrasonics Ltd., and this worked by feeding the two liquids past a metal reed vibrating at ultrasonic frequencies.

3.2 Microscopy and Photomicroscopy

All optical microscopy was carried out with an American Optical Microstar L10TG-HW trinocular microscope using transmitted light. Illumination was varied stepwise by means of a control box from 1·0 to 7·5 watts. The light reached the object through an adjustable condenser. There were three objective lenses, 10x, 20x and 45x so with an eyepiece of 10x the overall magnifications were 100x, 200x and 450x. The eyepiece was mounted alternately with a 35 mm. Kodak "Colorsnap 35" camera which had a 5x eyepiece.

The emulsion specimen was normally diluted but to avoid introducing sampling artifacts a fairly large sample (2 - 3 cm^3) was taken and added to the continuous phase. Only gentle stirring was applied to disperse it. The diluted emulsion was added dropwise by means of a fine glass rod to a haemocytometer cell with a depth of 20 μm. A cover slip was applied both to prevent evaporation of the oil phase and also to provide a thin enough sample to avoid the problem of opacity.

Black and white photographs were taken using Ilford 1P4 film. From droplet size analysis considerations, it was necessary to give the emulsion droplets sufficient time to sink to the bottom of the haemocytometer cell in order to obtain the maximum number of droplets in focus. This could be as long as ten minutes if Tia Juana crude oil was being used. Exposure time for Kuwait and Brega crude oils was generally 0·5 second at 7·5 and 5·5 watts illumination respectively. Tia Juana crude oil generally required a one second exposure at 7·5 watts. These exposure times refer to maximum magnification; for lower magnifications, lower illuminations were normally employed. Several photographs were taken of the same sample to ensure that a statistically significant number of countable droplets was obtained. Although the general areas to be photographed were chosen by moving the sample on the microscope stage to a set pattern, the specific field of view was not adjusted to "get a good photograph"; so in this sense, a random sample was taken. If the stage had been moved totally at random, there was a chance that the same area would have been photographed and perhaps counted twice. At the end of each film, a photograph was taken of a graticule marked with eleven lines, 100 μm apart. The space between one pair of these was divided equally into lines 10 μm apart. The films were developed using ID 11 developer and ID 25 fixer. Prints were made either to A4 size or the size at which the largest droplet could be counted on the sizing machine, whichever was the smaller.

3.3 Droplet Size Analysis

The apparatus used was the Carl Zeiss "Particle Size Analyser TGZ 3". The mode of operation is described in section 2.1.2. The general principles can be seen in Fig. 3-1. There were two size ranges with forty eight counters each, the reduced range was one third the size of the standard range. The diameter in millimetres of each counter for the standard range is tabulated in Appendix 2. The absolute value of the droplet size was obtained by direct comparison between the graticule photograph and the light beam of the apparatus. A sample calculation is also given in Appendix 2. All mean diameters in Chapter 4 are in microns.

Computing was carried out using Algol 60 language on an ICL 1906A computer using punched cards. A copy of each program is given in Appendix 3.

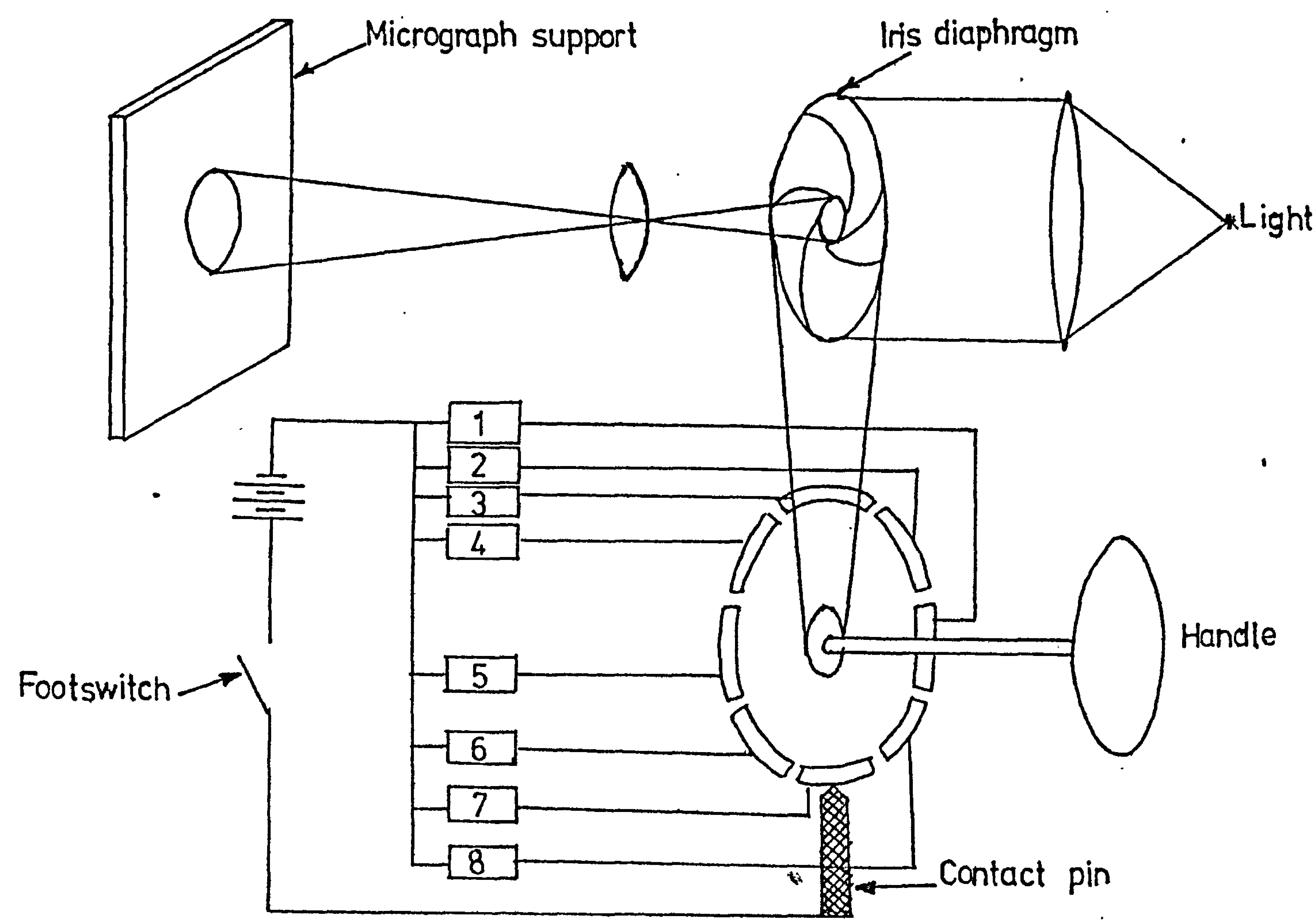

Micrograph support
Iris diaphragm
Light
1
2
3
4
5
6
7
8
Handle
Footswitch
Contact pin

FIG. 3-1

3.4 Emulsion Systems

The three naturally occurring crude oils used were Kuwait, Tia Juana (from Venezuela) and Brega (from Libya). They were stored in closed forty gallon drums and tapped off by the half gallon when required. Loss of low boiling fractions was avoided constantly by topping up the laboratory supply.

The asphaltenes used in the model crude oil systems were obtained from the heavy residue of Kuwait crude oil. The asphaltenes were prepared by shaking 12·5 cm^3 of the residue with 250 cm^3 of n-pentane overnight on a standard laboratory shaker. The precipitate was collected on a grade 4 sintered glass crucible with the aid of a water pump, washed in fresh pentane, left to dry and stored in a vacuum dessicator.

The model oil phase was a mixture of an aliphatic and an aromatic hydrocarbon and the standard laboratory reagents used are shown in Table 3-1.

Aromatic	Aliphatic
benzene	n-heptane
toluene	n-octane
m-xylene	
o-xylene	
p-xylene	
ethyl benzene	
tetralin	
α-methyl naphthalene	

Table 3-1

Two aqueous phases were used. As the "mousses" were formed at sea, the majority of emulsions were made using a simplified simulated sea water of 0·5m sodium chloride and 0·05m magnesium sulphate in tap water. The remaining emulsions were made with deionised water.

3.5 Detergents

Most oil slick dispersants are based on non-ionic detergents, and at the time of the "Torrey Canyon" these were toxic to marine life [4, 74]. This was due to the high aromatic content of the detergent solvent. Present dispersants have toxicities some three orders of magnitude lower [74]. One of these is BP 1100X and the detergent that comprises the active ingredient was used. Standard solutions were made in the three crude oils on a weight per litre basis.

Two ionic detergents of opposite charge were also used. These were the anionic detergent sodium dodecyl sulphate ($C_{12}H_{25}SO_4^- Na^+$) and the cationic detergent cetyl pyridinium bromide ($C_{16}H_{33}C_5H_5N^+ Br^-$). These were both used in solution in the water phase.

3.6 Nmr Studies

The spectrometer used for ^1H nmr was a 60 MHz Perkin-Elmer R10 model. A tetramethyl silane reference peak was used for all experiments. ^{13}C spectra were obtained using a Jeol Fourier Transform spectrometer.

3.7 Rheological Studies

The viscometer used was a Rheotest II, imported from East Germany by F. Copley and Sons of Nottingham, and this is shown in Plate 1. The drive was supplied by a 12-step synchronous motor with

Plate 1 Rheotest 2 Viscometer with cylinder S1 in position. The instrument is set at gear 2b on spring I.

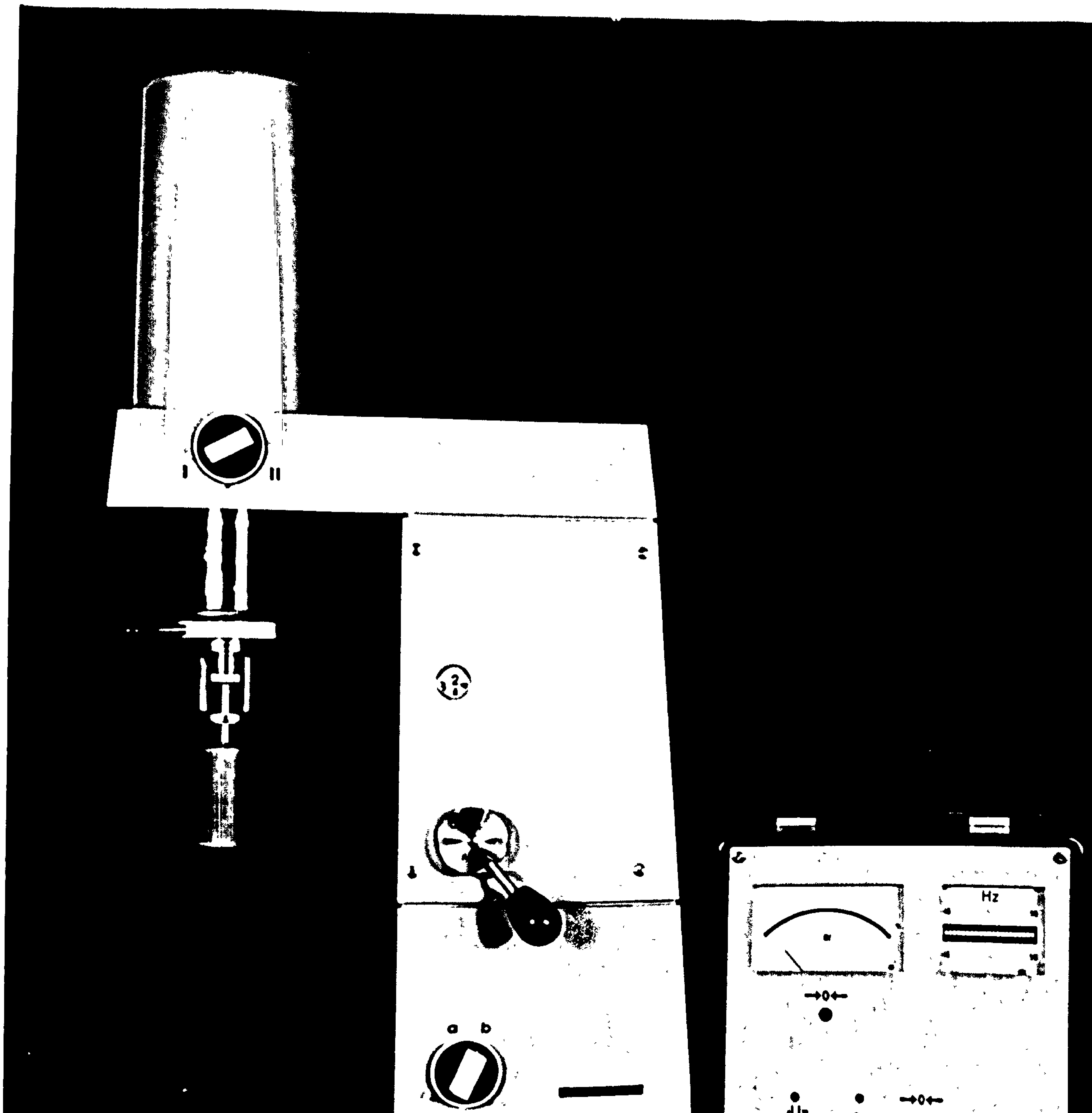

I
II
a b
Hz

a reduction gear of 1/2 giving a total of twenty four possible speeds. The inner cylinder was rotated and the outer cylinder thermostatted to $\pm$ 0·1 K. The shear stress was measured by means of a spring and transducer, the torque being indicated on an arbitrary scale of 0 - 100 (α). Two springs, I and II were incorporated and the switch from one to the other could be carried out while the machine was running. II was approximately ten times stronger than I.

Three inner cylinders were used, and the manufacturers provided a table of shear rates for each of the gear speeds and the corresponding cylinder pair. The outer cylinder diameter was 4·00 cm, and the diameters of the three inner cylinders are shown in Table 3-2.

Cylinder	Diameter (cm)
S 1	3·92
S 2	3·76
S 3	3·24

Table 3-2

3.8 Freeze Etching and Electron Microscopy

This was carried out in the Cell Biology Unit of the School of Biological Sciences at this university.

Balzers A.G. of Balzers, Liechtenstein manufactured the freeze etching unit, model BA 360M and the collared gold specimen holders, Cat. No. 11-3654. Arcton 22 (a di-chloro-monofluoroethane) was used as the coolant for specimen freezing and was made by I.C.I. Mond Division, Runcorn. Johnson Matthey Chemicals Limited supplied the platinum used for shadowing. This was a 1·5 mm bar insert in a 2 mm diameter graphite bar from an electron beam source. The same company supplied the carbon for making the replicas, 6·5 mm diameter graphite rods, Cat. No. J.M.B.2206.

The completed replicas were floated free and washed in tetrahydrofuran (normal reagent grade) and rinsed in distilled water. They were then mounted on standard electron microscope grids coated with formvar (polyvinyl formaldehyde). An A.E.I. EM6B electron microscope was used and photographs of specimens were taken on glass plates for the earlier work and film for the later exposures.

4. RESULTS

4.1 Introduction

As each emulsion was made, it was numbered in strict chronological order. Groups of emulsions have been classified by letters according to the oil phase, the phenomenon being investigated and in some cases by the detergent added. As different phenomena may have been investigated at around the same time, the emulsion numbers in a given group are not necessarily sequential. Numbers missing between 1 and 156 indicate, for example, emulsions made for samples, for trials to locate the level of experimentation or simply faults in techniques corrected in a later series. The letters designated are shown in Table 4-1.

When quoted in isolation in the text, the emulsion is given its full description, e.g. KR:92 is emulsion 92 which was made in a series of rheology experiments using Kuwait crude oil. If an emulsion was sampled, photographed and sized at different times whilst being stirred and/or aged, a further number has been added in the form of a decimal, e.g. KR:92·4. This can be understood from the tables in this chapter. To avoid confusion with laboratory made emulsions, the Admiralty samples have been numbered from 200 in order of receipt. In some cases one emulsion has been used in two investigations. In this situation the second letter is used according to the phenomena under discussion.

Letter	Meaning
First	
A	Admiralty emulsion
K	Laboratory made Kuwait crude oil emulsion
T	Laboratory made Tia Juana crude oil emulsion
B	Laboratory made Brega crude oil emulsion
M	Laboratory made model crude oil emulsion
O	Comparative series using Kuwait, Brega, and Tia Juana crude oils
Second	
M	Method of manufacture
V	Variation of ϕ (volume concentration)
S	Effect of salt
P	Variation of aromatic to aliphatic proportions
A	Variation of asphaltene concentration
R	Rheological investigations
O	Rate of formation/ageing studies
F	Freeze-etching experiments
D	Determination of detergent level
Third	
A	Anionic detergent
C	Cationic detergent
N	Non-ionic detergent
R	Rheological investigation (when V or A is the second letter)

Table 4-1

4.2 Preliminary Experiments with Kuwait Crude Oil

4.2.1 Admiralty Emulsions

The Admiralty Oil Laboratory maintained a barge in Langstone Harbour, Portsmouth containing Kuwait crude oil and water which were emulsified under wave action. Samples from these trials, together with a Kuwait crude oil-slick emulsion were received at various times during this study and are listed in Table 4-2.

Group A Emulsion	Admiralty Code	Date of Receipt	ϕ	Type
201	AOL 1469/69	-	0·60	Barge
202	-	12/3/71	0·60	Barge
203	-	7/1/72	?	Barge
204	AOL 1922/1/72	31/8/72	0·275	Barge
205	AOL 1054/70	-	0·61	Oil-slick
206	AOL 1922/2/72	-	0·60	Barge

Table 4-2

As ϕ for emulsions A:201 and A:202 was about 0·60, the initial laboratory experiments were carried out at this water concentration.

4.2.2 Laboratory Methods of Manufacture

Five different methods were tried for establishing a reasonable technique for making laboratory emulsions. Table 4-3 lists the different emulsions made and the methods used. In all cases the water-phase was simulated sea water.

Group KM Emulsion	Method	ϕ	Total Time
1	"Magimix"	0·60	80 secs.
2	Shaker	0·60	$1\frac{3}{4}$ hours
3	Ultrasonic Tank	0	$2\frac{3}{4}$ hours
5	Stirrer	0·60	28 mins.
10	"Magimix"	0·74	6 mins.
13	"Magimix"	0·75	60 secs.
14	"Magimix"	0·60	70 secs.
15	"Magimix"	0·60	70 secs.
16	Ultrasonic "Whistle"	0·60	-
21	Stirrer	0·79	55 mins.

Table 4-3

Emulsion KM:1 was effectively emulsified within 20 seconds as no water separation was evident after this time. On further stirring it rapidly developed a cocoa-colour, much lighter, in fact, than A:201 with which it was being compared.

Emulsions KM:10 and KM:13 were attempts to make emulsions with ϕ at 0·85 and 0·75 respectively in the "Magimix". The usual charge of 250 cm^3 was used and for KM:10, 37·5 cm^3 of this was Kuwait crude oil. Stirring was continued in bursts of 30 seconds, with an over-night break after three minutes, until the water separation was constant. By this time the emulsion was highly viscous. The separated water was measured by volume and the fractional water content in the emulsion was found to be 0·74. Emulsion KM:13 was made with 62·5 cm^3 of Kuwait crude oil. All the water was emulsified within one minute.

The laboratory shaker emulsified all the water in the flask in KM:2 (at $\phi = 0{\cdot}60$) after 1¾ hours. However, it was very dark in colour and on standing overnight it separated into three distinct phases. The bottom phase was a very stiff, cocoa-coloured W/O emulsion, the middle phase was a dark "runny" W/O emulsion, and the top phase appeared to be only crude oil.

A flask containing oil and water was left in an ultrasonic tank for 2¾ hours but gave no apparent emulsification (KM:3).

The stirrer method after Berridge et al [7] was used to make an emulsion at $\phi = 0{\cdot}60$ (KM:5). The water was added dropwise in four equal batches. Even after 18 minutes of stirring at full speed, overnight standing revealed considerable creaming. A further 10 minutes stirring did not appear to change the overall effect. An additional problem was that as the emulsion became more viscous, the stirrer laboured and the rate of stirring became less consistent. For emulsion KM:21, the water was added again in four batches but a regime was adopted of 5 minutes for adding the batch, 5 minutes stirring and 5 minutes rest. After 55 minutes, some separation had occurred, leaving an emulsion at $\phi = 0{\cdot}796$.

Emulsion KM:16 was made with the ultrasonic whistle device and was of the same cocoa-coloured appearance as emulsion made with the "Magimix".

Four of the five methods tested yielded concentrated emulsions. The ultrasonic whistle was lacking in versatility, as the frequency could not be changed thus restricting the droplet size to the same narrow range each time. Both stirrer and shaker gave reasonable emulsions which, if the process had been continued longer, might have been similar to the natural emulsion A:201. However, for the number and variety of experiments to be carried out, such emulsification times were not practical.

The "Magimix" had several advantages. Emulsification was rapid. A cocoa-coloured, rigid "mousse" could be made in one minute. The droplet size of a given emulsion scheme could be varied by taking readings at times within one minute. The power input was such that there was little apparent difference in stirring speed after the emulsion had thickened. The fast speed control was constant from one experiment to the next whilst both the stirrer and the shaker had to be varied for optimum stability. One further test for the reproducibility of the "Magimix" was the manufacture of emulsions KM:14 and KM:15 under identical conditions.

4.2.3 Photography and Counting

The counting method was limited by the sharpness of resolution of the individual emulsion droplets. At the microscope magnifications used (450 X), thick black rings were always present around the droplets and these are clearly seen in the plates of emulsions KM:1 and A:202, (2 and 3). The rule used in this work was always to size around the outside of the ring.

The raw data from all the counting is given in Appendix 4. As soon as it was obtained, the data was processed by a computer program (PST48 in Appendix 3) to obtain the basic information necessary to draw out a histogram. The print-out gave the number of drops as counted, as a percentage and as a cumulative percentage. The interval centre of the scale reading of the counter was converted into microns by means of a factor, Q, obtained from the

Plate 2 Emulsion KM:1 (X850)

Plate 3 Emulsion A:202 (X850)

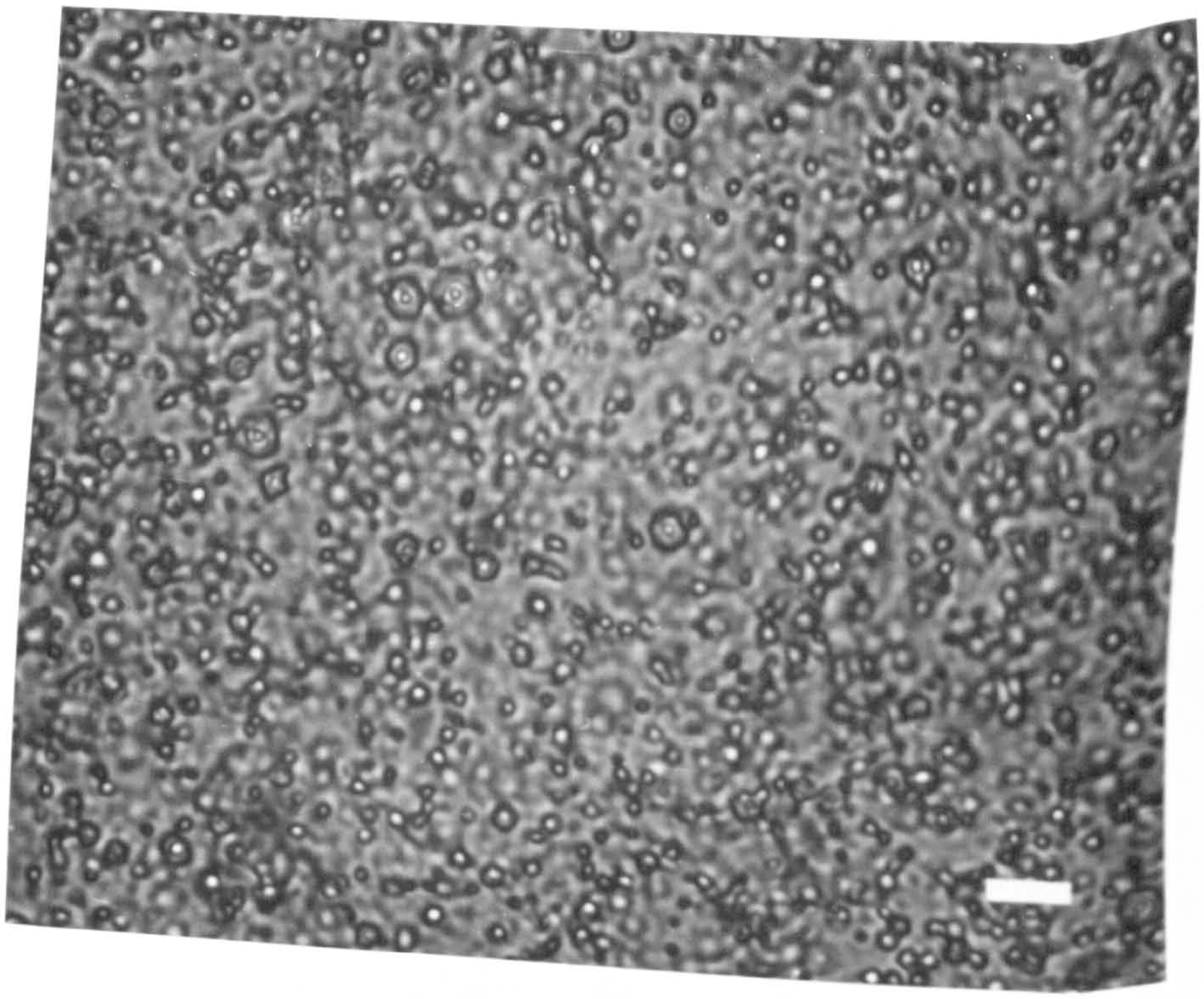

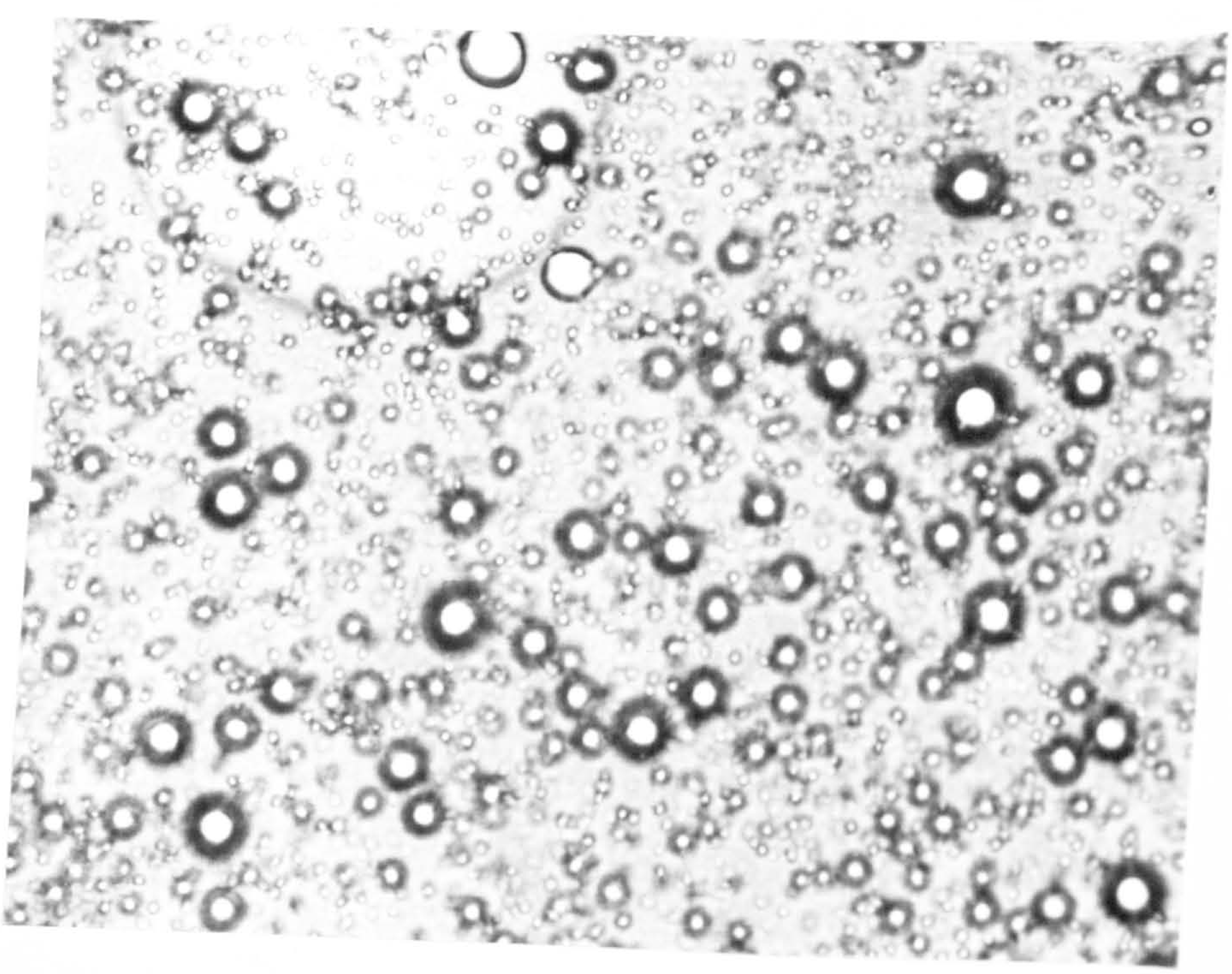

Plate 2 Emulsion KM:1 (X850)

Plate 3 Emulsion A:202 (X850)

matching of the graticule with the light beam. This was also expressed in natural logarithms. A further column gave the normalised values of the droplet number such that the area under the frequency histogram would be unity, thus allowing direct comparison with relevant distribution equations. This was calculated by dividing the number percentage in a class by one hundred times the class width.

The remainder of this section and the next three sections will be exemplified by reference to the results obtained from Plates 2 and 3 for emulsions KM:1 and A:202. The data from program PST48 for these two is shown in Tables 4-4 and 4-5. The scale reading column showed the class interval centre in millimetres and this together with the print-out of the original data were presented as a check that the system was working correctly. Histograms drawn from this data are shown in Figures 4-1 and 4-2. Each distribution is clearly skewed.

4.2.4 Application of A.D.E.

Figure 4-3 shows the droplet size data for emulsion KM:1 as applied to the Schwarz and Bezemer treatment [44] in the linear form represented by equation 2-18. There is clearly a marked discontinuity in the graph which occurs at a diameter of about 2·1 μm. It is interesting to note that Sherman found, that for unpublished data of his own, this particular equation does not hold at droplet sizes less than 2 μm. The reason for this breakdown is not obvious, but as there are a number of emulsions reported in this thesis with the majority of droplets with diameters less than 2 μm, this approach to droplet size analysis is clearly unsuitable.

TABLE OF VALUES FOR EMULSION 1.0 FROM DATA IN FILM 1 1 NO TOTAL = 1061 Q = 4.492

CLASS NO.	NO OF DROPS	DROP P/C	CUM NO P/C	NORMALISED	X(MICRONS)	LOGE X	S READING
1	0	0.0000	0.0000	0.0000	0.393	-0.9336	1.49
2	0	0.0000	0.0000	0.0000	0.516	-0.6625	2.04
3	0	0.0000	0.0000	0.0000	0.638	-0.4494	2.59
4	0	0.0000	0.0000	0.0000	0.760	-0.2738	3.14
5	0	0.0000	0.0000	0.0000	0.865	-0.1220	3.70
6	0	0.0000	0.0000	0.0000	1.008	0.0075	4.25
7	1	0.0943	0.0943	0.0077	1.130	0.1222	4.80
8	2	0.1885	0.2828	0.0153	1.252	0.2251	5.35
9	9	0.8483	1.1310	0.0690	1.375	0.3184	5.90
10	19	1.7908	2.9218	0.1457	1.500	0.4057	6.46
11	33	3.1103	6.0320	0.2531	1.622	0.4847	7.01
12	82	7.7286	13.7606	0.6290	1.744	0.5564	7.56
13	190	17.9076	31.6682	1.4575	1.867	0.6243	8.11
14	228	21.4892	53.1574	1.7490	1.989	0.6878	8.66
15	167	15.7399	68.8973	1.2811	2.114	0.7486	9.22
16	117	11.0273	79.9246	0.8975	2.236	0.8049	9.77
17	81	7.6343	87.5589	0.6214	2.359	0.8582	10.32
18	39	3.6758	91.2347	0.2992	2.481	0.9038	10.87
19	26	2.4505	93.6852	0.1994	2.604	0.9569	11.42
20	12	1.1310	94.8162	0.0921	2.728	1.0037	11.98
21	11	1.0368	95.8530	0.0844	2.851	1.0426	12.53
22	3	0.2828	96.1357	0.0230	2.973	1.0897	13.08
23	8	0.7540	96.8897	0.0614	3.096	1.1300	13.63
24	2	0.1885	97.0782	0.0153	3.218	1.1668	14.18
25	6	0.5655	97.6437	0.0460	3.343	1.2068	14.74
26	5	0.4713	98.1150	0.0384	3.465	1.2428	15.29
27	3	0.2828	98.3977	0.0230	3.588	1.2775	15.84
28	5	0.4713	98.8690	0.0384	3.710	1.3111	16.39
29	4	0.3770	99.2460	0.0307	3.833	1.3435	16.94
30	2	0.1885	99.4345	0.0153	3.957	1.3755	17.50
31	2	0.1885	99.6230	0.0153	4.080	1.4060	18.05
32	1	0.0943	99.7172	0.0077	4.202	1.4356	18.60
33	0	0.0000	99.7172	0.0000	4.325	1.4643	19.15
34	1	0.0943	99.8115	0.0077	4.447	1.4922	19.70
35	0	0.0000	99.8115	0.0000	4.572	1.5199	20.26
36	0	0.0000	99.8115	0.0000	4.694	1.5463	20.81
37	0	0.0000	99.8115	0.0000	4.817	1.5721	21.36
38	0	0.0000	99.8115	0.0000	4.939	1.5972	21.91
39	0	0.0000	99.8115	0.0000	5.061	1.6216	22.46
40	1	0.0943	99.9057	0.0077	5.186	1.6460	23.02
41	1	0.0943	100.0000	0.0077	5.309	1.6693	23.57
42	0	0.0000	100.0000	0.0000	5.431	1.6921	24.12
43	0	0.0000	100.0000	0.0000	5.553	1.7144	24.67
44	0	0.0000	100.0000	0.0000	5.676	1.7342	25.22
45	0	0.0000	100.0000	0.0000	5.801	1.7579	25.78
46	0	0.0000	100.0000	0.0000	5.923	1.7788	26.33
47	0	0.0000	100.0000	0.0000	6.045	1.7993	26.88
48	0	0.0000	100.0000	0.0000	6.168	1.8193	27.43

Table 4-4

TABLE OF VALUES FOR EMULSION 202.0 FROM DATA IN FILM 3 7 NO TOTAL = 1429 Q = 4.824

CLASS NO.	NO OF DROPS	DROPS P/C	CUM NO P/C	NORMALISED	X(MICRONS)	LOGE X	S READING
1	0	0.0000	0.0000	0.0000	0.366	-1.0048	1.49
2	0	0.0000	0.0000	0.0000	0.480	-0.7339	2.04
3	5	0.3499	0.3499	0.0306	0.594	-0.5207	2.59
4	10	0.6998	1.0497	0.0612	0.708	-0.3451	3.14
5	50	3.4990	4.5486	0.3058	0.824	-0.1933	3.70
6	146	10.2169	14.7656	0.8930	0.938	-0.0638	4.25
7	238	16.6550	31.4206	1.4557	1.052	0.0507	4.80
8	185	12.9461	44.3967	1.1316	1.166	0.1538	5.35
9	238	16.6550	61.0217	1.4557	1.280	0.2471	5.90
10	172	12.0364	73.0581	1.0520	1.396	0.3339	6.46
11	97	6.7880	79.8460	0.5933	1.510	0.4123	7.01
12	37	2.5892	82.4353	0.2263	1.624	0.4851	7.56
13	43	3.0091	85.4444	0.2630	1.738	0.5530	8.11
14	40	2.7992	88.2435	0.2447	1.852	0.6165	8.66
15	31	2.1693	90.4129	0.1896	1.968	0.6773	9.22
16	13	0.9097	91.3226	0.0795	2.082	0.7336	9.77
17	17	1.1896	92.5122	0.1040	2.197	0.7869	10.32
18	18	1.2596	93.7719	0.1101	2.311	0.8375	10.87
19	12	0.8397	94.6116	0.0734	2.425	0.8856	11.42
20	4	0.2799	94.8915	0.0245	2.541	0.9324	11.98
21	3	0.2099	95.1015	0.0183	2.655	0.9763	12.53
22	7	0.4899	95.5913	0.0428	2.769	1.0184	13.08
23	7	0.4899	96.0812	0.0428	2.883	1.0587	13.63
24	4	0.2799	96.3611	0.0245	2.997	1.0975	14.18
25	3	0.2099	96.5710	0.0183	3.113	1.1355	14.74
26	10	0.6998	97.2708	0.0612	3.227	1.1715	15.29
27	5	0.3499	97.6207	0.0306	3.341	1.2062	15.84
28	4	0.2799	97.9006	0.0245	3.455	1.2398	16.39
29	2	0.1400	98.0406	0.0122	3.569	1.2722	16.94
30	4	0.2799	98.3205	0.0245	3.685	1.3042	17.50
31	3	0.2099	98.5304	0.0183	3.799	1.3347	18.05
32	3	0.2099	98.7404	0.0183	3.913	1.3643	18.60
33	4	0.2799	99.0203	0.0245	4.027	1.3930	19.15
34	3	0.2099	99.2302	0.0183	4.141	1.4209	19.70
35	0	0.0000	99.2302	0.0000	4.257	1.4486	20.26
36	0	0.0000	99.2302	0.0000	4.371	1.4750	20.81
37	1	0.0700	99.3002	0.0061	4.485	1.5008	21.36
38	2	0.1400	99.4402	0.0122	4.599	1.5259	21.91
39	0	0.0000	99.4402	0.0000	4.713	1.5503	22.46
40	1	0.0700	99.5101	0.0061	4.829	1.5747	23.02
41	2	0.1400	99.6501	0.0122	4.943	1.5980	23.57
42	1	0.0700	99.7201	0.0061	5.057	1.6208	24.12
43	0	0.0000	99.7201	0.0000	5.171	1.6431	24.67
44	1	0.0700	99.7901	0.0061	5.285	1.6649	25.22
45	1	0.0700	99.8600	0.0061	5.401	1.6866	25.78
46	0	0.0000	99.8600	0.0000	5.515	1.7075	26.33
47	0	0.0000	99.8600	0.0000	5.629	1.7280	26.88
48	2	0.1400	100.0000	0.0122	5.743	1.7480	27.43

Table 4-5

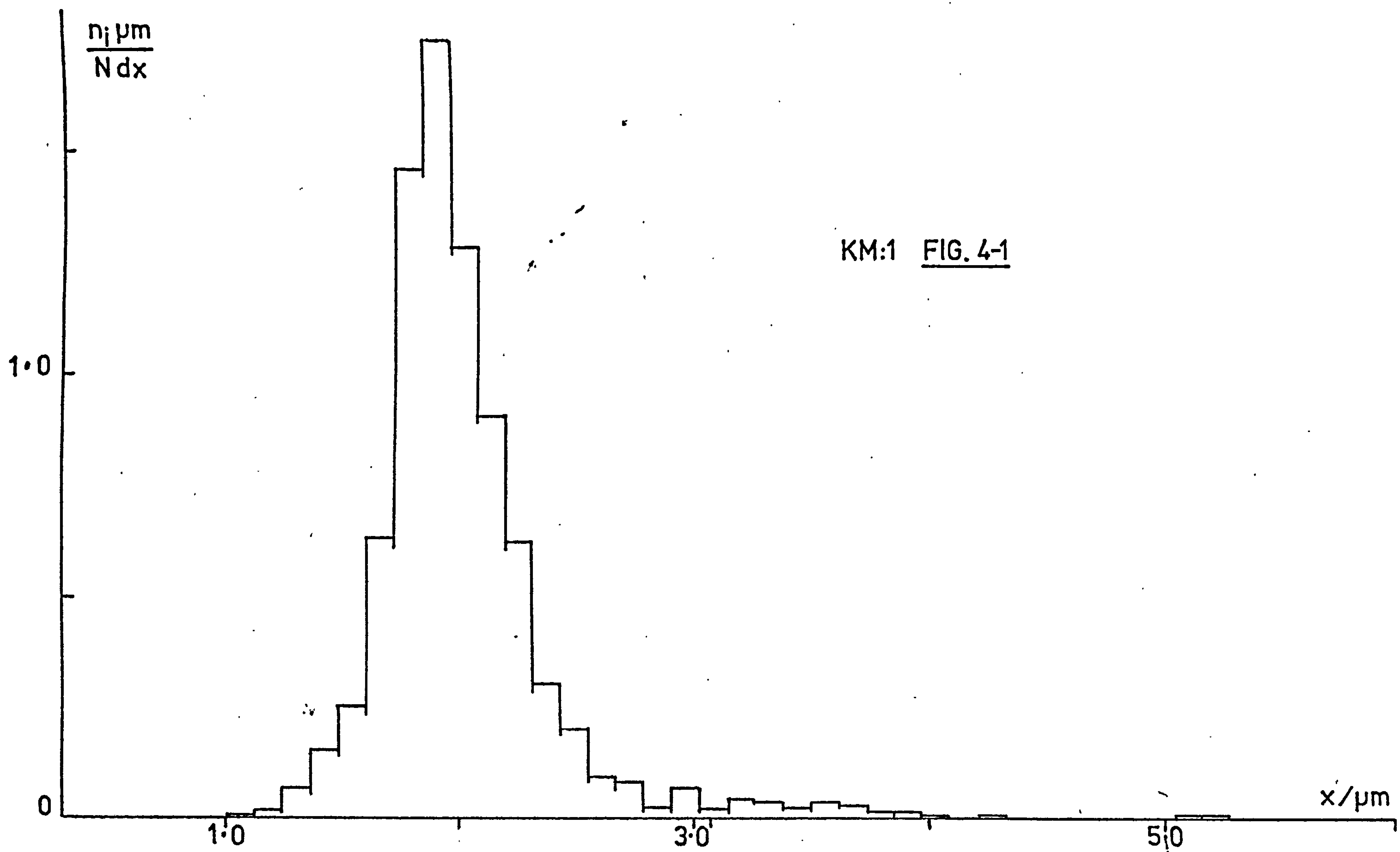

KM:1 FIG. 4-1

A:202 FIG. 4-2

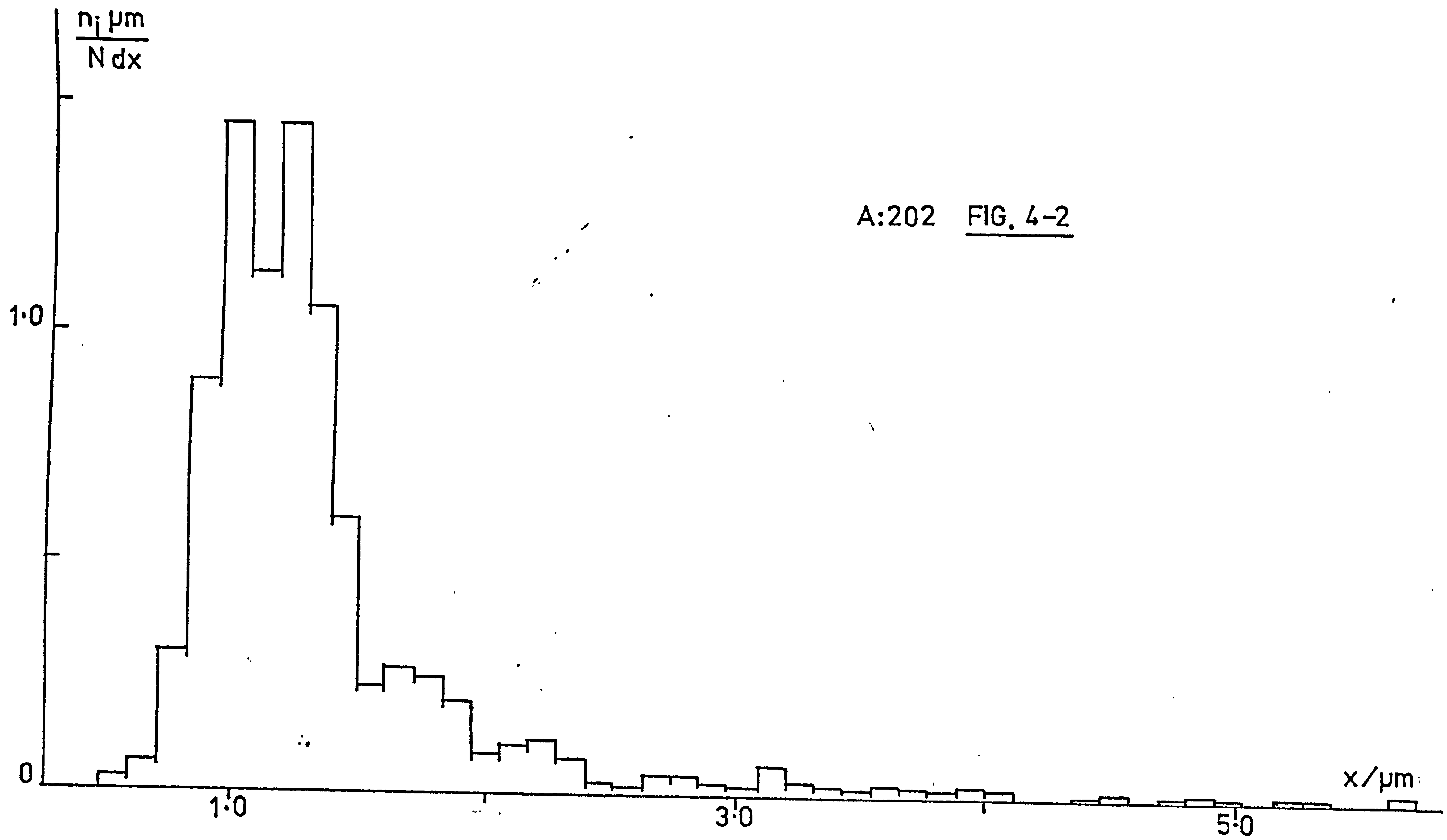

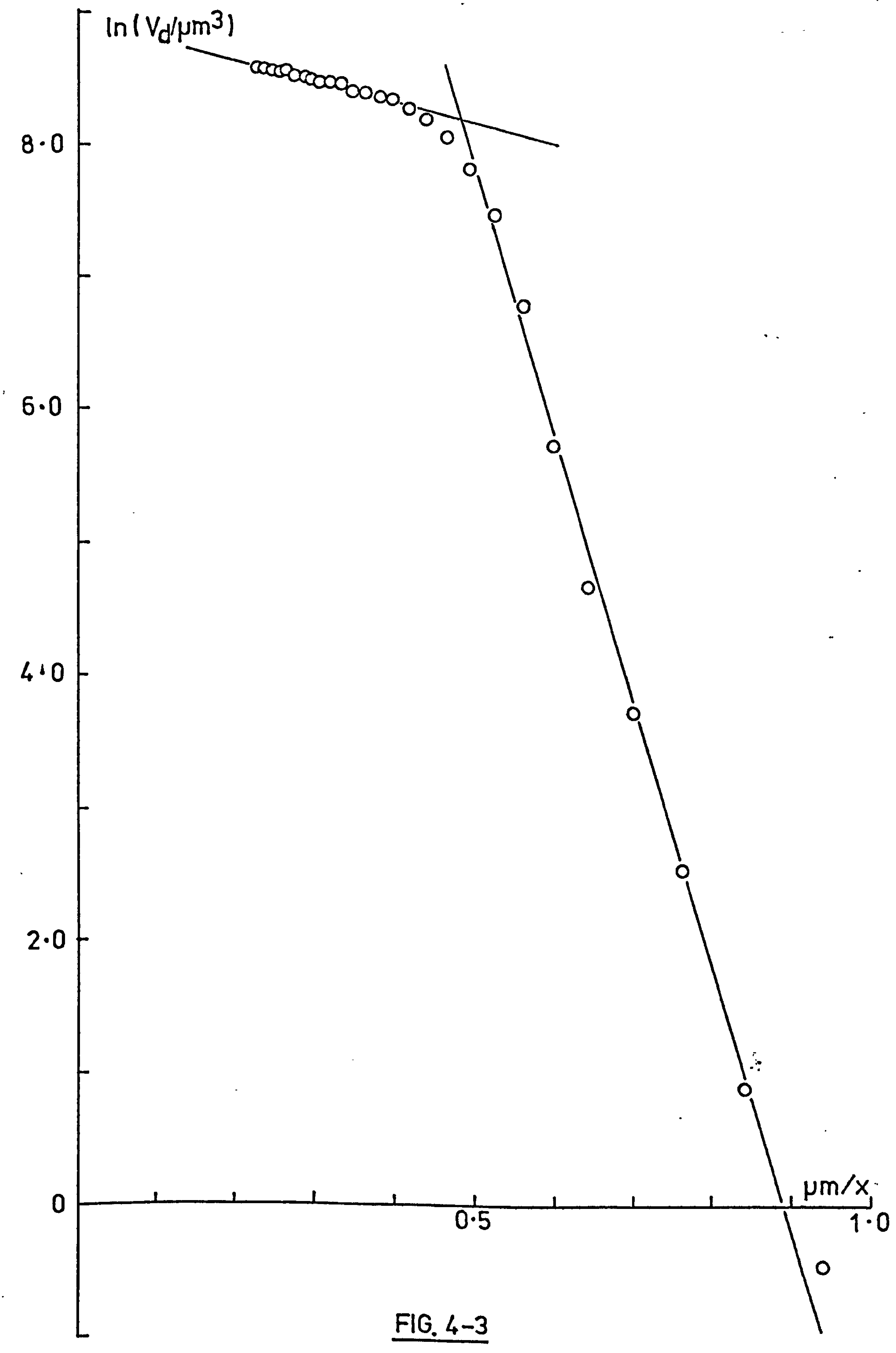

FIG. 4-3

4.2.5 Logarithmic-Normal Equations

Data for emulsion KM:1 was used in Figure 2-3 to illustrate the theory behind this equation. The corresponding graph for emulsion A:202 is shown in Figure 4-4. There is apparently a large deviation for the tail of the graph in each case even with the 1% error lines, however the 5% error lines show the true significance of the discrepancy. The justification of using the method of least squares has been discussed in section 2.1.7. For emulsions KM:1 and A:202 and subsequent emulsions, "by eye" values of M and σ_g have been found to be very close to the computerised least squares results.

The computer procedure was as follows :- The results falling between 10% and 90% in the cumulative percentage column from program PST48 were selected, and those values less than 50% were subtracted from 50·0. All these values were looked up in probability tables, the subtracted values counting as negative. This data was fed into program LT (Appendix 3). Tables 4-6 and 4-7 show the output for KM:1 and A:202 respectively. As with PST48 the input data was printed, the LOGE X values correspond to the upper interval limits of the classes. The gradient and intercept (b' and a' in equations 2-33 and 2-34) are given but are not relevant. M and the variance ($\ln \sigma_g$) are shown next with σ_g on the next line. In order to draw a straight line on the graph, five values of Z with the corresponding values of ln x were printed as calculated from the M and ln σ_g values. These last two values were used to calculate x_v and x_{sv} which comprise the remainder of output.

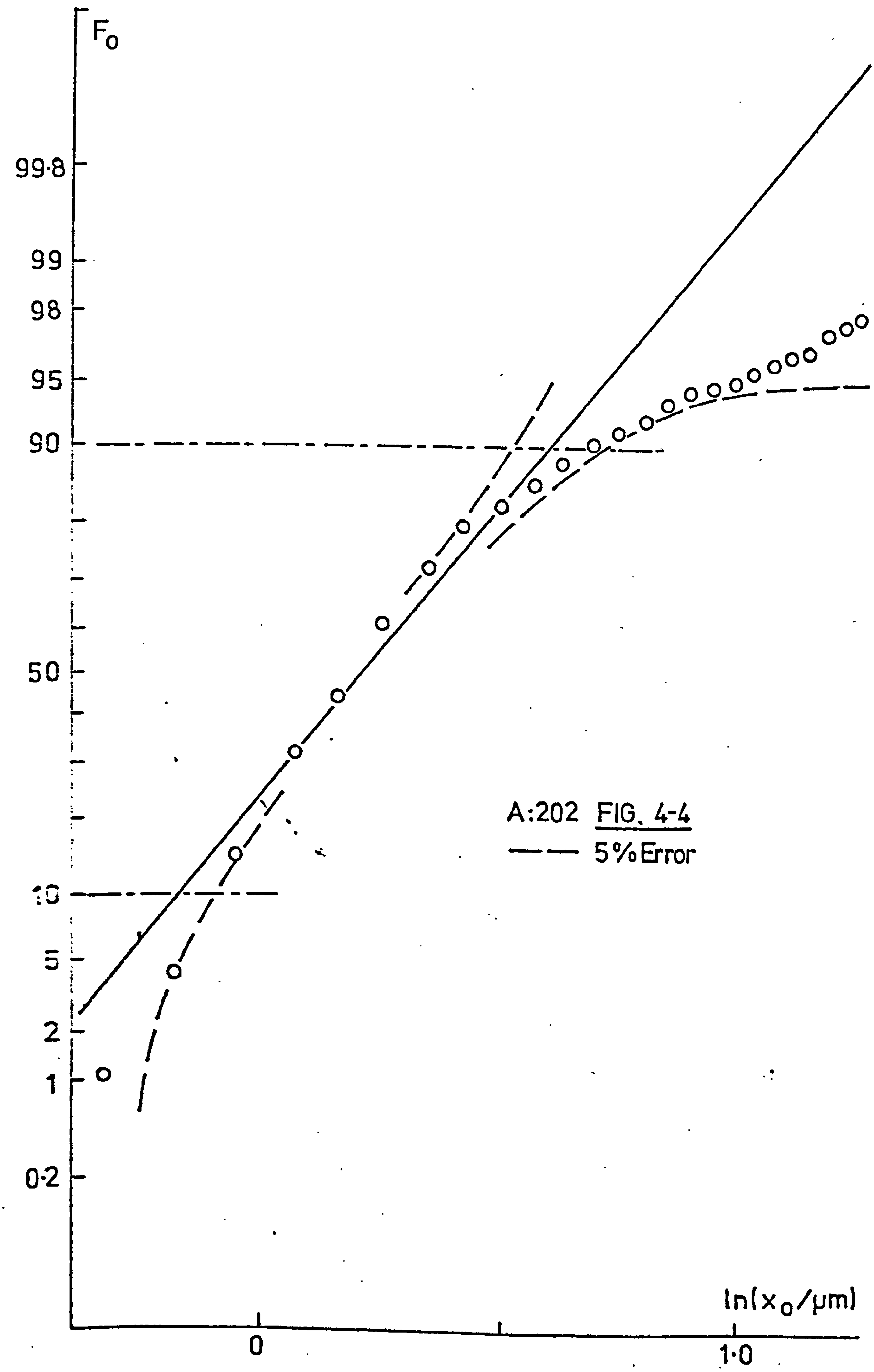

F0
99·8
99
98
95
90
50
10
5
2
1
0·2
A:202 FIG. 4-4
5% Error
ln(xo/μm)
0
1·0

FOR EMULSION 1.0 FILM NO. 1 1

LOGE X	Z
0.5569	-1.0910
0.6247	-0.4770
0.6882	0.0790
0.7479	0.4930
0.8043	0.8390
0.8586	1.1530

GRADIENT = 7.427 INTERCEPT = -5.133

XI = 1.996 VARIANCE = 0.135

GEOMETRIC STANDARD DAVIATION = 1.144

Z	LOGE X
-2	0.422
-1	0.556
0	0.691
1	0.826
2	0.960

Table 4-6

MEAN VOLUME DIAMETER = 2.051

MEAN SURFACE/UNIT-VOLUME DIAMETER = 2.088

FOR EMULSION 202.0 FILM NO. 3 7

LOGE X	Z
-0.0651	-1.0490
0.0517	-0.4840
0.1545	-0.1420
0.2477	0.2600
0.3330	0.6190
0.4115	0.8360
0.4850	0.9320
0.5534	1.0520
0.6169	1.1670

GRADIENT = 3.262 INTERCEPT = -0.653

XI = 1.221 VARIANCE = 0.306

GEOMETRIC STANDARD DAVIATION = 1.358

Z	LOGE X
-2	-0.413
-1	-0.106
0	0.200
1	0.506
2	0.812

Table 4-7

MEAN VOLUME DIAMETER = 1.406

MEAN SURFACE/UNIT-VOLUME DIAMETER = 1.544

4.2.6 Analysis of Various Means

Program VMNS (Appendix 3) was written to take the same data as PST48 in order to calculate the mean diameters given in section 2.1.5. Tables 4-8 and 4-9 show the output for emulsions KM:1 and A:202. Other means are also shown, but as they have not been used in this work they may be ignored.

The complete tables of values for the various mean diameters and the log-normal distribution for groups KM and A are given in Table 4-10. The photographs for emulsions A:201, A:203 and A:204 were too poor for sizing to be carried out. Similarly, an excellent print was available for emulsion KM:15, but for emulsion KM:14 the quality was much poorer, probably due to a thicker sample in the haemocytometer cell. These early experiments showed the need for good exposures and the resulting variations when they were not obtained. This explains the absence of the other emulsions listed in Table 4-3 from Table 4-10.

Emulsion KM	G	d_v	d_{sv}	M	x_v	x_{sv}	σ_g	n
1	2.02	2.14	2.25	2.00	2.05	2.09	1.14	6
14	1.33	1.43	1.51	1.31	1.38	1.43	1.20	6
15	1.56	1.72	1.87	1.53	1.62	1.69	1.22	7
21	2.47	4.07	5.47	2.41	5.01	8.16	2.01	12
A								
202	1.27	1.69	2.16	1.22	1.41	1.54	1.36	9
205	2.07	4.12	7.03	1.88	3.11	4.35	1.79	9
206	1.94	3.76	5.97	1.64	3.96	7.14	2.15	9

Table 4-10

VARIOUS MEAN DIAMETERS FOR EMULSION NO. 1.0

FROM DATA IN FILM 1 1

GEOMETRIC MEAN DIAMETER	2.0164
ARITHMETIC MEAN DIAMETER	2.0508
MEAN DIAMETER LENGTH	2.1349
MEAN SURFACE DIAMETER	2.0924
MEAN VOLUME DIAMETER	2.1447
RECIPROCAL MEAN DIAMETER	1.9356
MEAN VOLUME-SURFACE DIAMETER	2.2533

Table 4-8

VARIOUS MEAN DIAMETERS FOR EMULSION NO. 202.0

FROM DATA IN FILM 3 7

GEOMETRIC MEAN DIAMETER	1.2656
ARITHMETIC MEAN DIAMETER	1.3577
MEAN DIAMETER LENGTH	1.6466
MEAN SURFACE DIAMETER	1.4652
MEAN VOLUME DIAMETER	1.6910
RECIPROCAL MEAN DIAMETER	1.1112
MEAN VOLUME-SURFACE DIAMETER	2.1629

Table 4-9

4.2.7 Effect of Salt

Group KS Emulsion	ϕ	Water Phase	Stirring time (secs.)
36, 37, 38, 39, 40	0·50	Salt	5, 10, 15, 30, 60
41, 42, 43, 44, 45	0·50	Deionised	5, 10, 15, 30, 60
46, 47, 48, 49, 50	~~0·50~~ 0·75	Salt	5, 10, 15, 30, 60
51, 52, 53, 54, 55	~~0·50~~ 0·75	Deionised	5, 10, 15, 30, 60

Table 4-11

Table 4-11 shows the twenty emulsions made for this series. Dealing with the series at ϕ = 0·50 first, emulsions KS:36 and KS:41 appeared very similar. In the following four corresponding pairs however, the deionised water series appeared to be a lighter brown colour than the salt specimens. For the series at ϕ = 0·75, direct comparison was difficult due to separation of some of the water phase on emulsions KS:46 - 48 and KS:51 and 52. Table 4-12 gives an indication of the water percentage in the emulsions. These figures are uncertain due to the high viscosity of the emulsion since although water may not have been emulsified, separation of trapped macrodroplets would have been slowed down considerably. Gentle stirring with a glass rod freed some of them, but possibly not all. The volume of separated water was measured in a glass measuring cylinder.

Emulsion (Salt)	ϕ	Emulsion (Deionised)	ϕ
46	0.50	51	0.68
47	0.58	52	0.75
48	0.63	53	0.75
49	0.74	54	0.75
50	0.75	55	0.75

Table 4-12

Emulsions KS:54 and 55 were very difficult to stir due to the high viscosity and a certain degree of "gelling". This last effect prevented effective circulation of emulsion around the stirrer. The droplet size data is shown in Table 4-13.

Group KS Emulsion	G	d_v	d_{sv}	M	x_v	x_{sv}	σ_g	n
36	2.22	3.90	5.72	2.00	4.09	6.59	1.99	10
37	1.96	2.82	3.65	1.83	2.86	3.73	1.71	7
38	1.64	2.45	3.41	1.59	2.14	2.61	1.56	6
39	1.51	1.85	2.16	1.48	1.70	1.87	1.37	11
40	1.32	1.47	1.62	1.29	1.37	1.46	1.25	7
41	2.33	4.19	6.40	2.20	3.79	5.46	1.83	10
42	1.93	2.93	4.02	1.88	2.62	3.28	1.60	7
43	1.80	2.54	3.29	1.77	2.40	2.94	1.57	7
44	1.68	2.12	2.51	1.65	2.01	2.29	1.43	14
45	1.51	1.72	1.90	1.45	1.67	1.83	1.36	9
49	1.65	2.57	3.63	1.56	2.32	3.02	1.67	6
50	1.53	2.15	2.80	1.45	2.01	2.51	1.60	5
52	2.39	4.85	7.59	2.21	5.30	9.48	2.15	14
53	2.27	3.79	5.38	2.21	4.03	6.02	1.88	11
54	1.78	2.97	4.50	1.74	2.43	3.05	1.61	7
55	1.88	3.07	4.53	1.76	2.96	4.18	1.80	7

Table 4-13

4.2.8 Variation of Water Concentration

In order to find the most feasible maximum water concentration at which to conduct further investigations, five emulsions were made at progressively higher water concentrations. All the emulsions were made with Kuwait crude oil and were stirred for ten seconds on the fast setting of the "Magimix"; ϕ was decided by the initial measurement of the two phases as no separation was observed. All five emulsions were dark in colour and were visually indistinguishable; the only difference appeared to be the viscosity, which became progressively higher (qualitatively). The droplet size data is given in Table 4-14.

Group KV Emulsion	ϕ	G	d_v	d_{sv}	M	x_v	x_{sv}	σ	n
31	0•50	1•54	2•25	2•95	1•42	2•27	3•11	1•75	16
32	0•55	1•86	2•63	3•31	1•77	2•81	3•82	1•74	22
33	0•60	1•82	2•64	3•39	1•70	2•85	4•02	1•80	22
34	0•65	2•07	3•37	4•71	1•83	3•69	5•91	1•98	9
35	0•70	2•11	3•60	5•22	1•84	4•49	8•13	2•16	10

Table 4-14

4.3 Model Crude Oil Experiments

4.3.1 Separation of Asphaltenes

The definition of the asphaltenes by method of separation is discussed in Chapter 1. As most investigations, including a parallel study to this work [75], have used n-pentane precipitated asphaltenes, this method was the one used here. A mixture of 250 cm^3 of n-pentane and 12·5 cm^3 of Kuwait crude residue (a 20x excess) were shaken overnight. After filtration the asphaltenes were washed in n-pentane and dried and stored in a vacuum dessicator. They were used as soon as possible after preparation.

The same method was used to determine the asphaltene content of the three crude oils and the results are shown in Table 4-15 together with the average yield for Kuwait crude residue.

Crude Oil	Asphaltene Yield wt/vol (g/dm^3)
Kuwait	3·68
Brega	0·459
Tia Juana	5·94
Kuwait residue	6·55

Table 4-15

4.3.2 Determination of Aromatic to Aliphatic Ratio in Crude Oil

Speight [76] and Williams [77] both required a relatively accurate hypothetical average crude oil molecule. They assigned peaks in the ^1H nmr spectrum to protons on carbon atoms in different environments. They also incorporated elemental analysis and molecular weight information into their procedures. In this thesis, the aim was merely to obtain an indication of the aromatic to aliphatic ratio in the crude oil. Hopefully, this would provide a slightly more realistic environment for the asphaltenes than that achieved by Lawrence and Killner [17] with their nujol solutions or Mackay et al [19] with m-xylene solutions.

Figure 4-5 shows the ^1H nmr spectrum for a Kuwait crude oil. The integration data from this is given in Table 4-16. The use of this data in formulating a hypothetical average crude oil system is exemplified using tetralin as the aromatic component and n-heptane as

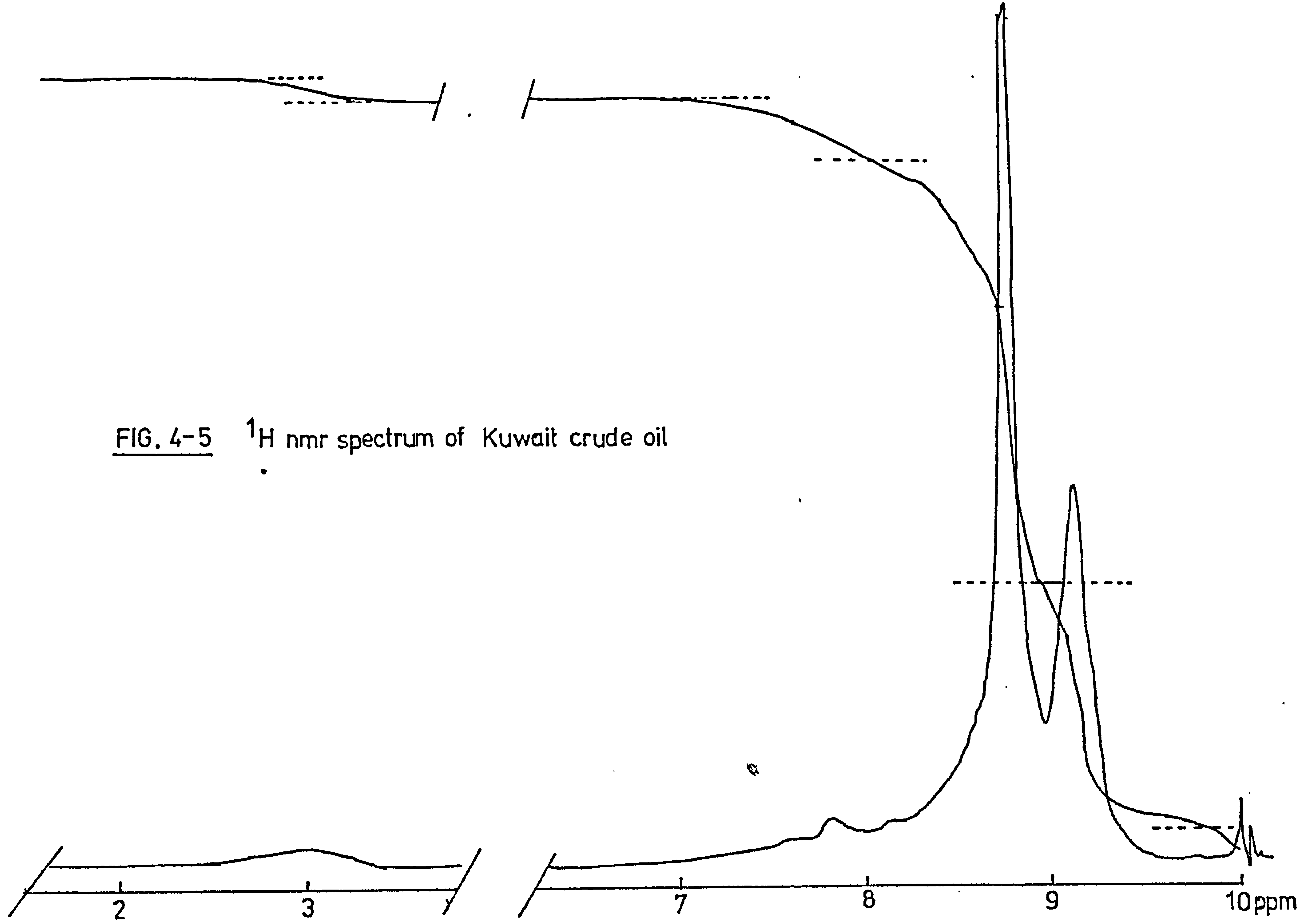

FIG. 4-5 ^1H nmr spectrum of Kuwait crude oil the aliphatic part.

Chemical Shift	Designation	Integration Units
2·8 - 3·3	Aromatic	1
6·9 - 8·0	Benzylic	3
8·0 - 8.95	- CH_2 -	20
8·95 - 9.5	- CH_3 -	11

Table 4-16

Two immediate approximations are made. First, the contribution of the asphaltenes to the aromatic part is neglected. Secondly, the benzylic part of the crude oil is ignored despite there being four benzylic protons in tetralin in this example. This enables simpler aromatic molecules to be used. In the following and all subsequent ratios, the first figure refers to the aromatic protons and the last to the aliphatic protons. Thus in crude oil it can be seen from Table 4-16 that the ratio is 1:31.

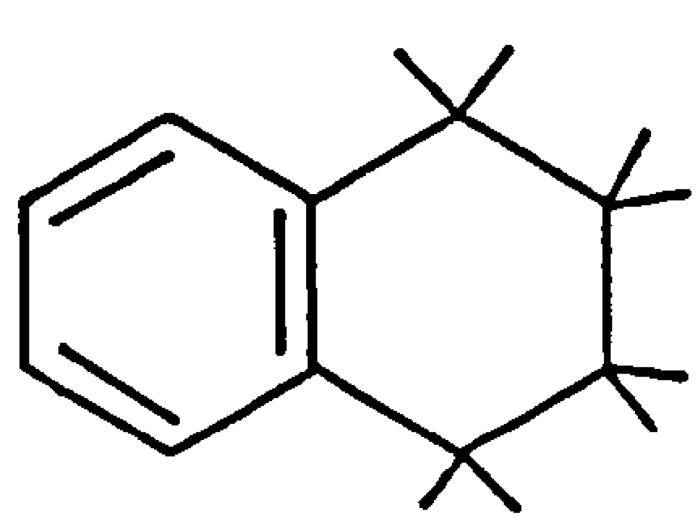

CH_3-$(CH_2)_5$-CH_3

0:16

4:4 1:31 ≡ 4:124

For one mole of tetralin (represented by four protons of each type), (124-4)/16 moles of n-heptane are required = 7·5. From the molecular weight, this gives a weight ratio of 1:5·68. The ^1H nmr spectrum for such a mixture is shown in Figure 4-6.

^{13}C nmr provides a means of determining the ratio of aromatic to aliphatic carbon present rather than the ratio of protons attached to such carbon atoms. Full analyses have been published by Knight [78] and

FIG. 4-6 ^{1}H nmr spectrum of n-heptane/tetralin (molar ratio 7·5:1)

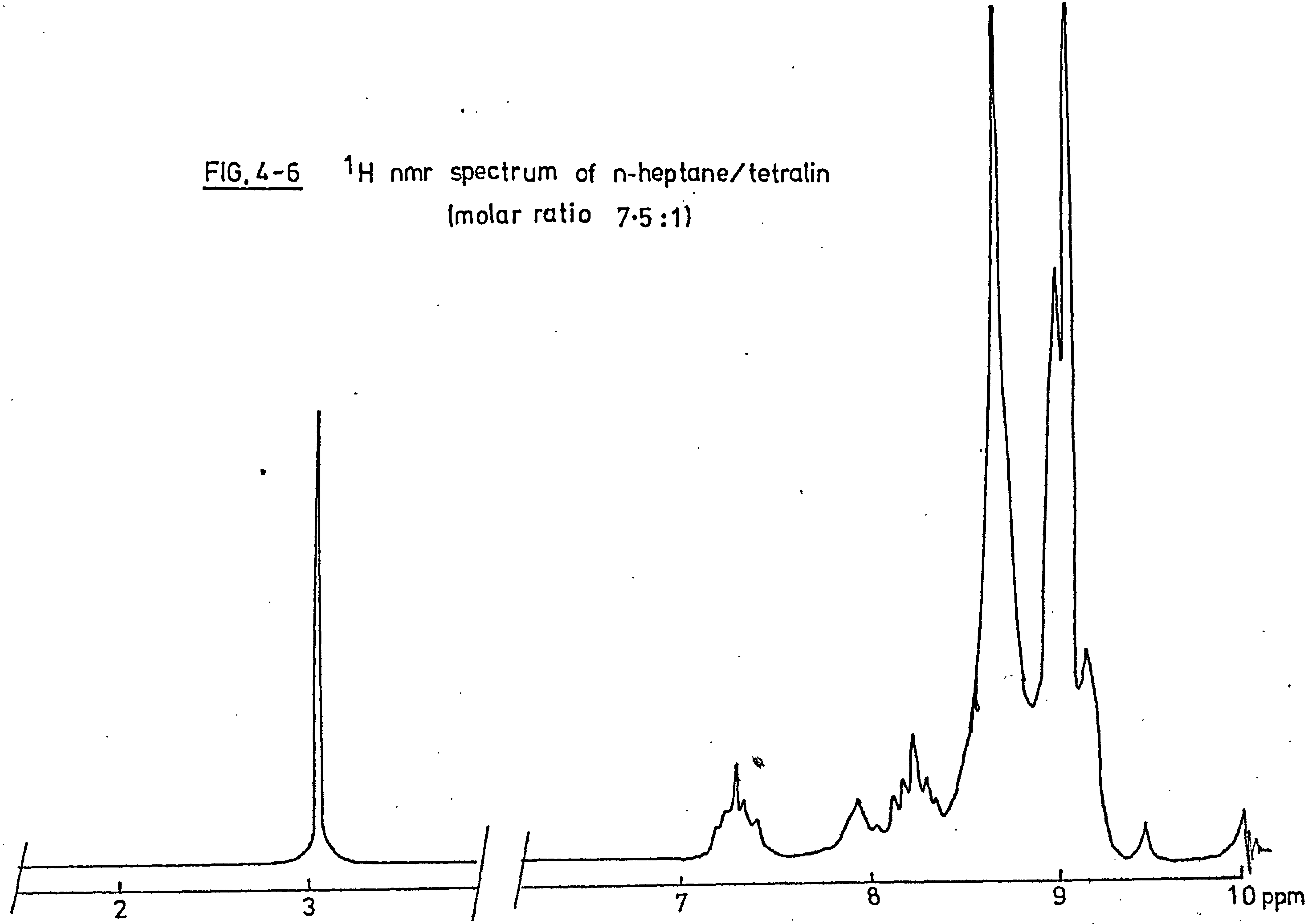

Clutter et al [79]. The latter authors have used the integrated intensities of the characteristic resonances in both ^{13}C and ^{1}H nmr spectra. However, the former is all that is required in this work, and the ^{13}C nmr spectrum of Kuwait crude is shown in Figure 4-7. Two methods were used for determining the integration and the results are shown in Table 4-17.

Method Used	Aromatic to Aliphatic Ratio
Planimeter	1 : 12•2
Planimeter	1 : 12•3
Planimeter	1 : 11•8
Planimeter	1 : 12•2
Planimeter	1 : 11•5
Planimeter	1 : 10•6
Weighed Cardboard cut out	1 : 12•2
Weighed Cardboard cut out	1 : 11•2

Table 4-17

The average ratio of all these values is 1 : 11•75. The analysis is the same as for the ^{1}H nmr treatment. Table 4-18 shows the molar ratio for various aromatic compounds with (a) n-heptane and (b) n-octane using this ratio of 1 : 11•75. In each case the aromatic portion is unity.

Aromatic Component	Aliphatic Component	
	n-heptane	n-octane
benzene	10.07	8•8
toluene	9•93	8•69
o-xylene m-xylene p-xylene	9•79	8•56
ethyl benzene	9•79	8•56
tetralin	9•50	8•31
α-methyl naphthalene	16•64	14•5

Table 4-18

FIG. 4-7 ^{13}C nmr spectrum of Kuwait crude oil

4.3.3 Asphaltene Addition to the Hypothetical Oil Phase

It was found that the only satisfactory method of making a reasonable model oil was to dissolve the asphaltenes in the aromatic part and then to add the aliphatic component. This resulted in the asphaltenes being thrown out of solution again in the form of a very fine dispersion. If, however, the aliphatic were added first, a very coarse dispersion resulted. The eight aromatic components listed in Table 4-18 were tried for their solvent power on the asphaltenes. The importance of this can be seen by considering that if a 2% wt/vol. asphaltene dispersion were made, then 2 grams of asphaltene would need to be dissolved in about 10 cm^3 of aromatic phase. For convenience, the aromatic compound that dissolved the asphaltenes the easiest was preferred. On the basis of a 2% wt/vol. dispersion, the three xylenes dissolved the asphaltenes very well, m-xylene being the best. The worst was α-methyl naphthalene where a fairly coarse dispersion resulted. The other four were fair with medium dispersions. All model crudes were therefore based on an m-xylene aromatic component.

It was interesting to note the settlement that resulted on leaving a model crude to stand overnight. Compared to a similar vessel containing the same amount of asphaltenes alone, the asphaltenes in the model appeared to have double the volume. This is probably a solvation effect whereby the asphaltenes concentrate the aromatic portion with them when they precipitate.

4.3.4 Variation of Asphaltene Concentration

Five emulsions were made at increasing asphaltene concentrations on a m-xylene/n-heptane model oil. The original idea was to stir 50 cm^3 of oil phase with 200 cm^3 of simulated sea water in bursts of 10, 20 and finally 30 seconds on the fast setting of the "Magimix". The final details are shown in Table 4-19.

Group MA Emulsion	Asphaltene conc. c' g/dm^3	Stirring time (secs.)
24	0·275	10 + 20 + 30
25	0·489	10 + 20 + 30
26	1·11	10 + 20
27	1·51	10 + 20
28	1·95	10 + 5

Table 4-19

It can be seen that as the asphaltene concentration increased, the stirring time decreased. This was due to a complete uptake of water together with a gelling effect. This meant that circulation of emulsion around the mixer ceased, and that the mixer was just beating a hole in the centre of the emulsion.

The model emulsions were found to break down when the normal method of dilution was used. To avoid breakdown, it was necessary to put the emulsion sample on a watch glass and "paddle" diluent into it with a spatula. Microscopic examination then showed that despite emulsification, even emulsion MA:24 with the lowest asphaltene concentration showed clumps of unused asphaltenes. Coalescence was also obvious. One notable feature was the presence of polyhedral droplets. These are discussed in a wider context in Chapter 5. The droplet size data is given in Table 4-20.

Group MA Emulsion	G	d_v	d_{sv}	M	x_v	x_{sv}	σ_g	n
24	5•45	12•0	18•1	5•22	19•0	44•7	2•53	23
25	3•66	8•13	13•2	3•13	11•2	26•1	2•51	13
26	7•18	11•7	14•9	7•38	15•5	25•3	2•02	21
27	5•70	8•25	10•6	5•64	7•95	10•0	1•61	11
28	5•53	7•90	9•83	5•54	8•29	10•8	1•68	12

Table 4-20

4.3.5 Effect on Emulsification of Varying Aromatic to Aliphatic Ratio

Table 4-21 shows four model emulsions made when the mixer and the molar ratio were varied. Emulsions MP:19 and 20 were made using only m-xylene, and no emulsification resulted. Emulsions MP:17 and 18 were made with the standard aromatic to aliphatic molar ratio of 1 : 9•79 for m-xylene and n-heptane. Emulsion MP:17 gelled up within seconds. In emulsion MP:18, the water was added dropwise over a period of fifteen minutes. The reason for the poor emulsification was probably loss of n-heptane by evaporation causing concentration of the aromatic phase. One further point concerning emulsion MP:19 was the cloudy appearance of the water phase. Although no droplets were visible, it is possible that either an O/W microemulsion had formed, or else a very small fraction of the asphaltenes was soluble in water.

Group MP Emulsion	Asphaltene conc. g/dm^3	Mixer	ϕ	Stirring time
17	2•9	"Magimix"	0•792	10 secs.
18	2•9	Stirrer	0•597	15 mins.
19	2•9	"Magimix"	0	60 secs.
20	3•0	Stirrer	0	15 mins.

Table 4-21

Table 4-22 shows the effect of varying the aromatic to aliphatic ratio on the uptake of a possible total of 210 cm^3 of water by 40 cm^3 of model crude oil. The asphaltene content was kept constant in each emulsion by weighing out 0·400 g of asphaltenes for each 40 cm^3 of model oil. Each emulsion was stirred for fifteen seconds in the "Magimix". The results are plotted in Figure 4-8. The water uptake was calculated by measuring the unemulsified water in a measuring cylinder. The gel-like nature of the emulsion in the high ϕ range (>0·500) made it difficult to obtain an accurate figure as large water droplets were trapped in the gel structure. The emulsions concerned were stirred twice very gently before measuring the separation. This uncertainty is reflected in the spread of the points above ϕ = 0·500.

Group MP Emulsion	Aromatic : Aliphatic (by volume)	Percentage n-heptane	cm^3 water emulsified	ϕ
59	3 : 1	25·0	3	0·070
60	1 : 1	50·0	8	0·167
61	1 : 3	75·0	54	0·575
62	1 : 6	85·7	82	0·672
63	1 : 9	90·0	110	0·733
64	1 : 12	92·3	84	0·678
65	1 : 1·5	60·0	10	0·200
66	1 : 2·0	66·7	15	0·264
67	1 : 2·5	71·4	22	0·355
68	1 : 9	90·0	72	0·643
70	1 : 49	98·0	<2	<0·047

Table 4-22

FIG. 4-8

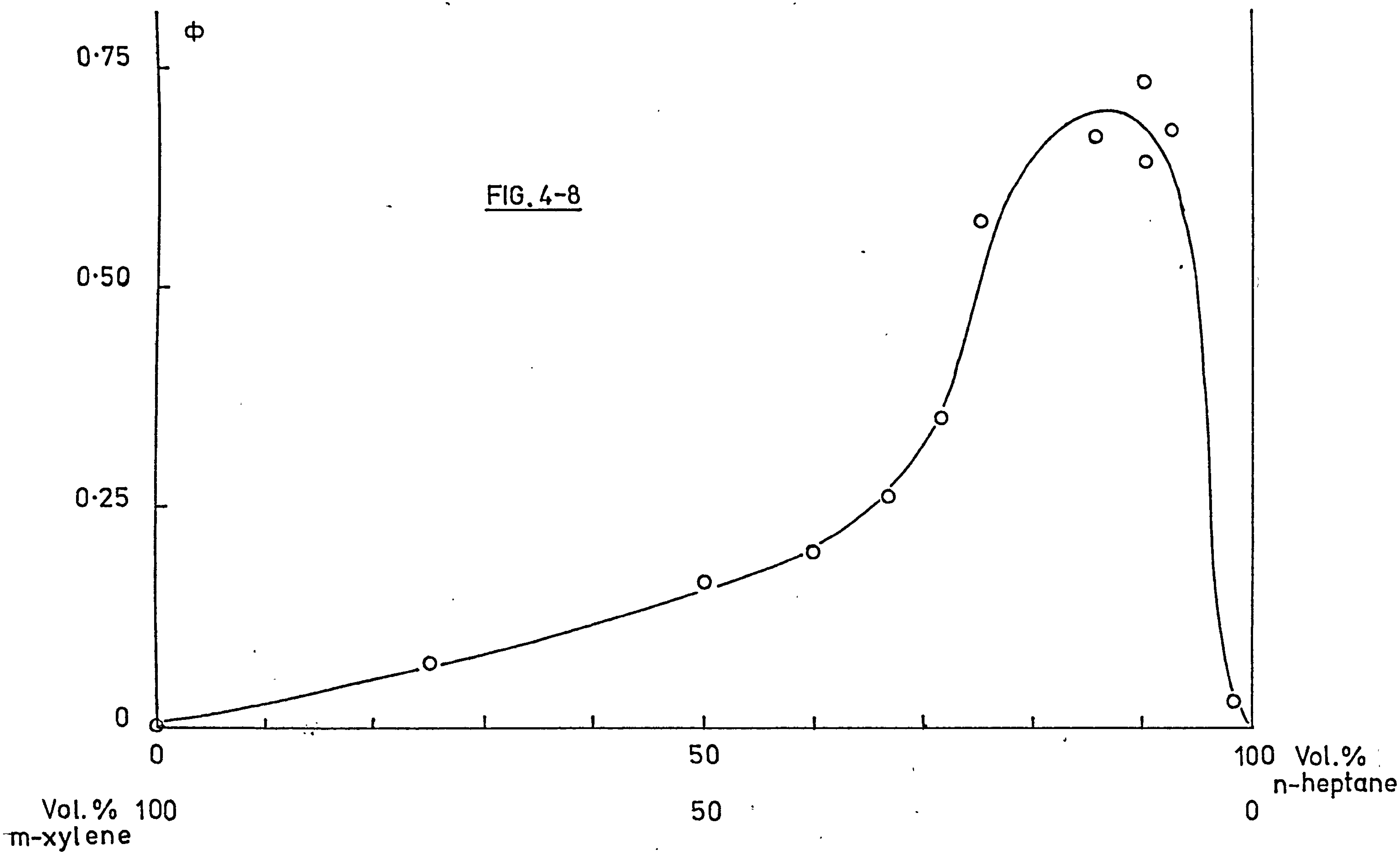

4.4 Rheology Experiments

4.4.1 Preliminary Investigations

During trials on the Rheotest II with various early emulsions, it was observed that a certain amount of slipping occurred between the inner cylinder and the emulsion, particularly those involving model crude oils. This has been reported previously [32, 80] and the only remedy reported was to slightly roughen all the cylinders by light sandblasting. The shearing stress, τ is related to the machine deflection α by a cylinder constant K :

$$\tau = K.\alpha \qquad 4\text{-}1$$

Although the manufacturers had provided values of K, they were re-checked after roughening for all three cylinder systems with dried glycerol of standard viscosity. The resulting calibration graphs are shown in Figures 4-9, 4-10 and 4-11. Each figure has two graphs, a value of K for each spring : K^{I} and K^{II} and these are recorded on the figures. The temperature had to be reduced for cylinder S3 so that the glycerol became viscous enough to register on scale II.

The viscosities of the three crude oils used were determined in cylinder system S1 at θ_c = 25·0 °C, the temperature at which all further investigations were carried out. Because of the problem of evaporation of n-heptane encountered in group MP, the higher boiling paraffin n-octane was used in model oil rheological experiments according to the molar ratio with m-xylene shown in Table 4-18. The viscosity of this mixture was too low for the Rheotest II, so it was determined in a standard Ostwald capillary viscometer. The viscosities of all four oil phases are shown in Table 4-23. A temperature variation of $\pm$ 1·0 K was found to make a difference of $\pm$ 5% for all three crude oils.

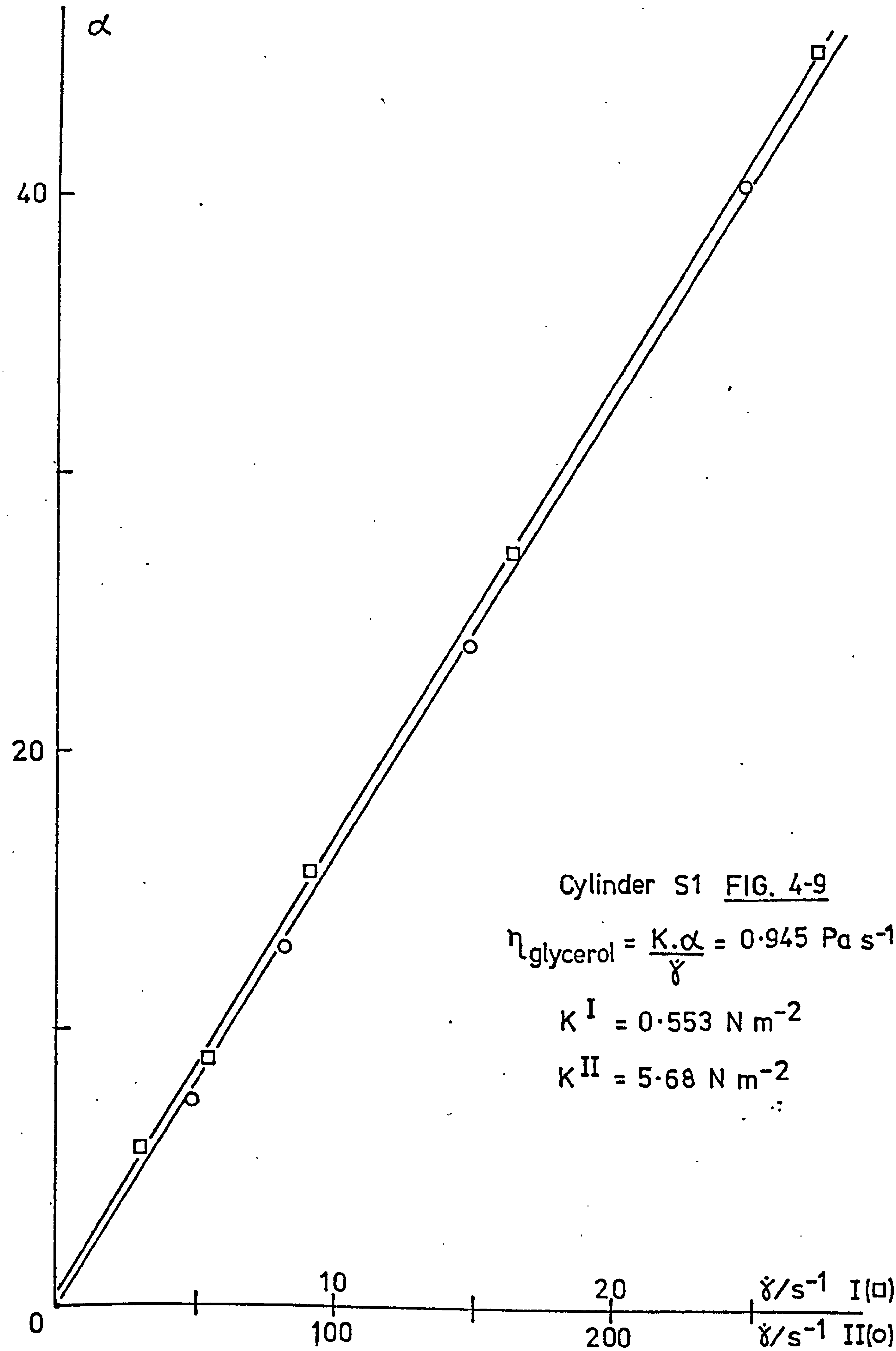

Cylinder S1 FIG. 4-9

$\eta_{glycerol} = \frac{K.\alpha}{\dot{\gamma}} = 0{\cdot}945$ Pa s^{-1}

$K^{I} = 0{\cdot}553$ N m^{-2}

$K^{II} = 5{\cdot}68$ N m^{-2}

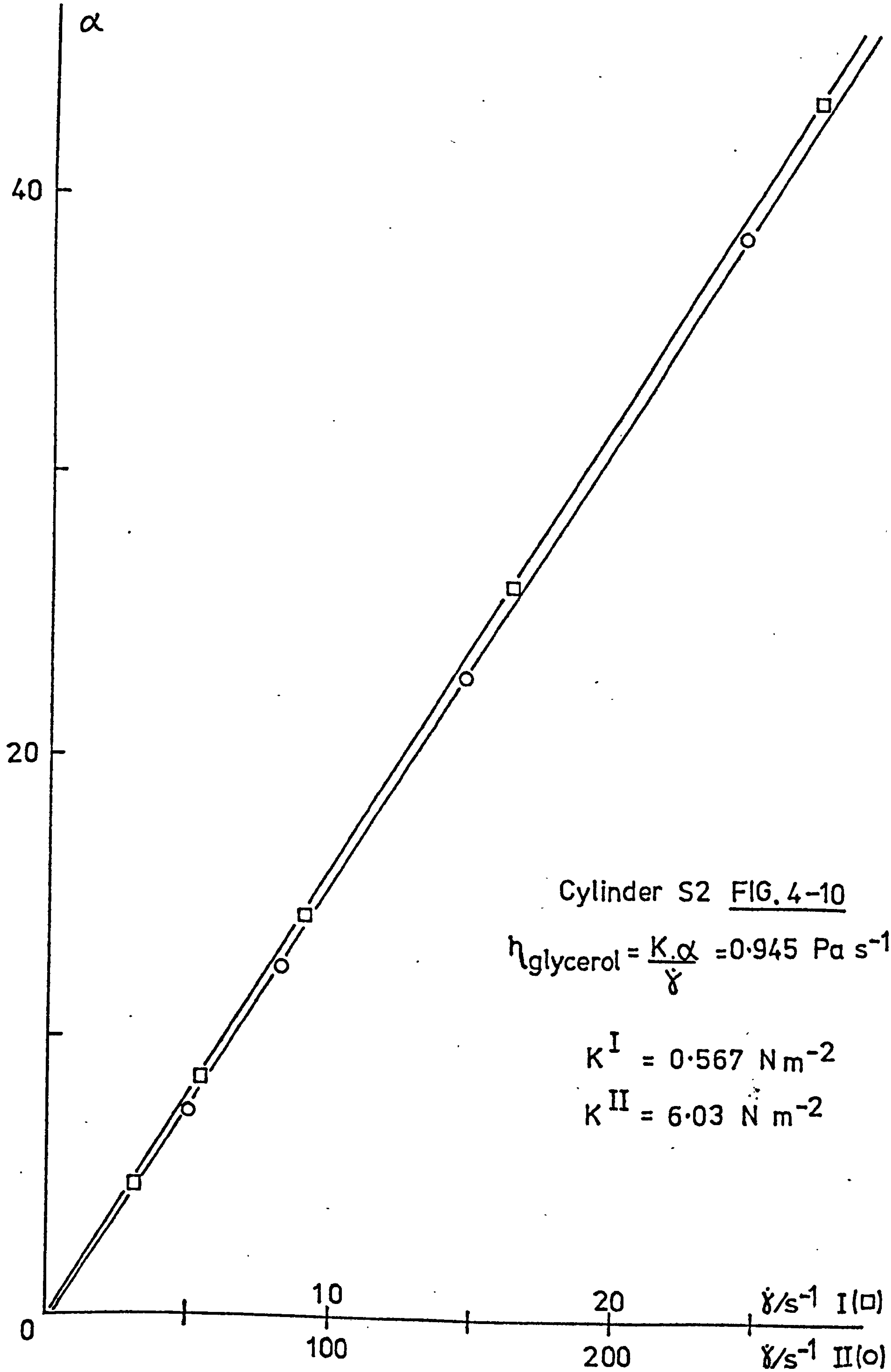
α
40
20
0
10
20
γ̇/s⁻¹ I(□)
100
200
γ̇/s⁻¹ II(o)
Cylinder S2
$\eta_{glycerol} = \frac{K.\alpha}{\dot{\gamma}} = 0{\cdot}945$ Pa s^{-1}
$K^{I} = 0{\cdot}567$ N m^{-2}
$K^{II} = 6{\cdot}03$ N m^{-2}

FIG. 4-10

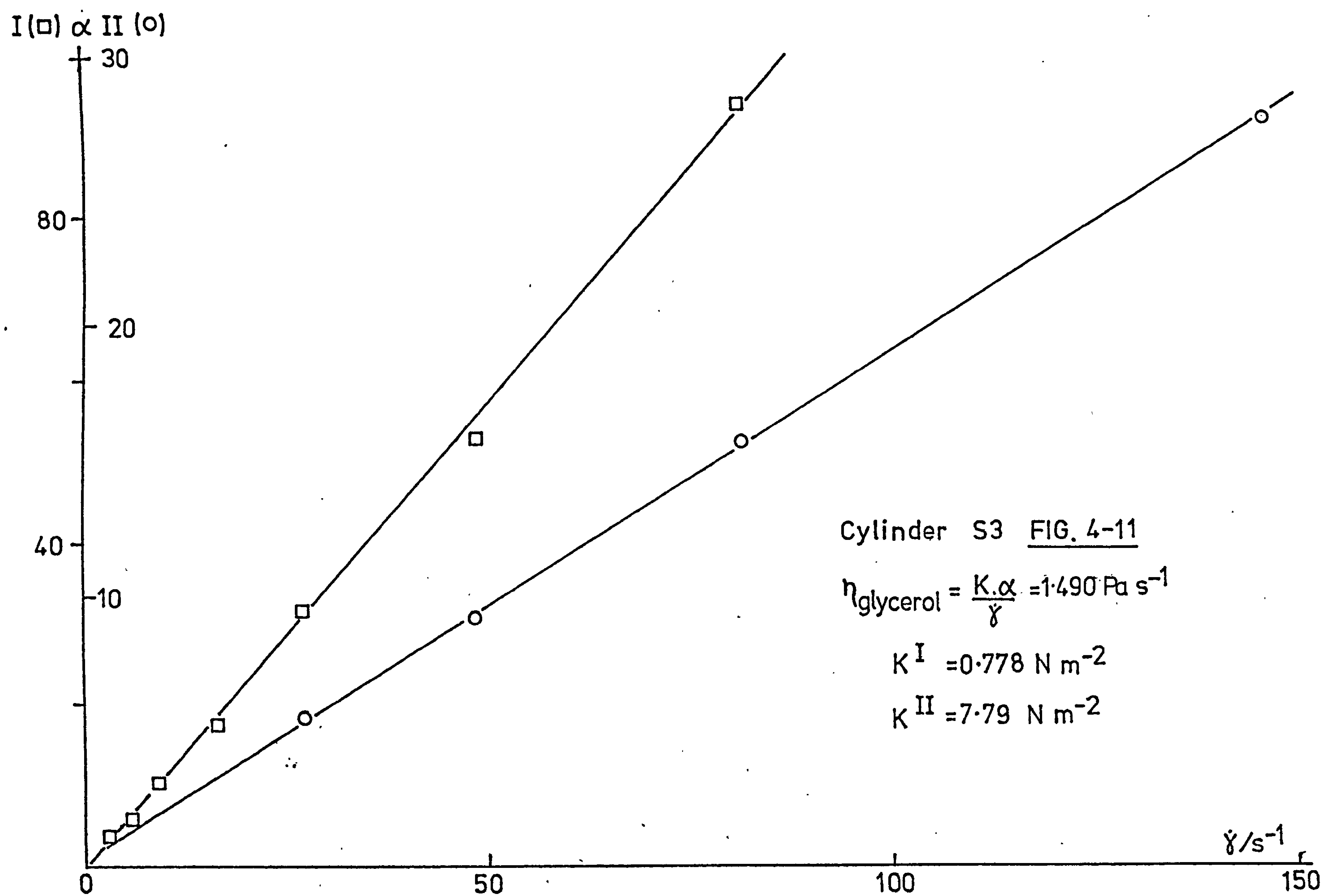

I(□) α II (○)
30
80
20
40
10
0
50
100
150
γ̇/s⁻¹
Cylinder S3
η_glycerol = K.α / γ̇ = 1·490 Pa s⁻¹
K^I = 0·778 N m⁻²
K^II = 7·79 N m⁻²

FIG. 4-11

Oil Phase	Viscosity mPa s
m-xylene/n-octane	0·53
Brega crude oil	4·73
Kuwait crude oil	12·6
Tia Juana crude oil	37·6

Table 4-23

A special emulsion, KR:81, was made at $\phi = 0.50$ in the "Magimix" (stirred at medium speed for 150 seconds) to determine the rheological characteristics. Cylinder system S2 was used; the shear rate was increased every 60 seconds and then decreased at the same time intervals. Such a cycle was carried out twice, and the result is shown in Figure 4-12. Hysteresis is not exhibited, but there is a pronounced curve at high shear rates. There are two possibilities. First, there is a heating effect or secondly, there is thixotropy present but with a very fast recovery time.

The second possibility was eliminated by shearing the emulsion (KR:81) at the maximum shear rate ($437{\cdot}4\ s^{-1}$) for 5 minutes and then rapidly reducing it to $24{\cdot}3\ s^{-1}$ to observe the build up if any. The scale reading changed over one minute from 6·6 to 6·8 units. However, the scale is marked in a similar way to a burette and the tenths are estimated by eye. So no matter how steady the needle is a change of the estimated tenths is negligible.

The heating effect possibility is more easily substantiated. Hediger [81] argued that with large gaps and high strain rates, heat would inevitably build up in the system. Indeed, he added that hysteresis loops due to heating effects are sometimes wrongly

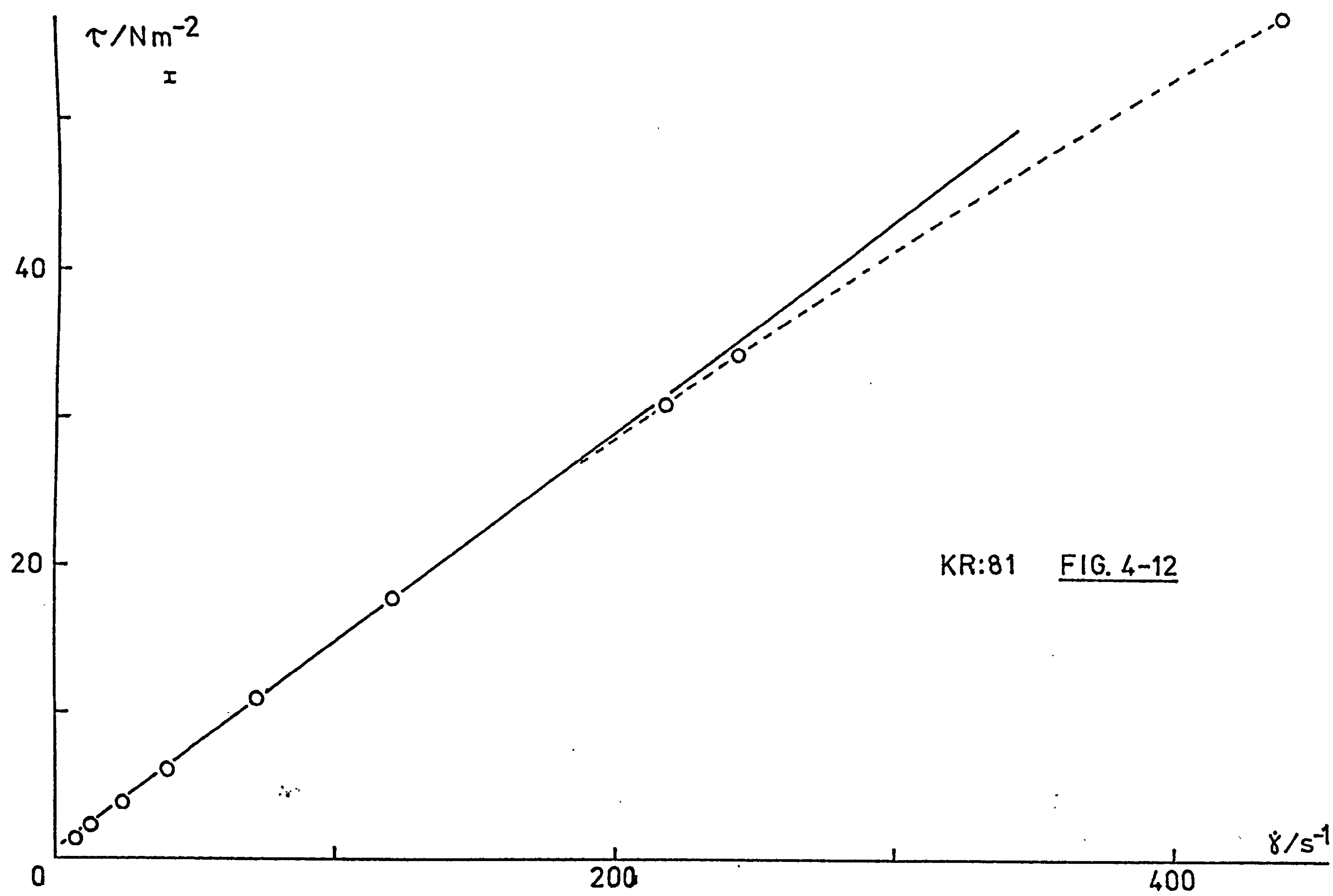

KR:81 FIG. 4-12

interpreted as thixotropy. He gave an expression for the temperature gradient over the gap for a particular make of viscometer (Contraves). This may be generalised as :

$$\Delta H = \frac{\tau_i \dot{\gamma}_i}{\lambda} \cdot C \qquad 4\text{-}2$$

where τ_i and $\dot{\gamma}_i$ are the shear stress and the shear rate at the inner cylinder, λ is the coefficient of thermal ~~capacity~~ conductivity and C is a constant unique to a given cylinder system. This equation is explored in greater depth in the discussion.

The problem of estimating α to tenths of a unit has been mentioned. One characteristic of the viscometer was that the needle seemed to keep very constant and that the estimation of α was quite reproducible. This can be seen from the data for emulsion KR:81 shown in Table 4-24.

Shear rate $\dot{\gamma}$	Values of α (estimated to tenths)			
	first upcurve	first downcurve	second upcurve	second downcurve
8·1	2·3	2·3	2·3	2·3
13·5	4·0	4·0	4·0	4·0
24·3	6·8	6·7	6·7	6·8
40·5	10·8	10·8	10·7	10·8
72·9	19·4	19·3	19·3	19·2
121·5	31·2	31·0	30·9	30·8
218·7	54·3	53·9	53·9	53·8
243·0	59·9	59·3	59·1	59·1
457·4	99·3	-	98·8	-

Table 4-24

Nevertheless, error bars are shown on the graphs corresponding to one scale unit.

The cone and plate attachment of the viscometer was tried for various emulsions, but they were all found to breakdown; possibly due to both high shear rates and because the tip was not removed. This method was therefore not used.

4.4.2 Procedure Adopted

Following on from emulsion KR:81, the procedure adopted for the rheological characterisation of the following emulsion systems was to increase the shear rate every minute. The linear portion of the graph was assigned as η_∞ as described in Chapter 2. The emulsion was weighed into the outer cylinder on a tared balance to ensure the correct height in the cylinder.

Three emulsion properties were varied. The first of these was droplet size. A given emulsion was stirred, weighed into the viscometer and while equilibrating, a sample was photographed for droplet size analysis. This ensured that the droplet size was measured as close to the rheological determination as possible. On finishing one such determination, the contents of the viscometer were emptied back into the stirrer. A new droplet size distribution was obtained by stirring and the process repeated. Altogether, four or five such determinations were made for a given emulsion. The second property varied was ϕ. For each of the three crude oils together with the model crude, three or four different values of ϕ were used. In addition, the emulsifying agent concentration was varied for the model crude oil. Of course the nature of the three crude oils effectively involved a variation in emulsifying agent concentration.

4.4.3 Rheological Determinations on Various Oil Systems

Each group is presented individually, but the emulsions within the group are listed in numerical order. In all cases, the "Magimix" was used on the fast setting and simulated sea water was used.

Four Kuwait crude emulsions were studied (group KR) and the rheograms are shown in Figures 4-13 to 4-16. The relevant properties of the emulsions, including size data and the rheological parameters obtained from the figures, are given in Table 4-25. A sample of emulsion, KR:87·5, was left on the slide for two days after the experiments, and a certain amount of clustering was observed. Although the droplets were not touching there was sufficient grouping for the phenomenon not to be a random event.

Four emulsions were made using Tia Juana crude oil (group TR) and the rheograms are shown in Figures 4-17 to 4-20. The emulsion properties and size data are shown in Table 4-26.

The low viscosity of Brega crude oil together with its low asphaltene concentration led to noticeable creaming, sedimentation and coalescence. Nevertheless, rheological experiments were carried out on three emulsions and the rheograms for group BR are shown in Figures 4-21 to 4-23. The emulsion details and size data are shown in Table 4-27. In all fourteen determinations, water droplets were visible in the outer cylinder at the end of the experiment. Coalescence was not observed in emulsion BR:105, but as ϕ increased so predictably did the coalescence.

Two sets of rheological experiments were carried out on model systems. In the first group (MAR), ϕ was kept at 0·50 and the asphaltene concentration was varied; in the second group (MVR), ϕ was varied and the asphaltene concentration was maintained at 0·5 g/dm^3. The first emulsion in the series, MAR:88, showed the two properties characteristic of the model system: "clumping" of droplets and the possibly associated feature of gelling or structuring. This "clumping", which made dilution for sizing difficult, was the basis for an interesting observation. In some instances throughout this work, a slight deficiency of sample was placed on the microscope slide and so when the cover slip was applied, there was capillary flow of emulsion to fill the remaining air spaces. In the case of a Kuwait emulsion the smaller droplets moved faster than the larger ones, as would be expected. However, in the model system, the "stickiness" of the droplets was shown up by clumps of droplets moving together, the force of attraction clearly overcoming the dynamic forces. A further feature was exhibited in emulsion MVR:109. When the cover slip was pressed, a certain clump was seen to rotate "on the spot". Although this induced flow, the three smaller droplets attached to the larger one all maintained their relative positions.

Although little or no coalescence was observed under the microscope, emulsion MVR:112 with ϕ = 0·40 showed a certain amount of creaming. The effect of this unavoidable phenomenon is discussed in Chapter 5. The last two viscosity readings of emulsion MVR:109 showed that considerable coalescence had occurred. The rheograms for group MAR are shown in Figures 4-24 to 4-27 and for group MVR in Figures 4-28 to 4-30. Emulsion 108 is common to both groups but is shown in detail in group MAR. Emulsion details and size data are shown for the model groups in Tables 4-28 and 4-29.

Group KR	Emulsion	ϕ	t (secs)	η_∞ (mPa s)	η_{rel}	G/μm	d_v/μm	d_{sv}/μm	M	x_v	x_{sv}	σ_g	n
87	1	0·50	5	101·6	8·06	2·29	4·49	7·02	2·20	3·89	5·68	1·85	11
	2		10	126·4	10·03	2·03	3·61	5·63	1·98	3·03	4·02	1·70	8
	3		15	145·6	11·56	1·64	2·91	4·62	1·51	2·60	3·75	1·83	7
	4		30	175·8	13·95	1·66	2·13	2·53	1·57	2·21	2·78	1·61	15
	5		60	225·8	17·91	1·39	1·65	1·89	1·35	1·50	1·61	1·31	9
91	1	0·40	5	56·7	4·50	2·17	4·46	7·24	2·07	3·98	6·15	1·91	11
	2		10	65·8	5·22	1·96	3·57	5·30	1·86	3·80	6·11	1·99	10
	3		15	71·1	5·64	1·73	2·62	3·62	1·71	2·41	3·03	1·61	6
	4		30	80·7	6·40	1·56	2·41	3·27	1·43	2·48	3·56	1·83	6
	5		60	87·0	6·90	1·41	1·75	2·06	1·32	1·79	2·15	1·55	13
92	1	0·60	10	252·3	20·02	2·22	3·82	5·51	2·09	3·95	6·03	1·91	10
	2		15	308·4	24·48	1·92	3·18	4·65	1·87	2·77	3·60	1·67	9
	3		30	450·2	35·73	1·63	2·20	2·69	1·59	2·31	2·97	1·65	6
	4		60	620·3	49·2	1·43	1·86	2·26	1·31	1·89	2·41	1·64	13
97	1	0·55	5	147·5	11·71	2·16	4·41	7·08	2·05	4·32	7·10	2·02	12
	2		10	181·4	14·40	1·97	3·18	4·31	1·89	3·57	5·46	1·92	8
	3		15	212·5	16·87	1·89	3·06	4·34	1·82	3·02	4·24	1·79	7
	4		30	268·8	21·33	1·50	2·09	2·69	1·43	2·17	2·88	1·70	15
	5		60	353·8	28·08	1·47	1·72	1·95	1·43	1·63	1·80	1·35	10

Table 4–25

Group TR	Emulsion	ϕ	t (secs)	η_∞ (mPa s)	η_{rel}	G	d_v	d_{sv}	M	x_v	x_{sv}	σ_g	n
101	1	0·40	5	162·2	4·46	1·94	3·83	6·16	1·79	3·69	5·96	2·00	9
	2		10	186·0	5·11	1·90	3·12	4·46	1·81	3·01	4·22	1·79	7
	3		15	214·8	5·90	1·72	2·51	3·30	1·64	2·48	3·25	1·69	6
	4		30	248·8	6·84	1·42	1·94	2·46	1·34	1·91	2·41	1·62	13
	5		60	299·1	8·22	1·24	1·52	1·79	1·17	1·41	1·60	1·43	8
102	1	0·50	10	315·4	8·67	2·26	4·12	6·61	2·05	3·81	5·74	1·90	7
	2		15	373·1	10·25	1·76	3·10	4·77	1·66	2·69	3·71	1·77	7
	3		20	450·1	12·37	1·60	2·71	3·93	1·39	2·90	4·74	2·01	6
	4		30	536·6	14·74	1·68	2·20	2·74	1·56	2·20	2·77	1·61	16
	5		60	770·0	21·15	1·36	1·81	2·26	1·28	1·74	2·12	1·57	14
103	1	0·60	20	765·6	20·34	2·53	5·27	8·30	2·45	5·71	10·04	2·12	15
	2		30	1301	34·59	1·68	2·92	4·63	1·57	2·61	3·66	1·79	6
	3		45	1681	44·70	1·50	2·12	2·81	1·42	2·02	2·56	1·63	5
	4		60	2357	62·69	1·48	1·79	2·08	1·47	1·68	1·84	1·35	4
104	1	0·55	15	448·1	12·31	2·47	4·22	6·37	2·37	3·74	5·08	1·74	9
	2		20	577·7	15·87	2·16	3·39	4·76	2·00	3·27	4·55	1·71	8
	3		30	785·8	21·59	2·07	2·65	3·18	1·97	2·64	3·26	1·56	17
	4		45	1023	26·59	1·95	2·44	2·87	1·78	2·65	3·45	1·68	15
	5		60	1387	38·10	1·70	2·03	2·34	1·59	1·93	2·19	1·43	12

Table 4-26

Group BR	Emulsion	ϕ	t (secs)	η_∞ (mPa s)	η_{rel}	G	d_v	d_{sv}	M	x_v	x_{sv}	σ_g	n
105	1	0·40	10	23·59	4·99	2·38	4·60	6·96	2·31	5·03	8·46	2·06	13
	2		15	23·81	5·03	2·39	4·20	6·01	2·24	4·60	7·41	2·00	11
	3		20	26·08	5·51	2·19	4·67	7·32	2·01	5·83	11·8	2·32	14
	4		30	26·76	5·66	2·18	4·09	5·82	2·05	5·84	11·8	2·31	13
	5		60	28·12	5·95	2·19	4·15	5·93	2·06	5·88	11·8	2·31	13
106	1	0·50	10	37·88	8·01	2·38	6·17	10·5	2·12	8·80	22·7	2·65	19
	2		15	41·73	8·82	2·63	5·54	8·71	2·34	7·01	14·5	2·35	16
	3		20	45·47	9·61	2·35	5·59	8·94	2·09	9·87	27·8	2·77	18
	4		30	47·97	10·14	3·54	7·64	10·4	3·58	20·9	67·8	2·96	28
	5		60	53·30	11·27	4·08	5·60	6·62	4·20	6·99	8·68	1·71	16
107	1	0·60	15	75·24	16·78	5·13	7·50	9·10	5·39	8·55	11·6	1·74	22
	2		20	94·69	20·02	3·81	7·69	10·7	3·83	13·3	30·6	2·49	27
	3		30	104·3	22·06	4·58	8·89	11·6	4·76	21·1	56·9	2·71	33
	4		45	124·2	26·25	5·10	7·78	9·72	5·29	9·4	13·8	1·86	24
	5		60	130·4	27·57	2·73	7·18	11·2	2·46	20·7	86·5	3·30	26

Table 4-27

Group MAR Emulsion		c′ g/dm^3	t (secs)	η_∞ (mPa s)	η_{rel}	G	d_v	d_{sv}	M	x_v	x_{sv}	σ_g	n
88	1	0·25	5	6·12	11·78	5·92	9·54	12·4	6·06	11·2	16·8	1·89	22
	2		10	9·07	17·45	4·72	7·35	9·76	4·74	7·42	9·99	1·73	16
	3		15	11·79	22·68	2·91	4·57	6·15	2·85	4·64	6·43	1·77	9
	4		30	12·81	24·64	2·94	4·23	5·24	2·98	4·49	5·89	1·68	13
	5		60	19·16	36·81	2·79	4·05	4·98	2·81	5·03	7·41	1·86	13
108	1	0·50	10	5·67	10·90	11·9	15·0	17·2	12·1	16·0	19·3	1·54	14
	2		15	6·35	12·21	11·5	15·0	17·2	11·9	17·3	22·1	1·64	15
	3		30	8·51	16·36	8·84	11·5	13·2	9·24	14·0	18·5	1·69	11
	4		45	8·96	17·23	9·17	11·2	12·5	9·46	12·7	15·5	1·56	10
	5		60	10·32	19·85	8·37	10·5	11·7	8·71	12·9	16·8	1·67	10
113	1	1·00	10	3·40	6·54	15·8	20·2	23·0	16·3	23·6	30·2	1·65	20
	2		20	7·37	14·17	13·1	18·3	21·1	14·1	30·5	51·0	2·05	20
	3		30	7·82	15·04	11·4	14·8	16·7	12·1	20·1	28·2	1·79	15
	4		45	8·28	15·92	10·3	13·2	14·7	11·0	16·6	22·0	1·69	13
	5		60	9·64	18·54	8·75	11·2	12·6	9·31	15·7	22·1	1·80	11
114	1	1·50	10	8·51	16·36	5·52	8·57	11·1	5·49	8·05	10·4	1·65	10
	2		20	11·68	22·47	5·34	7·21	8·76	5·36	7·26	8·89	1·57	9
	3		30	14·40	27·70	4·28	5·57	6·66	4·22	5·57	6·70	1·54	6
	4		60	18·37	35·33	3·53	4·51	5·22	3·59	4·61	5·45	1·50	15

Table 4-28

Group	MVR Emulsion	ϕ	t (secs)	η_∞ (mPa s)	η_{rel}	G	d_v	d_{sv}	M	x_v	x_{sv}	σ_g	n
109	1	0·60	15	17·58	33·81	22·9	25·6	27·1	23·6	26·6	28·8	1·32	18
	2		30	26·65	51·25	16·3	19·5	20·9	17·8	25·1	31·6	1·61	19
	3		45	24·15	46·45	13·9	16·5	17·9	14·9	19·8	23·9	1·59	13
	4		60	20·41	39·25	12·6	14·9	16·3	13·0	16·4	19·2	1·49	13
111	1	0·55	15	10·42	20·04	20·9	22·8	23·9	21·4	23·6	25·3	1·30	14
	2		30	12·13	23·33	19·4	22·2	23·6	20·7	24·4	27·2	1·39	15
	3		45	13·27	25·52	15·8	18·4	19·7	16·6	19·1	21·6	1·38	14
	4		60	15·88	30·54	14·9	17·6	19·0	16·1	20·2	23·4	1·47	14
112	1	0·40	10	2·61	5·02	11·9	14·8	16·8	12·0	15·7	18·7	1·53	13
	2		20	3·12	6·00	10·4	13·0	12·4	10·6	14·0	16·9	1·54	11
	3		30	3·52	6·76	8·79	11·0	12·4	8·90	12·4	15·4	1·60	10
	4		45	3·97	7·63	8·42	10·5	11·8	9·04	12·5	15·5	1·59	9
	5		60	3·97	7·63	7·50	9·14	10·3	7·68	9·47	10·9	1·45	7

Table 4-29

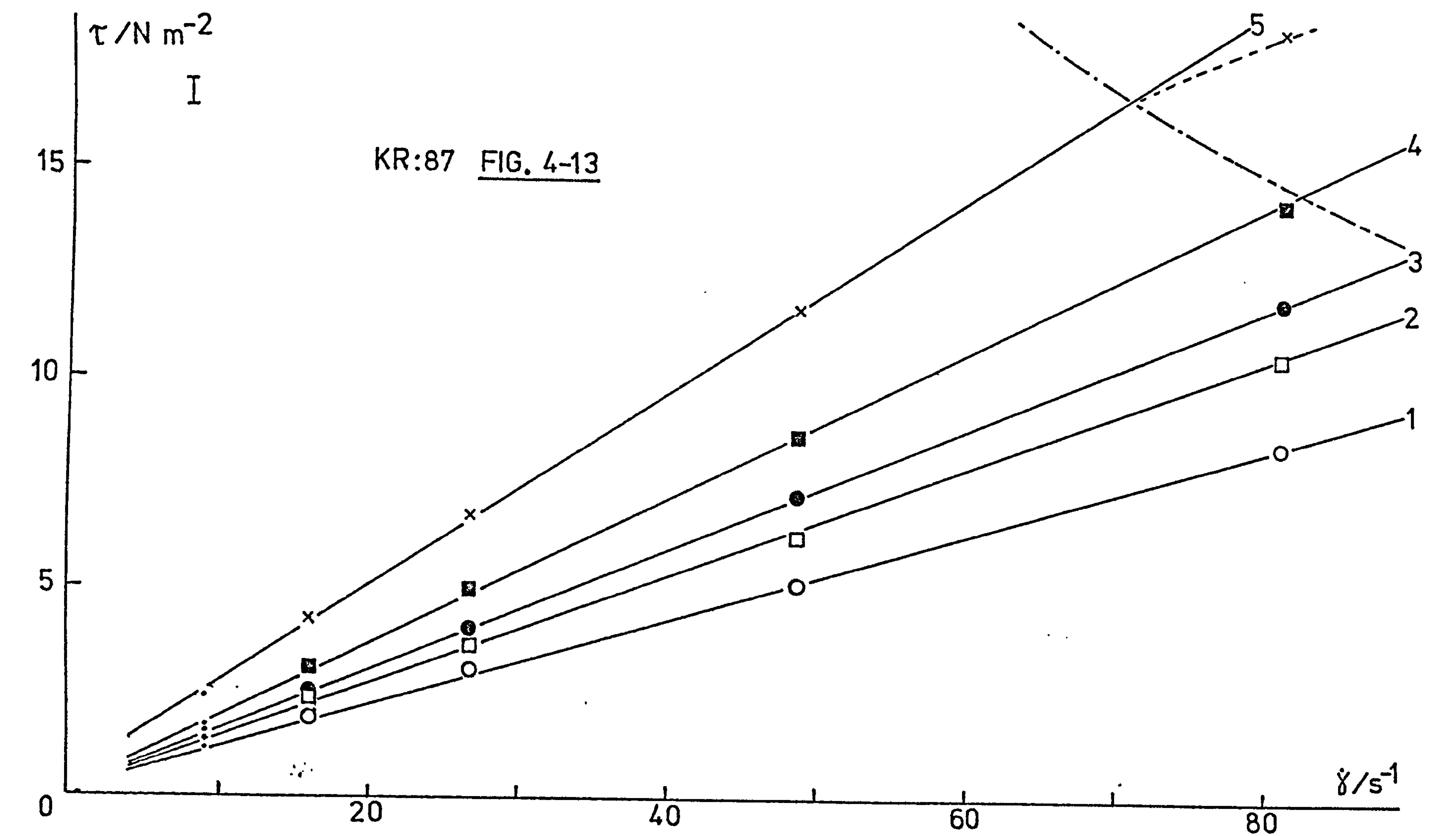
τ /N m⁻²
I
KR:87 FIG. 4-13
15
10
5
0
20
40
60
80
γ̇/s⁻¹
1
2
3
4
5

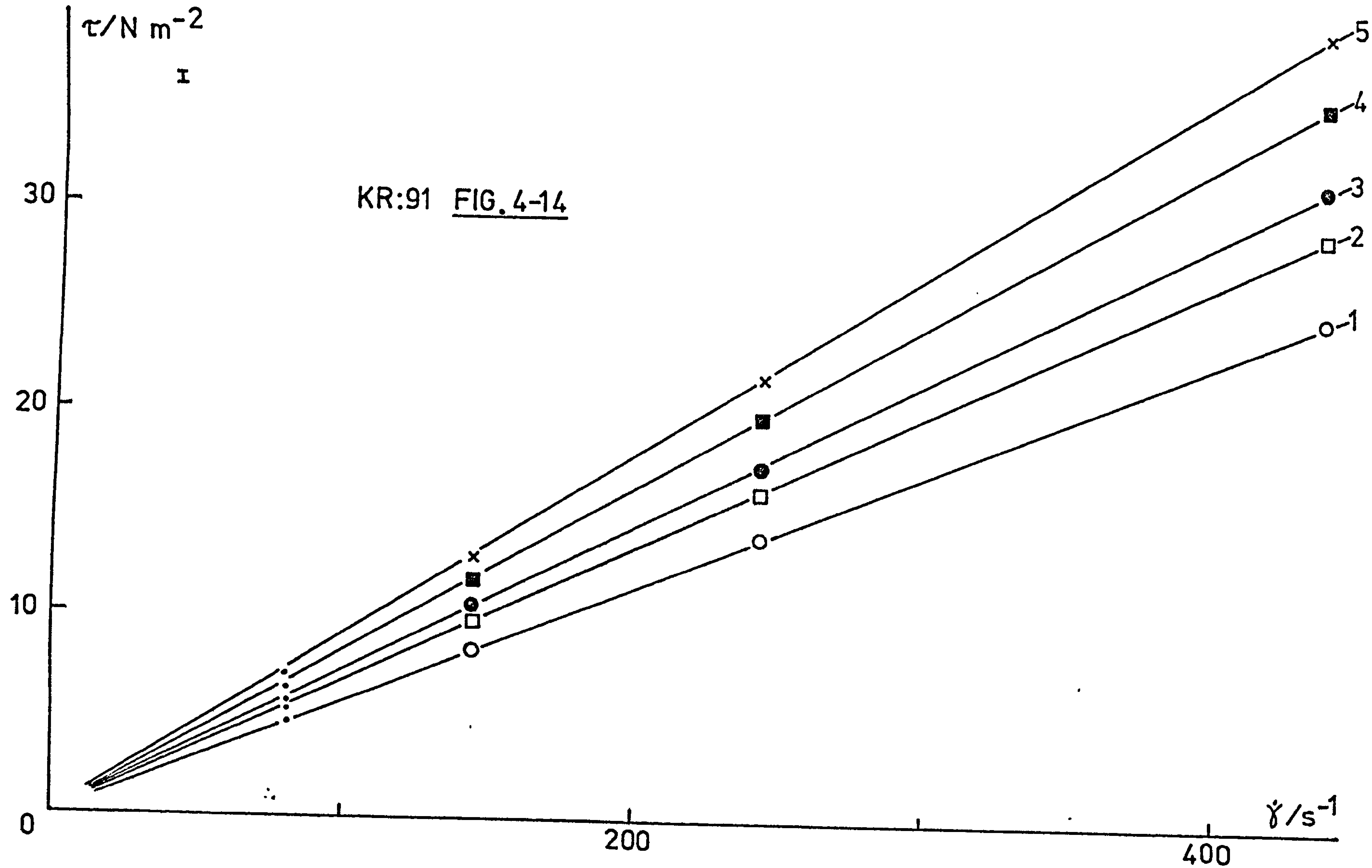

KR:91 FIG. 4-14

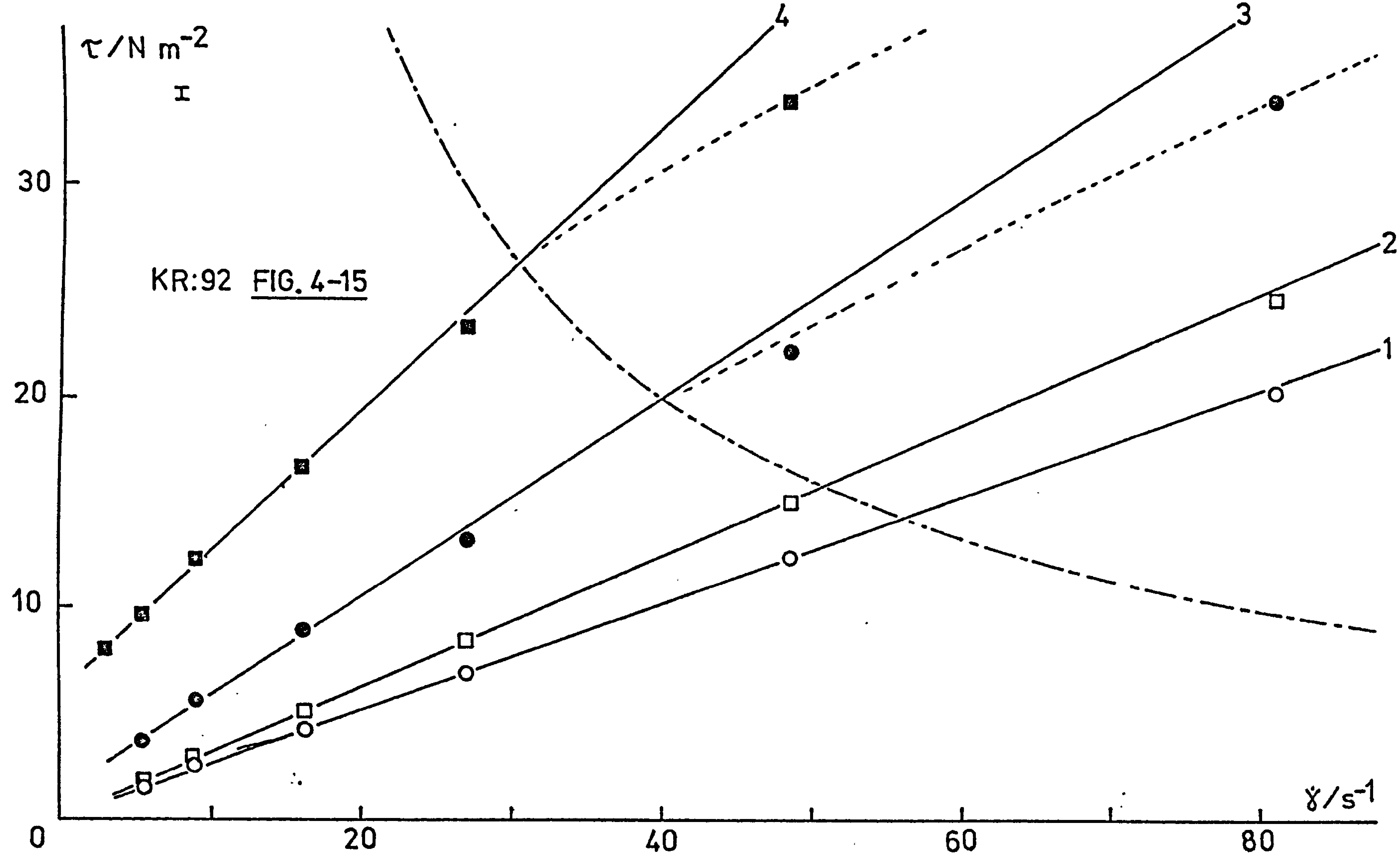

KR:92 FIG. 4-15

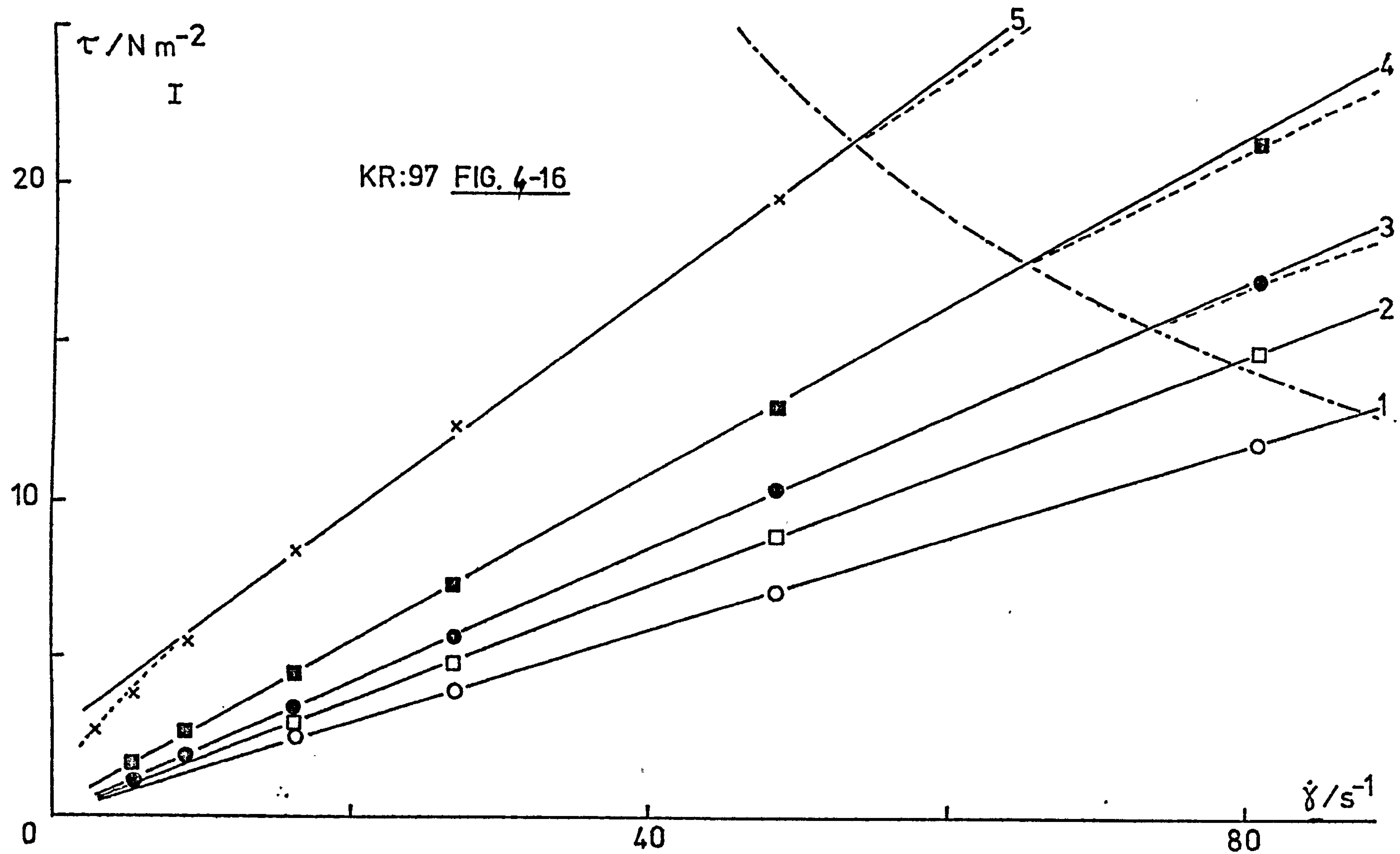

τ / N m^-2
I
KR:97 FIG. 4-16
20
10
0
40
80
γ̇ / s^-1
1
2
3
4
5

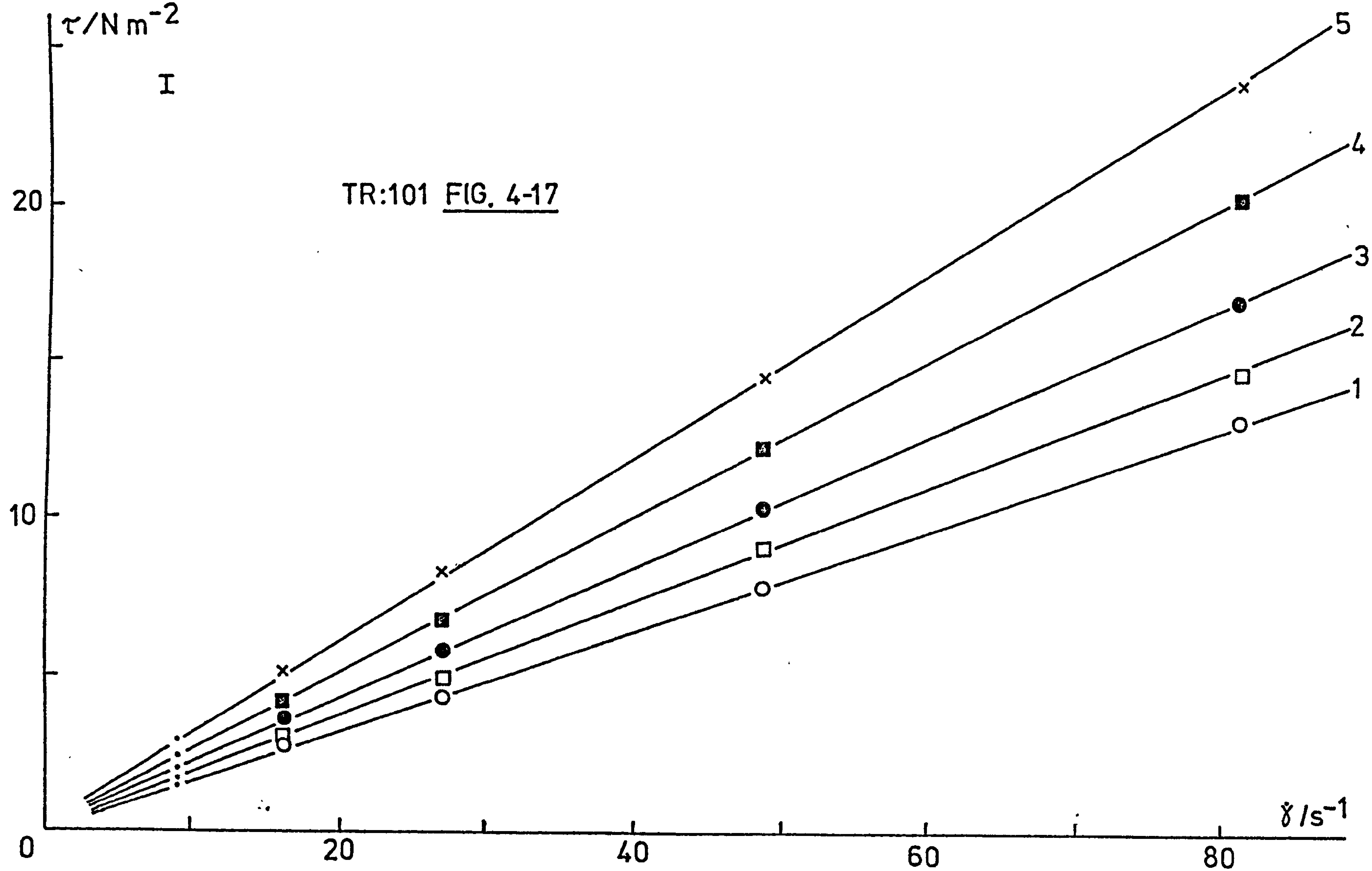

TR:101 FIG. 4-17

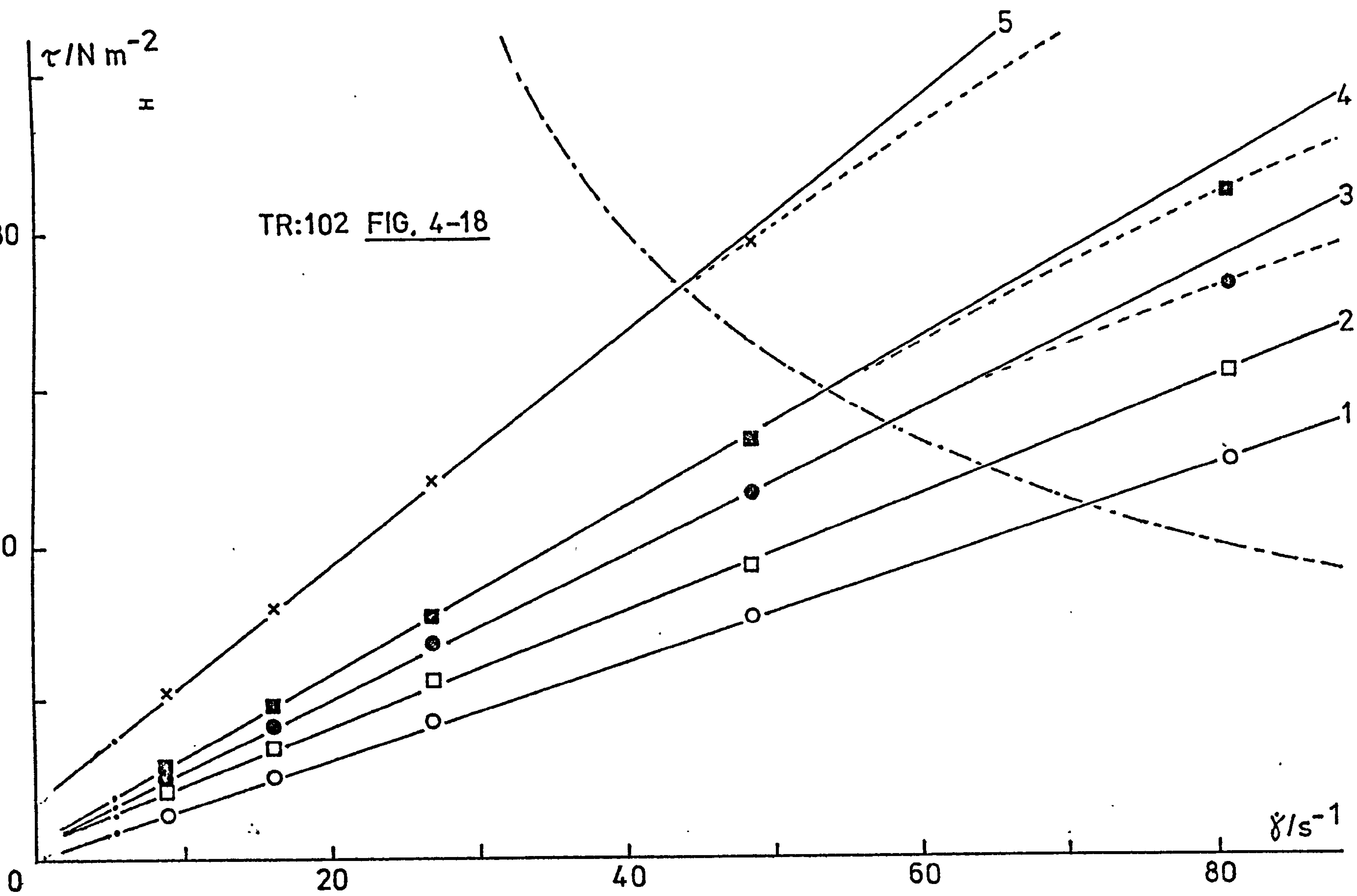

TR:102 FIG. 4-18
τ/N m^{-2}
$\dot{\gamma}$/s^{-1}
0
20
40
60
80
40
80
1
2
3
4
5

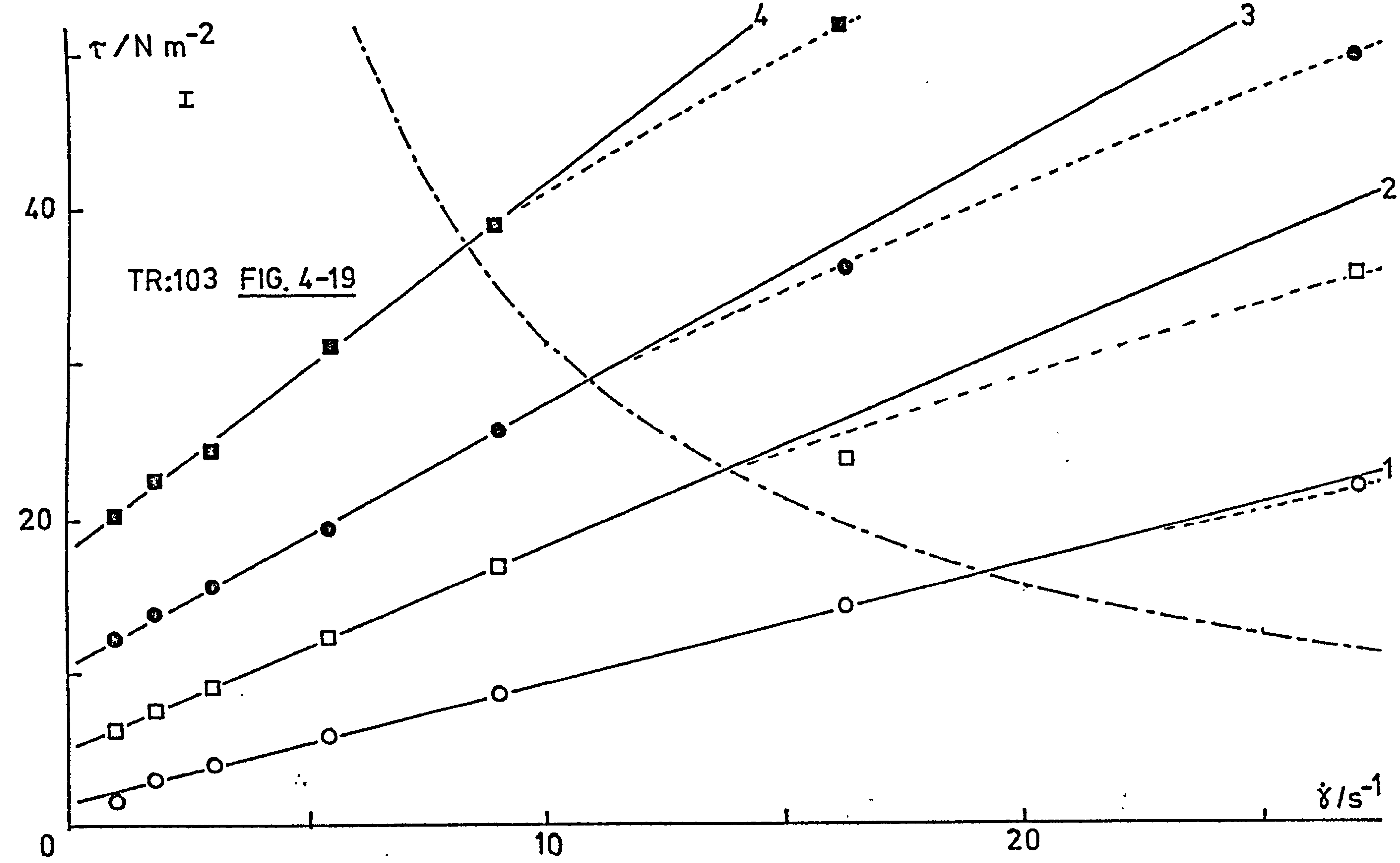

TR:103 FIG. 4-19

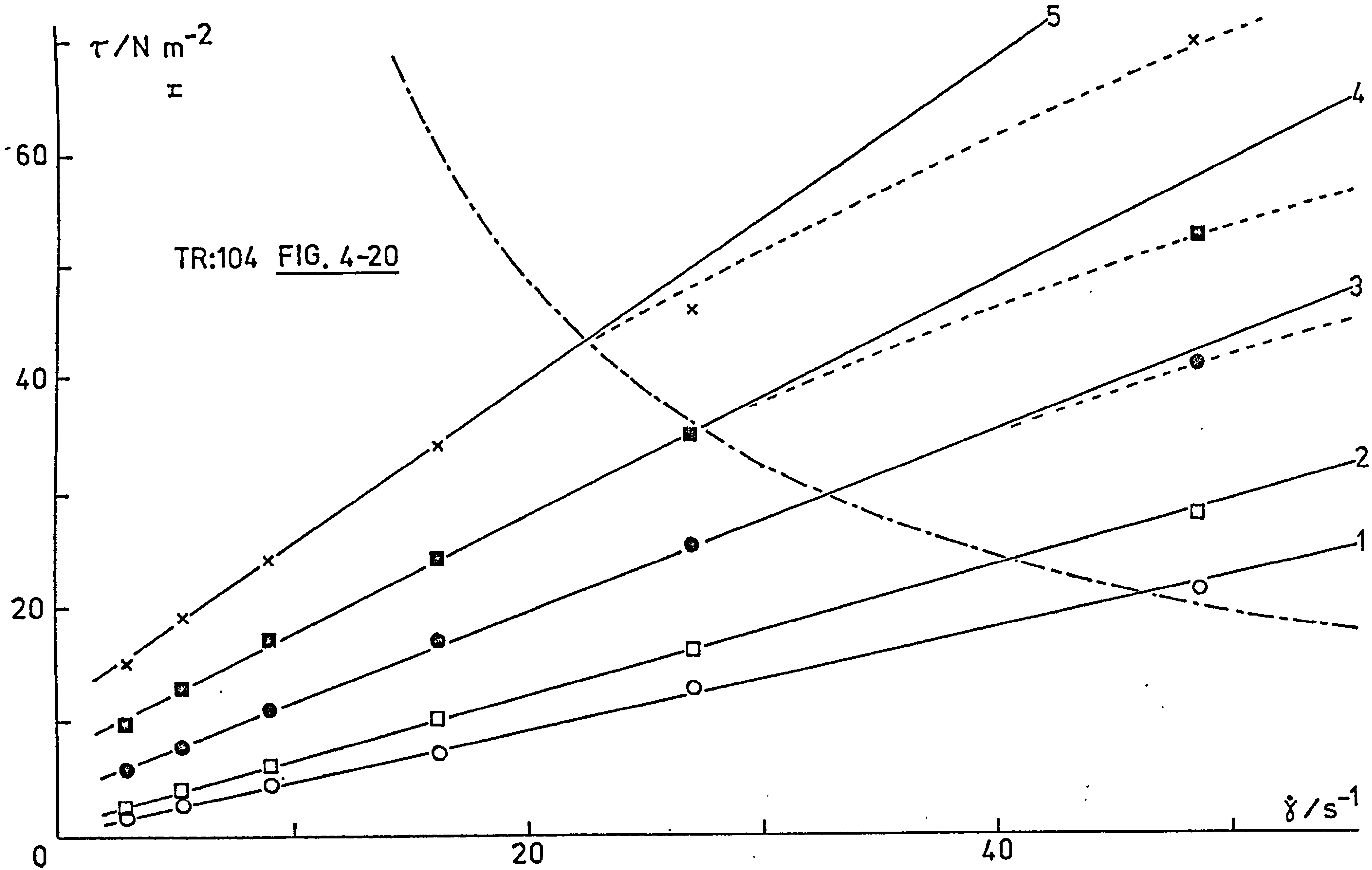
τ/N m⁻²
60
40
20
0
20
40
γ̇/s⁻¹
1
2
3
4
5
TR:104 FIG. 4-20

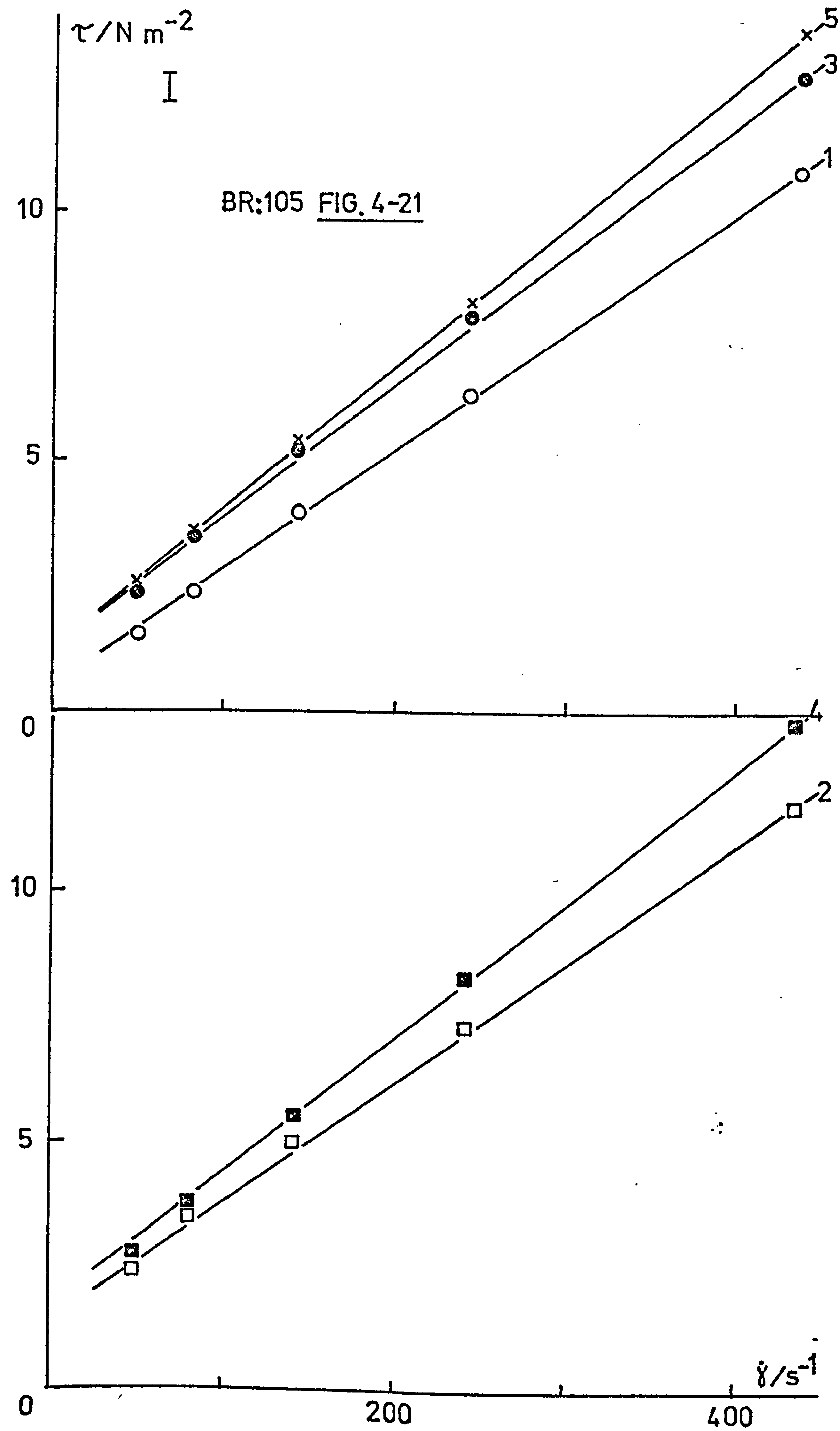

τ/N m^{-2}
I
BR:105 FIG. 4-21
10
5
0
5
3
1
4
2
10
5
0
200
400
$\dot{\gamma}$/s^{-1}

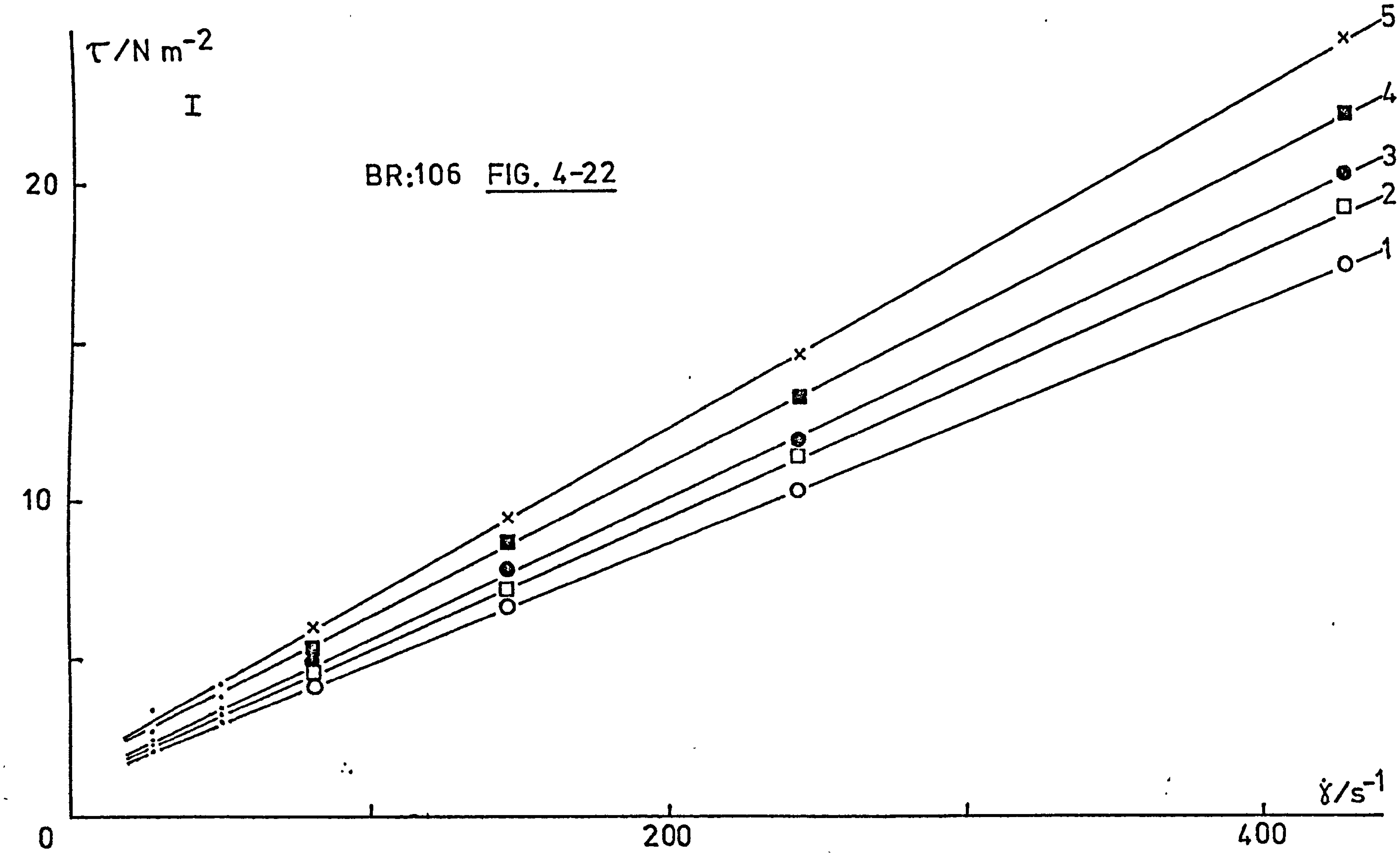

BR:106 FIG. 4-22

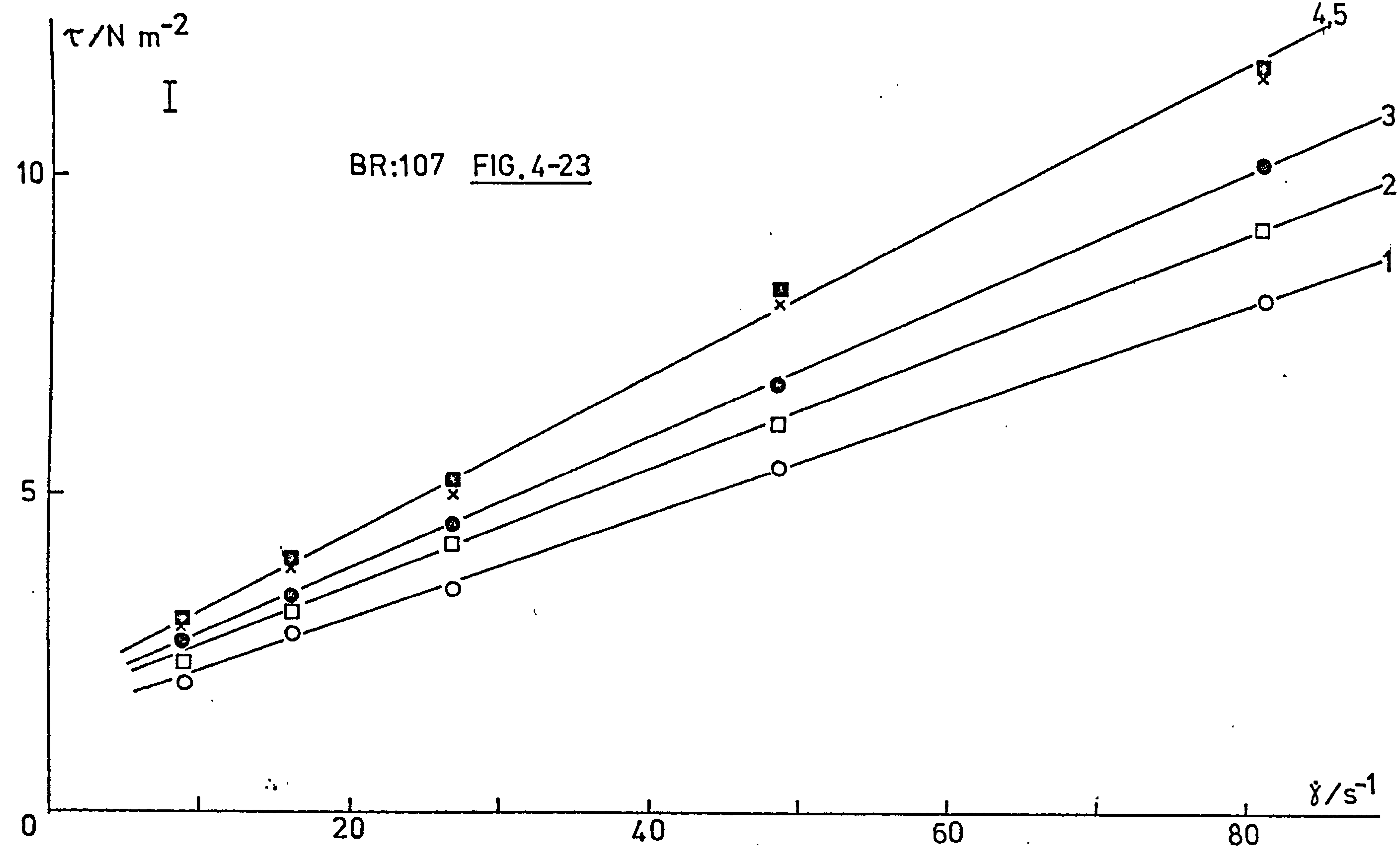
τ/N m-2
I
BR:107 FIG.4-23
10
5
0
20
40
60
80
γ̇/s-1
4,5
3
2
1

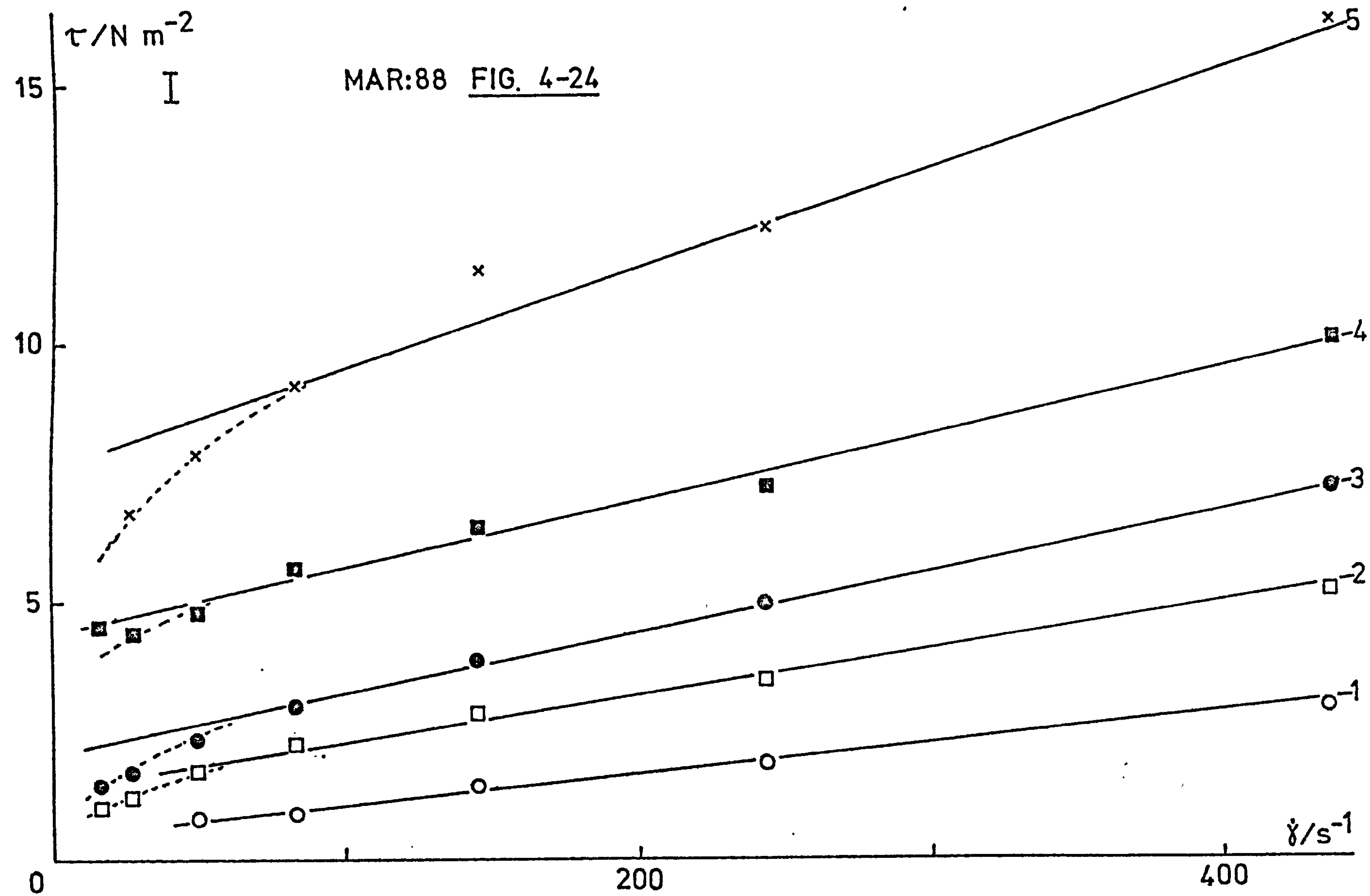

MAR:88 FIG. 4-24

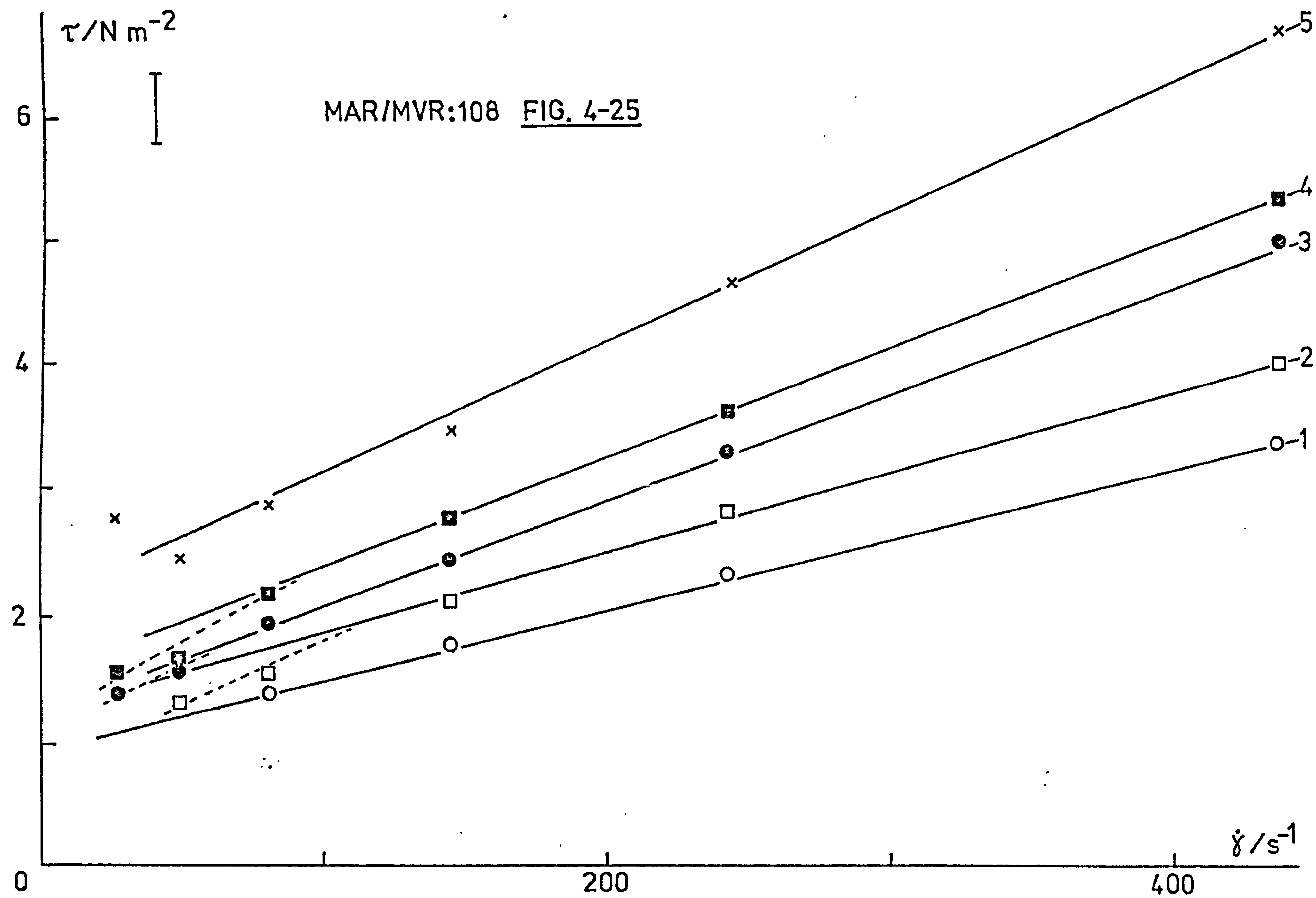

FIG. 4-25

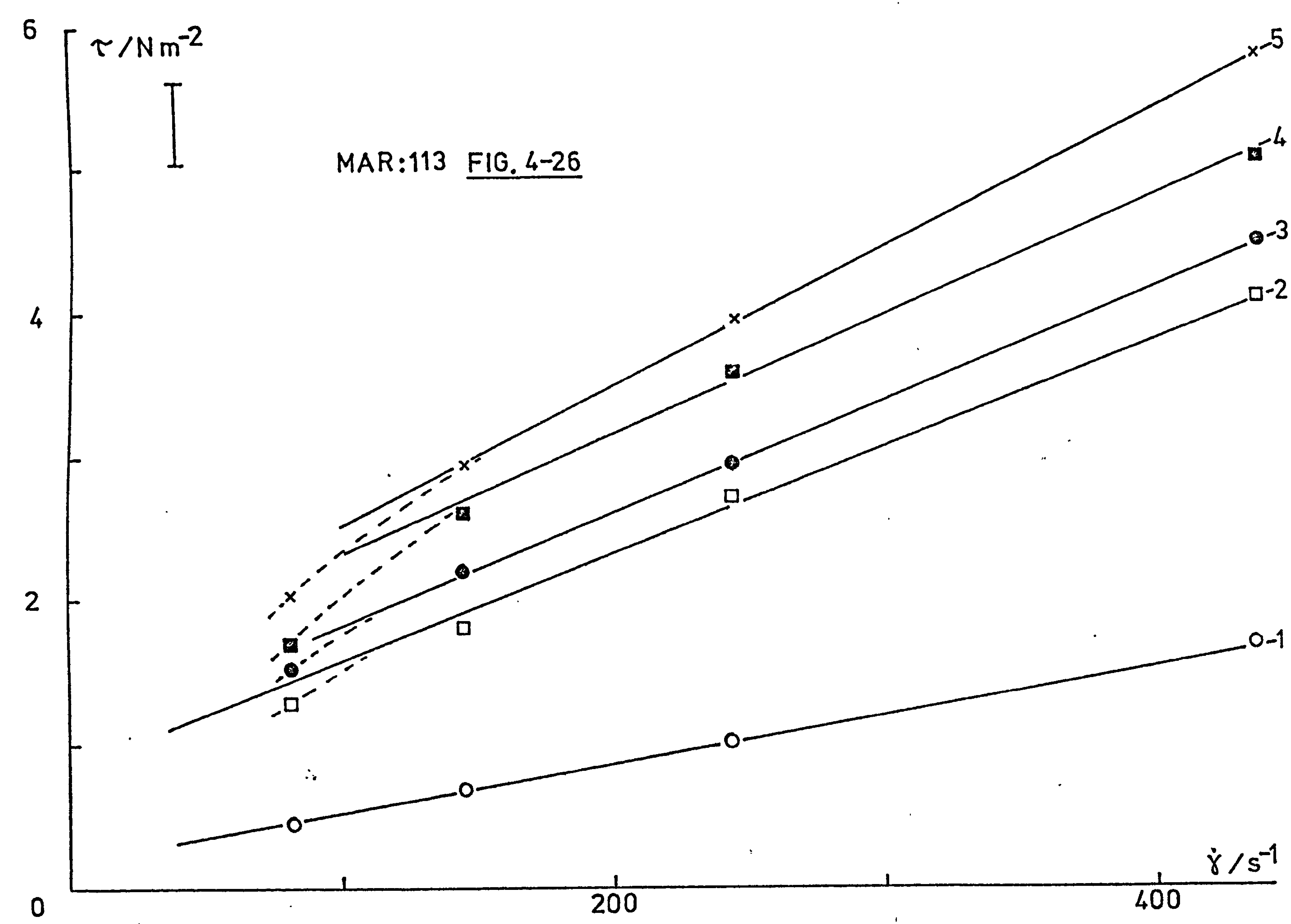
MAR:113 FIG. 4-26
τ / N m^-2
γ̇ / s^-1
6
4
2
0
200
400
5
4
3
2
1

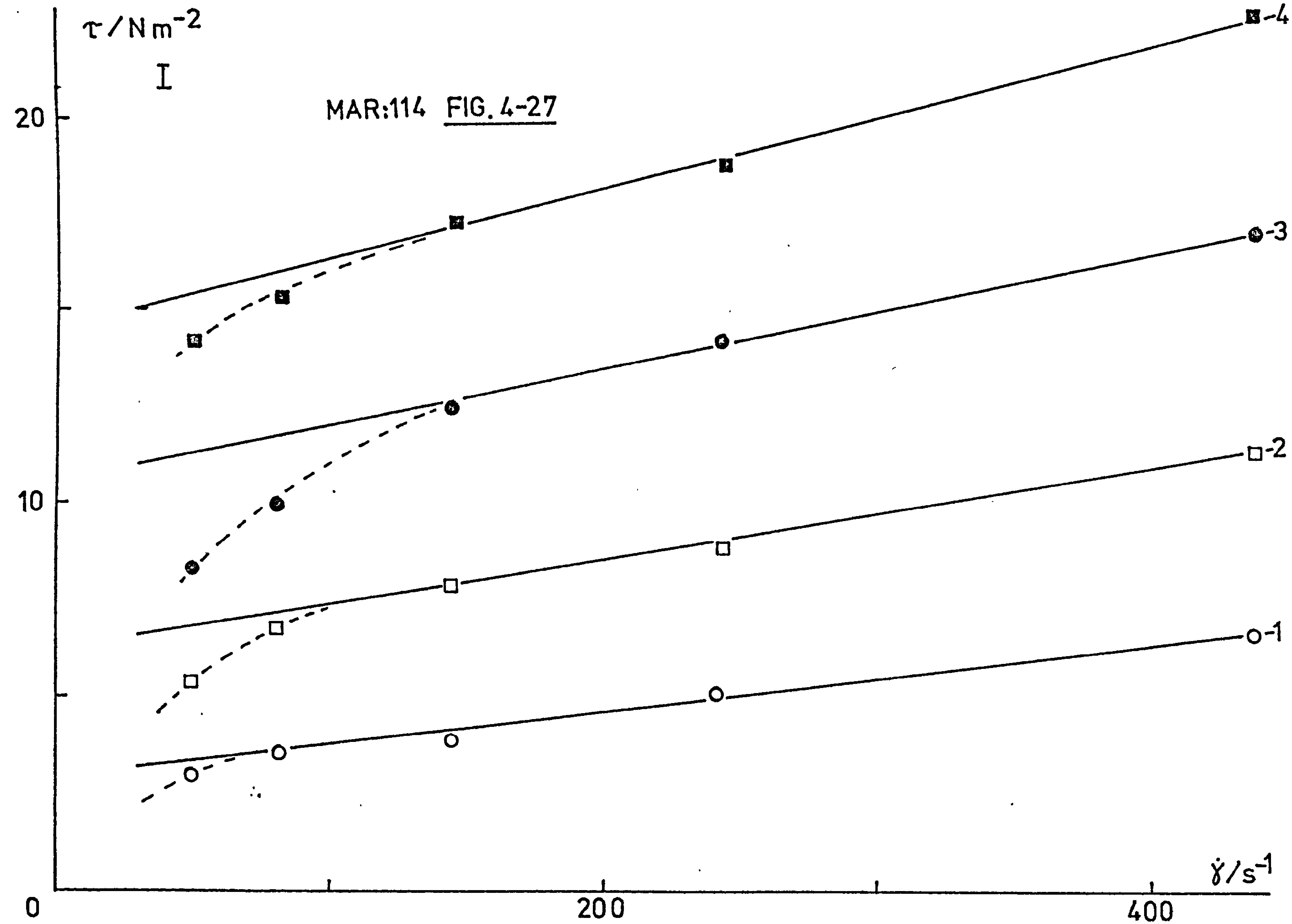

τ / N m⁻²
I
MAR:114 FIG. 4-27
20
10
0
200
400
γ̇ / s⁻¹
-4
-3
-2
-1

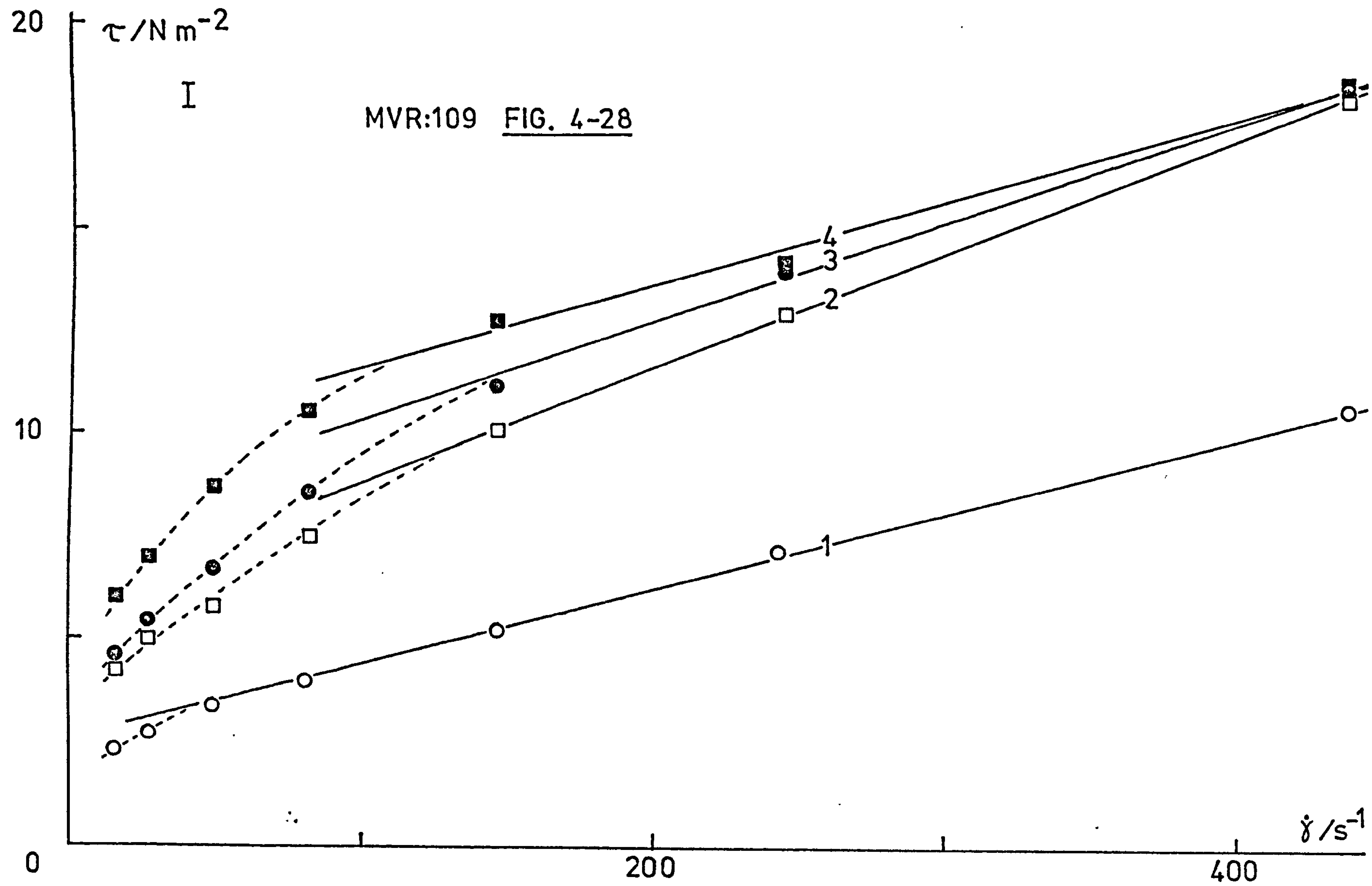

MVR:109 FIG. 4-28

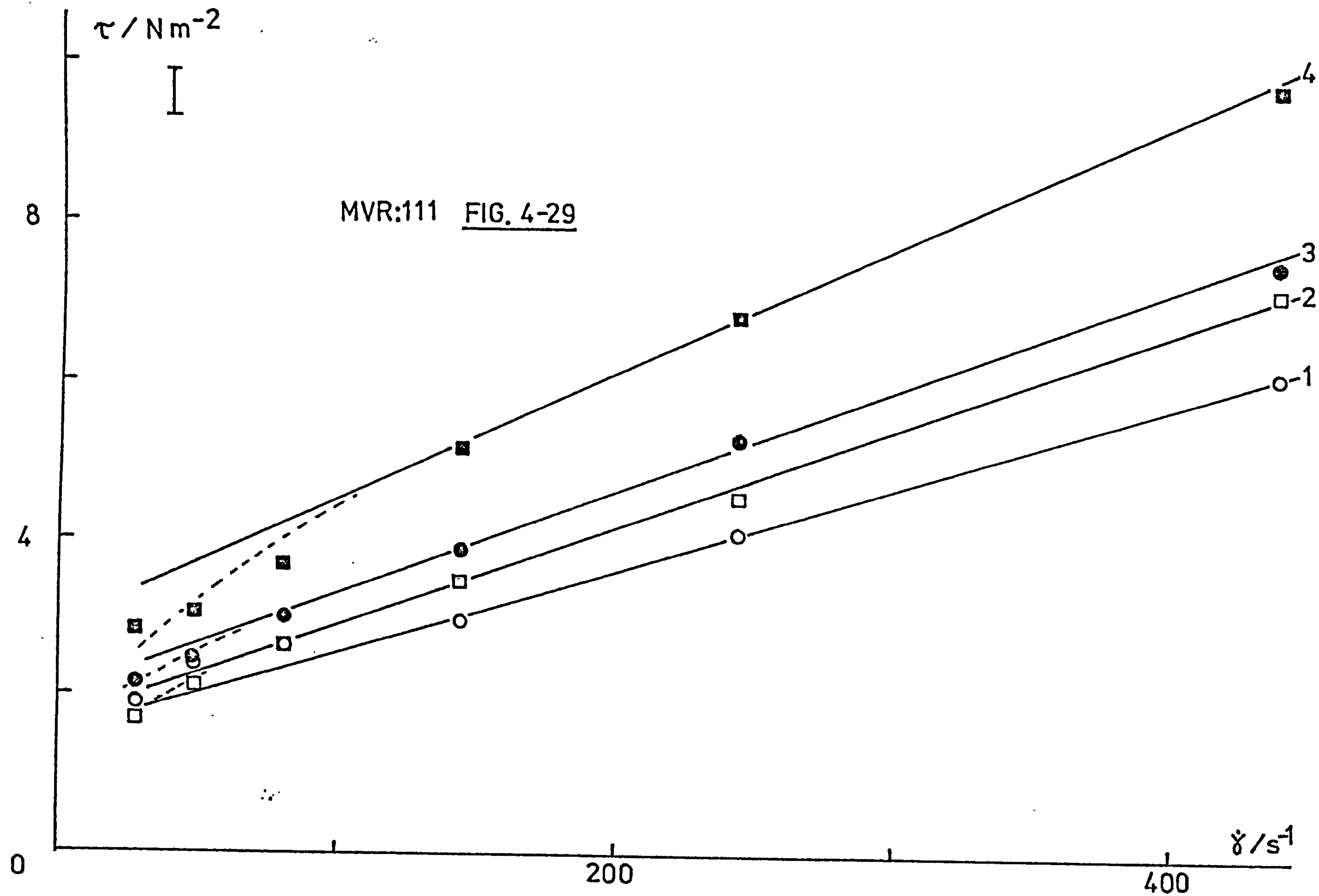

FIG. 4-29

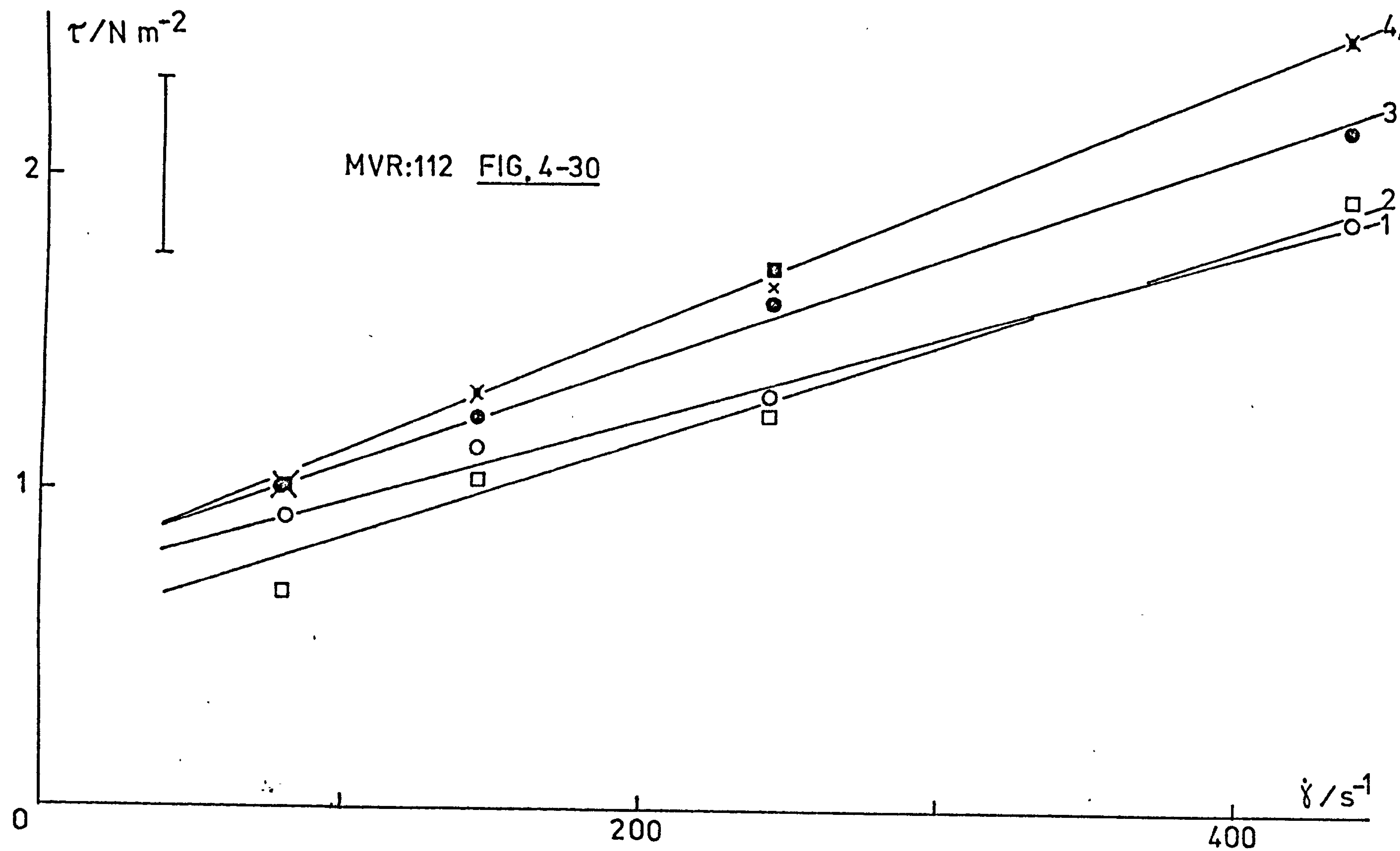
τ/N m⁻²
MVR:112
FIG. 4-30
2
1
0
200
400
γ̇ / s⁻¹
4,5
3
2
1

4.5 Effect of Detergent Addition on Formation Rates

4.5.1 Establishment of Detergent Addition for Inversion

In order to study the effect of detergent on emulsion formation it was first necessary to find the level of detergent required for inversion and then work at concentrations up to that value. All the work in this section was carried out with simulated sea water at $\phi = 0{\cdot}50$ in the "Magimix". Stirring was carried on, with intermittent microscope examination until the emulsion type had been established.

The same procedure was adopted for both sodium dodecyl sulphate and cetyl pyridinium bromide addition. Master solutions were made of both detergents in water. The cationic detergent had to be subjected to ultrasonic irradiation to reach a satisfactory dispersion. Pipetted aliquots from the master solutions were added to the water phase and in the case of cetyl pyridinium bromide complete solution was found to occur. In the earlier emulsions, further detergent solution was added as emulsification progressed, but this was found to make no difference once a W/O emulsion had formed. In the case of the non-ionic detergent, the active ingredient of BP 1100X is oil soluble and so solutions of it were made up in Kuwait crude oil. Details for all three systems are shown in Table 4-30.

In groups KDA and KDC foaming prevented further detergent addition and so it was difficult to find the point of inversion. However, one interesting feature was that although complex formation and a certain amount of water separation occurred after only a few seconds stirring, further stirring produced the characteristic "mousses". So detergent addition below the inversion point only appears to lengthen the stirring time necessary for emulsification.

It is possible that the point of inversion had been reached for KDN:130 for although it had been stirred for only thirty seconds, there was a definite O/W portion. One further feature of this emulsion was the observation of an O/W/O/W/O system after ten seconds stirring.

Emulsion	Master solution g/dm^3	cm^3 detergent solution added	t (secs)	Comments
KDA:93	1	1 (2,4,8, (16,32,64	10 20,30,40) 50,60,70)	No separation. ϕ increasing - no separation.
KDA:98	5	10	10 20	60 cm^3 water separated. No separation.
KDA:99	5	20	10	Foam - complex emulsion.
KDA:100	5	70	10	O/W plus foam
KDC:94	1	1 2,4,8,16	10 (20,30, (40,50	No separation. No separation.
KDC:95	1	16	30	No separation.
KDC:96	1	68	10 30	Very poor emulsion. No separation - foam.
KDN:129	-	0·1cm^3 added directly	10	No separation.
KDN:130	15·74	25	10 20	Complex formation. Complex formation O/W and W/O.

Table 4-30

4.5.2 Rate of Formation

In order to study the effect of detergent in delaying the rate of formation of emulsions, it was necessary to establish the formation rate for each of the crudes. In each case the only delay between stirring was the time taken to dilute a sample and take photomicrographs (about ten minutes). The emulsion details and size data are shown in Table 4-31.

The Kuwait and Tia Juana emulsions were formed with no problems. Because of the high speed of the stirrer, five seconds between stirring was not entirely satisfactory as the time was probably not accurate to more than $\pm$ 1 second. However, this was necessary to obtain a wide range of droplet size throughout the stirring period. This problem was accentuated with Brega as sixty seconds for emulsion 00:116 was too long and the emulsion started to break down much faster than if left after thirty seconds. One of the problems with the photomicroscopy of Brega emulsions was that coalescence was so rapid that the equilibrium reached on the glass slide did not necessarily coincide with that in the mixer. However, there was unfortunately no way of checking this.

Emulsions 00:128 and 00:156 were made at $\phi = 0{\cdot}40$ in an attempt to overcome coalescence. The first signs of coalescence appeared after twenty seconds of stirring in the former, and after thirty seconds in the latter. The droplets appeared to exist in flocs which coalesced before they could be separated or counted. In emulsion 00:147 there was a certain amount of coalescence after each stir. Clearly, an accurate analysis of Brega crude oil is not possible but certain trends are discussed in Chapter 5.

Group 00 Emulsion		t (secs)	oil	G	d_v	d_{sv}	M	x_v	x_{sv}	σ_g	n
115	1	5	K	3·13	4·69	6·06	3·06	4·88	6·66	1·75	12
	2	10		2·56	4·14	5·63	2·46	4·55	6·84	1·90	11
	3	20		2·37	3·17	3·86	2·32	3·23	4·03	1·60	8
	4	30		2·21	2·65	3·03	2·01	2·85	3·59	1·62	16
	5	60		1·86	2·20	2·50	1·74	2·22	2·60	1·49	13
116	1	5	B	3·09	5·71	8·38	2·96	6·36	10·6	2·04	13
	2	10		3·47	5·95	8·19	3·43	6·70	10·5	1·95	13
	3	20		3·86	5·91	7·43	3·88	7·55	11·8	1·95	14
	4	30		3·90	5·80	7·36	3·90	6·31	8·70	1·76	12
	5	60		4·52	5·55	6·22	4·61	6·18	7·52	1·56	10
117	1	5	T	2·72	5·85	9·46	2·43	6·55	12·7	2·25	13
	2	10		2·26	4·12	6·61	2·05	3·81	5·74	1·90	7
	3	20		1·94	2·70	3·47	1·87	2·48	2·98	1·56	12
	4	30		1·85	2·29	2·67	1·79	2·23	2·57	1·46	11
	5	60		1·63	1·89	2·11	1·61	1·78	1·92	1·31	7
128	1	5	B	3·16	5·62	7·89	1·43	6·42	10·5	2·01	17
	2	10		2·64	4·36	6·05	2·53	4·70	7·10	1·90	12
	3	20		2·58	3·68	4·56	1·76	4·14	5·72	1·77	10
	4	30		2·74	4·11	5·19	2·70	4·91	7·32	1·88	12
147	1	5	B	2·74	5·50	8·99	2·57	5·08	8·00	1·95	9
	2	10		2·91	5·23	7·66	2·78	5·88	9·67	2·04	10
	3	20		3·99	6·32	8·17	4·03	7·38	11·1	1·90	16
	4	30		3·38	6·95	9·92	3·27	12·4	30·7	2·59	20
156	1	15	B	2·87	4·58	6·11	2·82	5·07	7·49	1·87	13
	2	30		2·82	4·31	5·53	2·79	5·13	7·70	1·89	12

Table 4-31

4.5.3 Detergent Addition

All three detergents were used in experiments on Kuwait crude, but only the non-ionic BP 1100X active ingredient was added to Tia Juana and Brega crude oils. The dispersed phase concentration of all emulsions in this section was 0·50.

Group KOA comprises the emulsions in which sodium dodecyl sulphate was added to the water. In the cases where the detergent concentration was nearing the amount required for inversion, just one reading was taken after sixty seconds. Prolonged stirring would only have heated the emulsion and caused spurious results. The emulsion details and size data are shown in Table 4-32. Emulsions KOA:146 and KOA:150 both showed complex behaviour in the early stages and after fifteen seconds stirring, the latter was predominately O/W. They also both exhibited a non wetting of the glass walls of the stirrer in contrast to all previous oils which wetted them very well.

The emulsions in which cetyl pyridinium bromide was present in the water phase are grouped as KOC. The details are shown in Table 4-33. All emulsions were formed without difficulty and there was no water separation. One interesting feature is the comparison between emulsion KDC:96 and KOC:127 where similar amounts of detergent were added. In the first, there was separation and complex formation; but in the latter, continuous stirring for the first thirty seconds produced a stable W/O emulsion. This shows the delay-time phenomenon of detergent addition which is emphasised even further by emulsions KOC:151 and 152.

This phenomenon was also exhibited in group KON where BP 1100X active ingredient was made up into a Kuwait crude oil solution at a concentration of 15·74 g/dm^3. The volume of this solution used to make the oil phase up to 125 cm^3 is shown with other details for this group in Table 4-34.

The phenomenon of non-wetting of the glass slides and a metal spatula was shown by the last three emulsions in the series. Simple separation was exhibited in the early stages of stirring in the first three emulsions, but KON:144 and KON:145 both displayed complex formation which disappeared with further stirring. The reason that no data is given for the log-normal equation for KON:145 is the bimodal nature of the distribution. This is shown up in the histogram in Figure 4-31.

As with Kuwait crude, a solution of BP 1100X was made up in Tia Juana crude for group TON at a concentration of 34·1 g/dm^3. The principle of stirring only for sixty seconds and then measuring the separation (provided there was no complex behaviour) was adopted for the later emulsions in this series as well. Bimodal distributions are also shown in emulsions TON:138 and TON:139. However, despite having more detergent, TON:140 does not seem to exhibit this feature. The details for this group are given in Table 4-35.

The influence of a BP 1100X active ingredient solution in Brega crude oil at 8·416 g/dm^3 on emulsification was studied in Group BON. Because of the difficulties with coalescence in a detergent-free sample, the experimental procedure was simplified. Each emulsion was stirred in four bursts for a total of forty-five seconds. The droplet size analysis at this time in each case could then be compared. The intermediate stirring times would give an indication of the delay-time and complex formation. The emulsion details are shown in Table 4-36.

Group KOA	Emulsion	Master soln. g/dm^3	cm^3 soln. added	t (secs)	G	d_v	d_{sv}	M	x_v	x_{sv}	σ_g	n
118	1	5·02	3	10	2·75	4·82	7·27	2·66	4·30	5·91	1·76	12
	2			15	2·54	3·96	5·43	2·45	3·87	5·24	1·74	9
	3			20	2·28	3·10	3·89	2·22	3·00	3·67	1·57	7
	4			30	2·25	2·83	3·28	2·09	3·49	4·92	1·80	18
	5			60	1·85	2·30	2·68	1·73	2·47	3·14	1·63	15
119	1	5·02	6	15	3·02	5·42	7·96	2·91	5·34	8·01	1·89	14
	2			20	2·52	4·02	5·49	2·42	4·31	6·34	1·86	10
	3			30	2·17	3·04	3·86	2·05	3·19	4·28	1·72	7
	4			45	2·08	2·77	3·30	1·98	3·34	4·73	1·81	20
	5			60	1·82	2·22	2·57	1·71	2·31	2·82	1·57	15
120	1	5·02	10	20	2·83	4·98	7·40	2·72	4·61	6·55	1·81	12
	2			25	2·09	3·32	4·59	1·94	3·46	5·10	1·86	8
	3			30	2·01	3·19	4·39	1·75	4·17	7·44	2·14	7
	4			45	1·76	2·51	3·31	1·74	2·26	2·68	1·57	6
	5			60	1·87	2·41	2·88	1·73	2·58	3·37	1·68	17
121	1	5·02	15	25	2·52	4·48	6·49	2·38	5·15	8·63	2·05	12
	2			30	2·29	3·79	5·41	2·13	4·00	6·08	1·91	9
	3			40	1·84	2·84	3·88	1·78	2·68	3·50	1·68	7
	4			55	1·91	2·46	2·96	1·79	2·55	3·23	1·62	17
	5			70	1·82	2·09	2·34	1·74	1·97	2·14	1·33	11
122	1	5·02	18	30	2·67	4·05	5·45	2·62	3·86	5·01	1·66	10
	2			35	2·60	3·67	4·66	2·41	4·08	5·79	1·81	8
	3			45	2·15	2·90	3·65	2·09	2·70	3·21	1·52	6
	4			60	2·02	2·50	2·92	1·89	2·67	3·36	1·62	17
	5			75	1·85	2·25	2·61	1·69	2·24	2·70	1·54	13
146		5·02	25	60	1·89	2·32	2·74	1·76	2·20	2·55	1·47	9
150		9·98	25	60	2·26	3·00	3·70	2·16	3·00	3·74	1·60	7

Table 4-32

Group KOC Emulsion		Master soln. g/dm^3	cm^3 soln. added	t (secs)	G	d_v	d_{sv}	M	x_v	x_{sv}	σ_g	n
123	1	1·02	10	10	2·64	4·24	5·78	2·54	4·39	6·32	1·33	11
	2			15	2·54	3·66	4·79	2·38	3·75	5·07	1·73	7
	3			20	2·25	2·94	3·62	1·95	3·35	4·79	1·82	5
	4			40	2·05	2·52	2·73	1·94	2·51	2·98	1·51	14
	5			60	1·82	2·05	2·24	1·74	1·99	2·18	1·35	11
124	1	1·02	25	15	2·74	4·77	7·00	2·64	4·47	6·35	1·81	12
	2			20	2·39	3·67	4·92	2·29	3·70	5·10	1·76	9
	3			30	2·09	3·16	4·24	1·95	3·27	4·62	1·80	8
	4			45	1·94	2·48	2·97	1·85	2·45	2·96	1·54	5
	5			60	1·88	2·27	2·62	1·70	2·21	2·56	1·46	14
125	1	1·02	40	20	2·29	4·17	6·22	2·06	4·35	7·15	2·02	11
	2			25	2·12	3·10	3·99	2·02	3·26	4·49	1·76	8
	3			35	1·77	2·52	3·31	1·75	2·20	2·57	1·48	6
	4			45	1·90	2·43	2·87	1·82	2·53	3·14	1·60	18
	5			60	1·73	2·12	2·48	1·65	2·01	2·30	1·44	13
126	1	2·01	27	30	2·34	3·95	5·69	2·22	3·81	5·46	1·82	10
	2			35	2·07	3·45	5·11	1·92	3·39	4·94	1·85	8
	3			45	1·88	2·62	3·35	1·73	2·72	3·68	1·73	6
	4			60	1·85	2·32	2·72	1·78	2·32	2·76	1·52	15
	5			75	1·73	2·06	2·36	1·65	2·04	2·35	1·46	13
127	1	2·01	35	35	2·16	3·78	5·99	2·03	3·28	4·52	1·76	8
	2			40	1·99	3·01	4·02	1·84	3·10	4·40	1·80	7
	3			50	1·77	2·50	3·22	1·75	2·32	2·81	1·55	6
	4			60	2·01	2·70	3·27	1·91	3·02	4·10	1·74	20
	5			75	1·74	2·12	2·46	1·64	2·12	2·52	1·51	14
151		3·99	25	60	1·80	2·20	2·59	1·75	2·08	2·32	1·40	5
152		3·99	40	60	1·93	3·05	4·42	1·84	2·68	3·45	1·65	7

Table 4–33

Group KON Emulsion		cm^3 soln. added	cm^3 water separated	t (secs)	G	d_v	d_{sv}	M	x_v	x_{sv}	σ_g	n
131	1	5	-	10	2·54	4·49	6·42	2·38	5·11	8·52	2·04	10
	2			15	2·24	3·94	5·94	2·06	3·59	5·20	1·84	7
	3			25	2·11	3·06	4·04	2·04	2·89	3·65	1·62	6
	4			40	1·95	2·53	3·12	1·87	2·34	2·71	1·47	12
	5			60	1·62	1·96	2·28	1·56	1·86	2·08	1·40	9
132	1	10	-	20	2·66	4·67	7·28	2·58	3·90	5·13	1·69	8
	2			25	2·47	3·64	4·82	2·35	3·50	4·56	1·67	7
	3			30	2·21	3·18	4·04	2·09	3·50	4·95	1·80	19
	4			40	2·03	2·75	3·44	2·12	3·06	3·91	1·64	14
	5			60	1·88	2·34	2·73	1·69	2·53	3·30	1·68	12
133	1	15	-	25	2·35	5·71	9·94	1·81	7·17	17·9	2·61	15
	2			30	2·21	4·83	7·82	1·68	7·39	19·8	2·70	11
	3			40	2·34	3·52	4·66	2·22	3·72	5·26	1·80	8
	4			60	1·85	2·49	3·07	1·75	2·58	3·33	1·66	17
	5			70	1·76	2·16	2·53	1·61	2·24	2·79	1·60	13
144		18	-	60	2·09	4.91	8·93	1·48	4·85	10·7	2·44	8
145		22	11	60	2·08	6·82	12·4					

Table 4-34

FIG. 4-31

Group TON Emulsion	Sample	cm^3 soln. added	cm^3 water separated	t (secs)	G	d_v	d_{sv}	M	x_v	x_{sv}	σ_g	n
137	1	5	-	35	2·05	3·94	6·25	1·95	3·51	5·18	1·87	10
	2			40	2·07	3·60	5·26	2·02	3·42	4·86	1·81	10
	3			50	1·77	2·54	3·32	1·72	2·48	3·16	1·64	6
	4			60	1·85	2·48	3·07	1·79	2·38	2·89	1·65	17
	5			75	1·76	2·23	2·69	1·60	2·18	2·68	1·58	14
138	1	10	-	40	2·89	9·03	13·5					
	2			45	3·25	9·12	12·7					
	3			50	3·69	9·50	12·6					
	4			60	3·25	8·77	12·1					
	5			75	3·12	7·65	10·4					
139		15	72	60	1·47	4·97	9·31					
140		20	103	60	1·58	4·19	7·38	1·37	4·91	11·5	2·52	17
143	1	8	-	40	2·05	3·66	5·59	1·76	3·91	6·66	2·07	8
	2			45	1·93	2·79	3·65	1·79	2·74	3·64	1·71	6
	3			50	1·76	2·42	3·14	1·64	2·21	2·69	1·56	4
	4			60	1·73	2·16	2·56	1·69	2·00	2·23	1·40	13
	5			75	1·63	2·02	2·39	1·59	1·85	2·05	1·37	11
Group BON Emulsion												
141		5	-	45	4·76	7·33	9·17	4·70	11·1	19·7	2·13	10
142		10	-	45	3·98	7·51	11·3	3·33	10·2	21·1	2·34	9
148		15	-	45	2·58	5·50	8·92	2·40	4·94	7·98	2·00	11
149		25	-	45	1·75	2.30	2·86	1·66	2.15	2·54	1·51	11

Table 4-35

Table 4-36

The first two emulsions appeared to follow the trend so far with increasing coalescence, but no complex formation or separation. However, despite BON:148 showing a minimal separation and complex behaviour after fifteen seconds and pronounced coalescence after twenty-five seconds, after forty-five seconds there was no apparent coalescence and the sample seemed less prone to clumping of droplets than the detergent-free emulsions in group 00. Emulsion BON:149 was similar, but instead of complex formation, there appeared to be areas of water within the oil without any interface - the water would just "merge" into the oil. Very little coalescence occurred on the slide, and there was no immediate water separation in the emulsion.

4.6 Ageing Observations

These were generally carried out on the emulsions listed in section 4.5. All the way through this work, each completed emulsion was stored in a corked conical flask on a shelf in the laboratory. From the outset it was clear that the emulsions were exceptionally stable. Some were kept under these conditions for over four years without any signs of breakdown or even coalescence. The characteristic signs of ageing were exhibited by the early Kuwait emulsions, e.g. KM:1, 14, 15, 16 with $\phi = 0{\cdot}5$ or $0{\cdot}6$ and are as follows. A certain amount of syneresis occurred(4 or 5 cm^3 of oil) although this may have been creaming with submicron water droplets. The emulsion, through the walls of the flask, appeared to darken, although the interior was still the characteristic light brown colour. The consistency generally remained very stiff and no visible water separation occurred.

Details of the various emulsion systems on ageing are shown in Table 4-37. The state of the emulsion is described mainly in a qualitative manner. This is because the main aim of the work was the initial effect of detergent in the emulsion; however, general features of interest have been noted. Size data where feasible (i.e. no continual coalescence or unmeasureable water separation) is shown in Table 4-38.

Group 00 Emulsion	Time Aged	Comments
116	24 hours	Separation of large water droplets.
116	7 days	Considerable separation and continual coalescence.
116	14 days	Many droplets visible to naked eye.
128	7 days	Lot of oil separation, but no apparent water separation; many drops visible by eye.
147	24 hours	Droplets can be seen with naked eye.
115	11 months	Typical ageing Kuwait emulsion (see text.
116	11 months	Heavy creaming; a little water separation.
117	11 months	Very stiff emulsion; light oil separation.
128	11 months	Heavy creaming; a few drops visible in bottom.
147	11 months	Heavy creaming; a few cm^3 of water separated.
156	11 months	Heavy creaming; no apparent separation.
Group KOA		
118 - 121	5 days	Great amount of clustering - droplets difficult to separate. (Progressive through series).
118 - 121	7 days	Clusters more pronounced.
122	3 days	Clusters occur on the microscope slide.
122	7 days	Clusters occur on the microscope slide.
146	24 hours	A great amount of clustering.

Table 4-37

cont'd.

Table 4-37 cont'd.

Group KOA Emulsion	Time Aged	Comments
118	11 months	Substantial creaming - coalescence observed in cream. Lower emulsion stiff, no breaking and light brown.
119	11 months	As 118 - less creaming, but dark lower emulsion.
120	11 months	As 118 - lower emulsion darker still.
121	11 months	As 118 - signs of lower emulsion breaking.
122	11 months	As 121, lower emulsion less rigid.
146, 150	11 months	Complete separation.
Group KOC		
123 - 127	11 months	Cream shows breaking - but lower emulsion rigid - all are the same.
151	11 months	Heavy cream, slight separation of lower emulsion.
152	11 months	About 50 cm^3 of water separated. Water dark brown in colour.
Group KON		
132,133	24 hours	Clustering apparent.
132,133	3 days	Clustering more pronounced.
144	24 hours	Slight water separation.
145	24 hours	Slight water separation.
131 - 133	11 months	Creaming with stiff light brown lower emulsion. Slight separation under each.
144 - 145	11 months	Considerable but not complete separation.
Group TON		
139,140	24 hours	A little (immeasurable) separation.
139	3 days	Some further water separation. (79 cm^3 altogether).
140	3 days	Some further water separation. (106 cm^3 altogether).
143	24 hours	Very pronounced clumping.
137	11 months	Light cream with very stiff emulsion.
138	11 months	Very runny, no separation but very large drops.
143	11 months	Like 138 but slightly stiffer.
139,140	11 months	Apparently total separation.

cont'd.

Table 4-37 cont'd.

Group BON	Time Aged	Comments
141,142	24 hours	Complete water separation.
148,149	24 hours	Pronounced water separation.
148	11 months	Separation of 50 cm^3 of water

Table 4-37

Group OO Emulsion	G	d_v	d_{sv}	M	x_v	x_{sv}	σ_g	Time Aged
115	1·86 1·93	2·11 2·21	2·33 2·45	1·81 1·90	2·02 2·11	2·18 2·27	1·49 1·31	7 days 14 days
Group KOA								
118	1·91 1·66	2·36 1·99	2·74 2·27	1·86 1·61	2·31 2·02	2·67 2·36	1·46 1·49	5 days 7 days
119	1·87 1·80	2·18 2·15	2·46 2·46	1·77 1·67	2·13 2·11	2·40 2·47	1·42 1·49	5 days 7 days
120	1·94 1·81	2·42 2·23	2·84 2·60	1·88 1·74	2·45 2·18	2·92 2·53	1·57 1·47	5 days 7 days
121	1·95 1·67	2·33 2·19	2·67 2·69	1·85 1·58	2·33 2·13	2·72 2·59	1·48 1·56	5 days 7 days
122	1·65 1·86	1·95 2·02	2·22 2·16	1·67 1·82	1·92 1·92	2·10 1·99	1·36 1·21	1 day 7 days
Group KOC								
123	1·55	1·88	2·18	1·46	1·79	2·04	1·44	24 hours
124	1·83	2.31	2·73	1·74	2·41	3·01	1·60	24 hours
125	1·61	1·99	2·33	1·54	1·95	2·28	1·49	24 hours
126	1·77	2·28	2·76	1·61	2·29	2·89	1·62	24 hours
127	1·92 1·91	2·34 2·29	2·72 2·63	1·79 1·84	2·32 2·21	2·75 2·49	1·52 1·42	24 hours 7 days

Table 4-38 cont'd.

Table 4-38 cont'd.

Group KON Emulsion	G	d_v	d_{sv}	M	x_v	x_{sv}	σ_g	Time Aged
133	1·62	2·10	2·53	1·57	2·00	2·34	1·49	8 days
Group TON								
139	1·81	5·52	11·9	-	-	-	-	3 days
140	1·84	4·11	7·66	1·50	2·90	4·49	1·94	3 days

Table 4-38

4.7 Freeze Etching Studies

Plates 4 and 5 show the results of the preliminary investigations carried out into the technique using emulsions A:202 and KM:1. Attempts to make replicas of model crude oil emulsions or of Kuwait crude oil alone failed. In the first case the oil phase was soluble in the refrigerant and was cooled in liquid nitrogen. The resulting slower freezing time led to a breakdown of the emulsion system. The Kuwait crude oil specimen shattered as soon as the knife struck it. Evidently the water droplets in an emulsion provide an internal structure which overcomes this problem. In both cases, replicas might have been obtained had the spray freezing technique described by Bachmann and Schmitt [82] been available.

Once the optimum values of specimen temperature, etching time and replica cleaning had been established on the above emulsions, a further series of emulsions were studied (shown in Table 4-39).

Emulsion	Water Phase	ϕ	t (secs)	Table Temp. θ_c	Etching time (secs)
KF:45 *	Deionised	0·50	60	-108K	60
KF:91 * ‡	Salt	"	60	-108K	60
TF:103*	Salt	0·60	60	-105K	60
BF:153	Salt	0·60	45	-108K	60
TF:154	Deionised	0·60	75	-105K	60
BF:155	Deionised	0·60	45	-102K	60

* Originally made in groups KS, KR and TR.

‡ The cream on top of this emulsion was separated and used.

Table 4-39

As the various replicas were examined in the electron microscope, features of interest that appeared were photographed. These are shown in the remaining plates (6 - 18) but are discussed in Chapter 5.

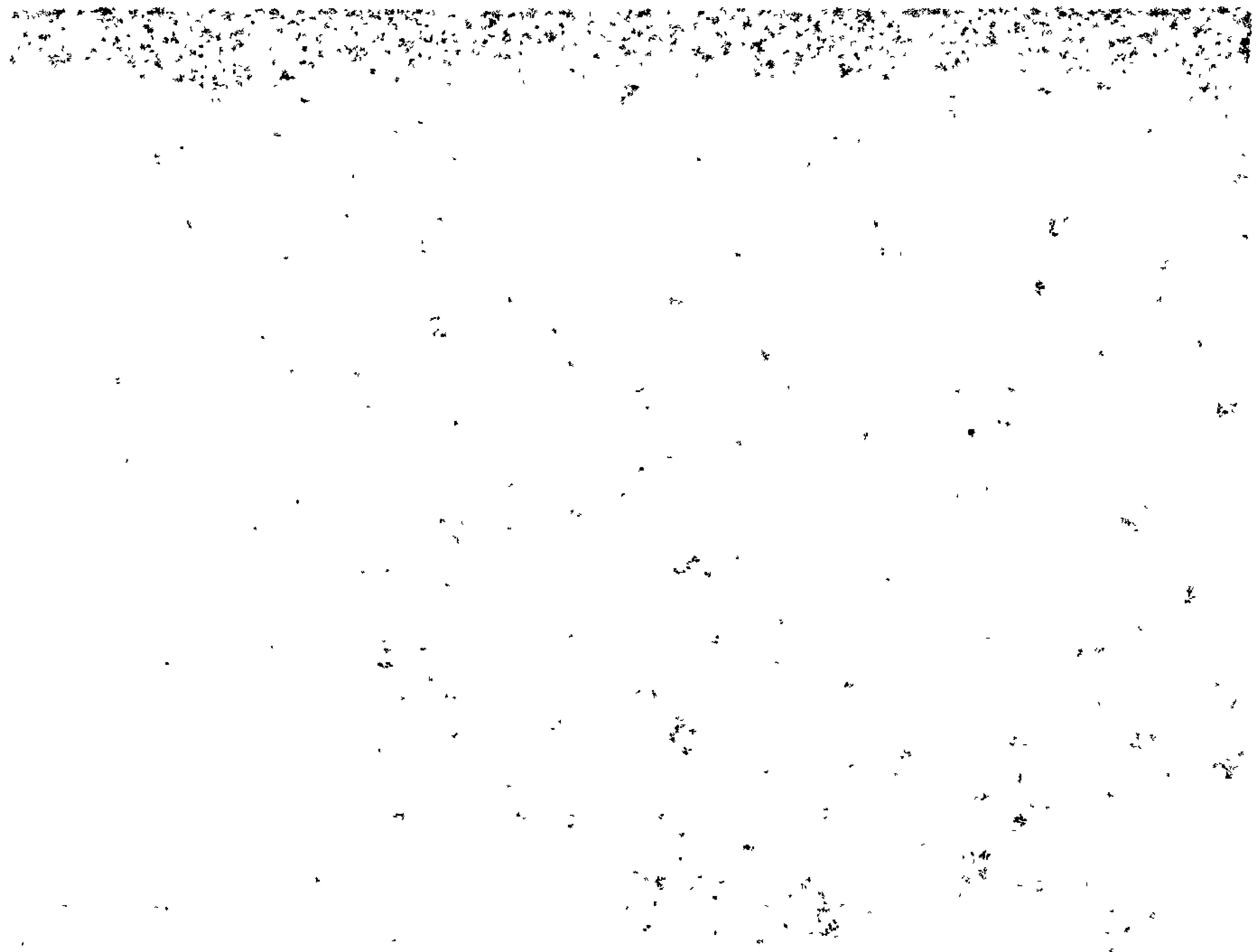

Plate 4 Emulsion A:202 (X6,400)

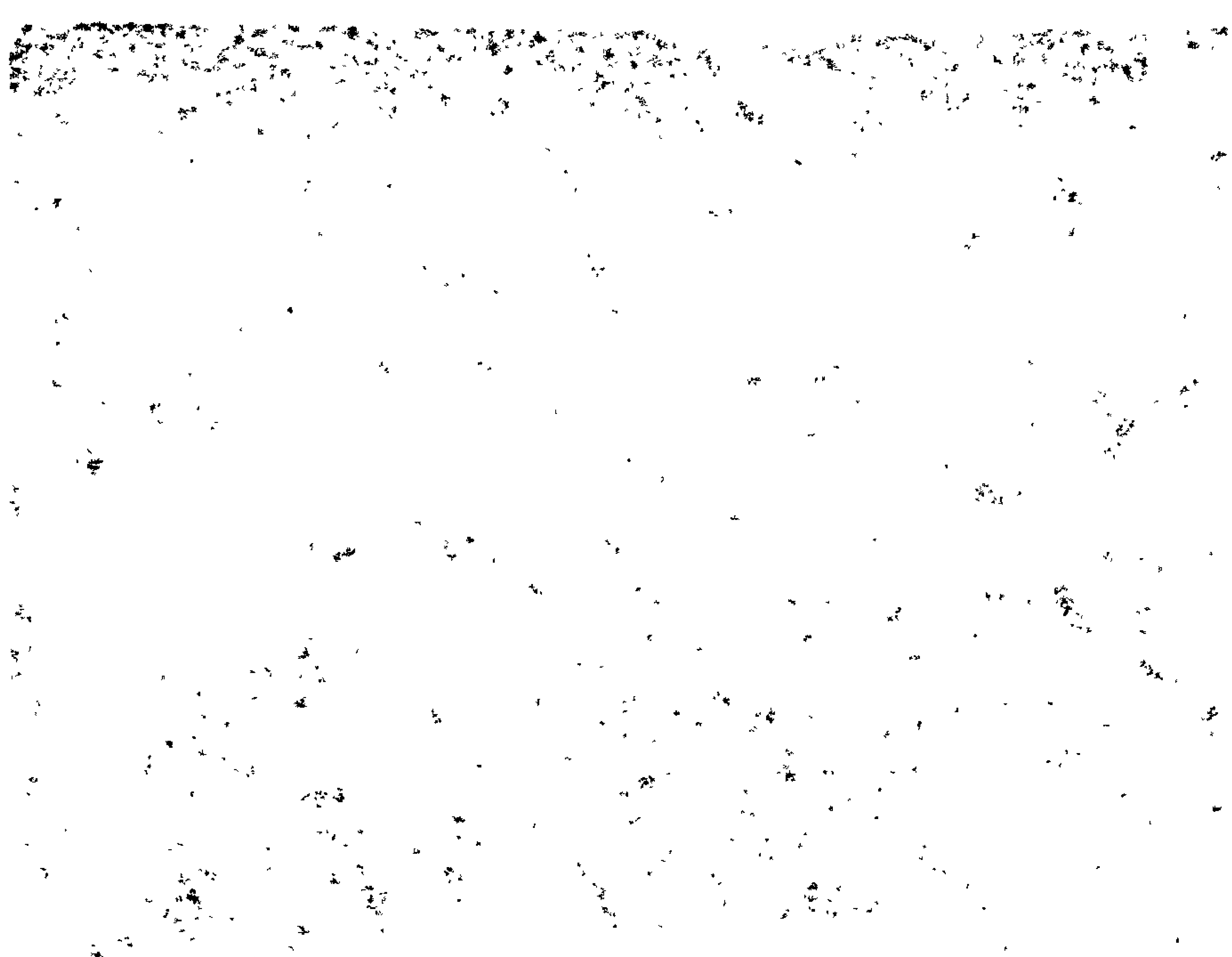

Plate 5 Emulsion KM:1 (X6,400)

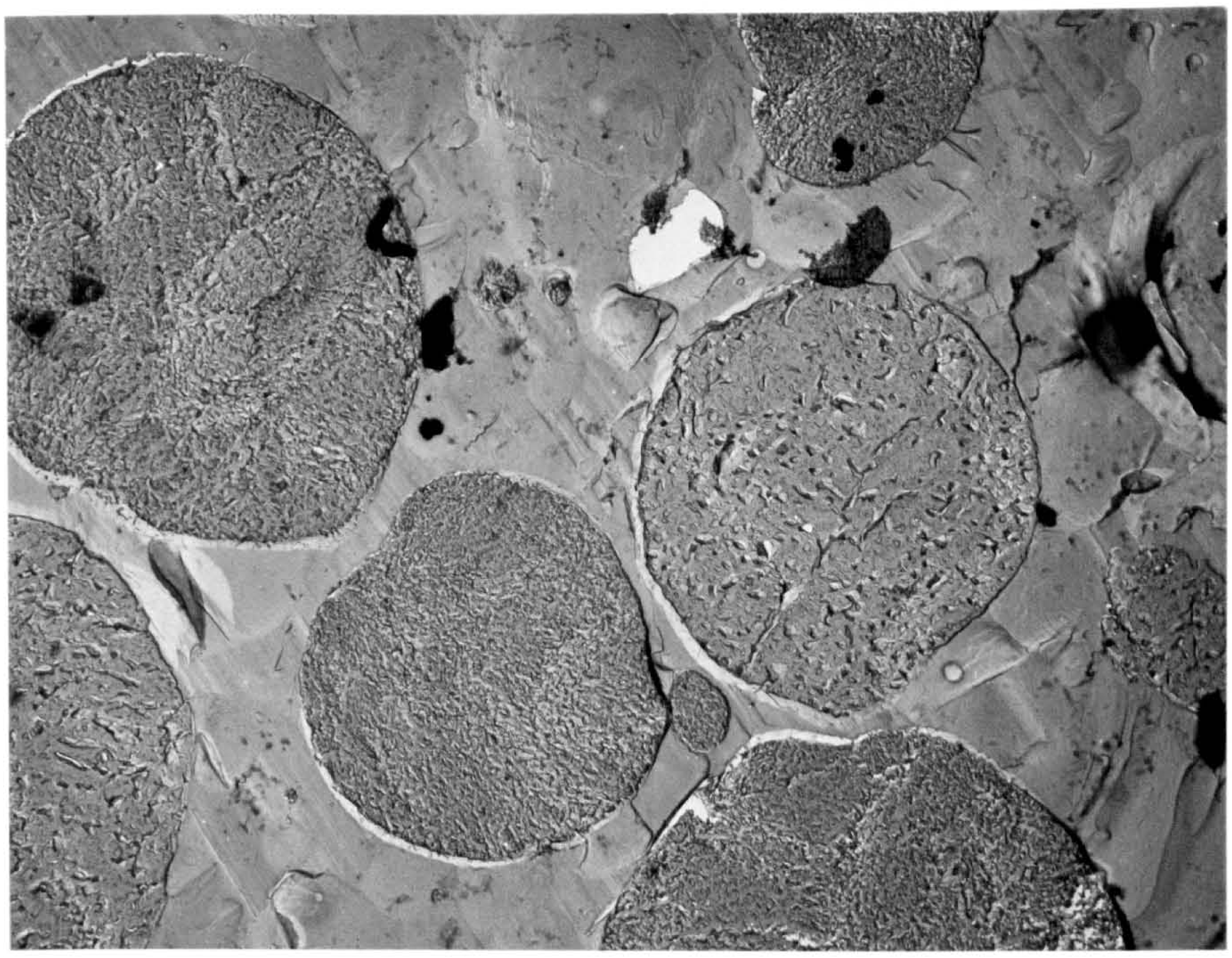

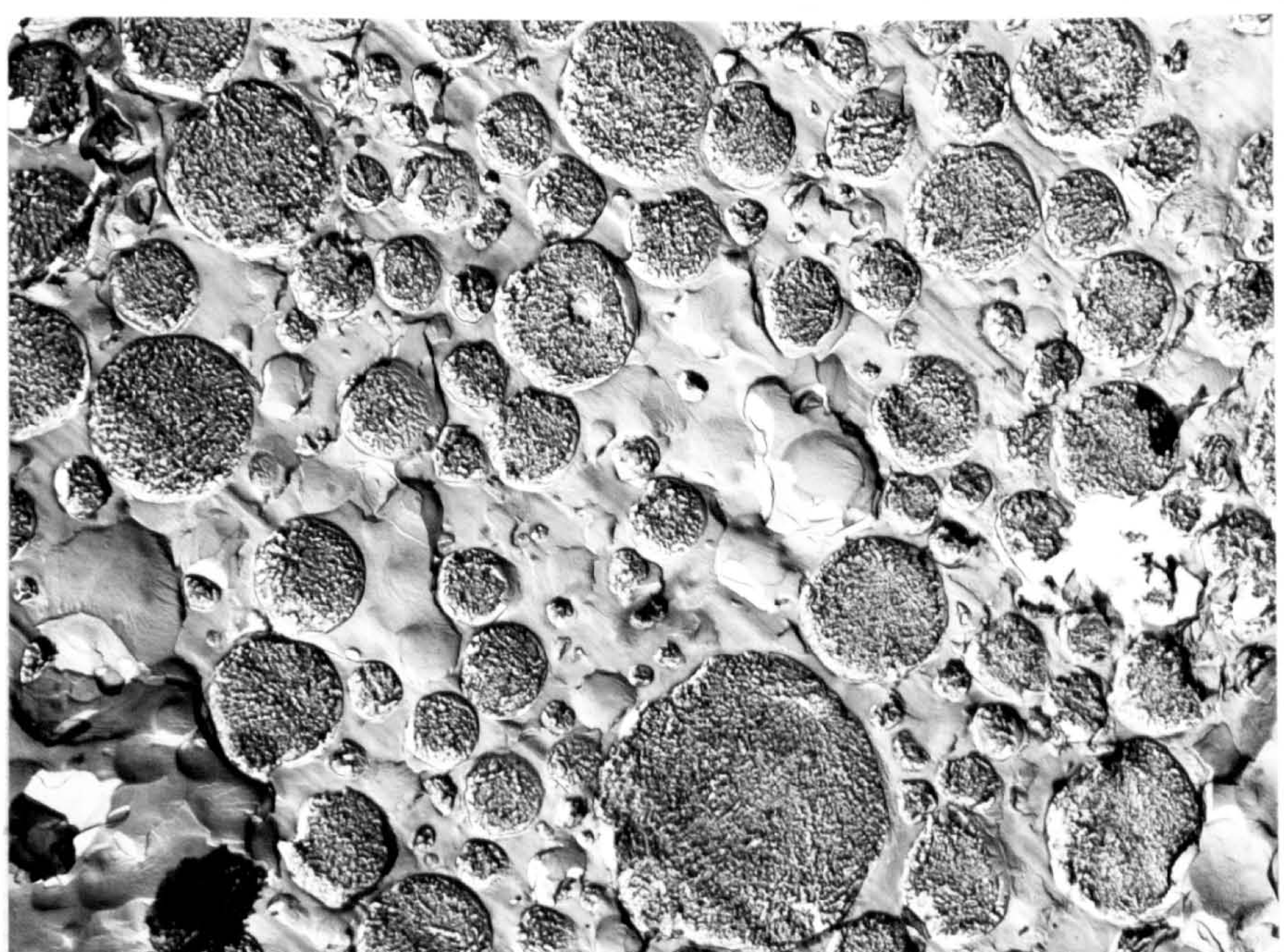

Plate 4 Emulsion A:202 (X6,400)

Plate 5 Emulsion KM:1 (X6,400)

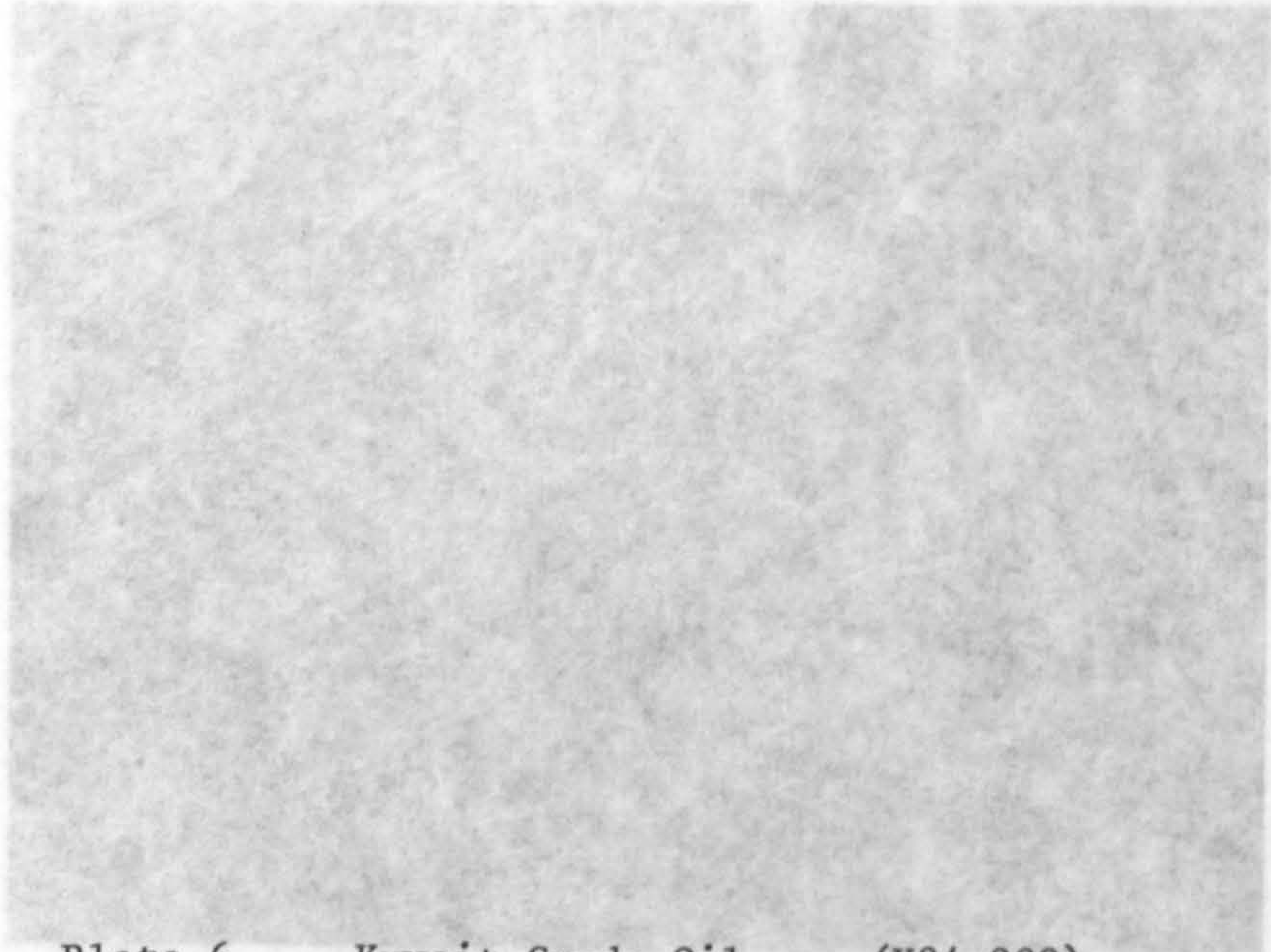

Plate 6 Kuwait Crude Oil (X34,000)

Plate 7 Brega Crude Oil (X29,400)

Plate 8 Tia Juana Crude Oil in bottom right hand corner (X23,600)

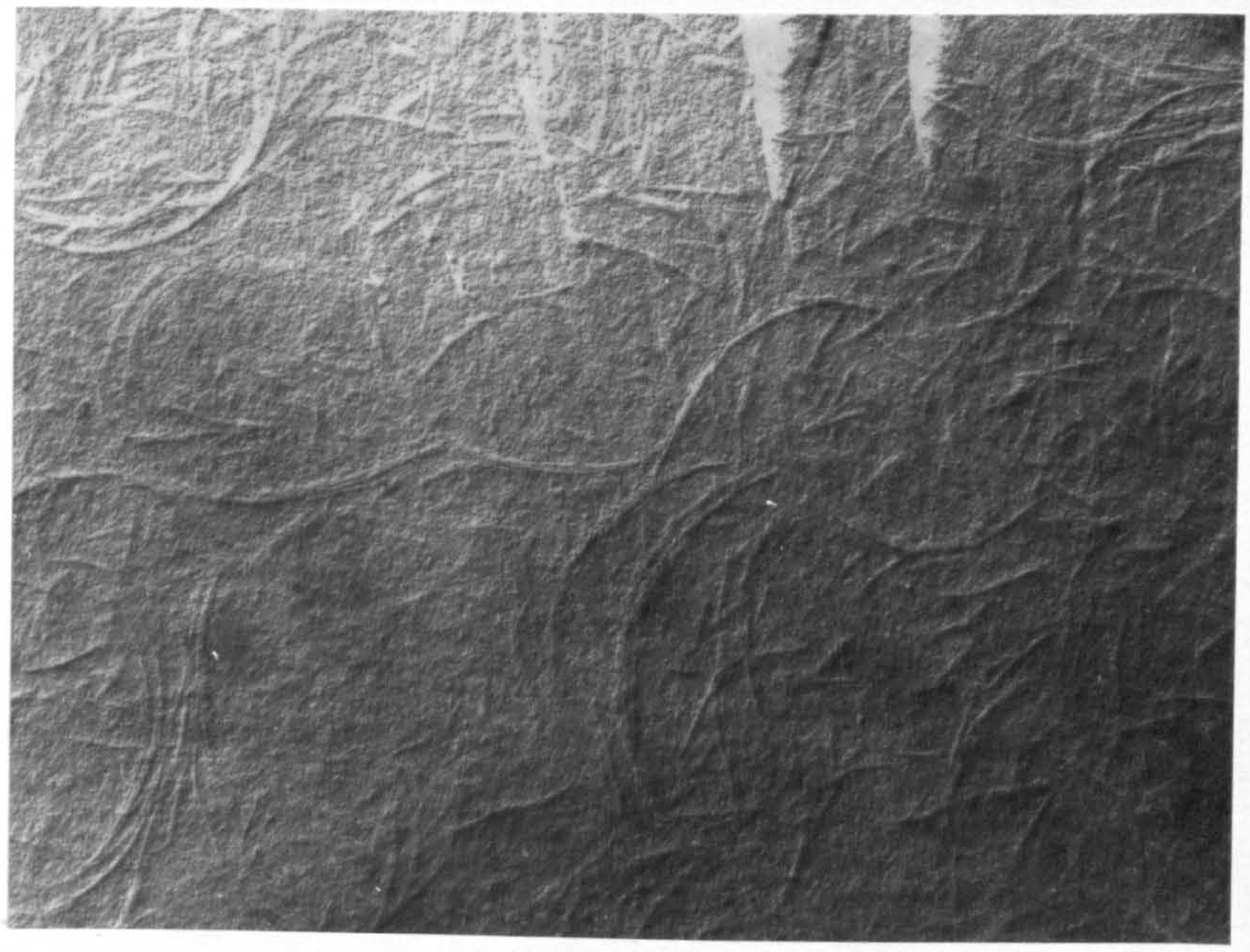

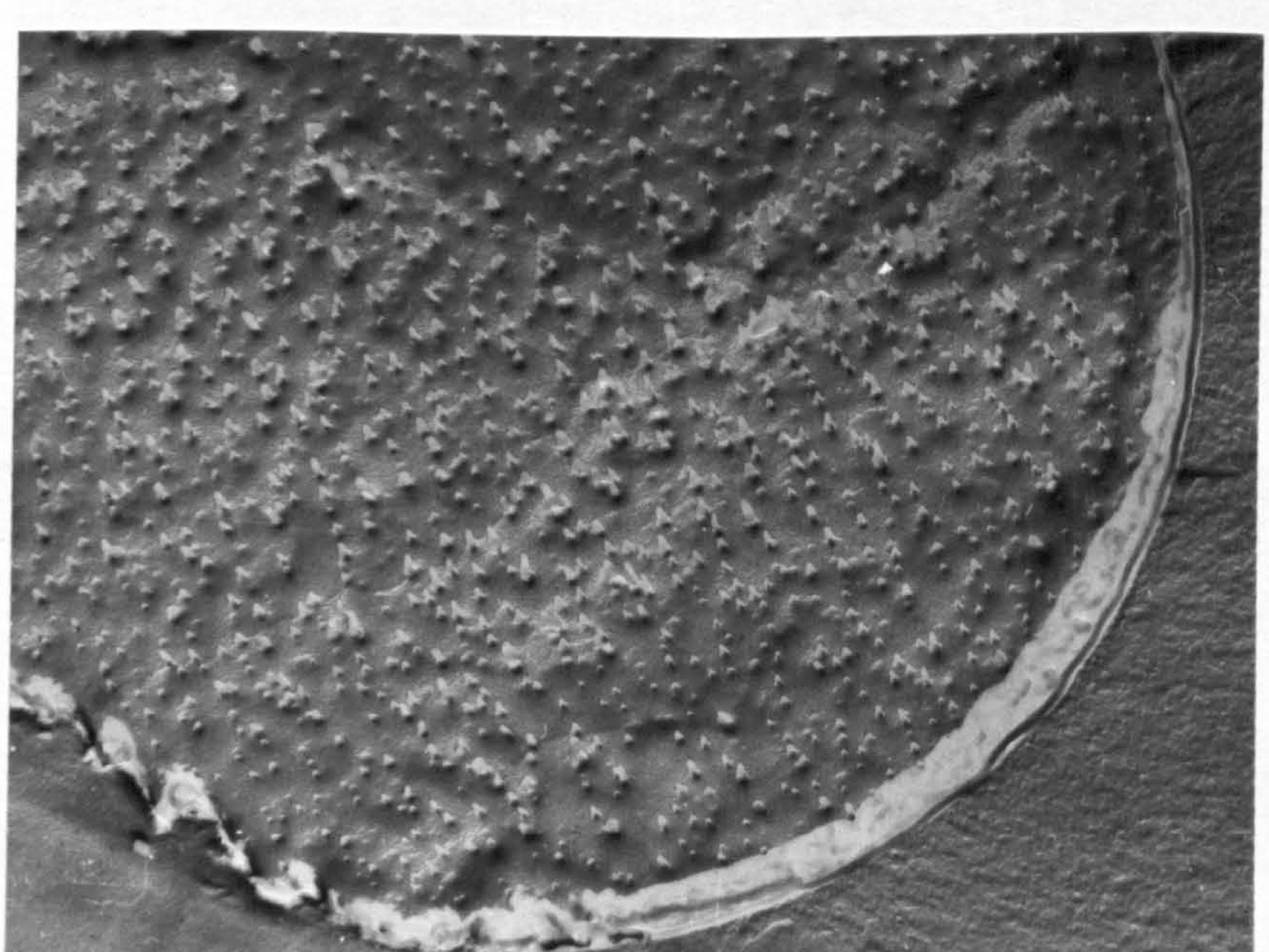

Plate 6 Kuwait Crude Oil (X34,000)

Plate 7 Brega Crude Oil (X29,400)

Plate 8 Tia Juana Crude Oil in bottom right hand corner (X23,600)

Plate 9 The Interface from the Aqueous side (X60,000)

Plate 10 The Interface from the Oil Side in emulsion KF:45 (right side of picture) (X69,600)

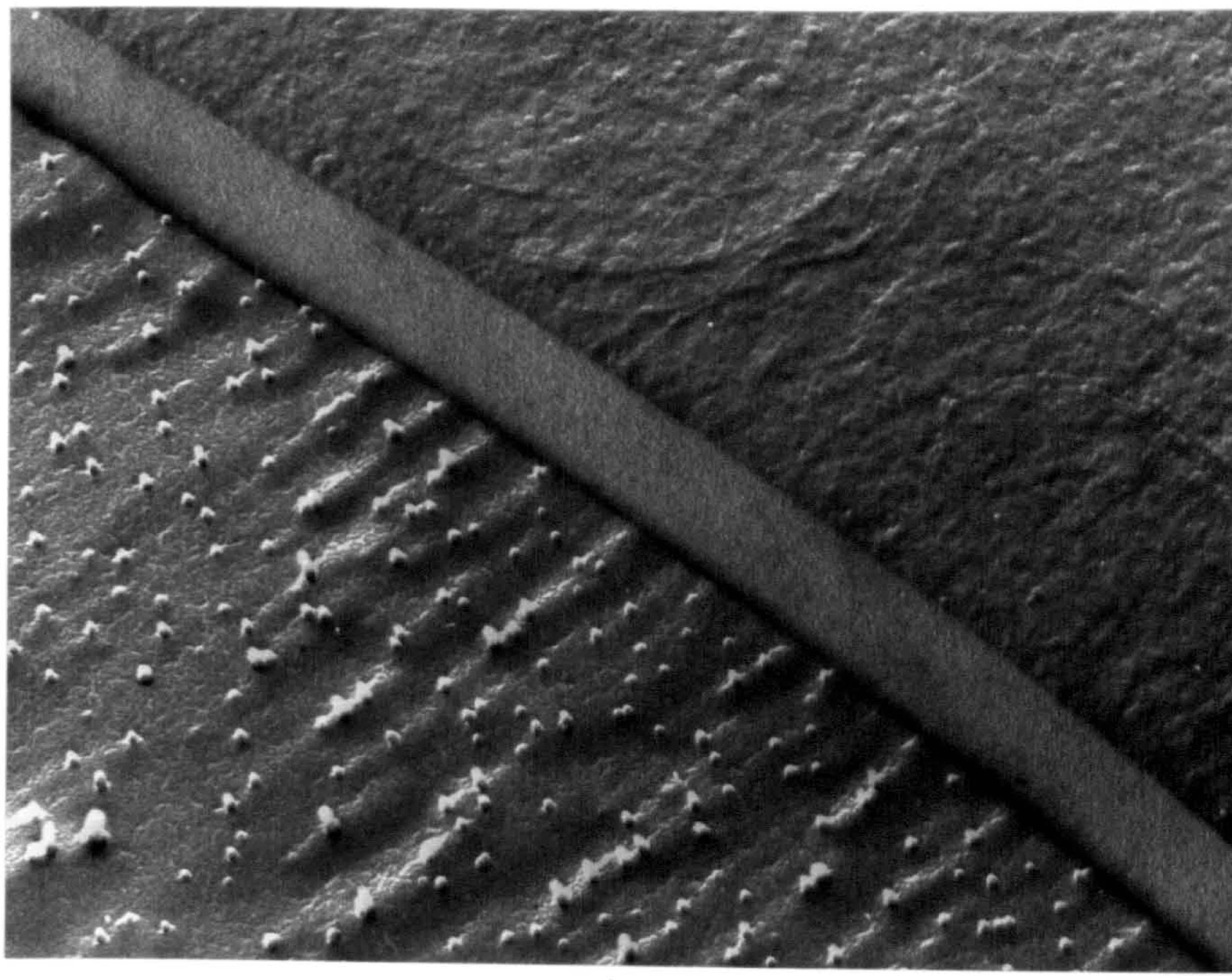

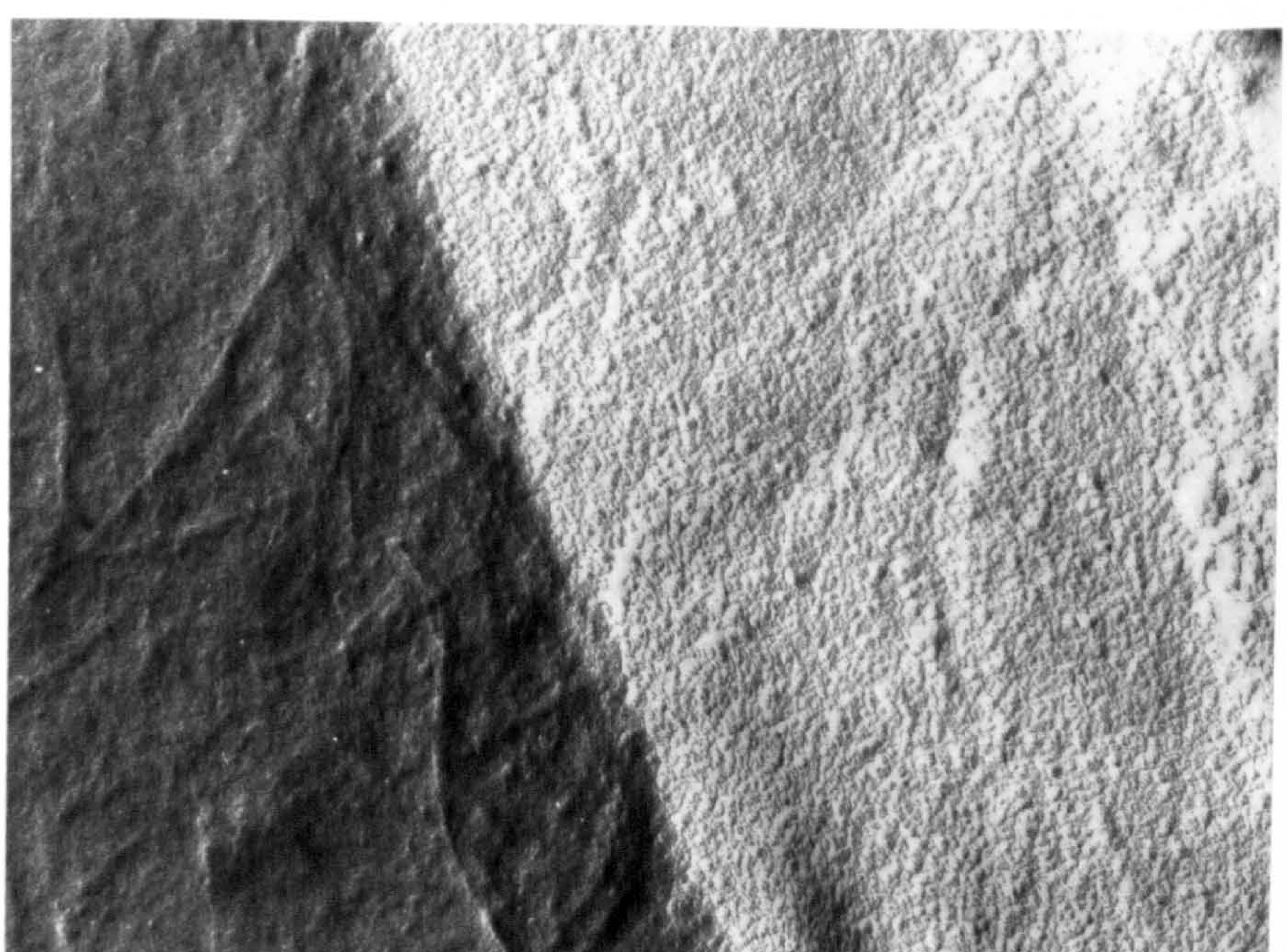

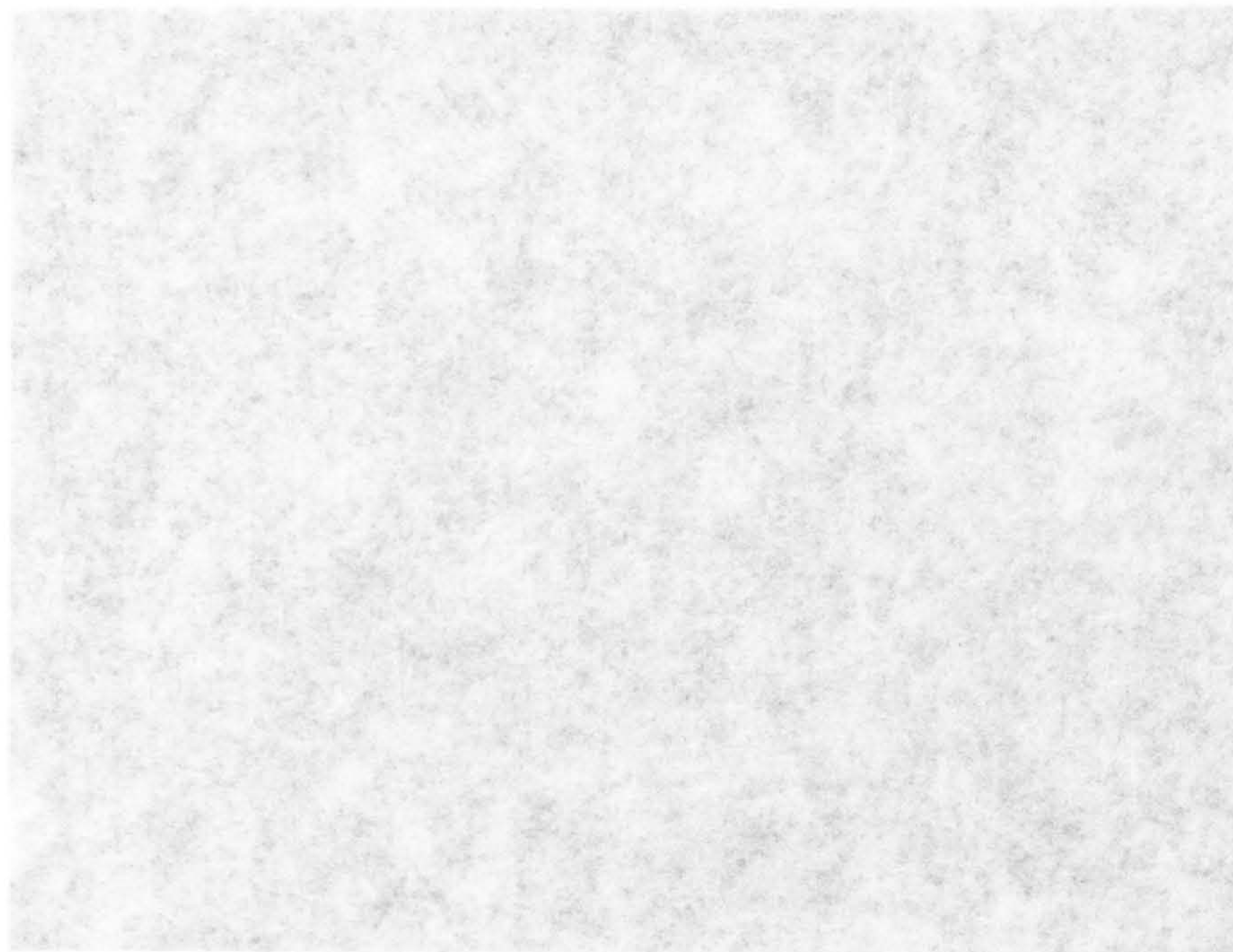

Plate 9 The Interface from the Aqueous side (X60,000)

Plate 10 The Interface from the Oil Side in emulsion KF:45 (right side of picture) (X69,600)

Plate 11 The Interface from the oil side in emulsion BF:153 (left side of picture) (X34,500)

Plate 12 The Interface from the Oil side (right side) and from the water side (left of centre) in emulsion TF:154 (X25,700)

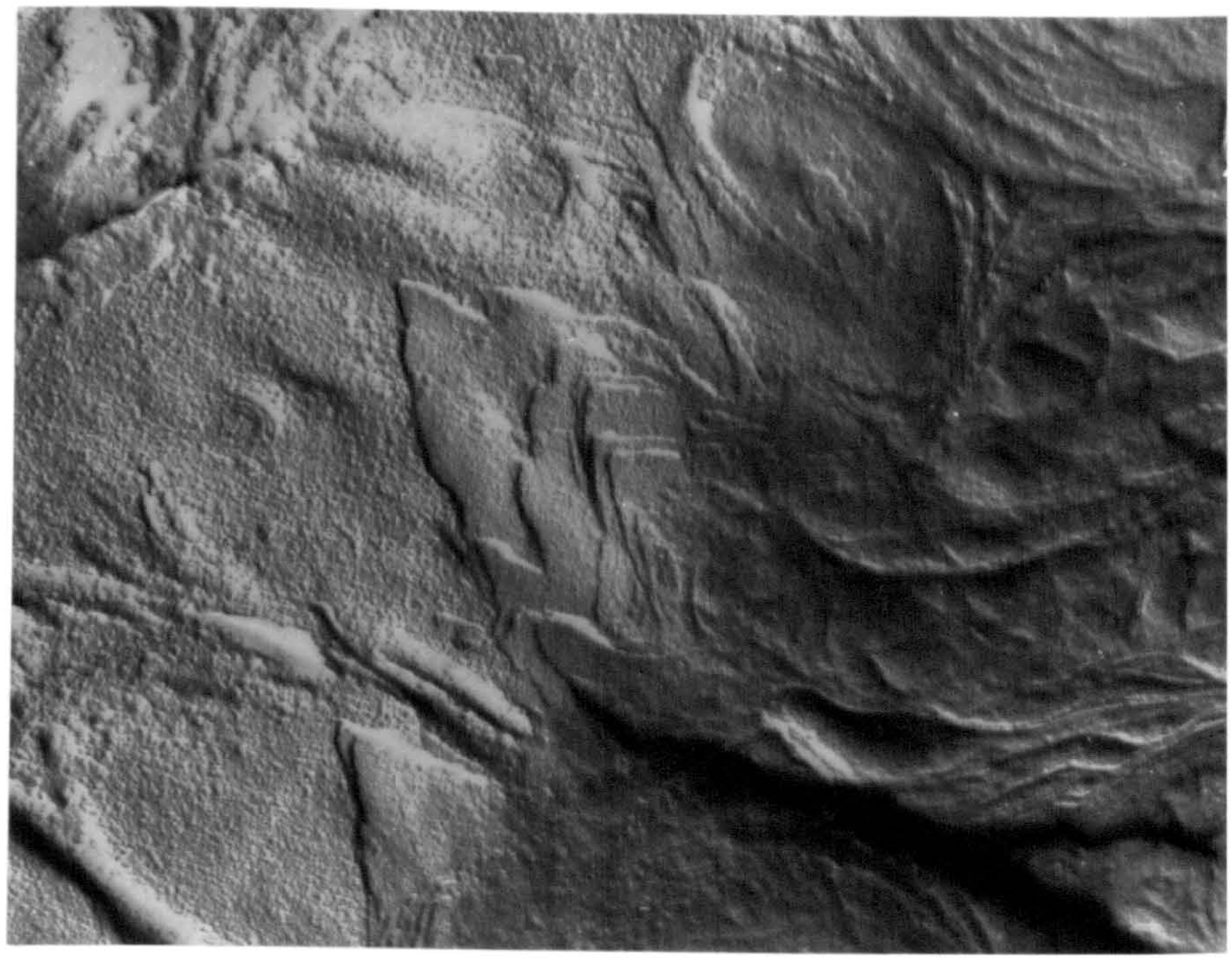

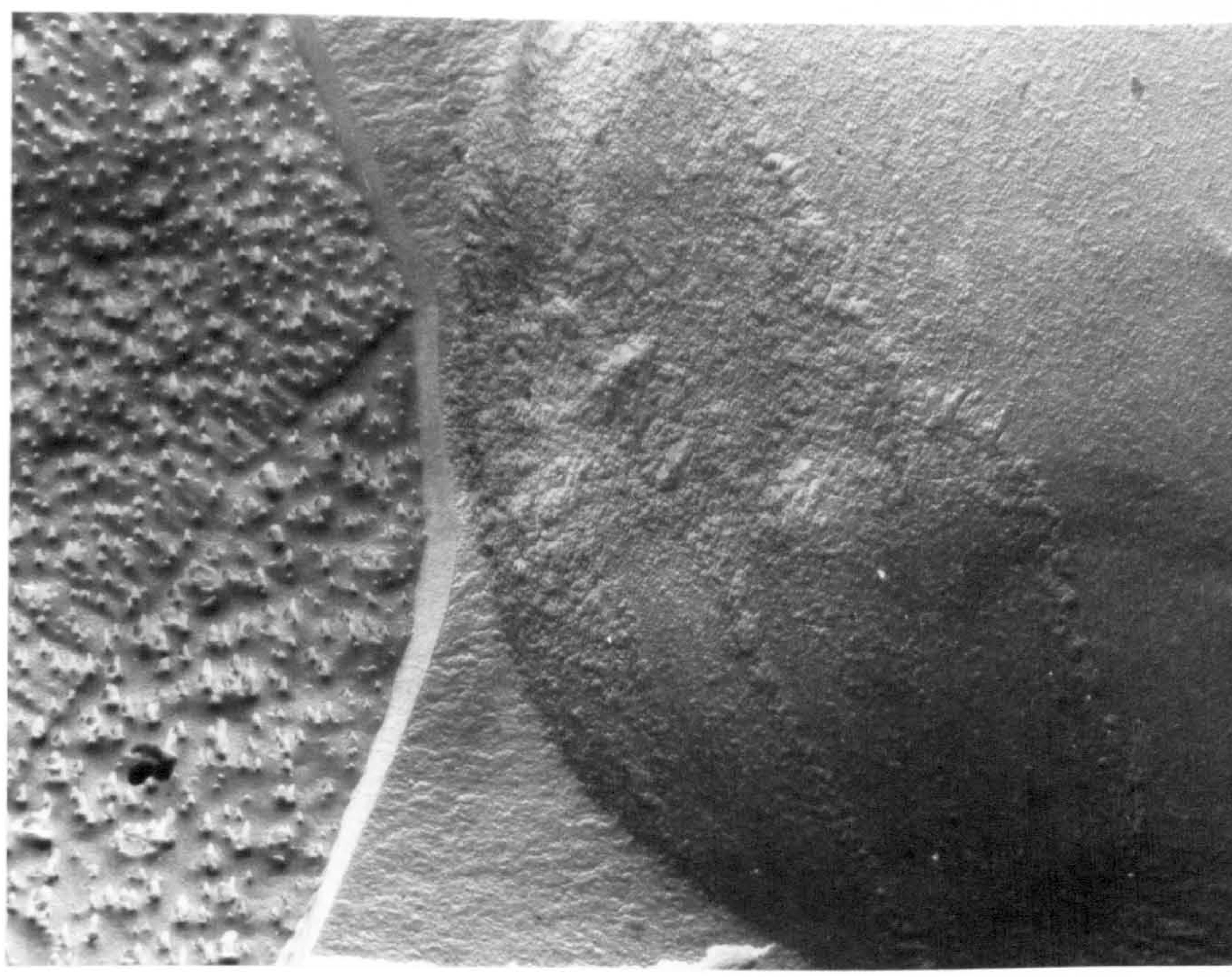

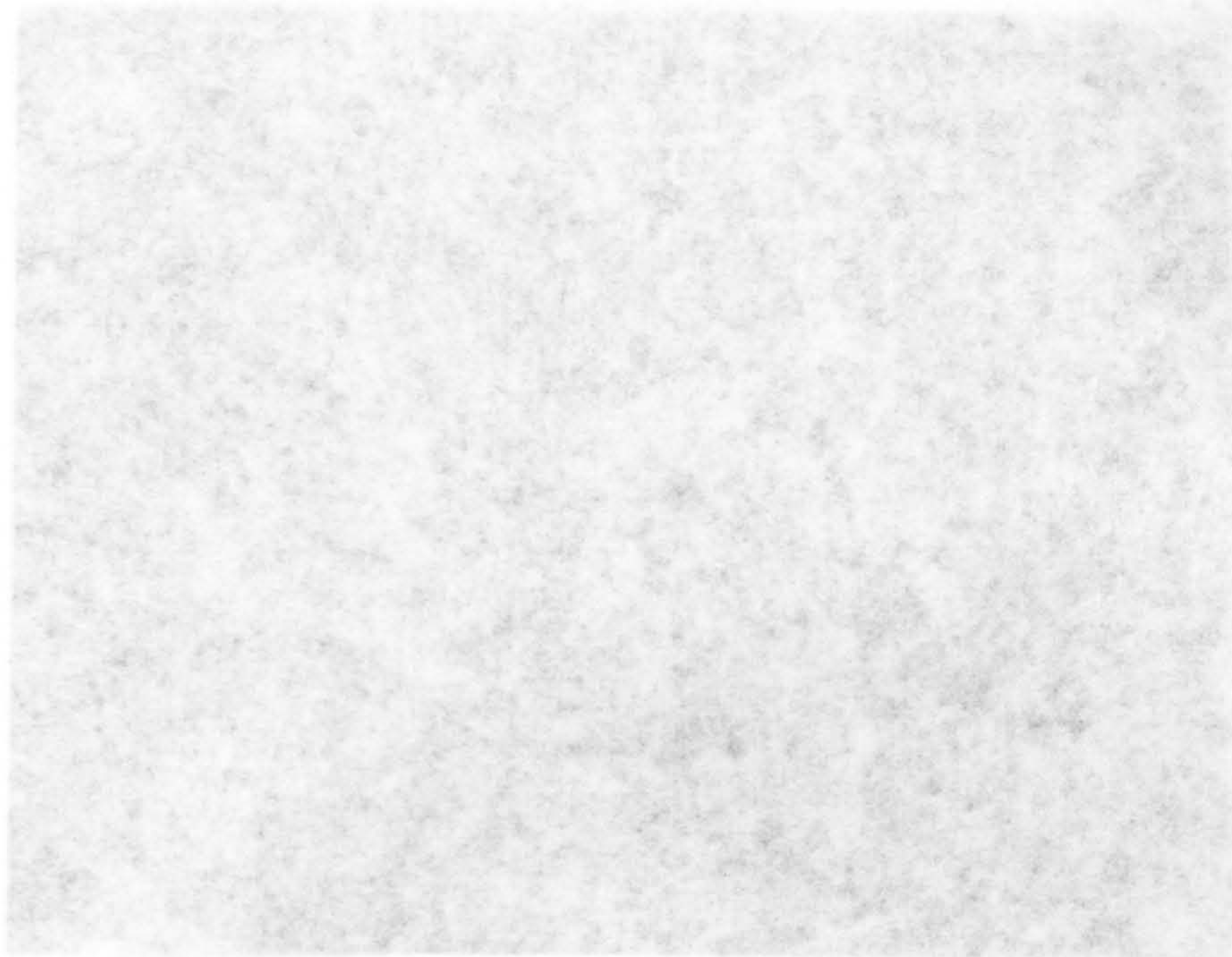

Plate 11 The Interface from the oil side in emulsion BF:153 (left side of picture) (X34,500)

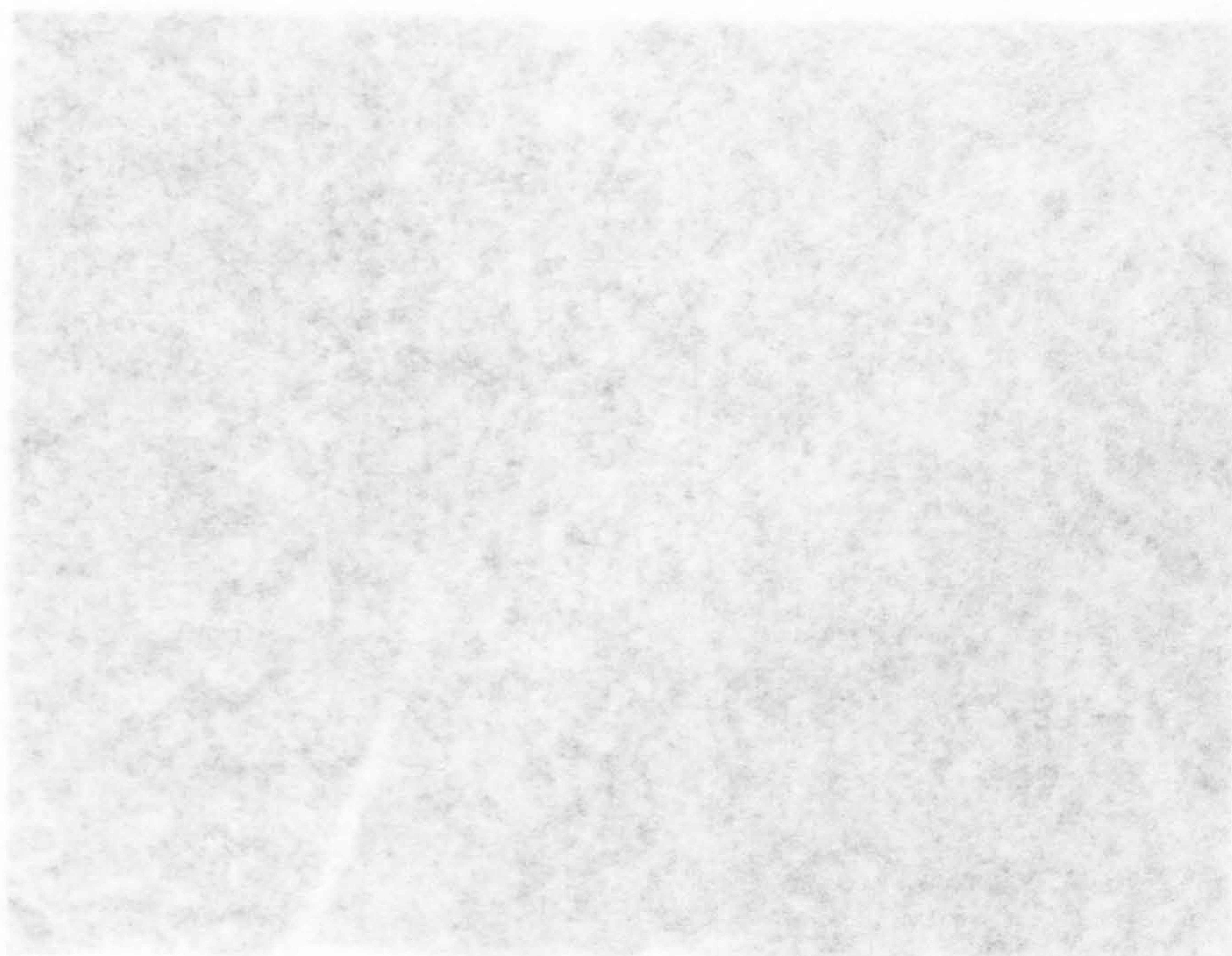

Plate 12 The Interface from the Oil side (right side) and from the water side (left of centre) in emulsion TF:154 (X25,700)

Plate 13 The encapsulating film in emulsion BF:155 (X53,300)

Plate 14 Alignment of waxy plates along the interface in emulsion BF:153 (X70,000)

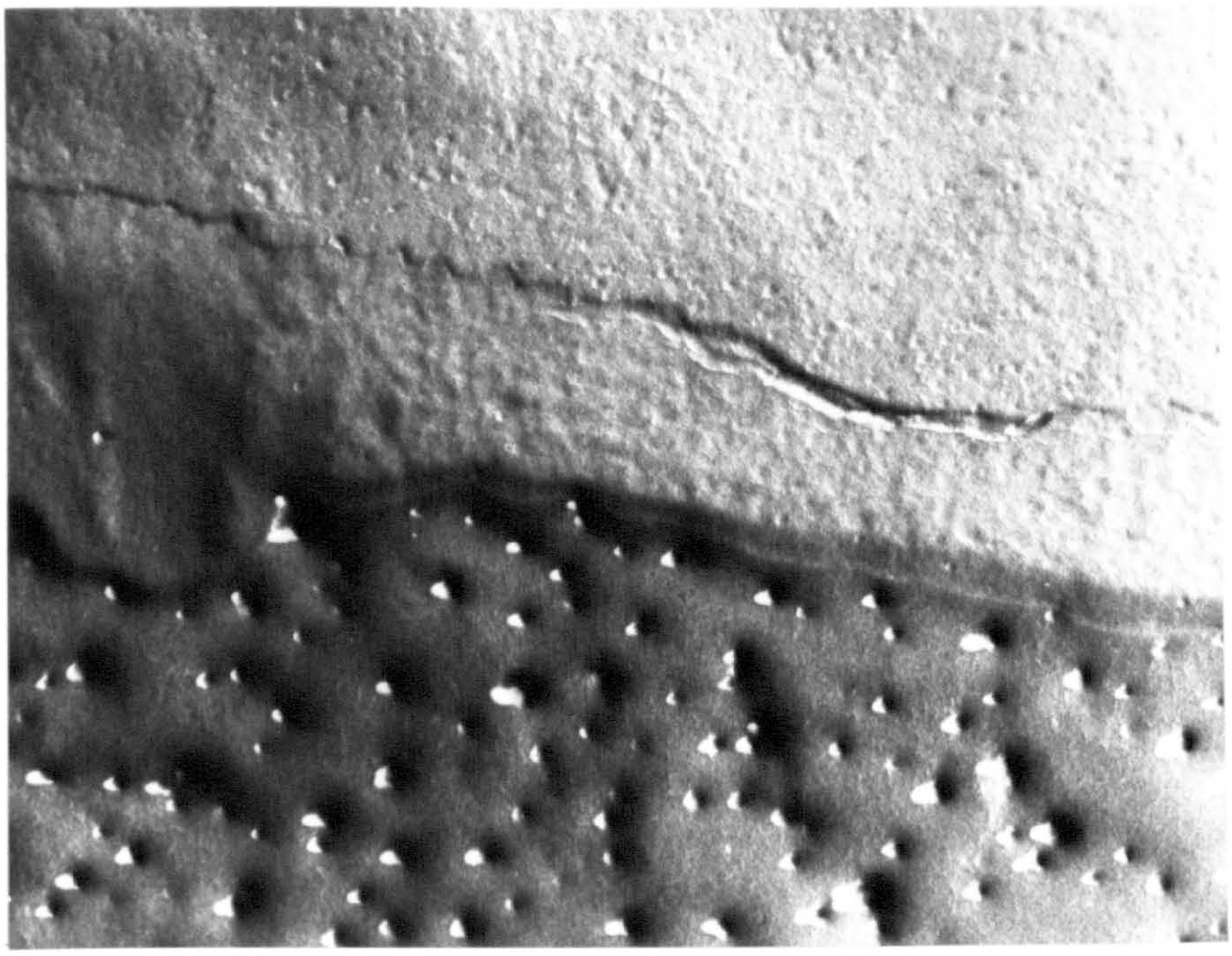

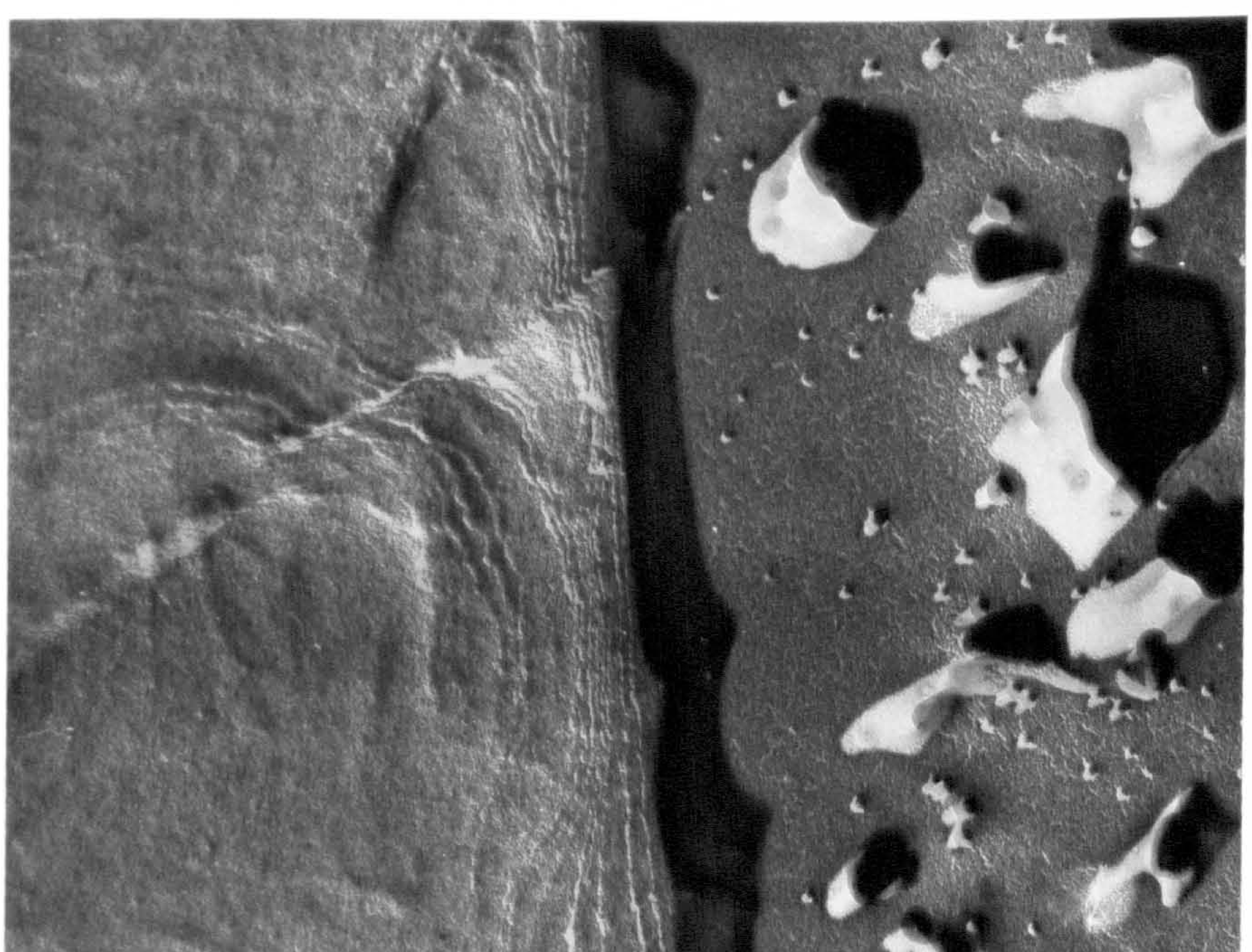

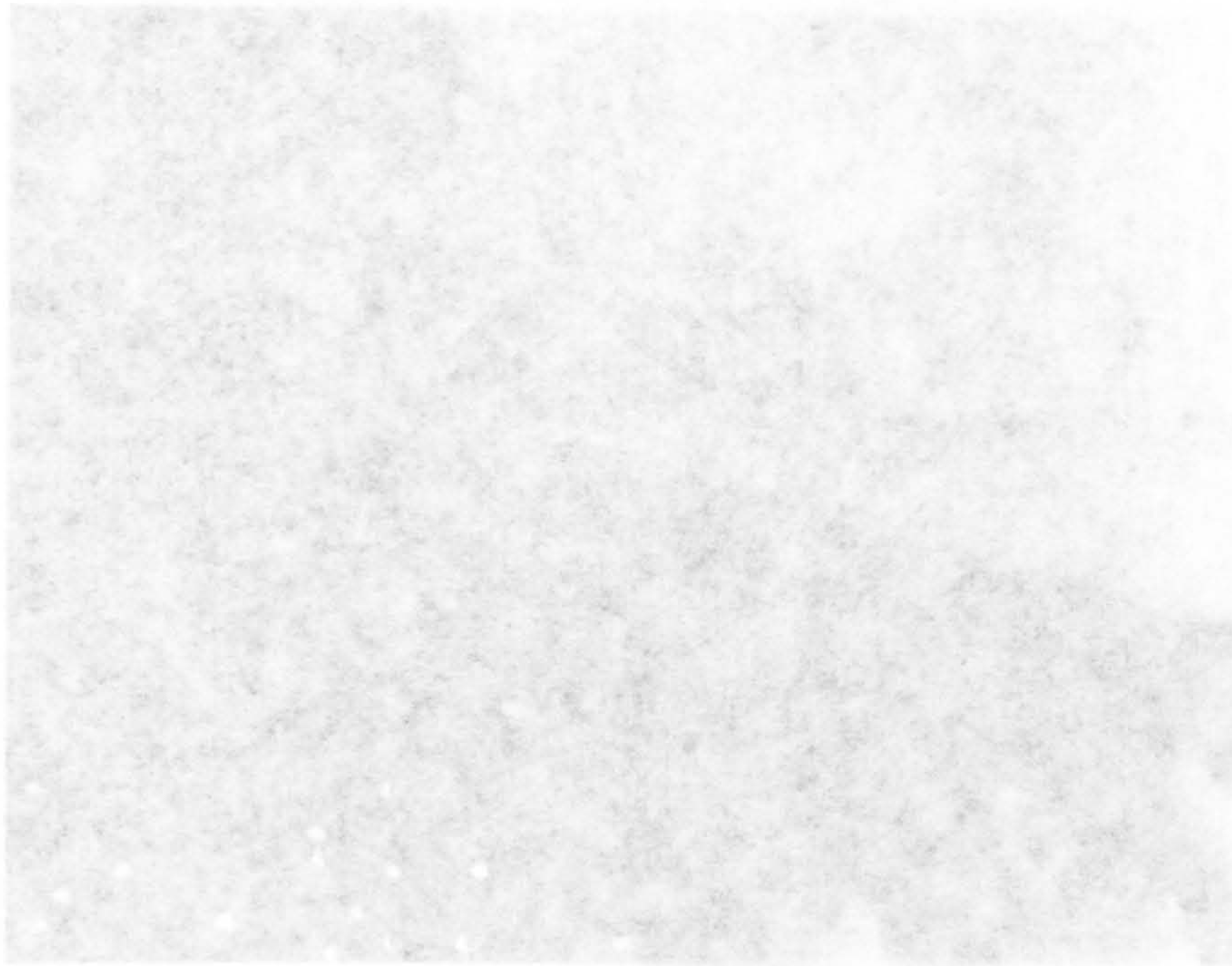

Plate 13 The encapsulating film in emulsion BF:155 (X53,300)

Plate 14 Alignment of waxy plates along the interface in emulsion BF:153 (X70,000)

Plate 15 Coalescence of small droplet in emulsion BF:155 (X26,700)

Plate 16 Coalescence of larger droplet in emulsion BF:155 (X8,700)

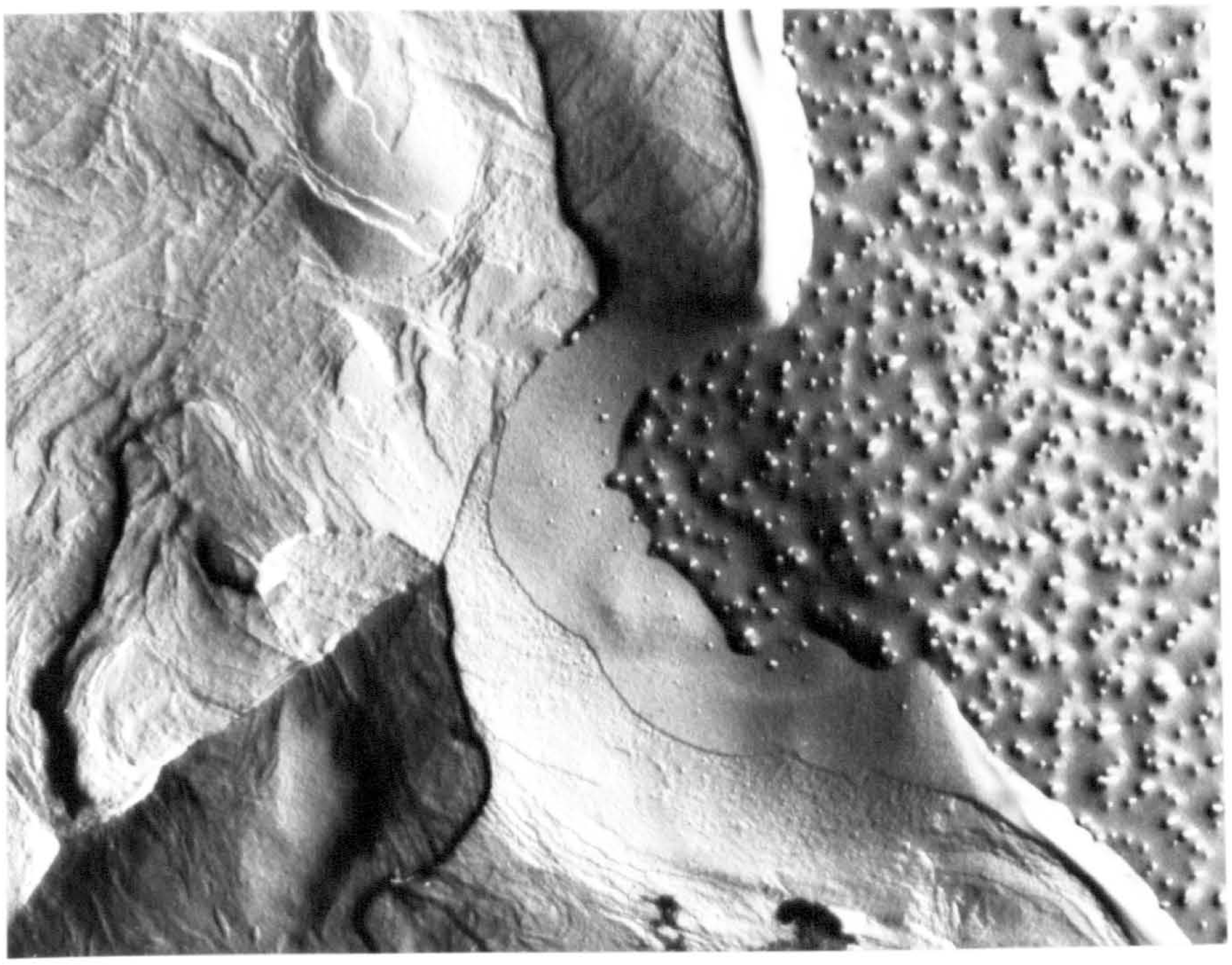

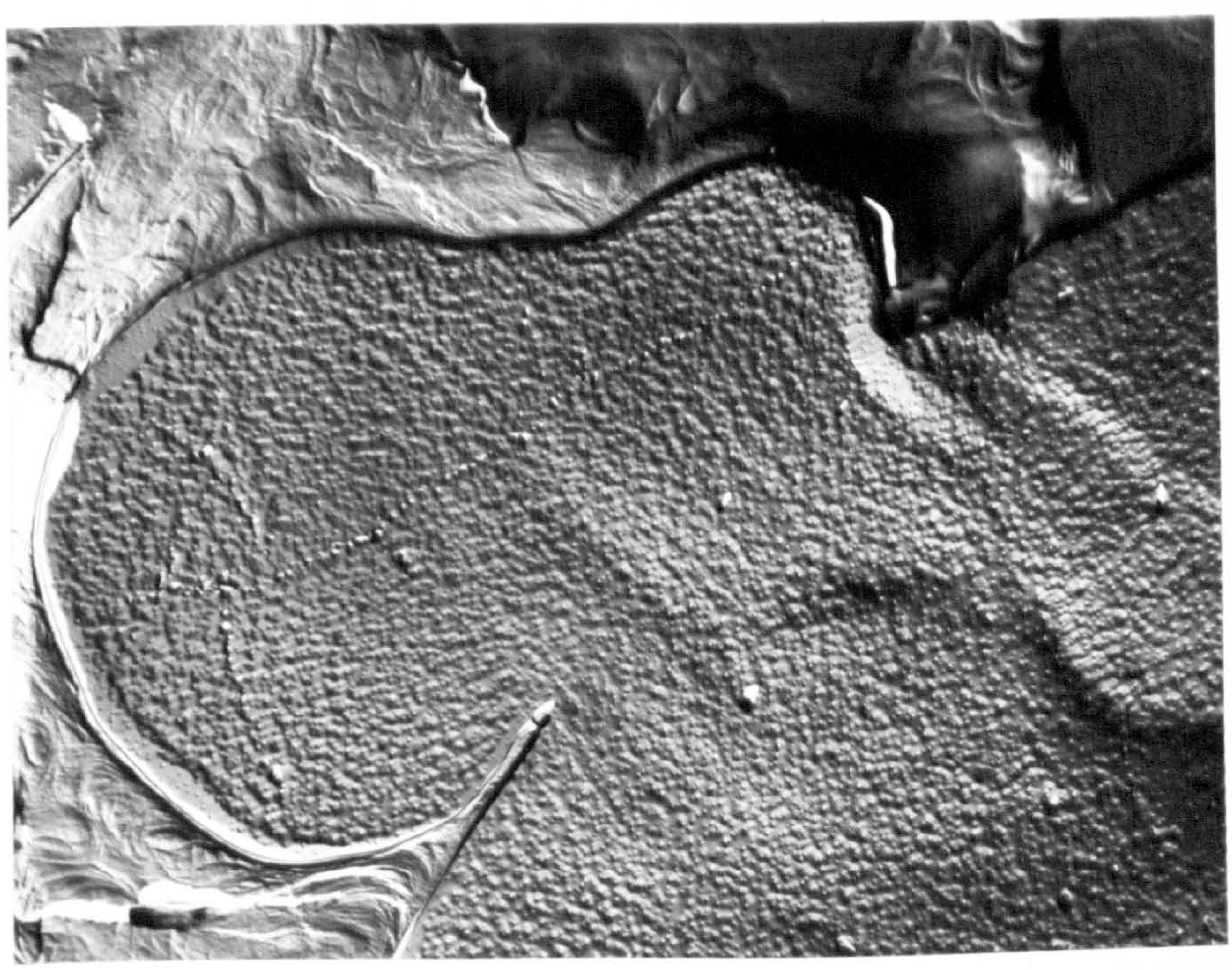

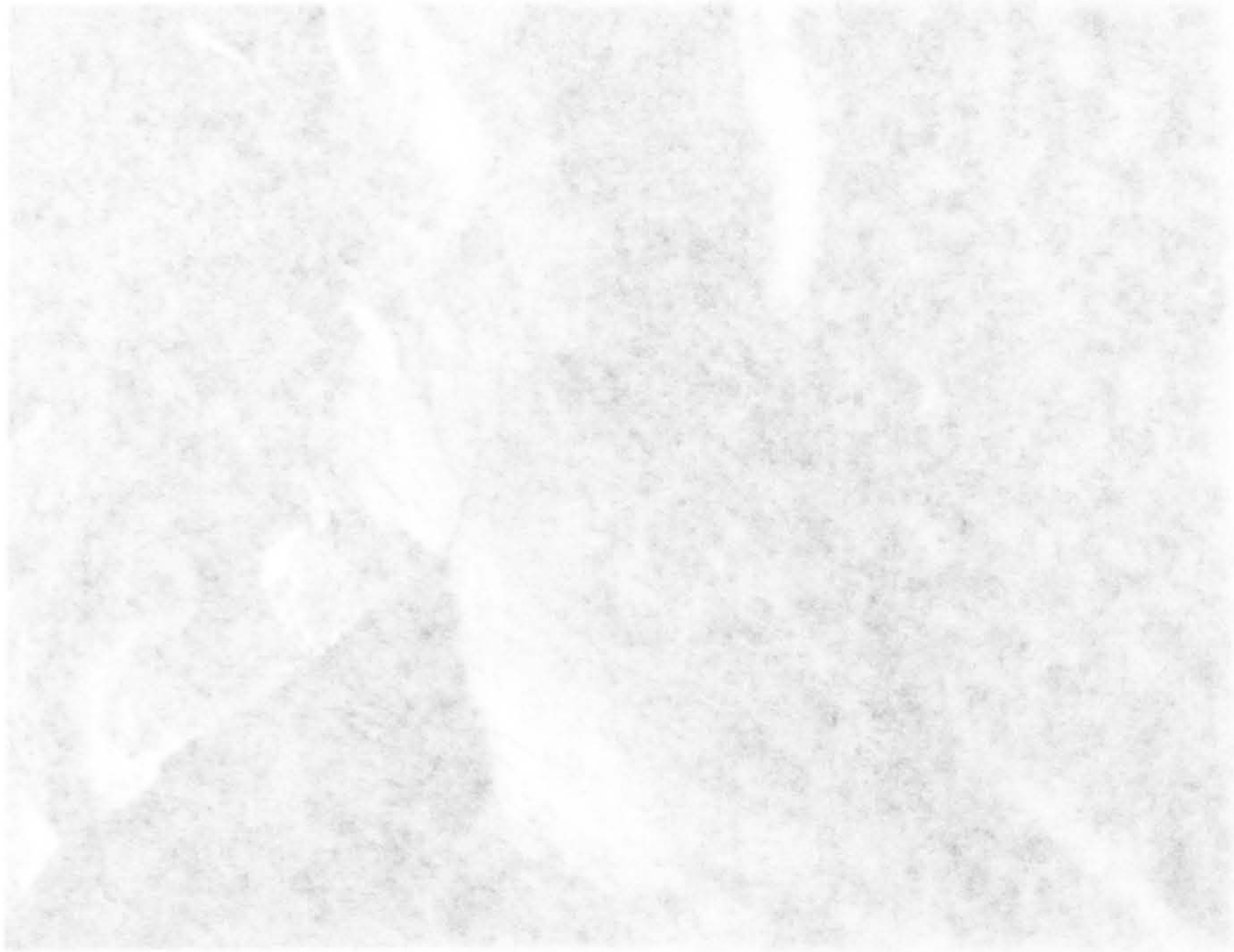

Plate 15 Coalescence of small droplet in emulsion BF:155 (X26,700)

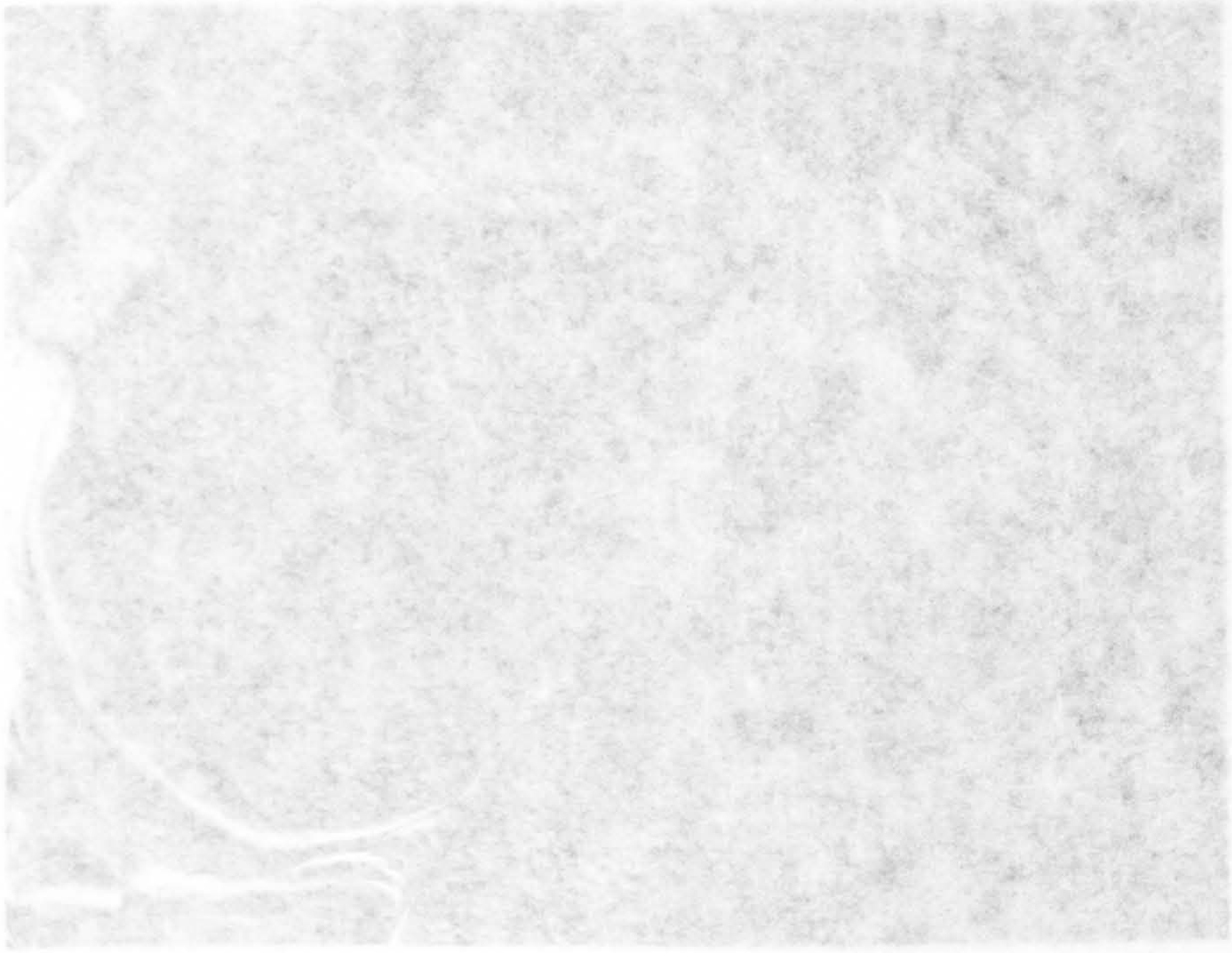

Plate 16 Coalescence of larger droplet in emulsion BF:155 (X8,700)

Plate 17 Cream from emulsion KF:91 (X8,900)

Plate 18 General view of cut and fractured region in emulsion TF:103 (X8,500)

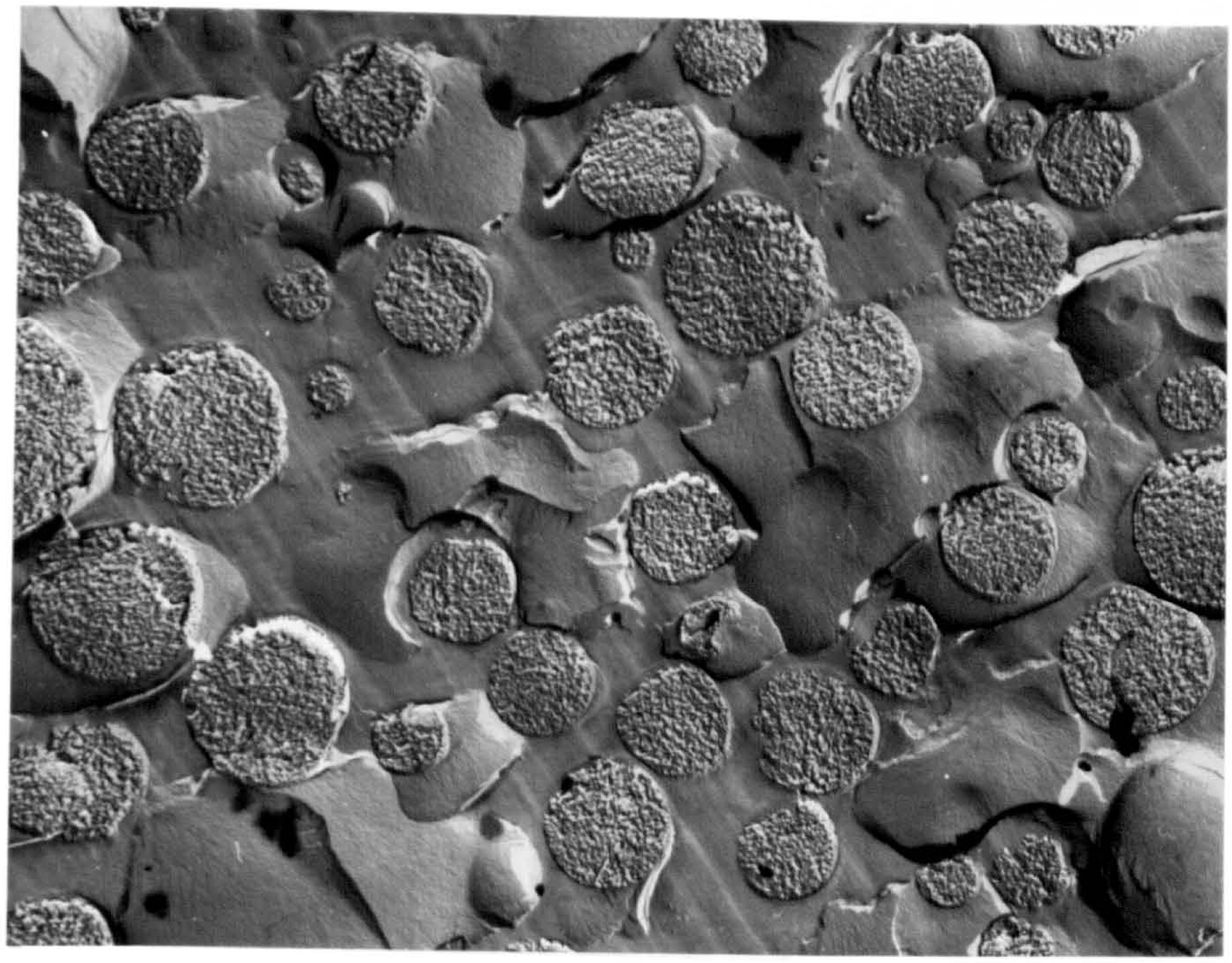

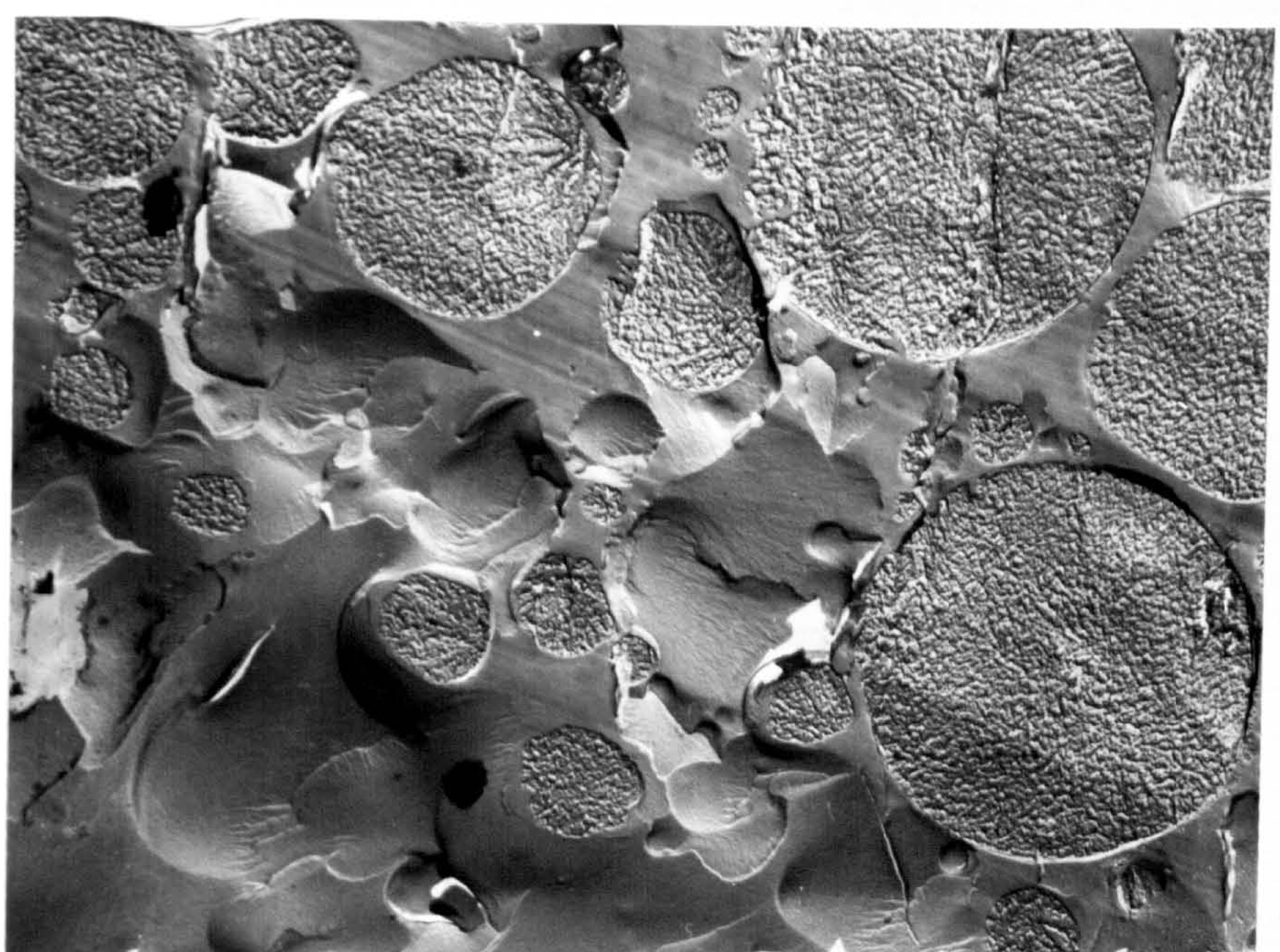

Plate 17 Cream from emulsion KF:91 (X8,900)

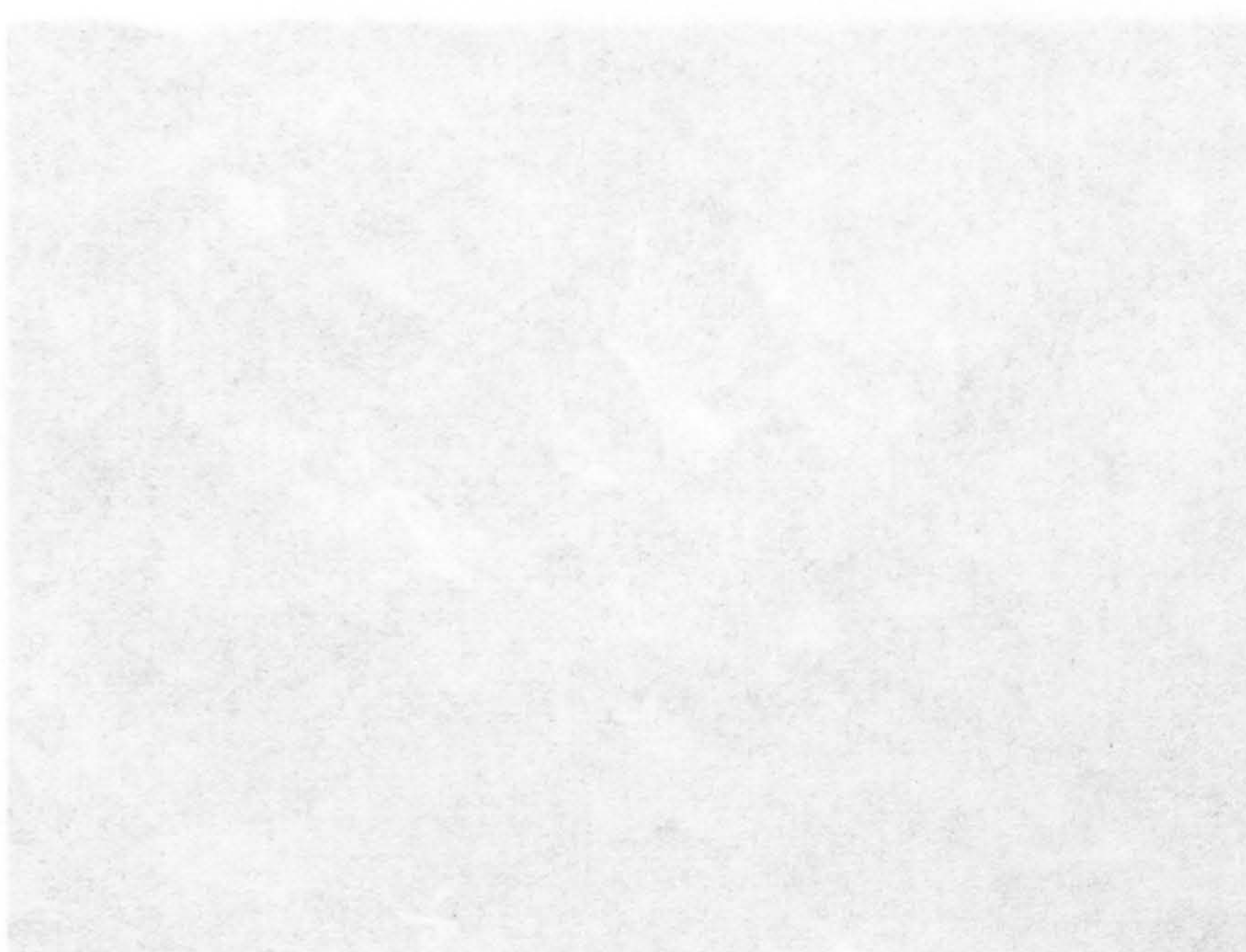

Plate 18 General view of cut and fractured region in emulsion TF:103 (X8,500)

5. DISCUSSION

5.1 Freeze Etching

5.1.1 General Features

Immediately apparent in plates 4 and 5 is the distinction between the oil and water phases. The water phases show the characteristic amorphous eutectic pattern of salt solutions (real and simulated sea water respectively). The oil phases show no distinct patterns, probably due to the short etching times. In plate 5, knife marks are clearly visible and in fact the majority of the droplets are cut or scuffed. Scuffing represents localised surface melting, sometimes accompanied by a rise in temperature which can lead to plastic deformation of the surface. In one corner of this plate, a very definite fracture region can be seen. This is brittle fracture which occurs with very little or no plastic deformation. The factors which determine the cut/scuff to fracture ratio are not well determined, but in any specimen from a microtome type process, both regions are always evident [71]. In general, the faster the knife is moved, the greater the likelihood of obtaining a fractured region.

5.1.2 Structure of the Two Phases

Plates 6, 7 and 8 show the characteristic etching patterns of the three crude oils which are all quite distinct. Kuwait has long filaments and fibrils with a granular matrix in between. Brega has a number of onion type structures but the etching, as might be expected from a lighter oil, is much deeper. Tia Juana shows barely any structure (the other features in plate 8 are discussed later).

There is a great similarity between the Kuwait structure and that of vaseline studied by Pajor et al [66] which also has a fibrous character. This suggests that the fibrils could be the edges of the aligned plates comprising the waxes in the oil as mentioned in Chapter 2. The onion type structures in the Brega may be an extreme example of this since it has a very high wax content. It must be emphasised that the crude oil is in the solid state and the situation may be different in the liquid phase.

Plate 9 shows very clearly the difference between deionised ice structures and the ice/salt eutectics of plates 4 and 5. Moor et al [62] were the first to publish observations on the small wart-like structures on the etched ice surface. Davy and Branton [83] have made a more detailed study of the vacuum sublimations of single oriented ice crystals. They found that the density of the warts did not seem to be affected by small amounts of impurity in the ice. The warts are useful for identifying the aqueous phase.

5.1.3 The Interface

5.1.3A The Interface from the Aqueous Side

Between the water and the oil in plate 9 is the interface as revealed from the aqueous side. Figure 5-1 gives a schematic representation of what has happened. The sample droplet was fractured in this case through its lower half. Davy and Branton [83] have given a table of values relating rate of sublimation to sample temperature and the pressure in the apparatus. From that it can be estimated that the water level has dropped by some 40 nm.

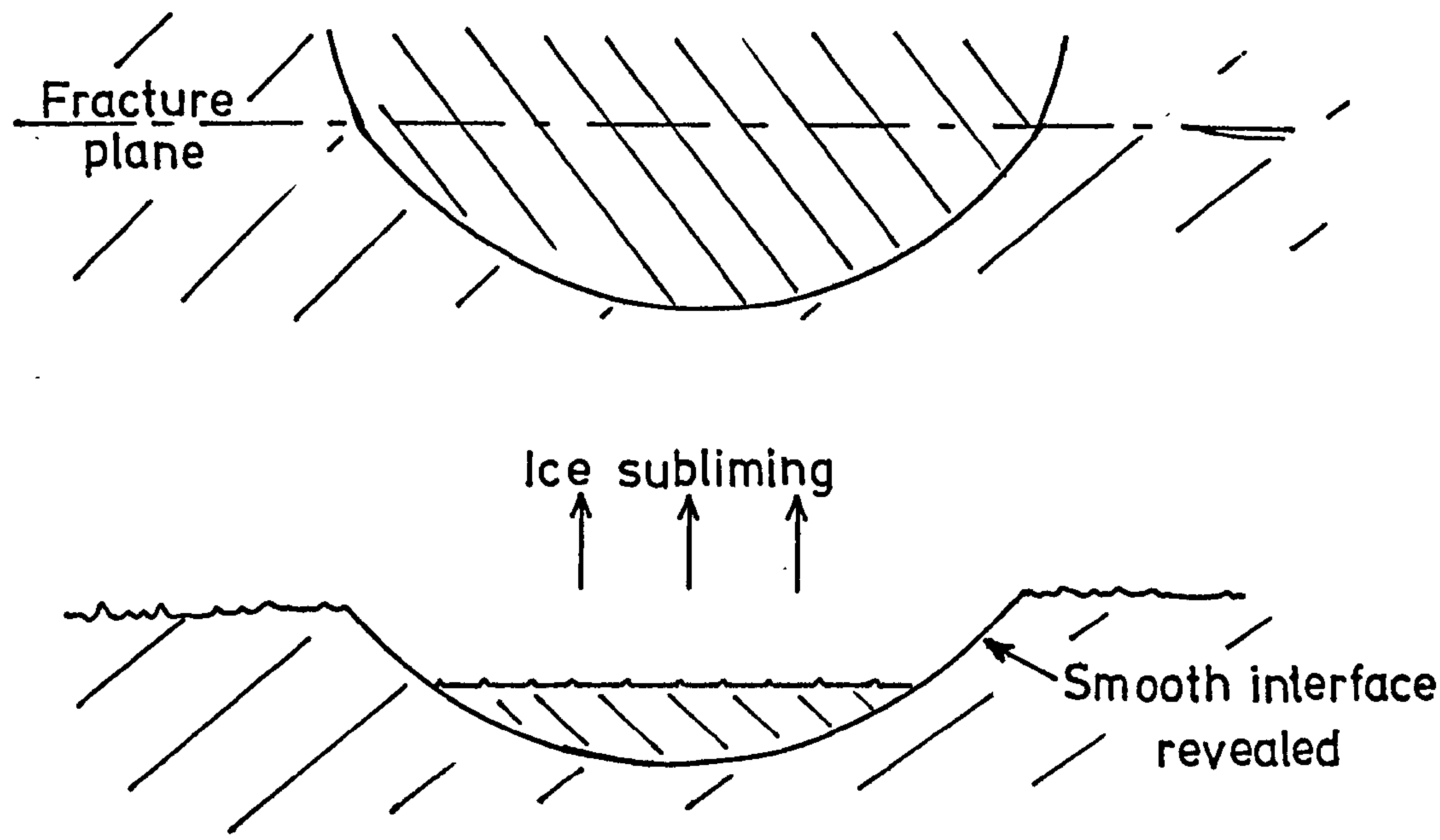

FIG. 5-1

In discussions on this smooth and structureless area it is necessary to mention the resolution limit of freeze etching. The technique is capable of resolving 5 nm detail [84] but below this it is necessary to be cautious in interpretation. Looking very closely at the smooth interfacial area, it is possible to make out granules of the order of 3 - 4 nm in size. These granules are platinum crystallites with a mean diameter of around 2 - 5 nm which tend to aggregate [71]. This smoothness then is highly significant. As asphaltene micelles are up to 3 nm in size [27], clusters consisting of a few micelles would be visible. With the implication that interfacial activity is due to single micelles, it is likely that they undergo rearrangement so that the more polar areas are in contact with the water.

5.1.3B <u>The Interface from the Oil Side</u>

When the fracture plane follows the surface of a droplet, very similar features for all three oils emerge as is shown in plates 10, 11 and 12. The interface thus revealed from the oil side has a distinctly granular surface and the size of the granules is of the order of 10 - 30 nm. There is also a certain granular structure to the Kuwait and Tia Juana oil phases and to a much lesser extent to the Brega. In view of the relative asphaltene concentrations of these three crudes, it seems reasonable to suppose that the granules are clusters or micelles of asphaltene molecules, each cluster containing around 250 molecules. The granular structure of the interface could then be explained as micelles of asphaltenes migrating to the area of the interface. It is interesting to note in plate 12 the particularly high concentration of these granules just where the two droplets are virtually in contact. It appears as though there is a physical barrier of asphaltenes preventing coalescence.

In plate 11 the waxy plates of the Brega seem to be aligning themselves along the interface; it may be that this is a second encapsulating film which compensates for the relatively low concentrations of asphaltene in this oil. Another example of this can be seen in plate 14.

5.1.3C <u>Evidence for an Encapsulating Film at the Interface</u>

Plate 13 shows evidence of the presence of a coherent film at the interface. Either side of the dark line, the structure is typical of the interface as seen from the oil side. One side of the line though has much sharper features than the other. It appears as though the fracture plane struck the droplet below its equator and started to remove the water complete with encapsulating film leaving an image of the typical interface as viewed from the oil side. However, a point was reached where the droplet extended below this phase and the knife cut through the film stretching it slightly (thus explaining what appears to be a slight curling.) Etching then revealed a much less structured surface but with the very low asphaltene content in Brega, this structure was considerably more than would be seen in Kuwait or Tia Juana emulsions. If this explanation is correct and can be extended to the situation at room temperature, then there are very strong intermolecular forces holding the asphaltenes together even when there is only a monomolecular film.

5.1.4 Coalescence

It is very difficult to observe coalescence under the optical microscope without either high speed film or unstable droplets in a fairly viscous medium. Plates 15 and 16 show droplets frozen whilst coalescing. The coalescing droplets in each case appears to be unsymmetrical. However, following the explanation in the previous section, the crescent shaped area around and below the droplet in plate 15 is the interface viewed from the oil side and when this is followed shows the drop to be quite regular. The diameter of this drop appears to be in the region of 2 μm.

In plate 16 the droplet is much larger (of the order of 10 μm diameter) and undergoes an asymmetrical coalescence. Ice crystal boundaries are visible in this droplet. It appears to be surrounded by a membrane type of interface.

5.1.5 Droplet Size Analysis

It was hoped that it would be possible to make an evaluation of the sub-micron range of a given emulsion. Plate 17 shows a sample of some of the oil phase that had separated to the surface of emulsion KF:91. These droplets were impossible to focus on the optical microscope. Plate 18 shows a typical view of an almost monodispersed Tia Juana emulsion. Herdan's [45] conditions for thin section analysis have been stated in Chapter 2. The knife marks in plate 18 show that some areas lie below the plane of cross-section. Furthermore there are strong indications that the interfacial film is so strong that unless the knife or fracture plane strikes the droplet near the equator then it will either jump over the top or lift the droplet out altogether. Clearly a truly random cross-section has not occurred.

5.2 Droplet Size Analysis Studies

5.2.1 Choice and Use of Mean Diameter

5.2.1A Mean Volume Diameter

Gopal [33] has reviewed the literature on emulsion formation and he described two competing processes: disruption and recombination. The mean droplet size will reduce very rapidly in the first few seconds and then gradually attain a limiting size. Gopal explained this in terms of the increasing number of collisions resulting from the greater number of droplets such that the rate of disruption is equal to the rate of coalescence. He considered the disruption to be directly proportional to N_n, the number of droplets at time t, and the recombination proportional to N (the collision approximation). The rate of change of N_t is given by :

$$\frac{\partial N_t}{\partial t} = B' N_t - A' N_t^2 \qquad 5\text{-}1$$

Assuming the initial number of droplets to be small, in terms of mean volume diameter :

$$d_{vt} = d_{vo} - (d_{vo} - d_{v\infty}) \{1 - \exp(-B't)\} \qquad 5\text{-}2$$

where $N_\infty = B'/A'$.

Gopal found that this equation was only moderately satisfactory as can be seen in the diagrams in reference 85. However, the mean volume diameter is essential for rheological studies and has already been described.

5.2.1B <u>Mean Surface Area per Unit Volume Diameter</u>

Jellinek [86] has pointed out the errors involved when calculating mean volumes from a sample of 2,000 droplets. He gave the example that if 99·5% of the droplets have a diameter of 1 μm and 0·5% have a diameter of 20 μm, the difference in such a sample will be negligible for a number distribution. However, 1,990 droplets of 1 μm diameter represents only 2·4% of the total volume, whereas 10 droplets of 20 μm comprise the remaining 97·6%. He suggested that ten large droplets are scarcely significant and that in this example it would be necessary to count 20,000 droplets. The surface area diameter, d_s is more representative with the larger droplets comprising 66·8% of the total area. However, in this research, the great majority of readings occur when the majority of droplets are in the range 1 - 4 μm, with the largest droplets generally less than 10 μm. The homogeneous nature of the distributions throughout, due to the use of the "Magimix" diminishes this error.

Gopal [33] has reviewed the efficiency of mixing machines and he found that the chemical engineers who predominated in the literature preferred to the use the specific area per unit volume of the emulsion in correlating agitation with droplet size. This is because d_{sv} combines two of the mean diameters and so essentially incorporates the spread of the distribution. It is possible for several distributions to give identical d_v values but different total surface areas.

It is not convenient to use d_{sv} alone as it is directly proportional to the reciprocal of the actual surface area per unit volume as can be seen from equation 2-14. However, this is only useful for comparative purposes if the volume of oil (and hence the amount of emulsifying agent) is also incorporated. So the total surface area per unit volume of continuous phase is given by :

$$S_c = \frac{6}{d_{sv}} \cdot \frac{V_d}{V_c} \qquad 5\text{-}3$$

Since

$$\frac{V_d}{V_d+V_c} = \phi \; , \quad \frac{V_d}{V_c} = \frac{\phi}{1-\phi} \qquad 5\text{-}4$$

Thus

$$S_c = \frac{6}{d_{sv}} \cdot \frac{\phi}{1-\phi} = \frac{F}{d_{sv}} \qquad 5\text{-}5$$

It can be seen that when $\phi = 0{\cdot}50$, $\phi/1-\phi = 1$. In equation 2-14, the surface area and volume are expressed as μm^2 and μm^3 respectively. If $S = (10^{-6})^2\ m^2$ and $V = (10^{-4})^3\ cm^3$ then $1/d_{sv}$ is expressed in m^2 per cm^3. If F has no units, S_c is the surface area in square metres per cubic centimetre of oil phase.

5.2.2 Errors in Droplet Size Analysis

Errors of sampling have been mentioned already. For the Kuwait and Tia Juana emulsions which were highly stable and not prone to breakdown on slight agitation, there were no sampling problems. The Brega and model crudes proved to be difficult to dilute, and so errors in these cases were likely. The instability of these two crudes which produced generally larger droplets means that errors due to depth of focus apply mainly to the Tia Juana and Kuwait emulsions with their majorities of smaller droplets. The technique of waiting for as many droplets as possible to settle down on the slide before taking photomicrographs is accurate provided there is a deep depth of focus. This however reduces as the magnification increases. At the maximum microscope magnification of 450X, the depth of focus was found to be of the order of 3 μm. With the natural tendency to focus on larger droplets, many of the smaller ones remained blurred. This is illustrated in Figure 5-2.

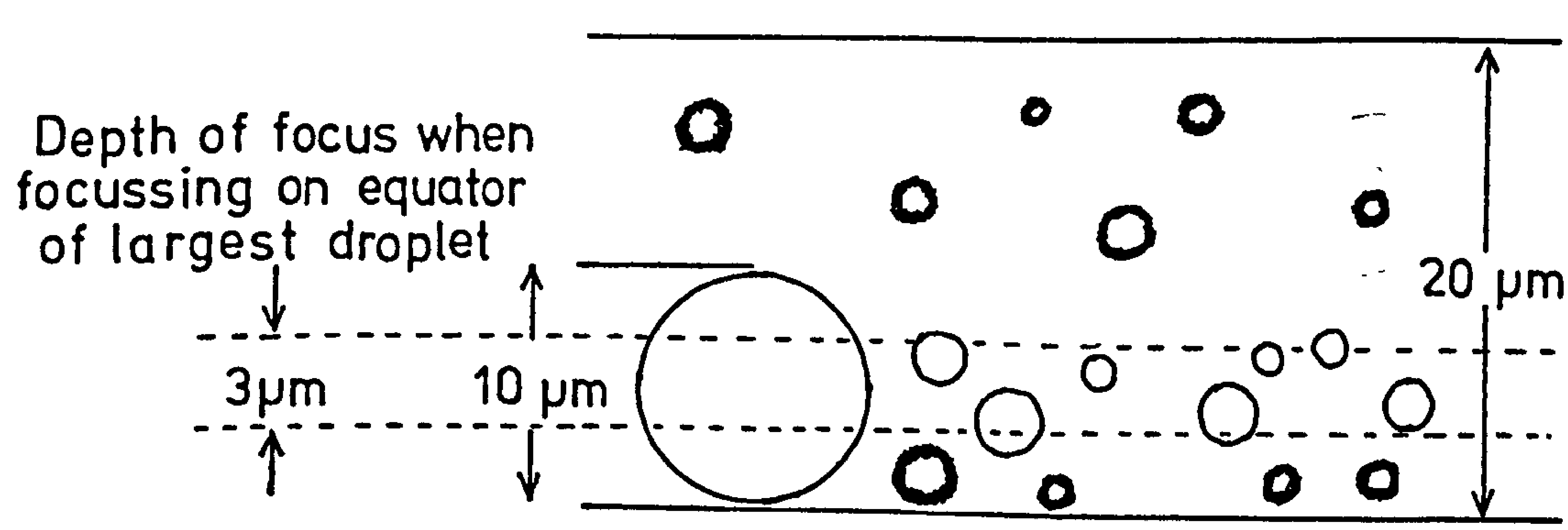

FIG. 5-2

This indicates the unavoidable tendency to emphasise the larger droplets and indeed the histograms show this for the more polydispersed systems as is shown in the next section. The more interesting emulsions in this work are relatively monodispersed, and in a range of five stirring times, only the first point shows an appreciable error for this reason.

Two groups of workers [41, 87] have investigated the accuracy of the Zeiss counter. The former were looking at irregular crystals, but Davison and Haller [87] obtained results by different operators using well defined circles on backgrounds of varying contrast. This showed errors on the whole of $\pm$5%. However, if the circles were less well defined, and the size range more polydispersed, then errors of $\pm$7% were found. Clearly, with the present emulsion systems, the rings of confusion existing anyway on droplets of less than 2 μm means errors of $\pm$7% are unavoidable and perhaps as much as $\pm$10% could be expected. The opacity of the oil and clarity of the points have already been suggested as the cause of the error between the identically prepared emulsions KM:14 and KM:15.

5.2.3 Comparison of Standard with Log-normal Means

The method used by Bezemer and Schwarz to test the applicability of distribution equations to raw droplet size data has been described in Chapter 2. Kunst and Mencer [88] have related the initial drop size distribution in mechanically prepared O/W emulsions to the speed with which droplets are stabilised. They postulated that the log-normal equation would only apply to those emulsions where droplets were stabilised almost immediately on formation, i.e. $B' >> A'$ in equation 5-1. Using the method proposed by Bezemer and Schwarz, they showed close agreement between the log-normal and the calculated means in sodium oleate stabilised emulsions, but poor agreement where no emulsifying agent was present. Unfortunately, they did not specify their emulsion systems.

In this work, the agreement on the basis of speed of stabilisation will be discussed in the particular section of work under study, but some general observations can be made. First, very good agreement was found in most cases between G and M; the former generally being slightly greater. This may be related to the tendency noted in the previous section in the focussing of the larger droplets on the slide. In the logarithmic-normal calculations, these would be the last few percent of the droplets which in this treatment have been omitted from the calculations. The largest differences were normally less than 15% and a more typical figure is 5 - 6%. These observations do not apply to model crude oil counts which support the postulate of a focussing error as all the droplets were large enough to be clearly visible and were therefore counted. This is shown up quite clearly in Tables 4-28 and 4-29 with M generally greater than G. This may be due to a cutting off of the larger droplets. The size distribution of the model systems and sometimes of the Brega emulsion was such that the 20 μm cell was probably too small for a few of the larger droplets in the range. The log-normal graph would thus "predict" droplets that the calculated means would not include, and so M would be larger. Conversely it is possible that the model system does not obey the log-normal distribution and that a form of limited coalescence occurs, in which case the largest droplets observed are truly the largest droplets in the sample and hence the standard mean is a true description of the distribution that exists.

Values of d_{sv} and x_{sv} were often quite different in cases where there was high polydispersity. This is the effect predicted by Jellinek [86], but differences between d_v and x_v were not quite so marked. However, the error may be accentuated by inaccuracy in values of σ_g carried by the arbitrary range of 10 - 90%. A long tail to the distribution sometimes fell below the 90% mark, thus increasing σ_g and therefore x_{sv} as well; at other times the opposite occurred giving smaller x_{sv} values. Once again, the problem appears to be one of focussing.

5.2.4A Variation of Water Concentration

Values of S_c are shown for five emulsions with ϕ from 0·5 to 0·7 in Table 5-1 using values of d_{sv} from Table 4-14.

Emulsion	ϕ	d_{sv}	F	S_c	Error ± %
31	0·50	2·95	6·00	2·03	5
32	0·55	3·31	7·33	2·21	11
33	0·60	3·39	9·00	2·66	17
34	0·65	4·71	11·14	2·37	24
35	0·70	5·22	14·00	2·13 ~2·6	50

Table 5-1

The discrepancy between d_{sv} and x_{sv} becomes larger as ϕ increases. This is due to the greater number of large droplets or the increasing polydispersity. Taking the difference between these values as the error and plotting out S_c versus ϕ including such error bars, a positive upward trend can be observed (Figure 5-3). Obviously, with a 50% error at ϕ = 0·70, firm conclusions cannot be drawn. There are clearly sufficient asphaltenes present to stabilise the

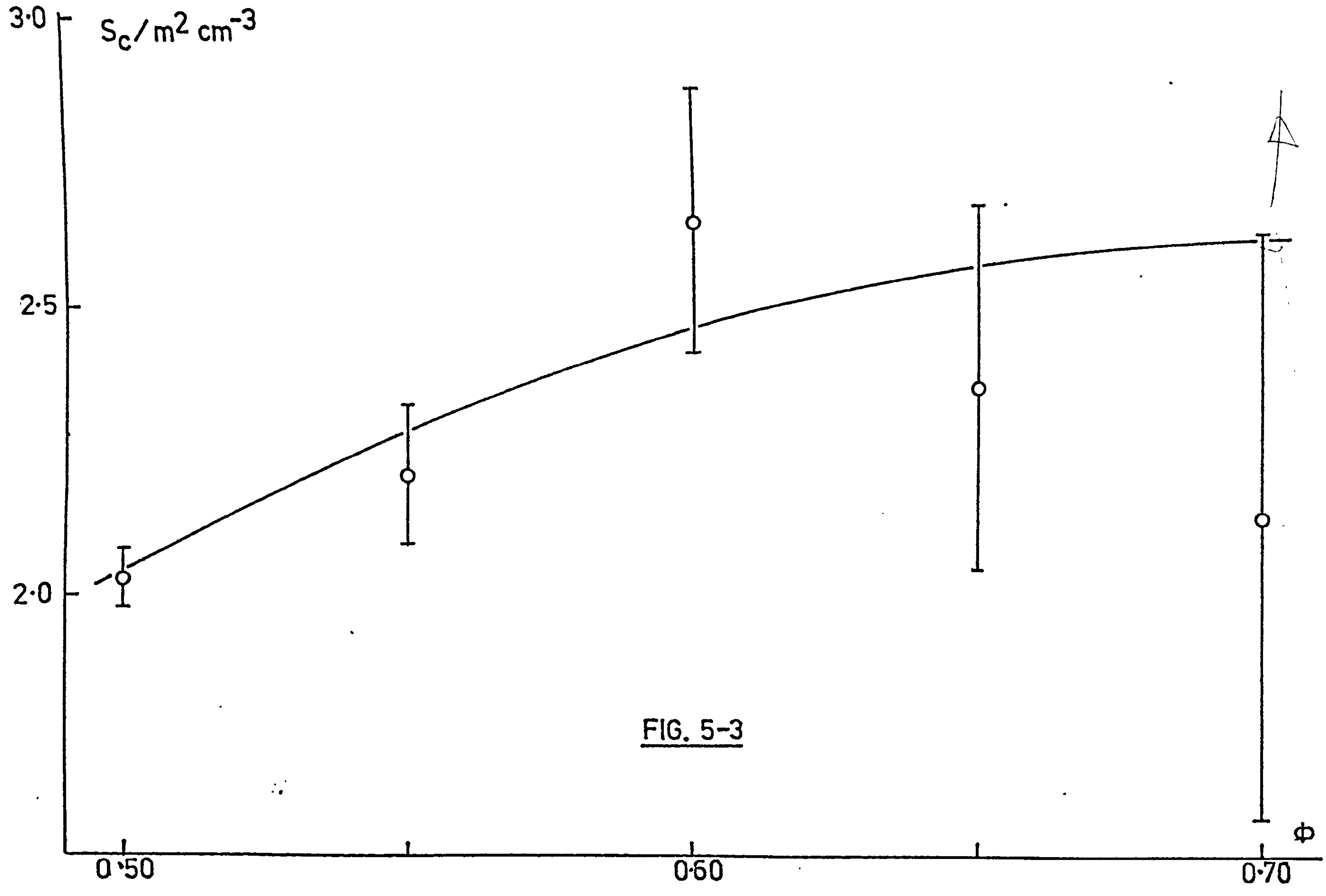

FIG. 5-3

larger interface formed on increasing ϕ. There is not enough data to determine whether the tail off is caused by asphaltene concentration becoming critical or because a smallest possible size of droplet is formed in the "Magimix" such that S_c can only increase as ϕ increases.

5.2.4B <u>Effect of Salt</u>

Values of S_c have been calculated from the values of d_{sv} shown in Table 4-4 with F = 6 and 18 for ϕ = 0·50 and 0·75 and these are shown in Table 5-2.

Salt Water		ϕ	Deionised Water	
Emulsion	S_c		Emulsion	S_c
36	1·05	0·50	41	0·943
37	1·64		42	1·49
38	1·76		43	1·83
39	2·78		44	2·39
40	3·70		45	3·16
-	-	0·75	52	2·47
-	-		53	3·35
49	4·96		54	4·00
50	6·43		55	3·98

Table 5-2

The results are plotted in Figure 5-4. Two features are immediately obvious. First, the emulsions made with salt water show a greater surface area stabilised and this is particularly pronounced at ϕ = 0·75. Secondly, a greater surface is stabilised in both cases at the higher ϕ values. This may be due to a more efficient exposure of the asphaltenes in the oil phase to the water interface. When salt is present, the asphaltenes are adsorbed slightly faster - a feature showing their polar nature. This may

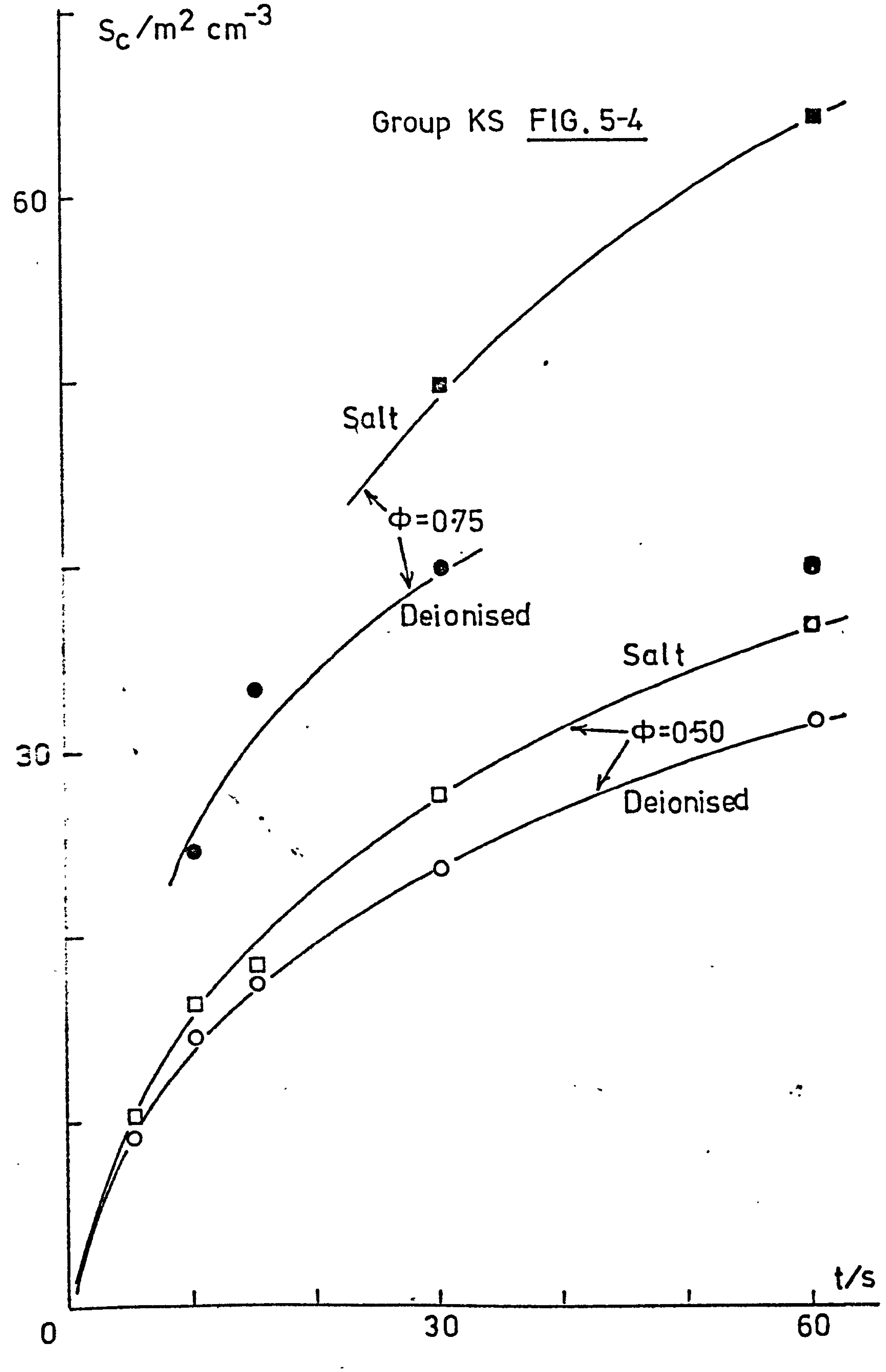

$S_c/m^2\ cm^{-3}$
Group KS FIG. 5-4
60
30
0
Salt
Φ=0·75
Deionised
Salt
Φ=0·50
Deionised
30
60
t/s

also explain the paradoxical behaviour exhibited in Table 4-13 where considerable water separation is shown by the salt water samples. The more rapidly adsorbed asphaltenes may have immediately stabilised the very large surface area of the large number of small droplets initially formed. The remaining asphaltenes would take longer to diffuse to the interface with the unemulsified water. In the case where the asphaltenes are not attracted so quickly to the water phase, the stabilisation of the interface occurs more slowly, but with larger droplets stabilised, the bulk of the water will be emulsified faster. However, given an unlimited time, these results suggest that an emulsion formed on the sea would be more stable than one formed in fresh water - although ageing effects show that both are highly resistant.

Hellmann and Bruns [18] found that fresh water emulsions stirred for the same length of time were more viscous than similar salt water emulsions and this was also observed in the present work. This can be explained on the basis of the above discussion. The slower uptake of the fresh water would lead to a more homogeneous dispersion shown by the smaller σ_g values for the fresh water emulsions. The low S_c values for KS:54 and 55 are explained from the observations in Chapter 4 where it was found that the high viscosity prevented effective stirring.

5.2.4C <u>Admiralty Emulsions</u>

One of the first observations that can be made is the apparently poor agreement between d_{sv} and x_{sv} in Table 4-10. A glance at a photomicrograph of an Admiralty emulsion (plate 3) shows the reason to be the polydispersity of the droplets. As with group KS, the salt appears to help stabilise very small droplets. However the later, larger droplets over-predominate on the microscope slide and although the tail containing these spurious larger diameters appears to have been cut off in emulsion A:205 giving $x_{sv} < d_{sv}$, the log-normal graph in A:206 predicts more larger droplets by giving $x_{sv} > d_{sv}$ the calculated mean. Comparison of surface areas stabilised is meaningless as time of exposure on the surface of the sea is unknown.

5.2.5 Effect of Detergent Addition on Rate of Formation

5.2.5A General Observations

Of the detergent-free emulsions, the Kuwait and Tia Juana emulsions 00:115 and 117 were the most satisfactory. As predicted there were high percentage differences between d_{sv} and x_{sv} at low stirring times but as stirring progressed these differences reduced to less than 10%. Agreement between M and G was excellent. The unsatisfactory method of computing the straight line is exemplified in doubtful σ_g values which affect calculation of x_{sv}. This is exhibited in 00:115·4 where σ_g at 1·62 is slightly greater than the trend would predict; consequently, x_{sv} is 20% higher than d_{sv} in a region where better agreement would be expected. The overall agreement supports the observations of virtually immediate stabilisation.

The Brega emulsions are not so encouraging. There are larger percentage differences between the two sets of means and it can be seen that the means do not always decrease with stirring time. In 00:147, d_{sv} increases after the second reading. The explanation is that these emulsions do not require very much stirring before the maximum possible surface area is stabilised. Once this point has been exceeded, the adverse effect of over-stirring can be seen.

Agreement between the two sets of means is very good for group KOC. Larger discrepancies arise in groups KOA and KON but the emulsions in these groups exhibited considerable clumping of droplets which made photography and counting more difficult. The general agreement shows that once the detergent has been displaced from the interface then it has no further effect. This observation is confirmed in group TON although the bimodal distributions found for emulsions TON:138 and 139 and for KON:145 are interesting. It seems that an initial distribution of small droplets was formed whilst the remaining water was eventually stabilised in much larger droplets. In emulsion TON:140, it would appear that the remaining water stayed unemulsified or emulsified very slowly; consequently there is no bimodal behaviour.

The effect of BP 1100X addition to Brega is enigmatic. BON:141 and 142 behave as would be expected with greater coalescence and complete breakdown after 24 hours. However apparently greater stability is imparted to BON:148 and 149 with further detergent addition. It is well known in the paint industry that a small addition of alcohol or water to a non-aqueous paint containing a bentone clay will develop the charge in the plate-like structure of the clay to make the paint thixotropic. One possibility is that the detergent somehow charges the wax plates which structure the emulsions thus preventing coalescence. Such a charge effect would also explain the absence of clumping or polyhedral droplets in these two emulsions. Furthermore, such a mechanical explanation does not contradict the observation that in BON:149 the interfacial tension between Brega and water is so low that the two phases at times appeared to "merge".

5.2.5B Proposed Mathematical Treatment

Gopal [85] based his treatment of emulsion formation on a first order rate law with a minimum size formed after an infinite time of emulsification. For a crude oil emulsion with no detergent addition, a first order law is proposed for increase in S_c with a theoretical maximum value of S_{max}

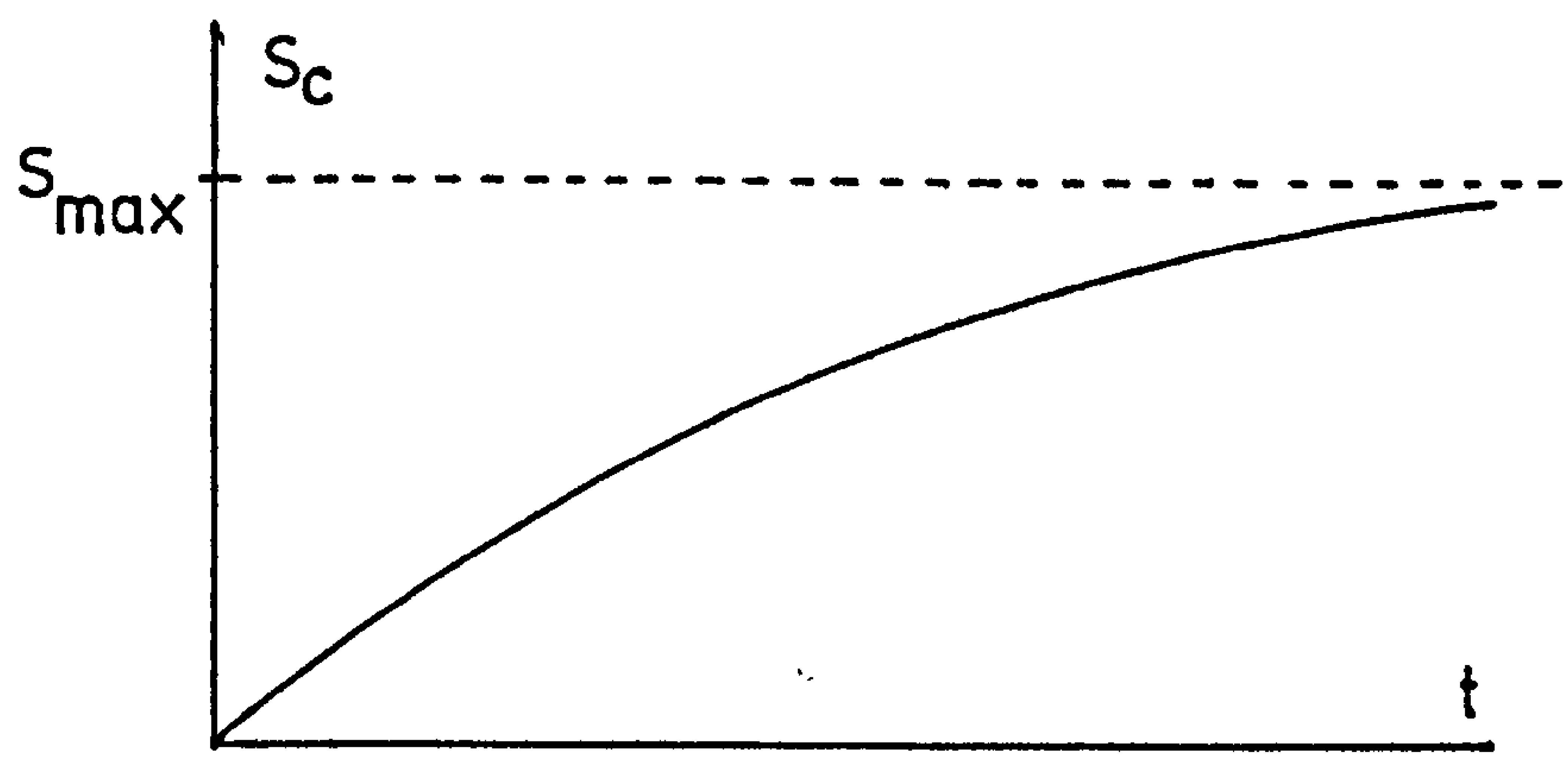

FIG. 5-5

$$\frac{dS_c}{d_t} = k_o (S_{max} - S_c) \qquad 5\text{-}6$$

k_o = rate constant for a given oil 0,

$$-\ln (S_{max} - S_c) = k_o t + \text{constant}$$

When $t = 0$, $S_c = 0$ (i.e. negligible)

$$\therefore \quad -\ln (S_{max} - S_c) = k_o t - \ln S_{max}$$

$$\ln \left(1 - \frac{S_c}{S_{max}}\right) = - k_o t \qquad 5\text{-}7$$

$$S_c = S_{max} \{1 - \exp(-k_o t)\} \qquad 5\text{-}8$$

The major observation when detergent has been added in quantities smaller than required for inversion is that after an initial delay time, when complex behaviour is observed, the asphaltenes eventually displace all the detergent which then has no further effect. This is demonstrated in Figure 5-6 where S_d represents the surface area per unit volume of continuous phase of an emulsion with detergent present.

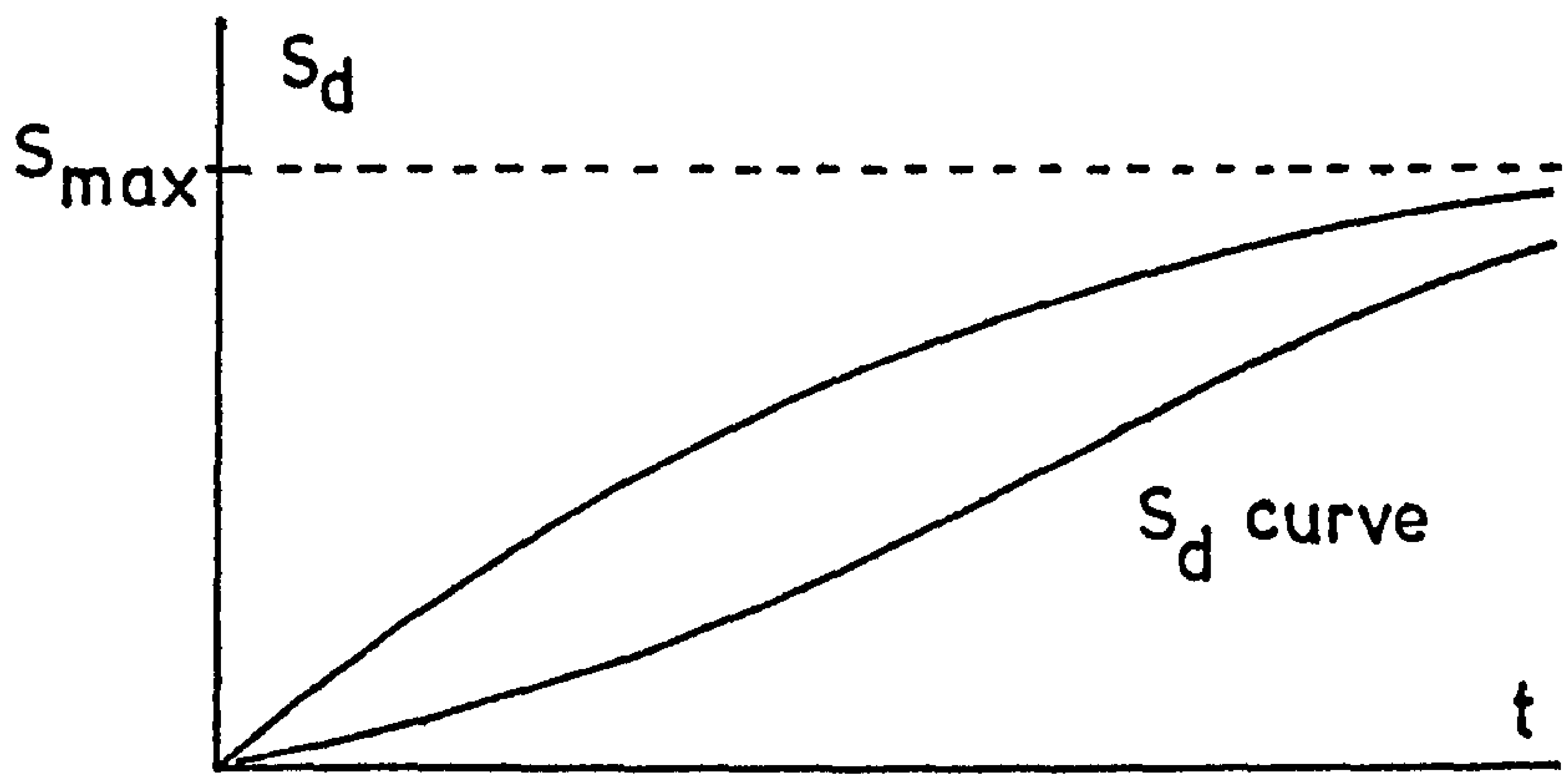

FIG. 5-6

The surface area of the O/W emulsion that is stabilised by detergent is ignored. The model so far assumes that the detergent is in dynamic equilibrium with the interface according to the Gibbs Adsorption Isotherm. Kitchener and Mussellwhite [31] have observed that certain emulsifying agents will reach the interface and stay there perhaps even changing their structure (e.g. casein in milk) so that such an equilibrium cannot exist. The asphaltenes appear to fit into this category. Assuming the detergents do not affect the asphaltenes in the bulk oil, then S_{max} should be the same whether or not detergent has been added. If the displacement of detergent by asphaltenes depends only on the rate at which the detergent leaves the interface then the gap between the S_c and S_d curves will possibly reduce according to a first order rate law.

$\omega = \frac{S_d}{S_c}$

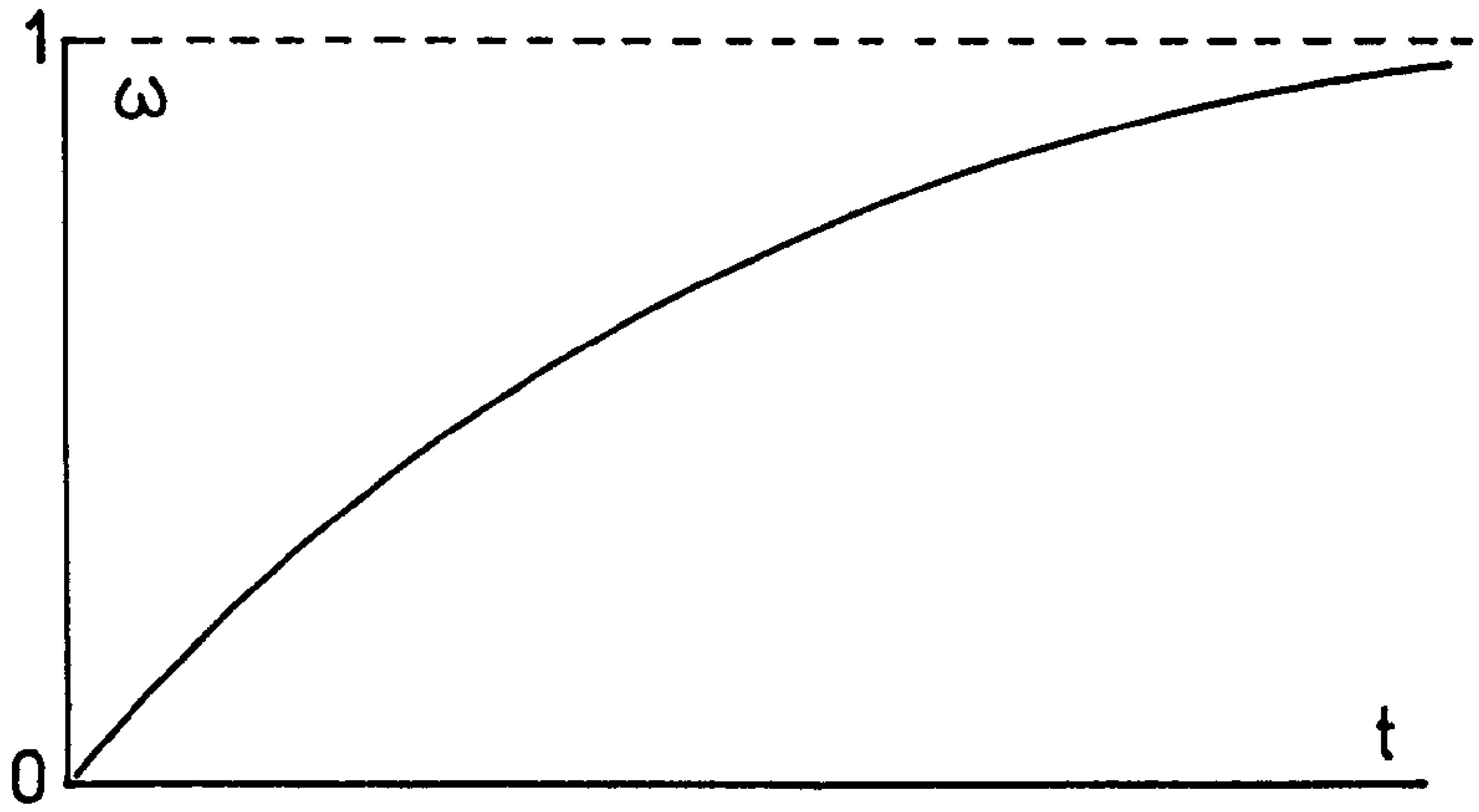

FIG. 5-7

$$\frac{d\omega}{dt} = (1 - \omega)\, k_d \qquad 5\text{-}9$$

k_d = rate constant for displacement of detergent by asphaltenes.

$$- \ln (1 - \omega) = k_d t + \text{constant}$$

When t = 0, $\omega = 0$; based on the assumption that the initial interface is stabilised by asphaltenes, i.e. $S_d = 0$ so $\omega = 0$

$$\ln (1 - \omega) = - k_d t \qquad 5\text{-}10$$

$$S_d = S_c \{1 - \exp(-k_d t)\} \qquad 5\text{-}11$$

Combining equations 5-8 and 5-11

$$S_d = S_{max} \{1 - \exp(-k_o t)\}\{1 - \exp(-k_d t)\} \qquad 5\text{-}12$$

5.2.5C Application of Treatment to Results

One of the problems with experimental exponential curves is in calculating the asymptotic values. Guggenheim's method [89] was tried, but this is best used in cases where the points are readily obtained over a small part of the graph representing a region of less than the half-life. Gopal [85] did not indicate how he obtained his ∞ values but presumably he extrapolated. Before applying equation 5-12 it is first necessary to apply equation 5-7 to emulsions 00:115 to 117 to obtain the values of S_{max} and k_o. A graphical iterative method was chosen.

First an assumed value of S_{max} was estimated from a plot of S_c versus t. A graph was drawn by plotting the L.H.S. of equation 5-7 versus t. Further lines were plotted by adjusting the values of S_{max}. The chosen value of S_{max} was the one where the points gave the best straight line; the other plots showed pronounced curves. These plots for emulsions 00:115 to 117 are shown in Figures 5-8 to 5-10 respectively. It can be seen that there is a very marked difference in changing S_{max} just by $\pm 3\%$. Values of k_o were taken from the gradient of the optimum plots and these are shown with S_{max} in Table 5-3. The theoretical graphs then obtained from equation 5-8 are shown for all three crude oils in Figure 5-11.

Group 00 Emulsion	S_{max} $m^2\ cm^{-3}$	k_o s^{-1}
115	2.50	0.0539
116	0.820	0.267
117	3.10	0.0415

Table 5-3

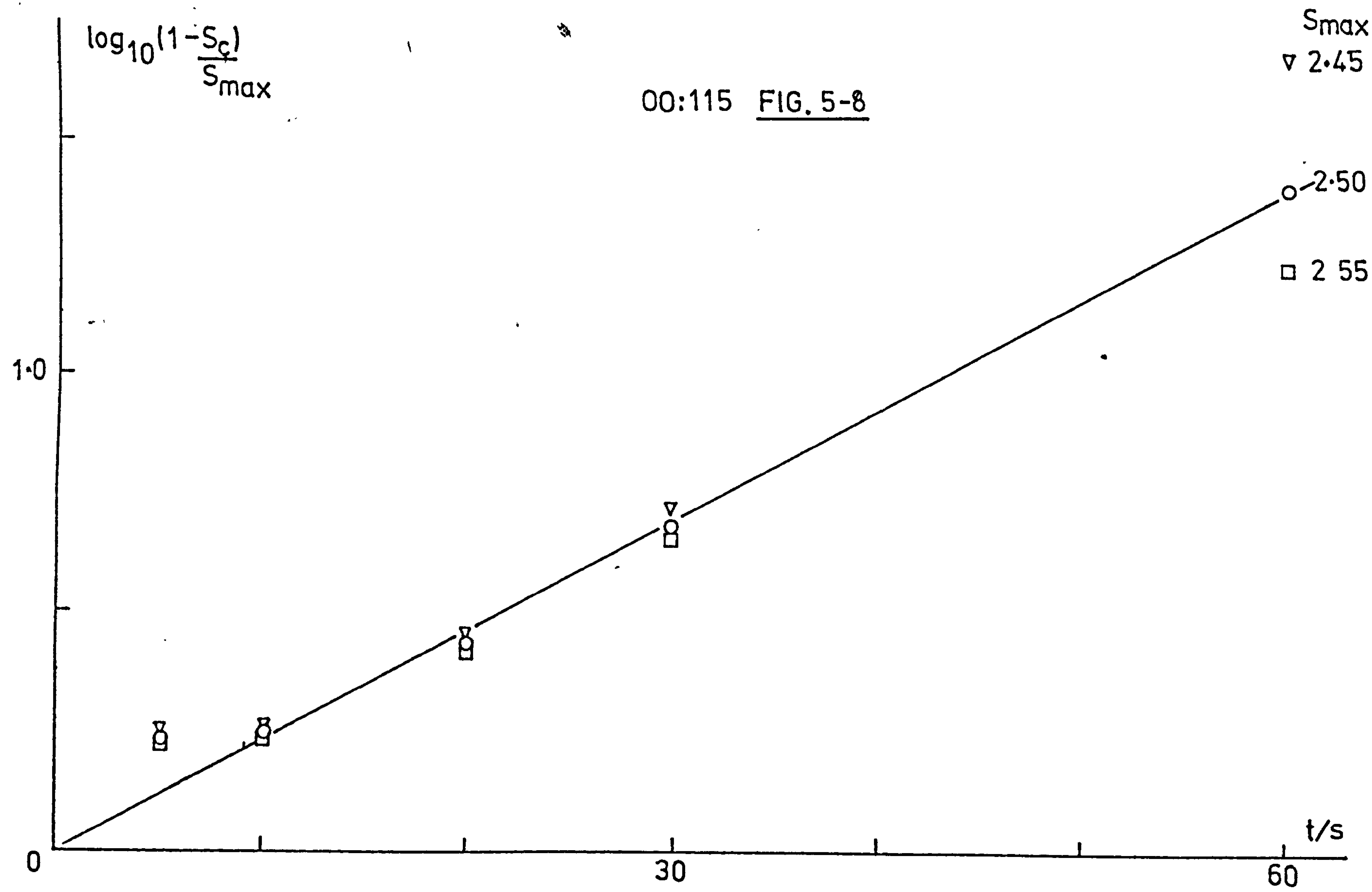

00:115 FIG. 5-8

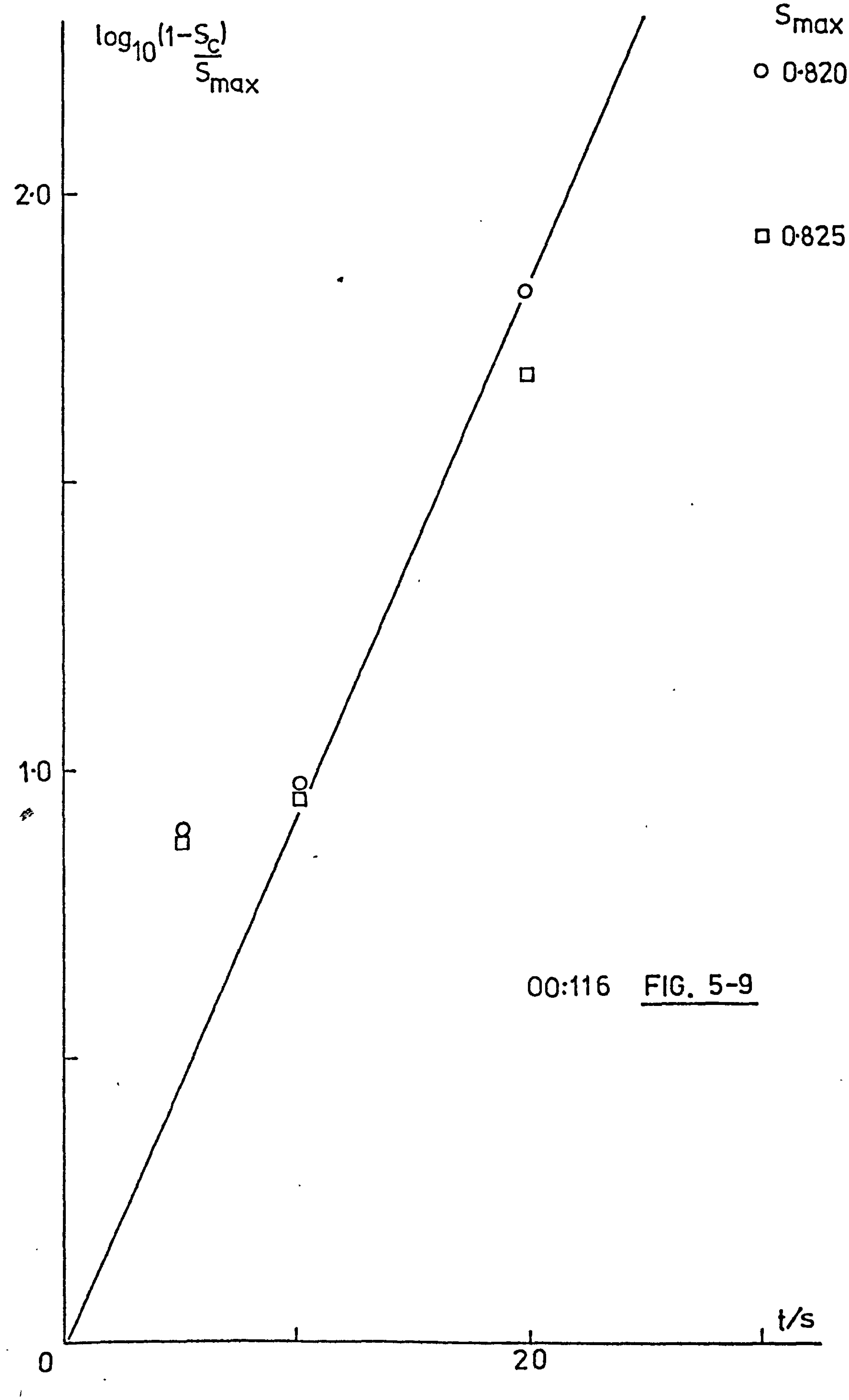

00:116 FIG. 5-9

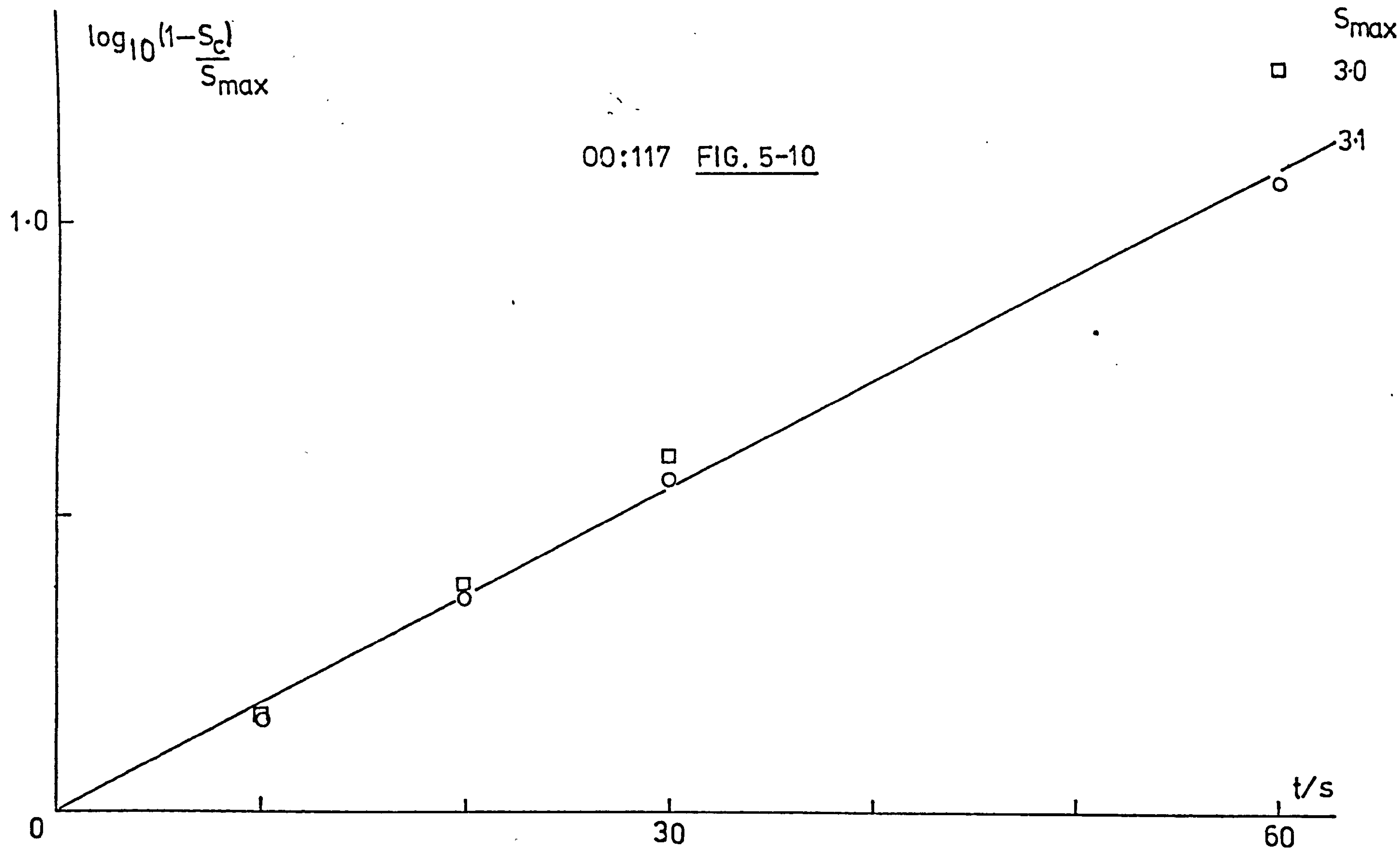

00:117 FIG. 5-10

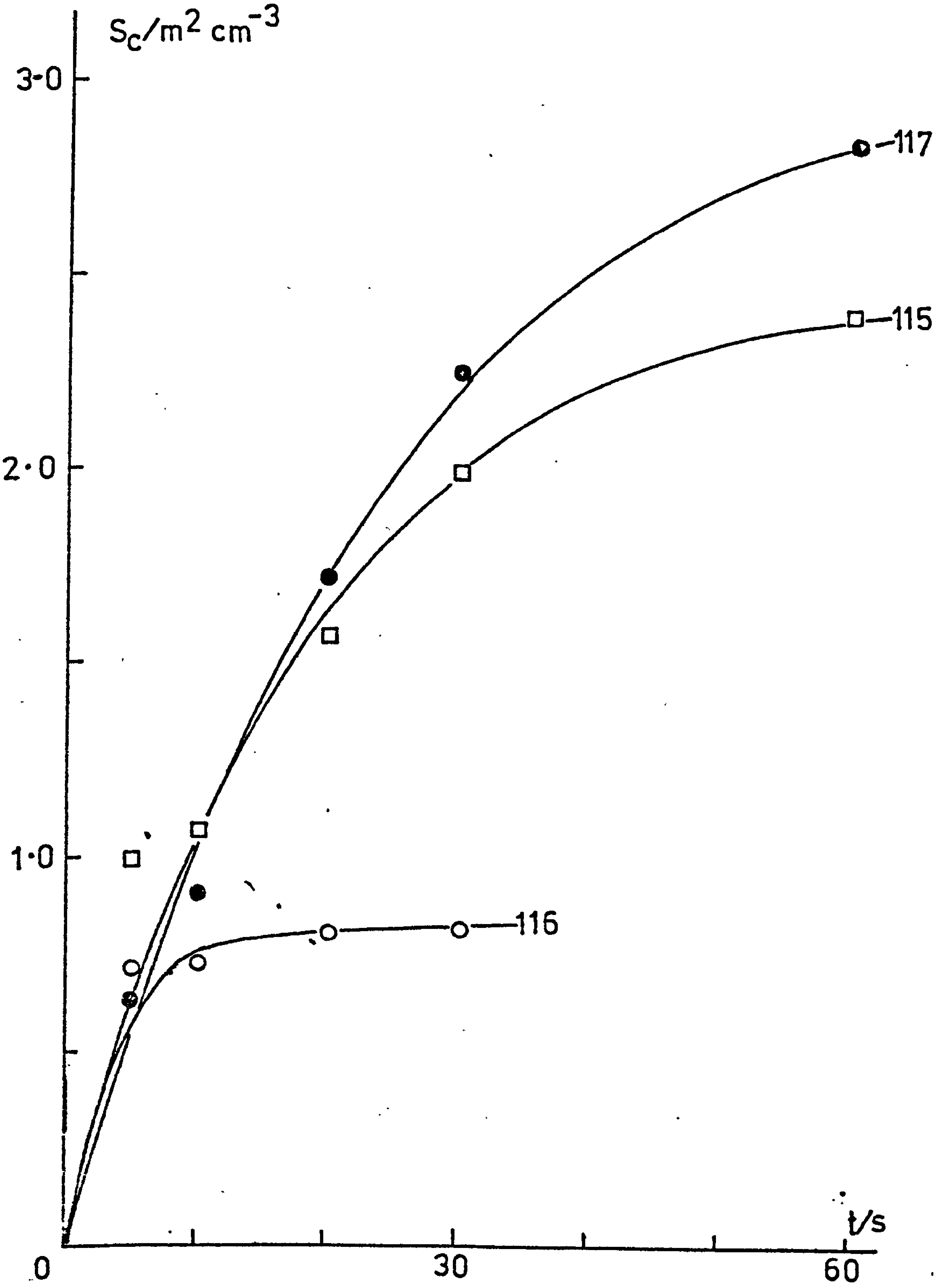

Group:00 FIG. 5-11

The values of S_{max} for Kuwait and Tia Juana do not differ as much as would be expected from their asphaltene concentrations. This may be because the minimum possible drop size in the "Magimix" (i.e. the maximum possible surface area) is not low enough for all the available asphaltenes to be used. The rate of stabilisation, k_o is probably related to the viscosity of the crude oil in that it reflects both the speed at which the oil/water mixture can achieve a dynamic equilibrium in the stirrer and also the speed at which the asphaltenes can diffuse through the oil to the interface in sufficient quantity to stabilise it.

Iterative methods are not required for equation 5-12 once S_{max} and k_o have been obtained. A direct plot of the two variables in equation 5-10 will give k_d. The full procedure adopted was as follows. A table of theoretical values of S_c was obtained using equation 5-8 and the parameters shown in Table 5-3. The mean diameter used to calculate S_d was d_{sv}. The theoretical value of S_c at the same stirring time as the particular value of S_d was used to obtain ω and the linear relationship to obtain k_d was plotted using logarithms to the base 10.
The various plots for groups KOA, KOC, KON and TON are shown in Figures 5-12 to 15 respectively and $\pm 10\%$ errors bars are shown. At first sight, the fit appears to be very poor. However, the error involved in the first point has already been discussed and a $\pm 10\%$ error is possibly conservative. A second consideration is that if S_d is within 10% of S_{max} then the upper limit of the error will indicate a negative $\log_{10}(1-\omega)$ value which is $-\infty$. The nearer S_d is to S_{max}, the faster this limit is approached. The

FIG. 5-12

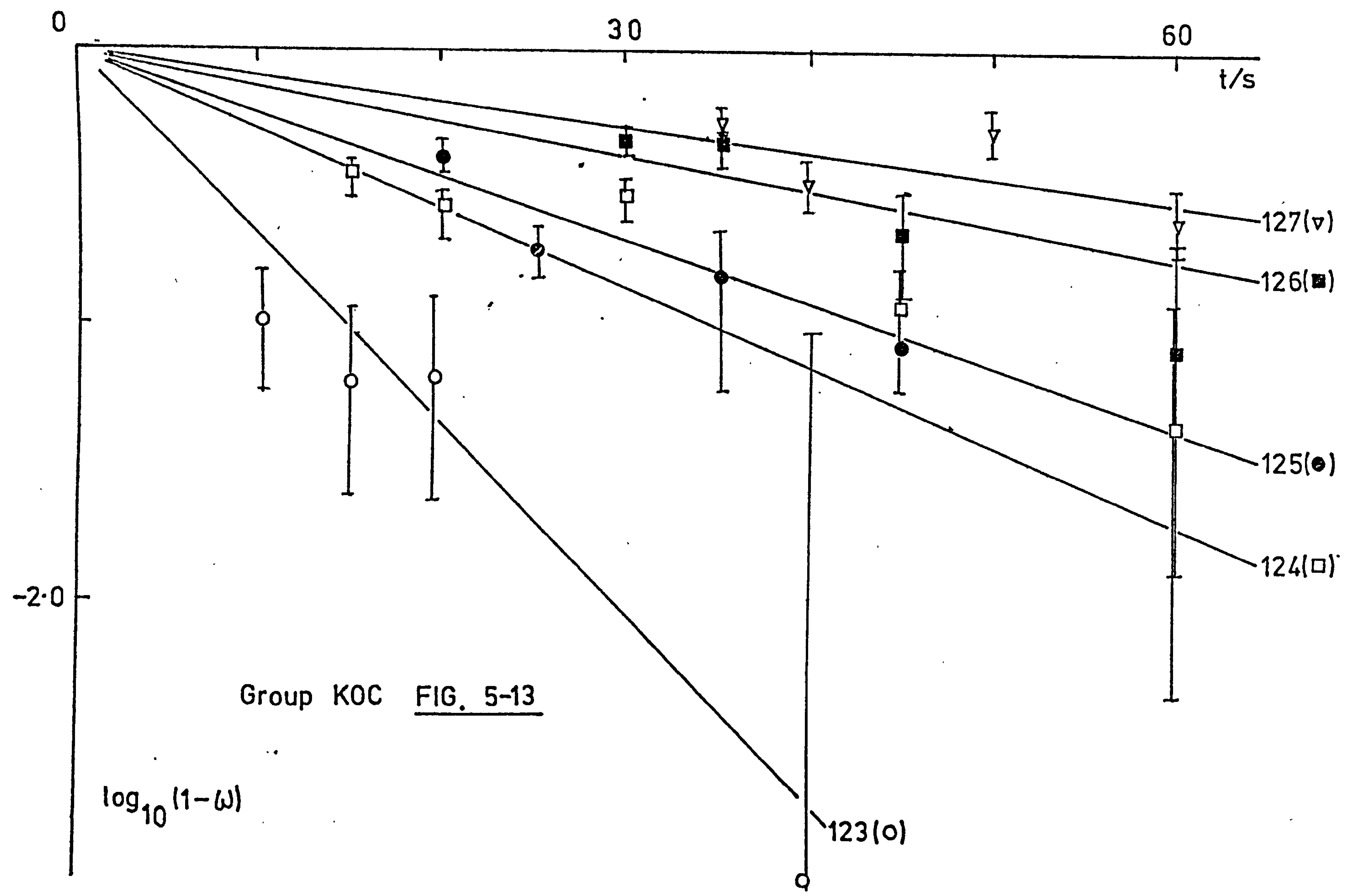

0
30
60
t/s
-2·0
$\log_{10}(1-\omega)$
127(▽)
126(■)
125(●)
124(□)
123(○)
Group KOC FIG. 5-13

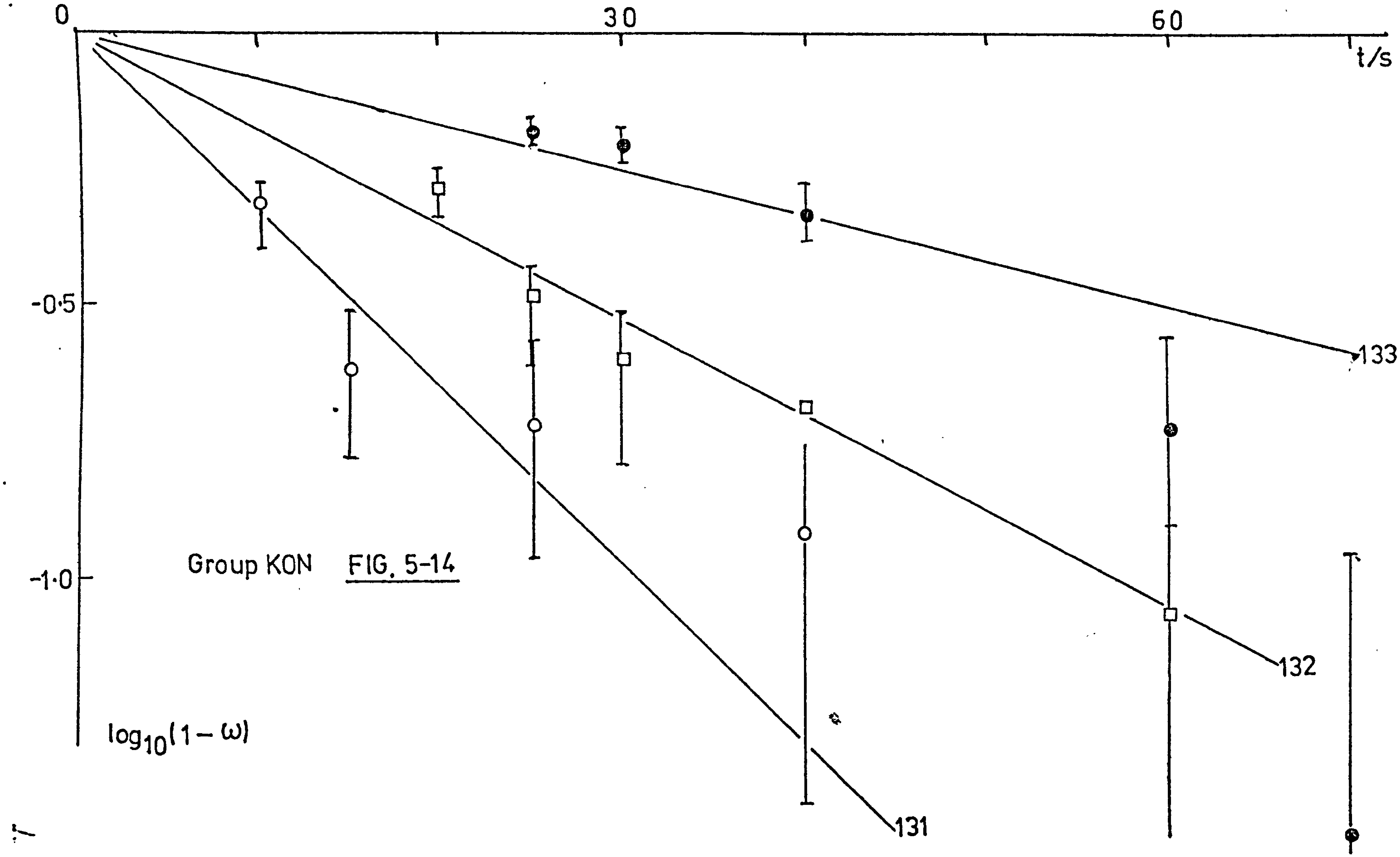

FIG. 5-14

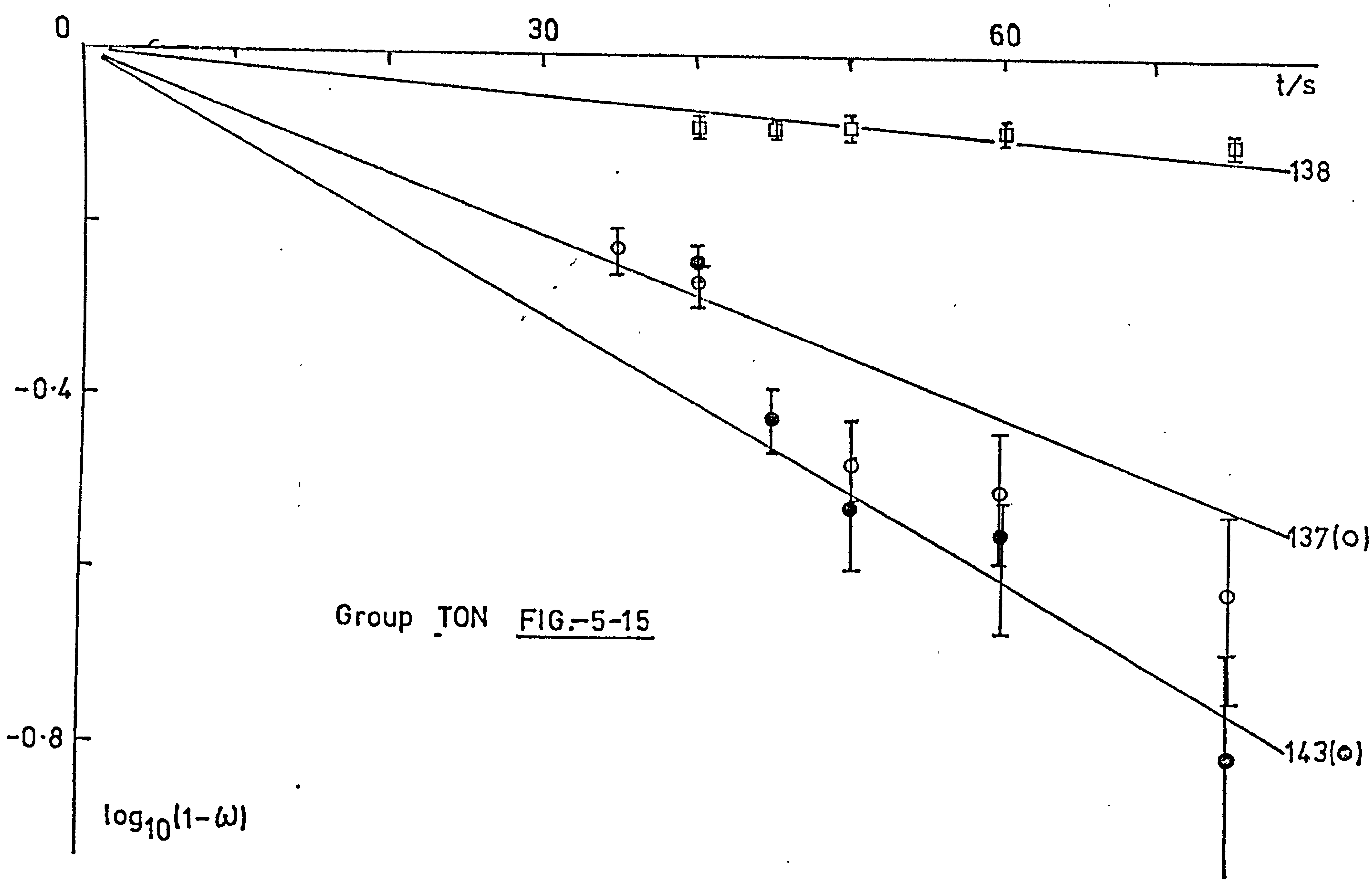

Group TON FIG.-5-15

most important points then are the three in the centre of the line. Despite the apparently poor fit on these graphs, when the k_d values so obtained are used in equation 5-12, a reasonable fit is obtained and the graphs obtained for the four groups are shown in Figures 5-16 to 19. The values of k_d are shown in Table 5-4.

Group KOA		Group KOC		Group KON		Group TON	
Emulsion	k_d s x10^3	Emulsion	k_d s x10^3	Emulsion	k_d s x10^3	Emulsion	k_d s x10^3
118	91·7	123	158	131	76·5	137	17·7
119	49·3	124	64	132	39·2	138	3·7
120	36·0	125	53	133	18·9	139	* 0·17
121	32·0	126	30	144	* 5·8	140	* 0·08
122	26·9	127	22	145	* 3·5	143	23·0
146	*41	151	*59	* Single point determinations			
150	*19	152	*14				

Table 5-4

5.2.5D <u>Implications in the Proposed Theory</u>

Figure 5-20 shows the values of k_d from Table 5-4 as plotted against the weight of detergent per unit volume of oil phase for groups KOA, KOC, KON and TON. Molar concentrations could not be used as the molecular weight of the detergent in BP 1100X is unknown. Initially, small increases in concentration of the water soluble detergents considerably reduced k_d; however with BP 1100X additions, the effect on k_d was much less pronounced. Although comparisons are difficult when molar concentrations have not been used, this effect may be due to the following factors. In section 5.2.5B, k_d was

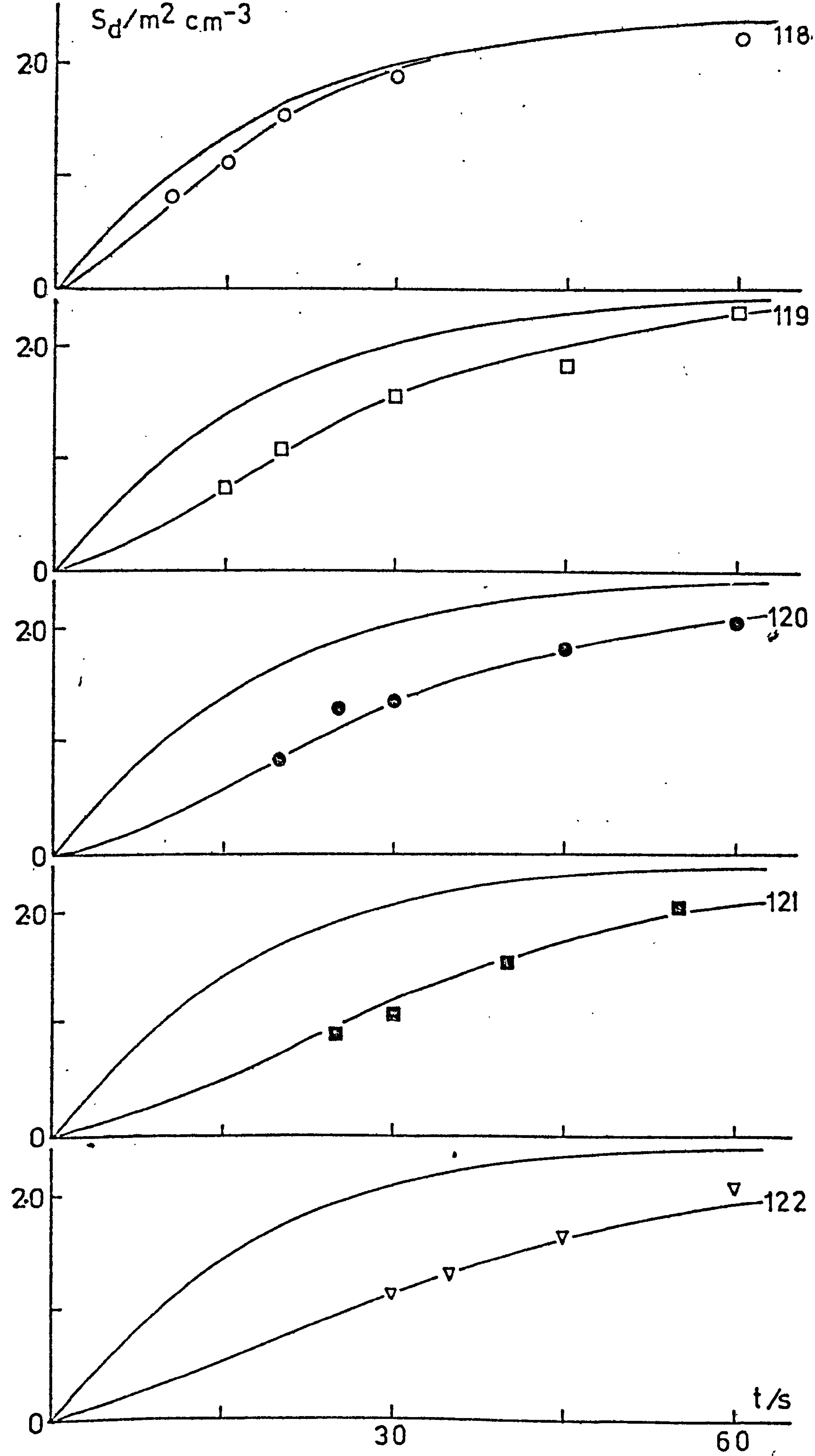

Group KOA FIG. 5-16

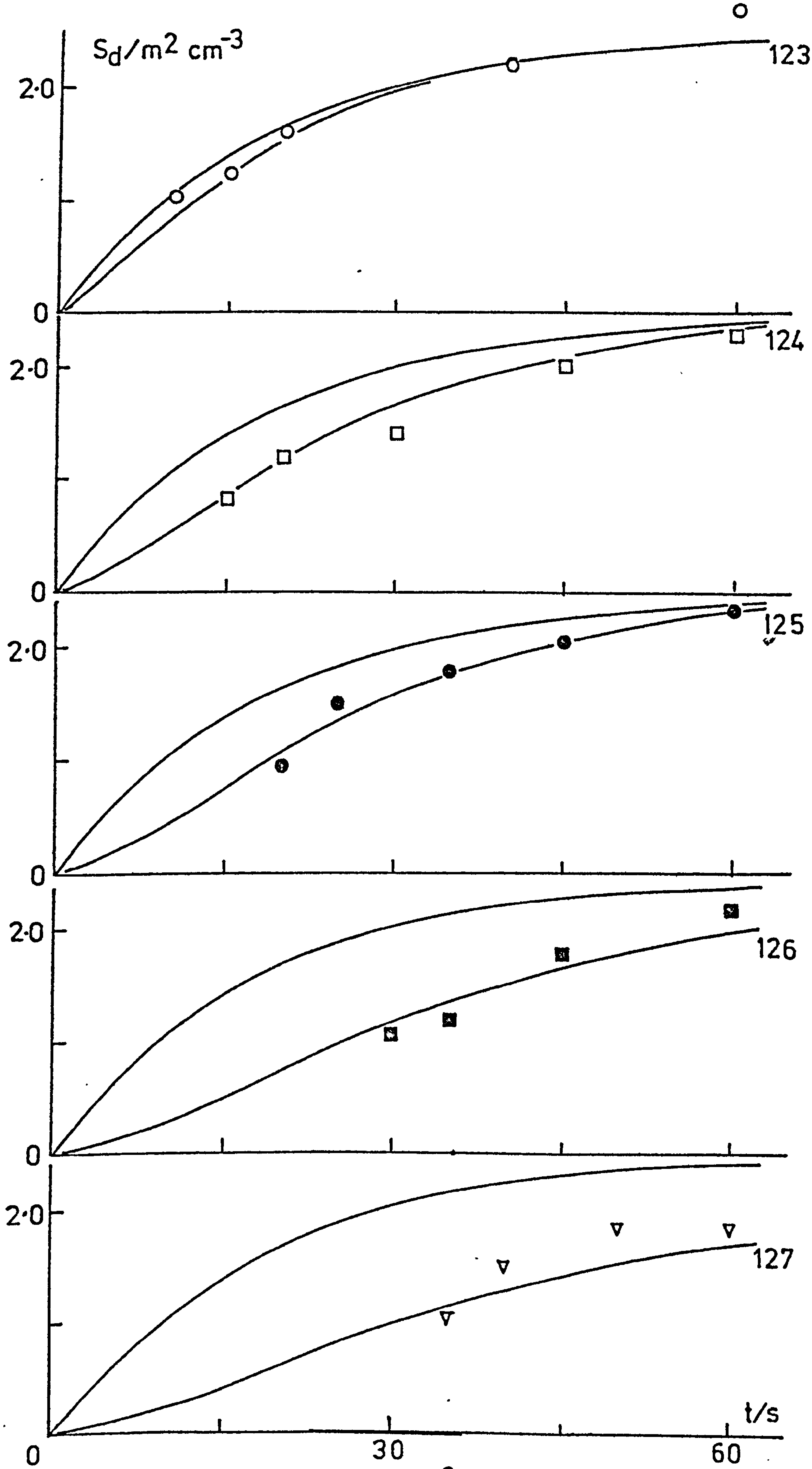

Group KOC FIG. 5·17

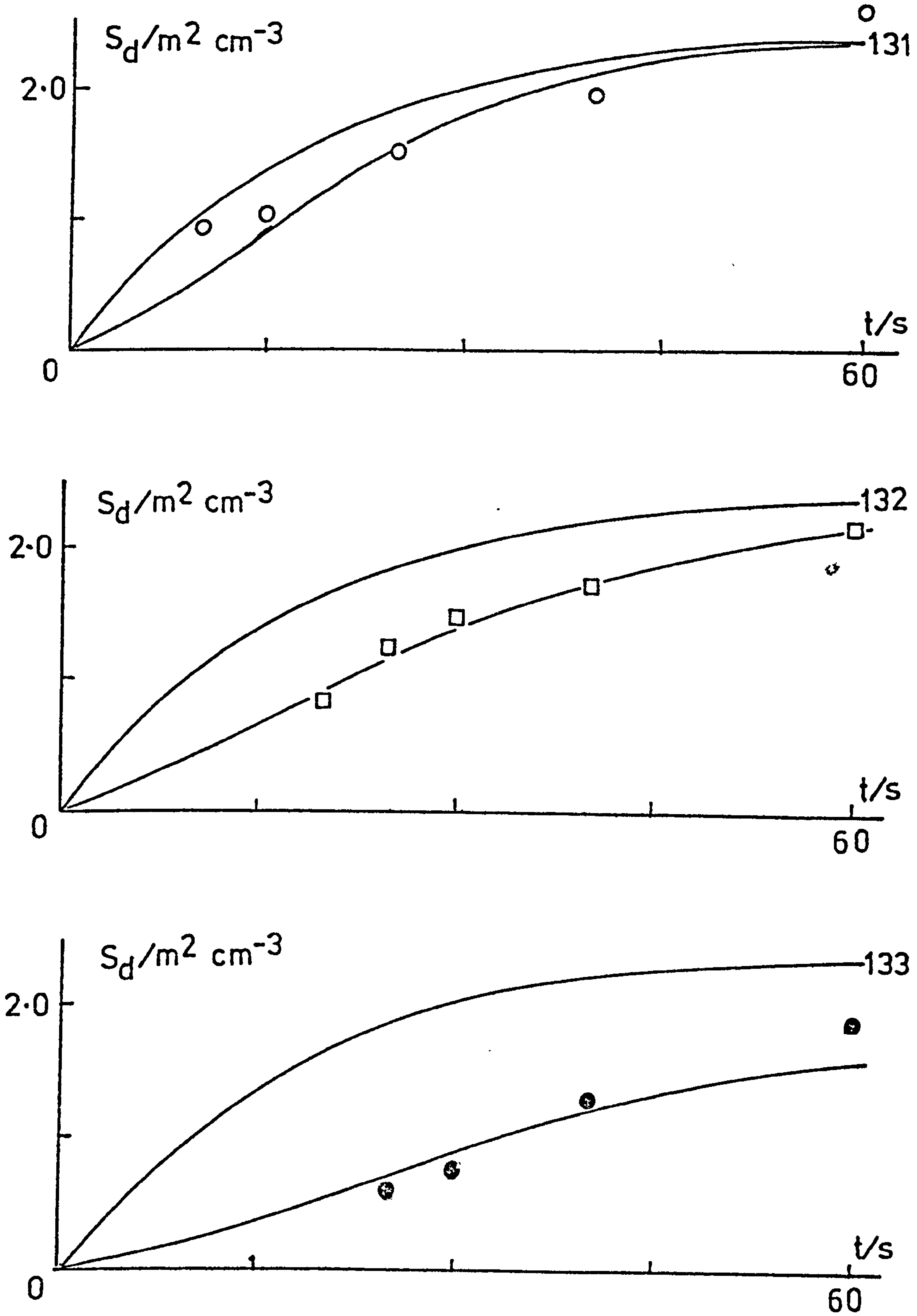

Group KON FIG. 5-18

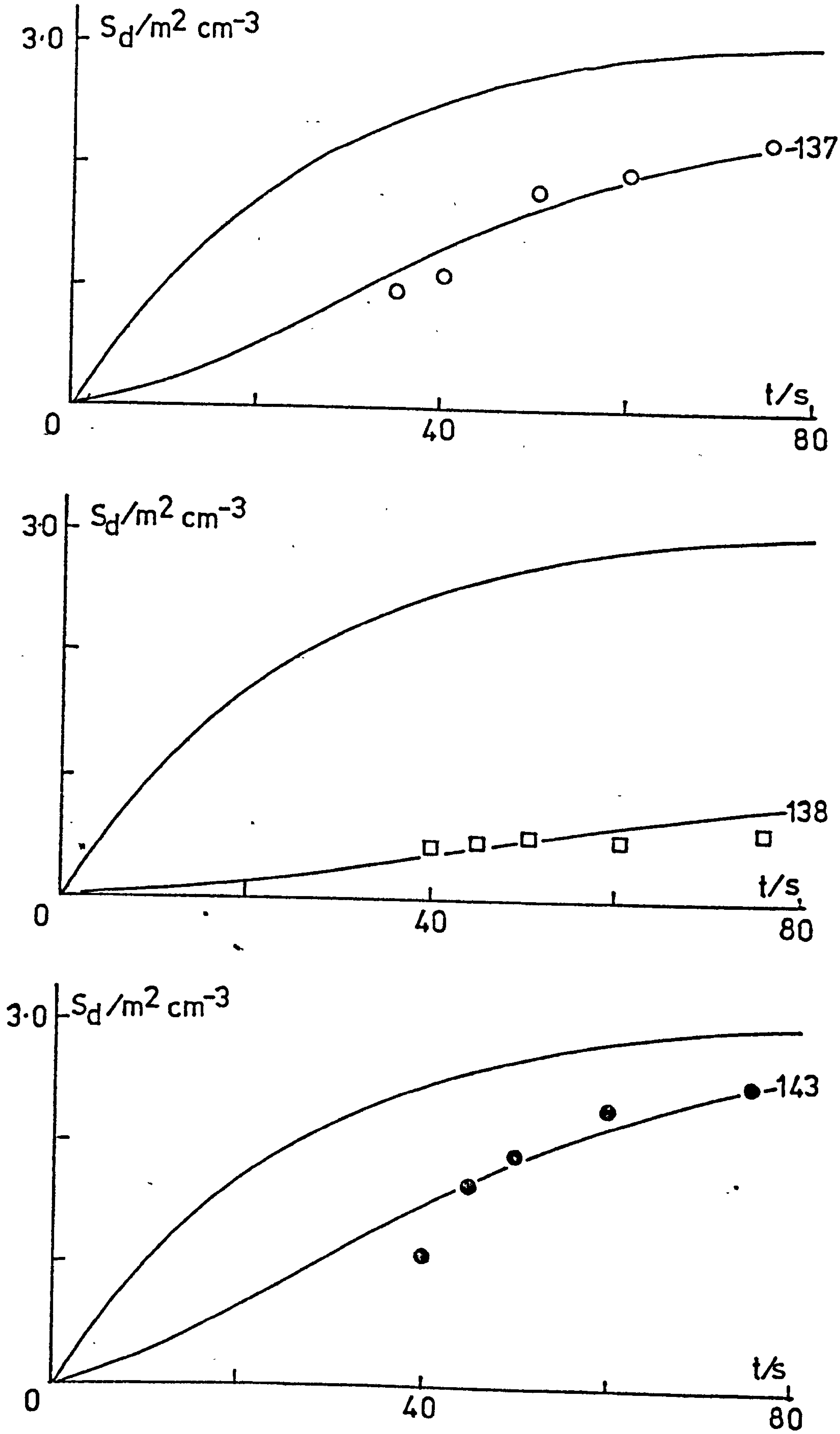

Group TON FIG. 5-19

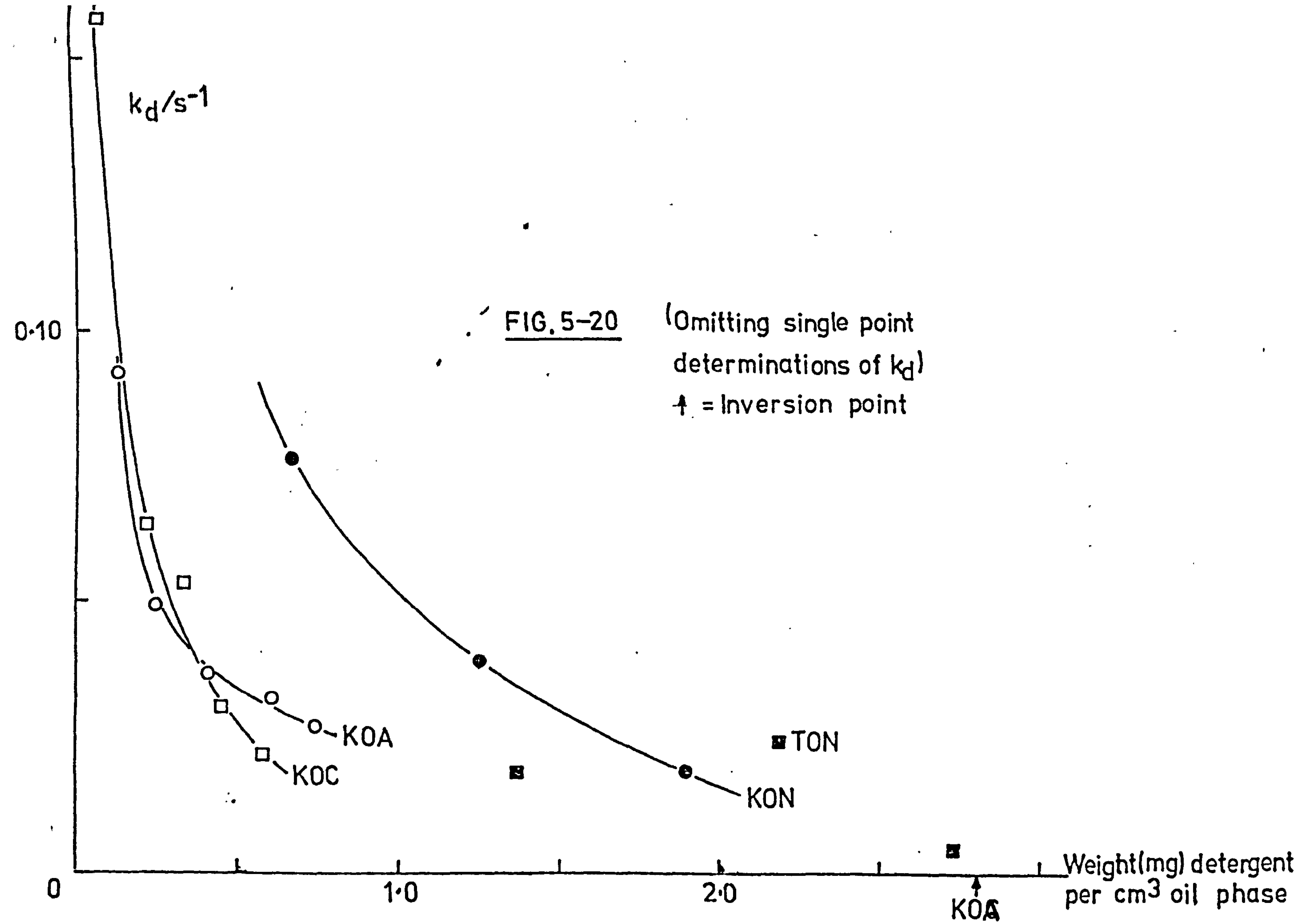

FIG. 5–20 (Omitting single point determinations of k_d)
↑ = Inversion point

postulated as the rate at which the detergent is displaced by the asphaltenes from the interface. In the first instance, areas of interface will be stabilised by both types of surface active agent. In the case of the water soluble detergents, initial access to the interface is unimpeded and relatively fast due to the low viscosity of the water. In the case of BP 1100X, the crude oil is quite viscous and in addition the detergent has to compete with the asphaltenes for these initial areas of stabilisation.

Without linearising the graphs in Figure 5-20 it is not possible to predict where the point of inversion will occur, although the empirical points are marked on. It is evident though that at low values of k_d ($<0{\cdot}02\ S^{-1}$), large changes in detergent concentration are accompanied by only slight changes in k_d. No account has been taken of the effect of the increased ionic strength of the water soluble detergents on S_{max}. However, as the concentration of these detergents was relatively small compared to the existing salt concentrations, this has been ignored.

Groups KS and KV indicated that S_{max} increased with ϕ and although no specific experiments were carried out, data from group KR was investigated for this phenomenon. A plot of S_c versus t for this data is shown in Figure 5-21 and it is clear that the values after thirty and sixty seconds stirring are too high. This is due to the loss of emulsion during the rheology experiments which led to a smaller emulsion sample in the stirrer and subsequent greater power input/unit volume. Comparison of KR:87 with OO:115 suggests reducing S_{max} for the former by about 25%. Despite this somewhat arbitrary approach, when the KR data was treated as

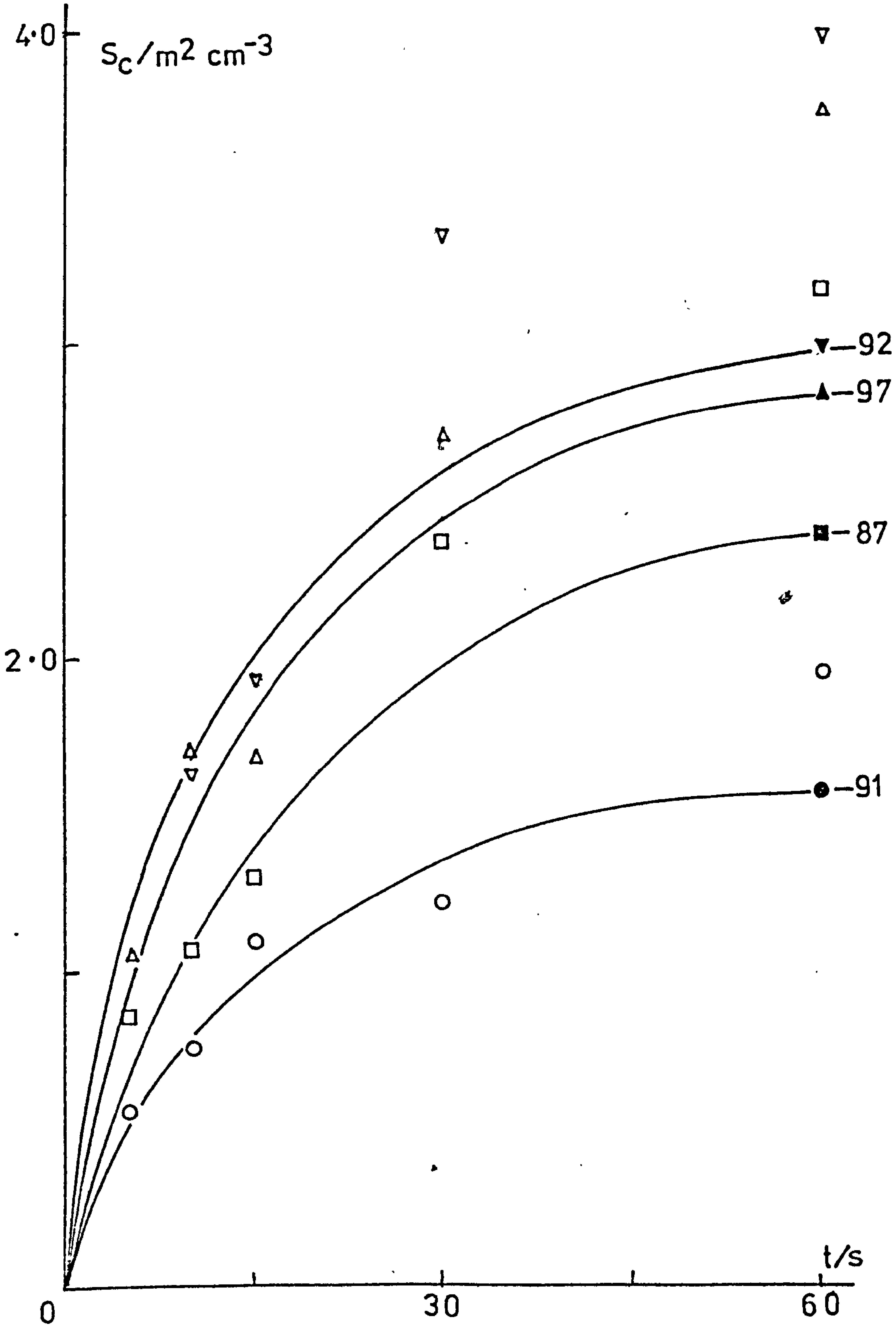

Group KR FIG. 5-21

Black symbols indicate a value reduction of 25%

described in section 5.2.5B the graph shown in Figure 5-22 emerges. The scatter is not as wide as might be expected and the indications are that k_o is the same for all four values of ϕ. This would confirm the earlier interpretation of k_o as being related to the diffusion of the asphaltene to the interface.

5.2.6 Ageing Studies

The first and most obvious feature was that Brega crude oil emulsions showed evidence of breakdown within twenty four hours whether or not detergent had been added. The apparent stabilisation by BP 1100X of certain Brega emulsions has already been dealt with.

None of the emulsions in groups KOA, KOC and KON exhibited any separation after standing for a few days, and this is supported by the droplet size data in Table 4-38. All the means obtained after a few days ageing appear to be equal (within the errors established for such means). Even after eleven months, no visible separation had occurred. However, the qualitative observations in Table 4-37 suggest a gradation of breakdown with detergent concentration. It is significant that the most stable group was KOC, the only system that did not exhibit clumping. Kitchener and Mussellwhite [31] have described the diffusion processes by which large droplets will grow larger at the expense of smaller droplets next to them. It appears that both sodium dodecyl sulphate and BP 1100X develop a secondary minimum so that the droplets are close enough for such a process to occur. In the case of the former detergent, this may be a genuine charge effect. For BP 1100X, it is more likely that the detergent replaces the secondary film and this allows the droplets to approach closer together such that the

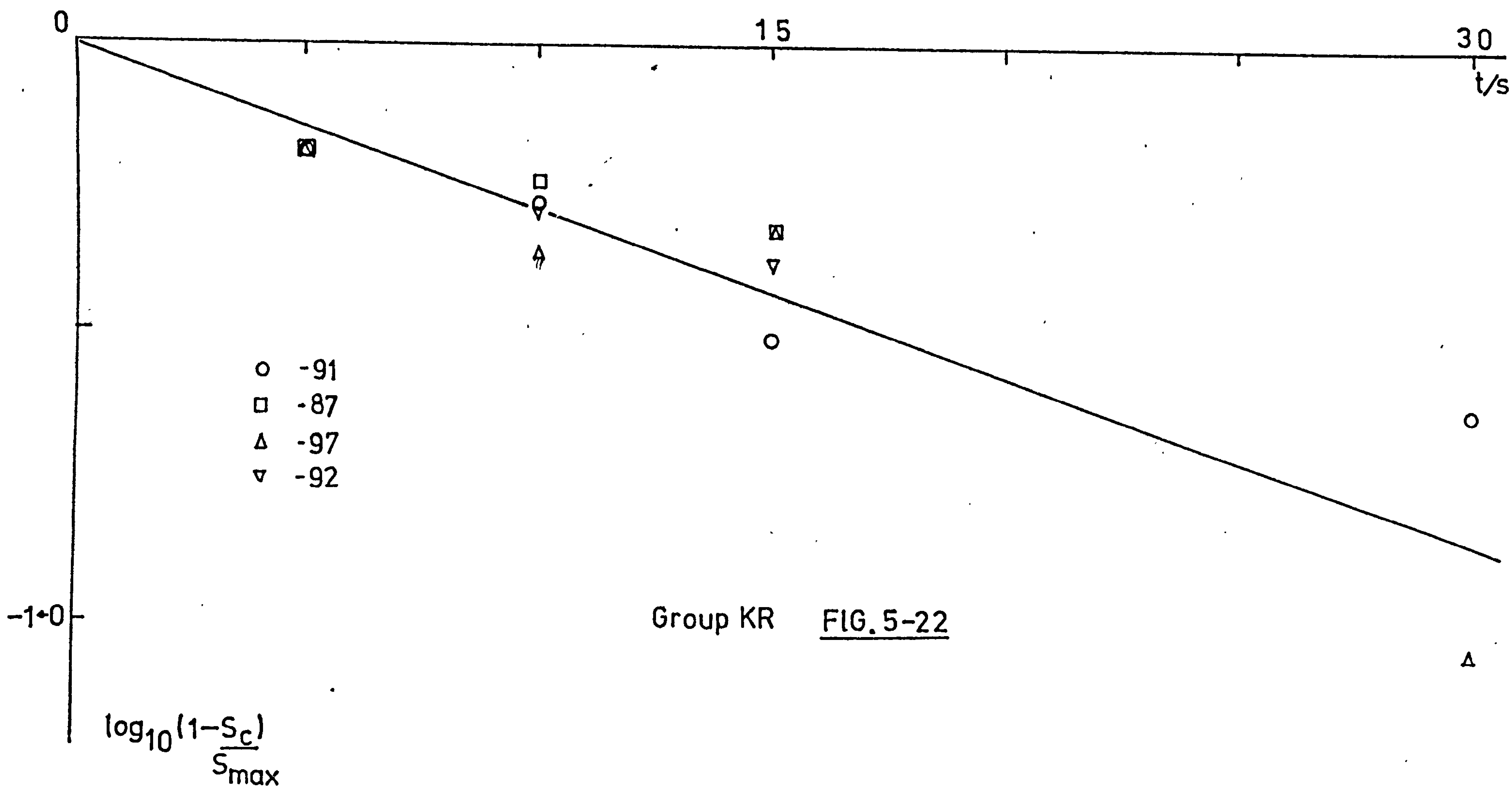

FIG. 5-22

the weaker charge will still have an effect. Group TON behaved in a similar way to group KON.

5.3 Rheology

5.3.1 Errors in Method and Results

As well as uncertainties in droplet size which have already been discussed, there were two further sources of error. The first, creaming, concerns mainly the Brega and model oil systems. This had the effect of concentrating the emulsions in the lower regions of the cylinder and at higher ϕ values this was followed by a certain amount of coalescence. For this reason, both the mean droplet size and the measured viscosity are unreliable. The problem was much more severe in the Brega systems and these can only be dealt with qualitatively; the model systems yield rather more information.

The second source has already been mentioned and that is the possibility of a heating effect which concerns mainly the Kuwait and Tia Juana systems. Hediger's equation (4-2) for the heat change is very similar in form to an expression derived by Eley [90], to calculate the viscous work involved in rolling plastics. Eley's expression (which has been translated into the present nomenclature) is :

$$\Delta H = \eta \cdot \dot{\gamma}^2 \cdot E \qquad \text{5-13}$$

where E is a constant for the system. Lines have been drawn on the rheograms at constant $\tau \cdot \dot{\gamma}$ values and these correspond to the start of the deviations. These values are summarised in Table 5-5.

Emulsion	ϕ	Oil	$\tau.\dot{\gamma}$ ($N_s\ m^{-2}$)	Cylinder system
KR:91	0·40	Kuwait	-	S2
KR:87	0·50	Kuwait	1180	S2
KR:97	0·55	Kuwait	1134	S2
KR:92	0·60	Kuwait	794	S2
TR:101	0·40	Tia Juana	-	S2
TR:102	0·50	Tia Juana	1588	S2
TR:104	0·55	Tia Juana	973	S3
TR:103	0·60	Tia Juana	778	S3

Table 5-5

The table shows up the trend that would be expected, namely that as ϕ increases and with it the total number of droplets, then less work is required to heat up the sample for the viscosity to change noticeably in the given experimental time period. As different cylinder systems were used for the Tia Juana oil, C will be different and hence a true comparison is not possible.

One further point is that τ and $\dot{\gamma}$ were obtained and used as if flow were Newtonian despite the expressions given in Chapter 2. This is justified on the grounds that once the initial curved portion has been passed, then flow is indeed Newtonian; a point supported by the absence of a curved portion at ϕ = 0·40 and at the large sizes at ϕ = 0·50 for Kuwait and Tia Juana systems.

5.3.2 Rheology of Kuwait and Tia Juana Systems

5.3.2A Sherman's Treatment [32]

The emphasis Sherman has continually put on the effect of droplet size on viscosity is easily justified by Figures 5-23 and

5-24 where η_{rel} has been plotted against d_v for Kuwait and Tia Juana respectively. Sherman observed a large curvilinear increase for W/O emulsions when d_v for a narrow size distribution fell below 2 μm. (in this work, 3 μm is a closer figure). He attributed this effect to the rigidity of the interfacial film and on that basis, the systems reported here are more rigid than his (sorbitan sesquioleate stabilised water-in-nujol)[91]. He suggested that the lines could be linearised by plotting η_{rel} versus $1/d_v$ and this is shown in Figures 5-25 and 5-26. However the linearity breaks down particularly at higher ϕ values. Table 5-6 shows the gradients of the linear parts of these lines.

ϕ	Gradient (μm)	
	KR	TR
0·40	6·0	8·8
0·50	24·4	29·2
0·55	39·6	72·0
0·60	61·2	86·0

Table 5-6

The gradients are larger for corresponding emulsions in group TR than in group KR and although this could be due to greater rigidity another explanation is based on the freeze etching observation of the build-up of a secondary layer of asphaltenes at the interface. This may provide a structured sheath around the droplets which although invisible under the optical microscope would effectively increase both the diameter of the droplets and also ϕ thus noticeably increasing η_{rel}.

$\phi = \frac{V_w}{V_w + V_o}$

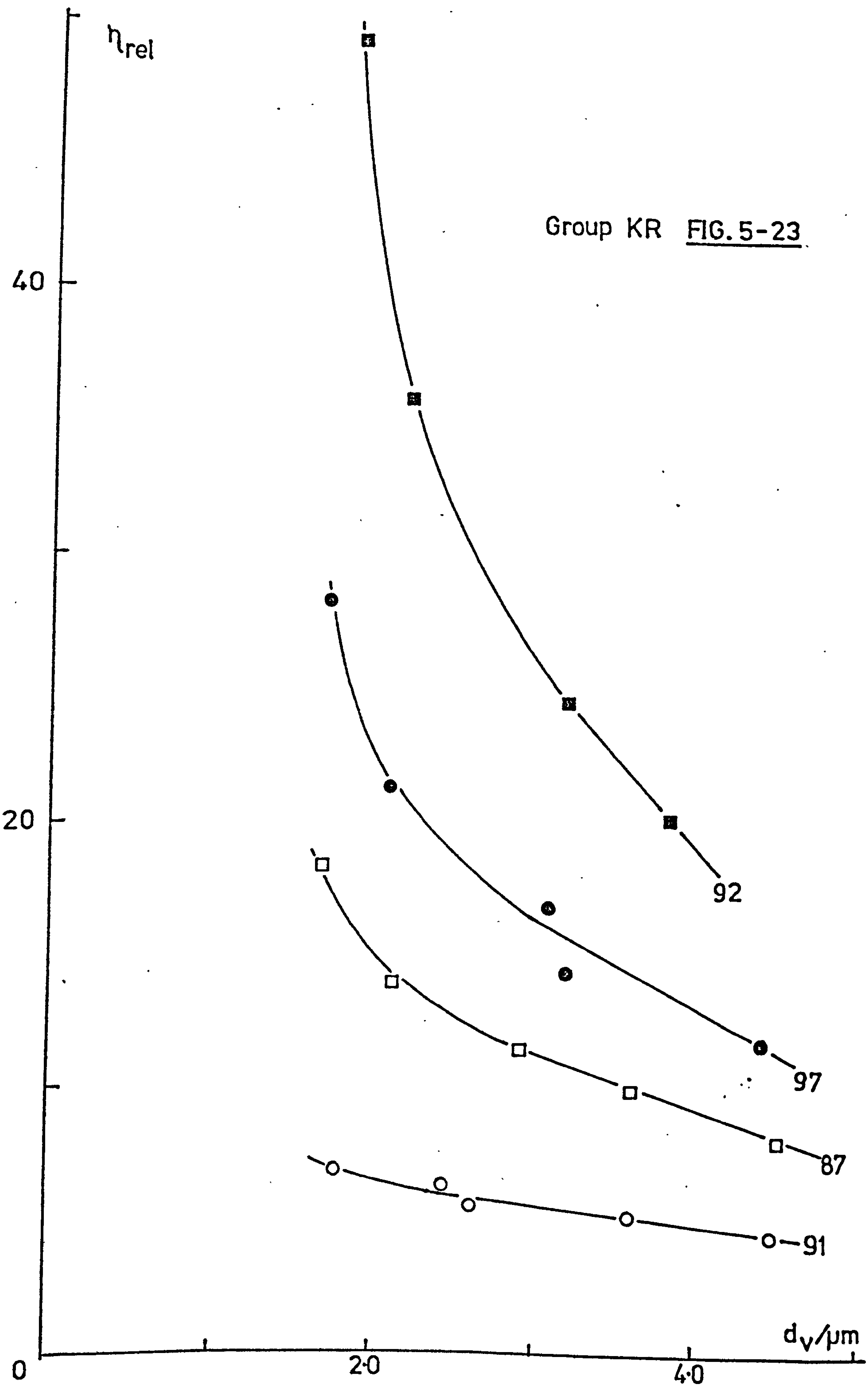

ηrel
40
20
0
2·0
4·0
dv/μm
92
97
87
91
Group KR FIG. 5-23

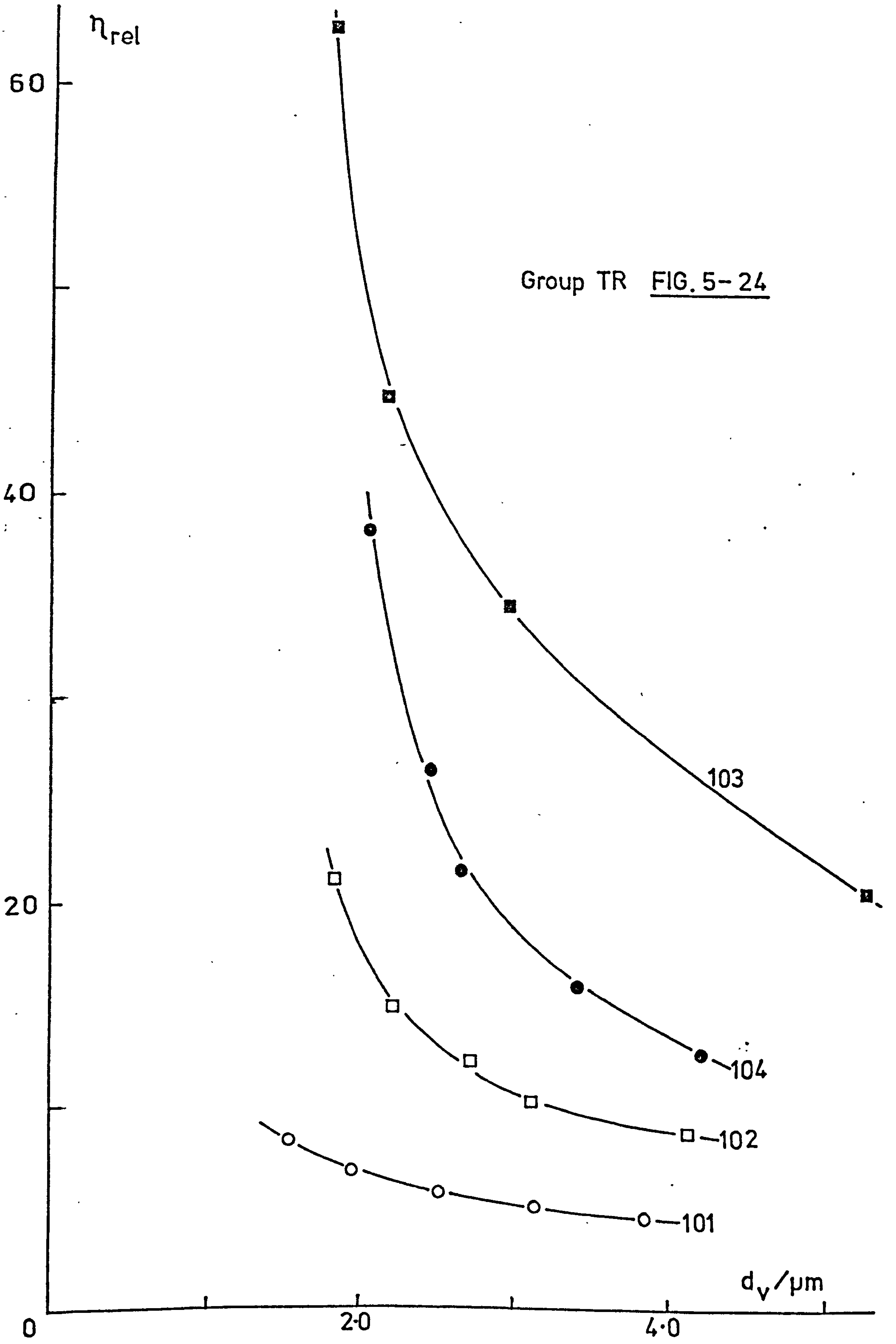

Group TR FIG. 5-24

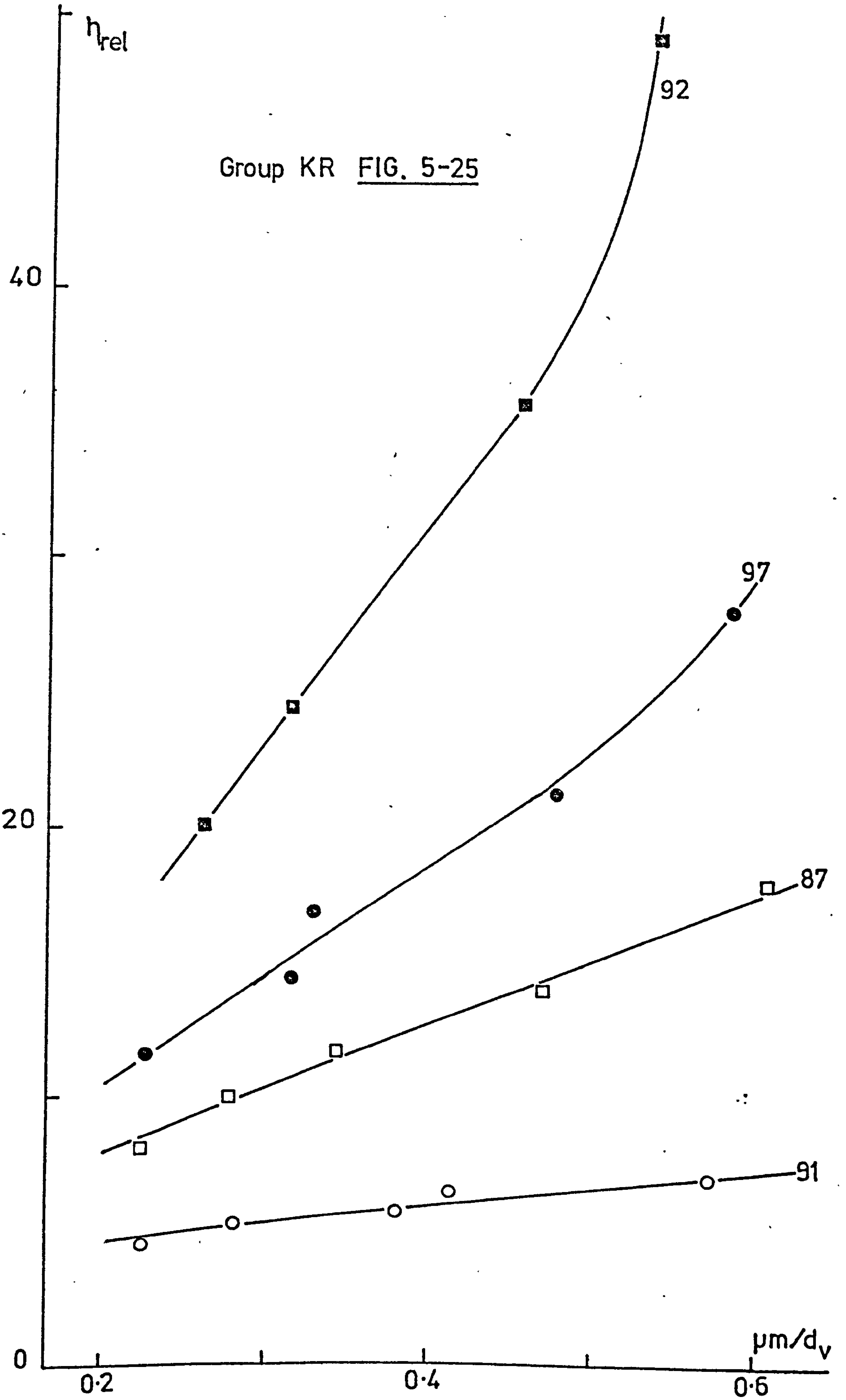

η_{rel}
Group KR FIG. 5-25
92
97
87
91
40
20
0
0·2
0·4
0·6
$\mu m/d_v$

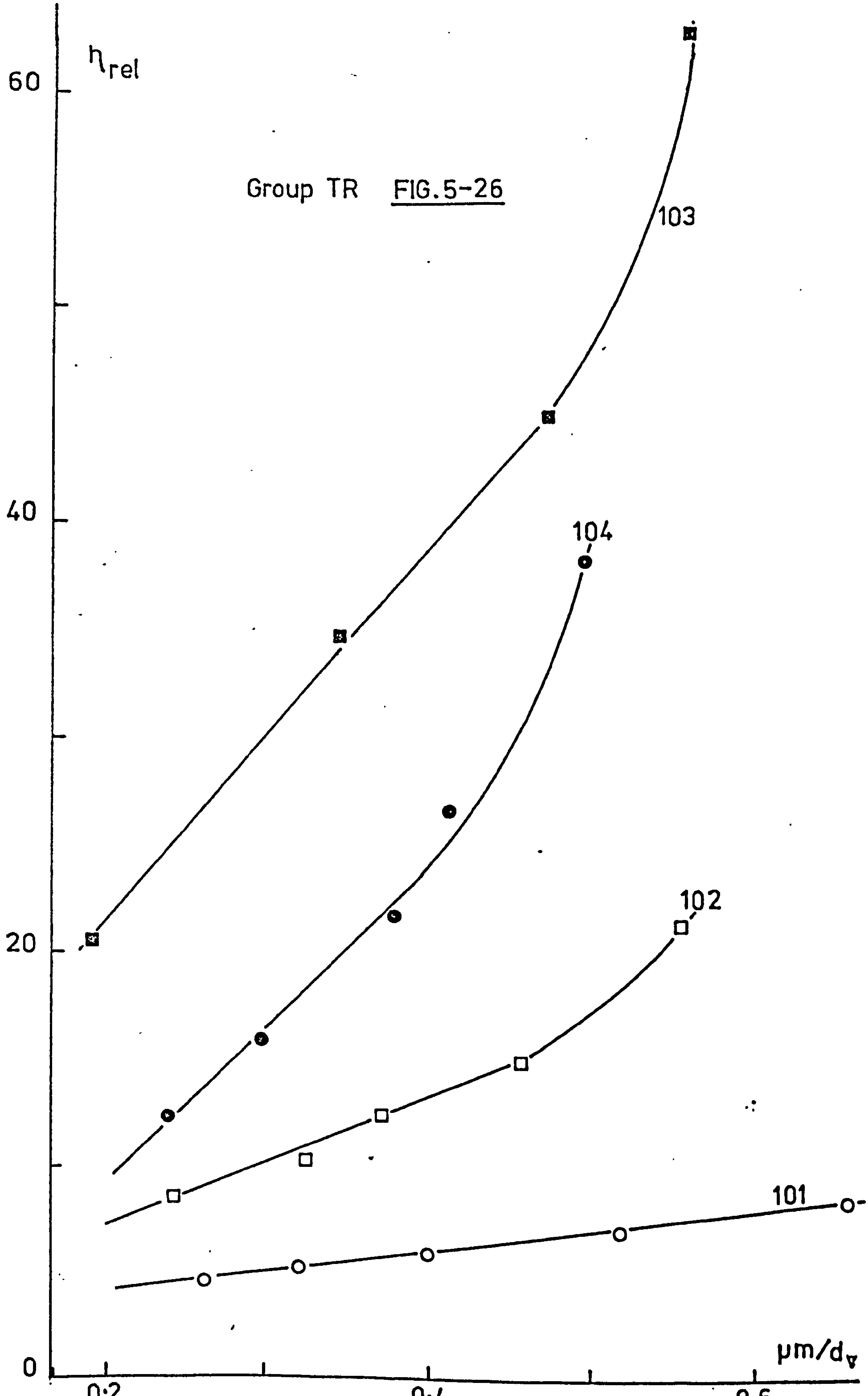

Group TR FIG.5-26

Plots of $\bar{a}$ versus η_{rel} for groups KR and TR are shown in Figures 5-27 and 5-28; values of η_{rel} appear to be asymptotic at an $\bar{a}$ of 0·1 μm in both cases.

5.3.2B <u>Difficulties in Interpretation of Rheological Data</u>

The previous section has shown up some of the difficulties in analysing rheological data of emulsions with complex phases even when the droplet size data is known. As Sherman [32] has stated, there is still a considerable amount of work to be done before the picture is clarified. Undoubtedly one of the more useful concepts is the mean distance of separation, $\bar{a}$. This expression is calculated on the assumption that the size distribution is monodispersed; however $\bar{a}$ increases with the polydispersity of the distribution. A more fundamental problem is that of ϕ_{max} which is normally taken as 0·74. It can be predicted that a monodispersed system of rigid spheres with ϕ just less than this figure would exhibit dilatant rather than pseudoplastic flow. Calculations based on the geometry shown in Figure 5-29 suggest that for pseudoplasticity, ϕ_{max} would need to be reduced to 0·605. At the other extreme, Lissant [92] has described the rheological behaviour of emulsions with ϕ as high as 0·98 where presumably the droplets distorted to allow flow. Unfortunately this author did not use a concentric cylinder viscometer. Nevertheless, the very low rigidity of some stable emulsion systems has been exhibited and as such ϕ_{max} will vary according to the emulsion system.

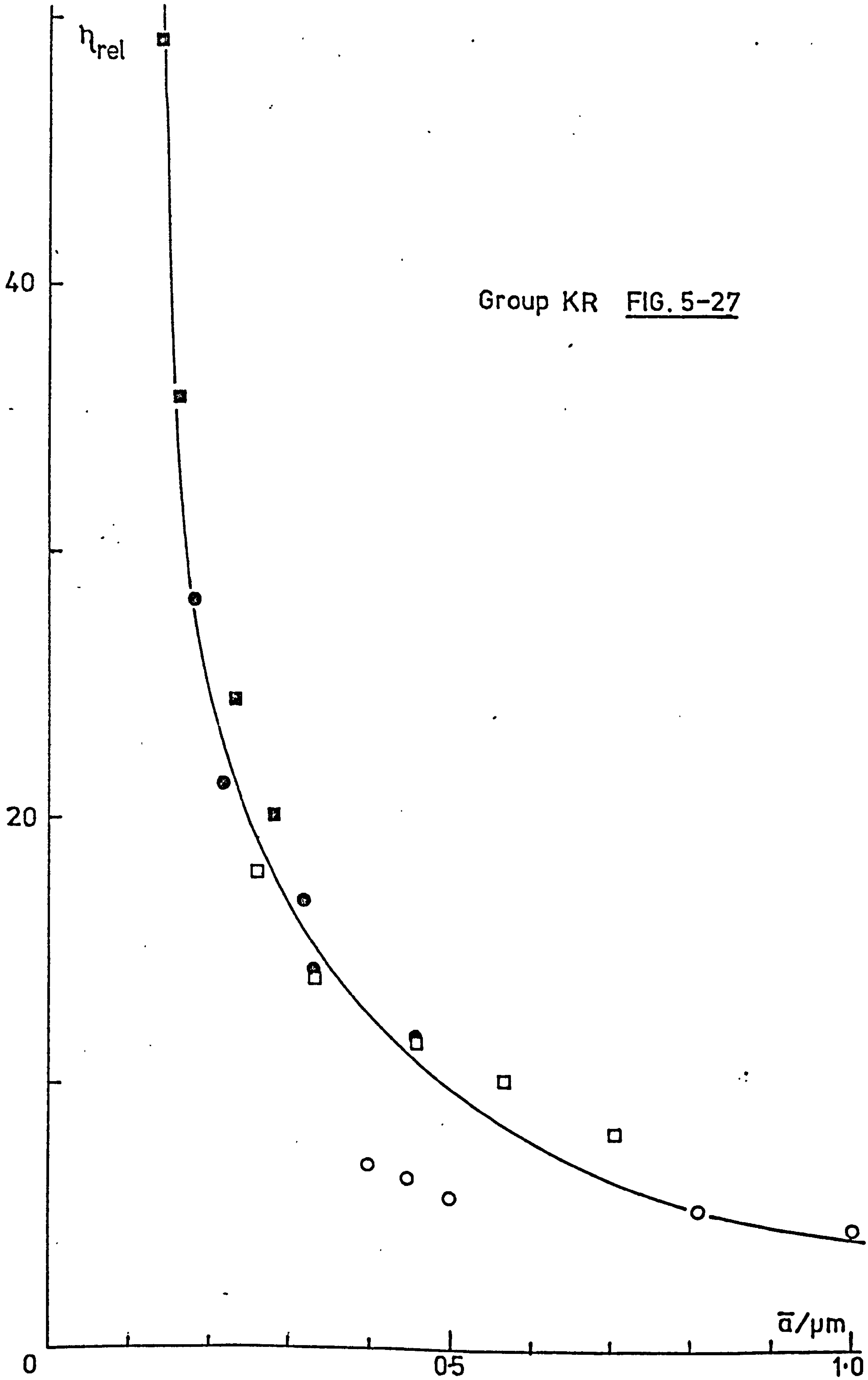

FIG. 5-27

η_{rel}
60
40
20
0
0·5
1·0
$\bar{a}$/μm
Group TR FIG. 5-28

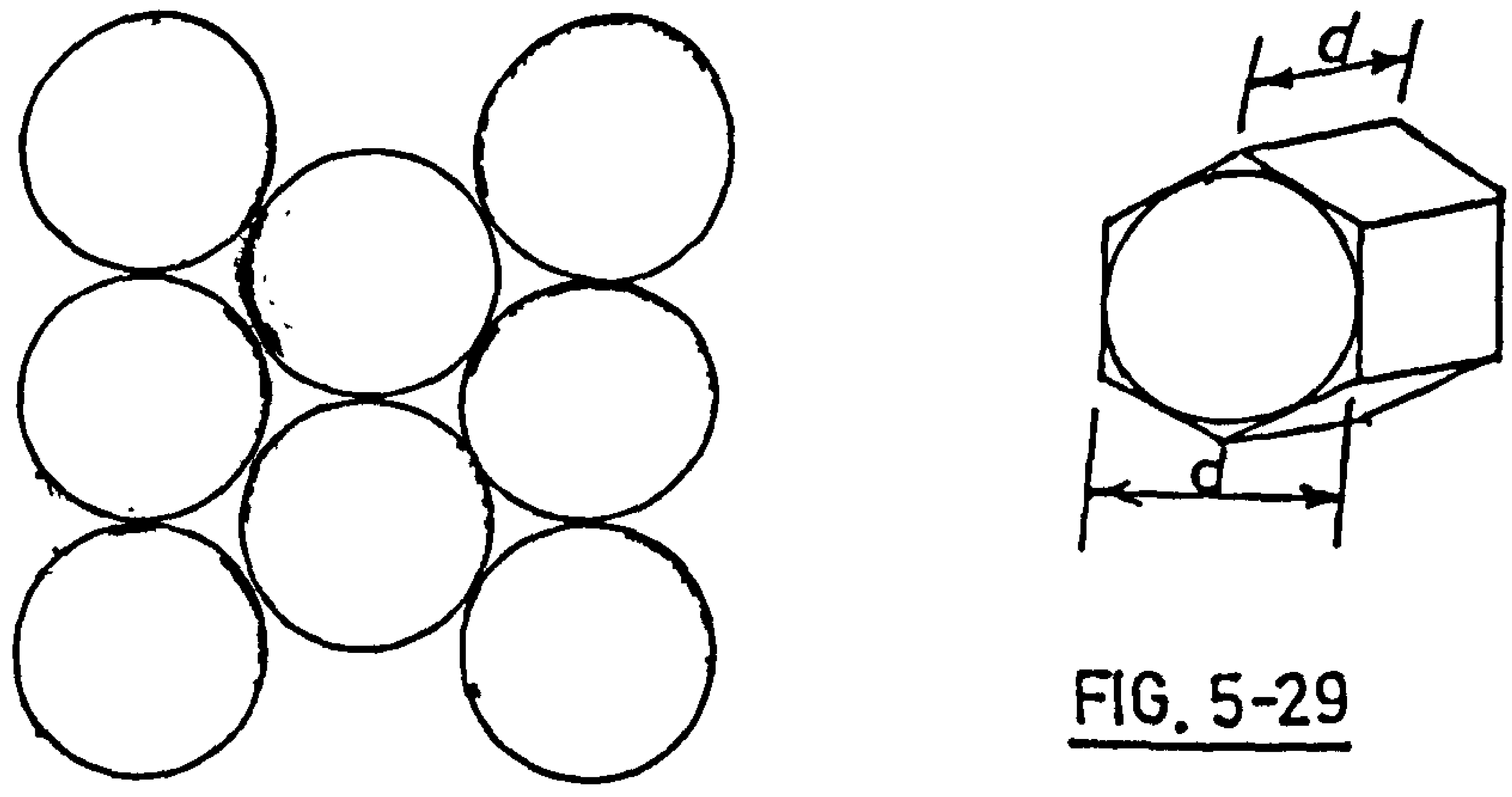

FIG. 5-29

5.3.3 Rheology of Model Emulsions

Plots of η_{rel} versus $\bar{a}$ (assuming $\phi_{max} = 0 \cdot 74$) for groups MAR and MVR are shown in Figures 5-30 and 5-31. In group MAR it would appear that the viscosity is a minimum at an asphaltene concentration of 1•0%. The explanation for the increase of viscosity on increasing asphaltene concentration from 1•0% to 1•5% is straightforward. Sherman [32] has discussed the effect of emulsifying agent concentration of η_{rel} and found the two to be directly proportional. He accepted that for certain emulsifiers such as proteins this may be due to adsorption greater than one molecule thick at the interface and this is the likely explanation in this work. However at asphaltene concentrations less than 1% the opposite relationship can be seen to occur. Sherman [32] has reviewed the work of Mason and his co-workers who found that emulsifying agent concentration was inversely proportional to the fluid circulation within a droplet in concentric cylinder viscometry. However, they found that increase of fluid circulation had the effect of decreasing η_{rel} albeit in dilute emulsions. In addition, these workers also found that when the ratio of the viscosities of dispersed phase to dispersion medium (η_i/η_o) was within the range 3•8 to 29 (as in this

Group MAR FIG. 5-30

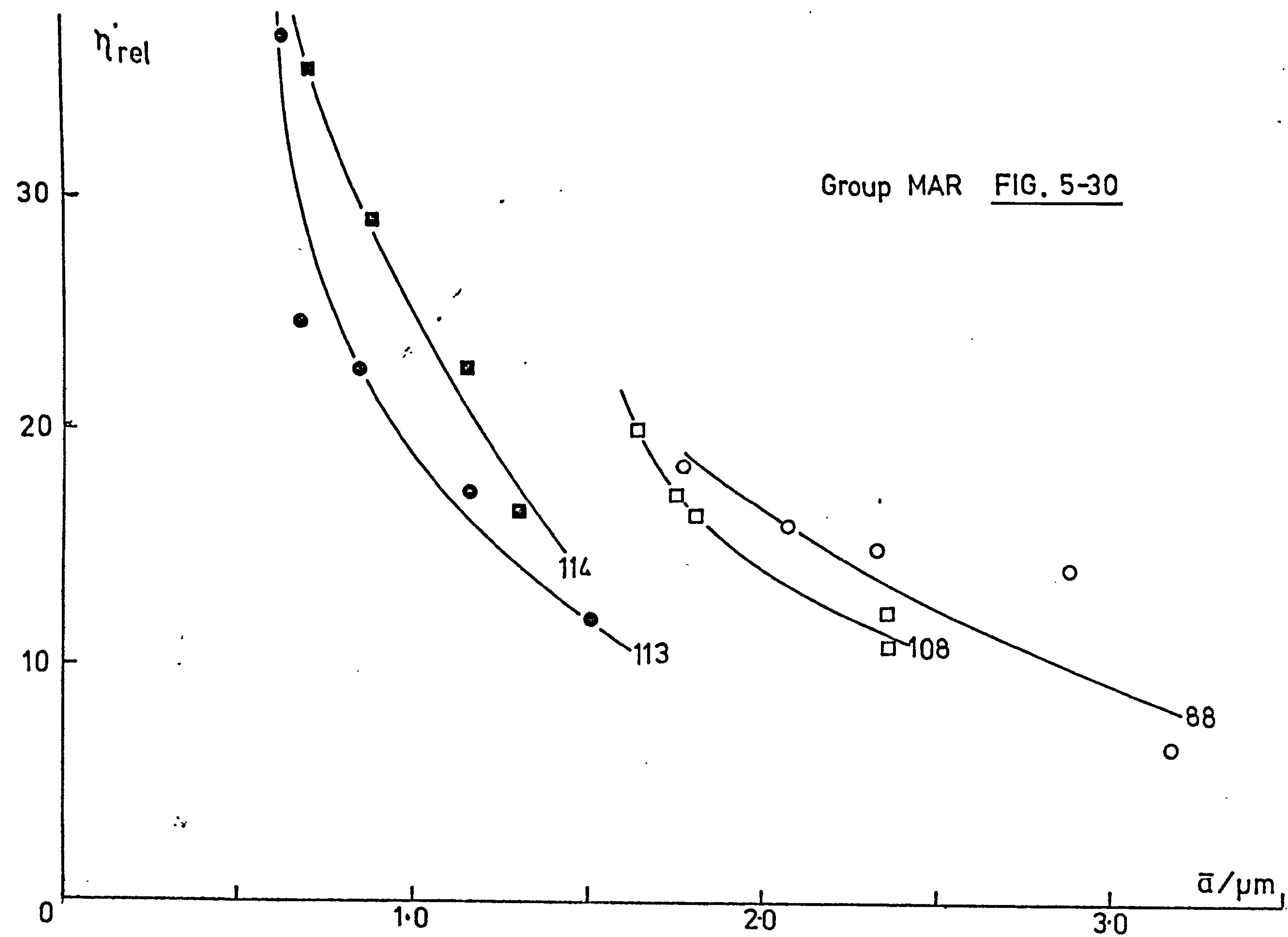

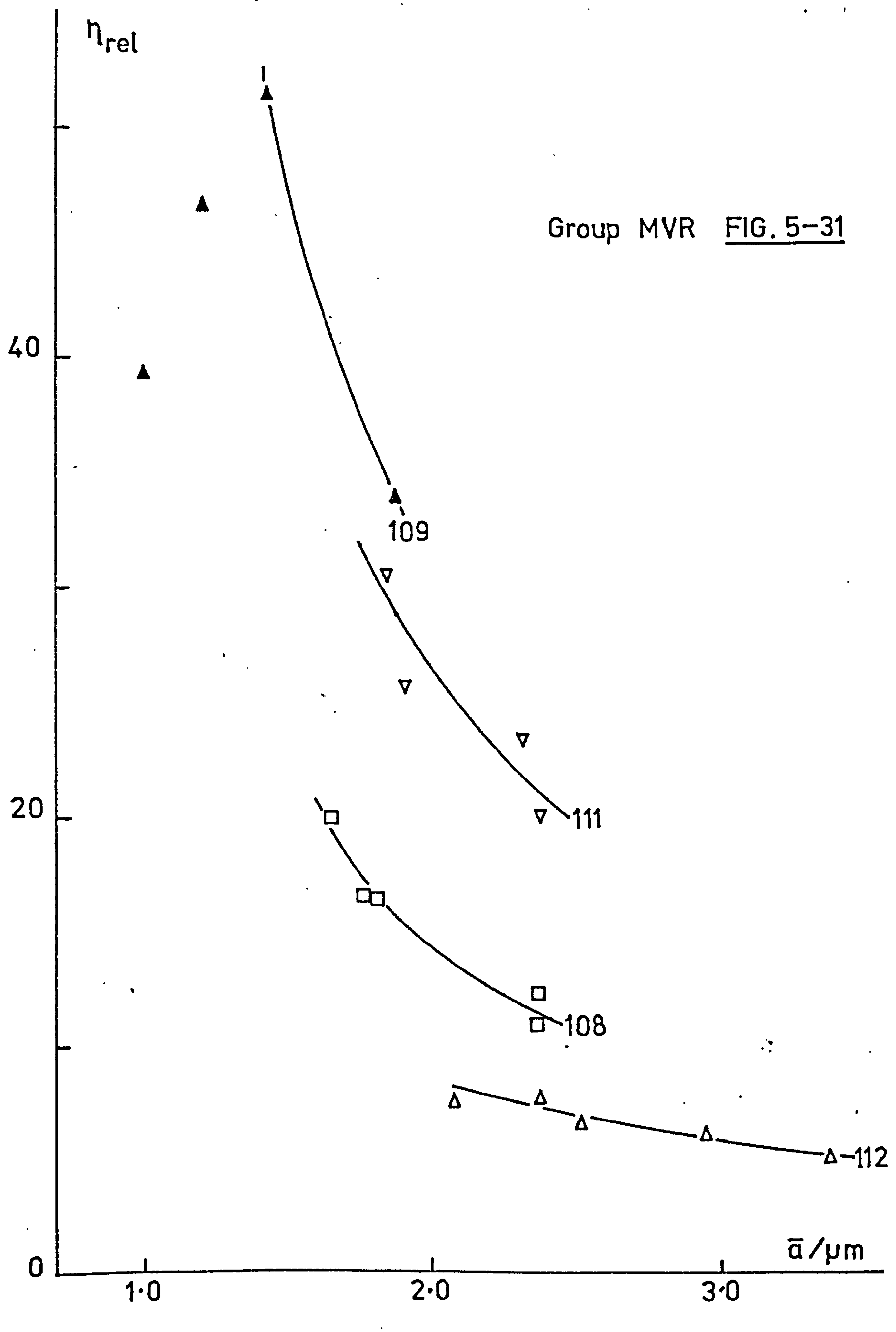

Group MVR FIG. 5-31

work) then any deformable droplets would become ellipsoids. In the two emulsions at asphaltene concentrations less than 1%, the majority of droplets are deformable (i.e. $> 5\ \mu m$ diameter) but such deformation in dilute emulsions should lead to reduced values of η_{rel}.

The work of Winterton [75] on the interfacial rheology of asphaltene films may provide an explanation. She found that the asphaltenes at the interface between water and toluene/n-heptane formed a viscoelastic film that could be represented, using viscous dashpot and elastic spring notation, by a Burgers model :

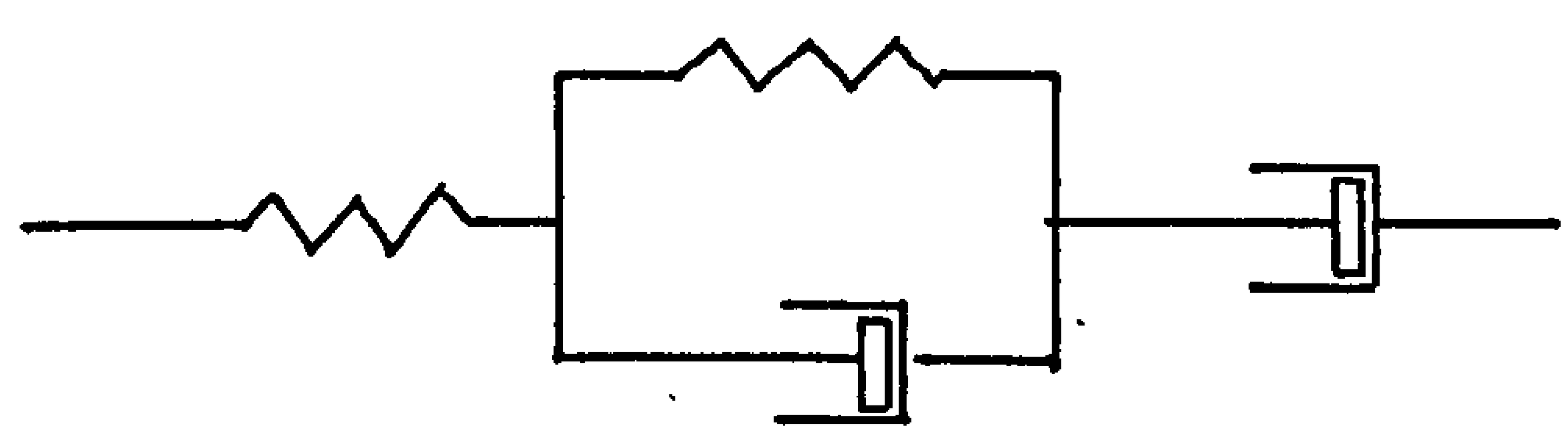

This model indicates the presence of instantaneous and retarded elasticity and viscous flow. Although she found it difficult to reproduce her work, the overall indication was that the shear elastic moduli of the film decreased as the asphaltene concentration increased. The implication is that at low asphaltene concentrations, the elasticity of the film would resist deformation and so more energy would be required for an equilibrium flow situation.

In Figure 5-31 one of the obvious features is the apparent coalescence exhibited at $\phi = 0{\cdot}60$ where anomalously low values of η_{rel} were obtained at low values of $\bar{a}$. The marked discontinuity between the curves at different values of ϕ may also be explained by the elasticity hypothesis. At higher ϕ, there are more droplets and hence proportionately more energy would be required.

5.3.4 Rheology of Brega Emulsions

The reasonable increase in η_{rel} with stirring time shown in Table 4-27 illustrates the problem of accurate droplet size analysis as values of d_v in the same table are highly erratic. A deviation from linearity can be seen at high $\dot{\gamma}$ at $\phi = 0{\cdot}60$ and this is probably a sign of coalescence at high rate of shear. However, the other lines show a remarkable steadiness that make the apparently rapid coalescence on the microscope slide rather puzzling.

5.3.5 Extrapolation Point and Critical Shear Rate

Reiner and Scott-Blair [52] defined the yield point as the point on the stress-strain curve at which yielding starts abruptly. Sherman [32] stated that to establish that a yield point exists, it is necessary to define the τ-$\dot{\gamma}$ relationship experimentally to low values of $\dot{\gamma}$ and that extrapolation is dangerous as the curve may be pseudoplastic. However, as some valuable information may be obtained by extrapolating the linear portion of the τ-$\dot{\gamma}$ curve back to the τ axis and yield point is clearly the incorrect term to use, extrapolation point Y will be used instead.

The critical shear rate, $\dot{\gamma}_{min}$ has been used by Albers and Overbeek [93] to obtain the London - van der Waals constant, $\bar{A}$ for their DLVO approach to emulsion stability. They assumed that when a shear is applied to a monodispersed emulsion system which does not exhibit shear deformation, the droplet aggregates are broken down until residual pairs of droplets remain. The critical shear rate is the point at which the forces of attraction holding these final pairs together is exceeded, and this is given by ;

$$\dot{\gamma}_{min} = \frac{\bar{A}}{18\,\pi.\,\eta_o\,D\,H_o^2\,\sin\,(2\beta)} \qquad 5\text{-}14$$

The critical angle between the lines joining the centres of the droplets and the direction of flow is β ($\approx 30^{o}$), H_o is the minimum distance between droplets, and D is the diameter of the monodispersed droplets. For emulsions with a narrow size distribution, d_v may be substituted for D. The authors assumed a value for H_o based on hydrocarbon chain length, but in this work, the uncertainties of resins and unused asphaltenes make such an estimation meaningless. However, a plot of $\dot{\gamma}_{min}$ versus $1/d_v$ would give A/H_o^2 from the gradient; $\dot{\gamma}_{min}$ being the point in the τ-$\dot{\gamma}$ curve where the line eventually becomes linear.

In group KR, Y only exists for those emulsions where $\bar{a}$ is less than 0·26 µm (based on ϕ_{max} = 0·74). Even in those examples, there is no detectable $\dot{\gamma}_{min}$. A similar pattern is observed for group TR, only $\bar{a}$ is critical at 0·45 µm. The absence of $\dot{\gamma}_{min}$ suggests that attractive forces are negligible, an observation supported by microscope studies. However, Y would appear to be a useful empirical measure of the deformability of the droplets. If the linear portion of the τ-$\dot{\gamma}$ graph (from which η_∞ is obtained) represents a situation of dynamic equilibrium with certain droplets deformed, then more work is required for Tia Juana droplets to achieve this situation than for Kuwait.

In group BR there are clear values of Y, but if $\dot{\gamma}_{min}$ has any effect it is at very low values. Under the microscope clumping has been evident, suggesting attractive forces are present. However, the contribution of the waxes to providing a certain amount of structure to the emulsion and rigidity to the droplets is possibly the cause for high values of Y.

In the model emulsions, there is a clear curve of experimental values leading up to $\dot{\gamma}_{min}$ and the linear portion. A graph of the estimated $\dot{\gamma}_{min}$ values versus $1/d_v$ for emulsions MAR:88 and 114 is shown in Figure 5-32; the scatter is due to the difficulty of estimation of $\dot{\gamma}_{min}$ possibly due to ϕ being too high which as Sherman explained means that a droplet from a dissociated pair will be attracted too easily to a neighbour in the immediate vicinity. Emulsions MAR:113 and 108 have not been included in the figure because equation 5-14 is not valid for deformable droplets, whereas it was shown in section 5.3.3 that the droplets in emulsions MAR:114 and 88 behaved as if they were rigid. It can be seen that the gradient, $\bar{A}/H_o^2$ is higher for the emulsion MAR:114 which has the higher asphaltene concentration. As Sherman [32] has commented that $\bar{A}$ is reduced by an increase in thickness of emulsifying agent and as this would be accompanied by an increase in H_o then a different mechanism to DLVO is required to explain the attractive forces between droplets at high asphaltene concentrations.

Davies [30] has suggested that certain macromolecules that stabilise emulsions may form bridges between the droplet surfaces such that the droplets are held quite far apart. He described this phenomenon as "stickiness". If correct, this theory would give an anomalously high value to $\bar{A}$ and thus increase $\bar{A}/H_o^2$. Supporting qualitative evidence for this comes from group MA where the emulsion with high asphaltene concentrations "gelled" in the stirrer due to the clumping of the droplets.

It is still necessary to explain how the $\dot{\gamma}_{min}$ values for MAR:108 and 113 are so much higher than for MAR:88 and this will be attempted in a qualitative manner. The

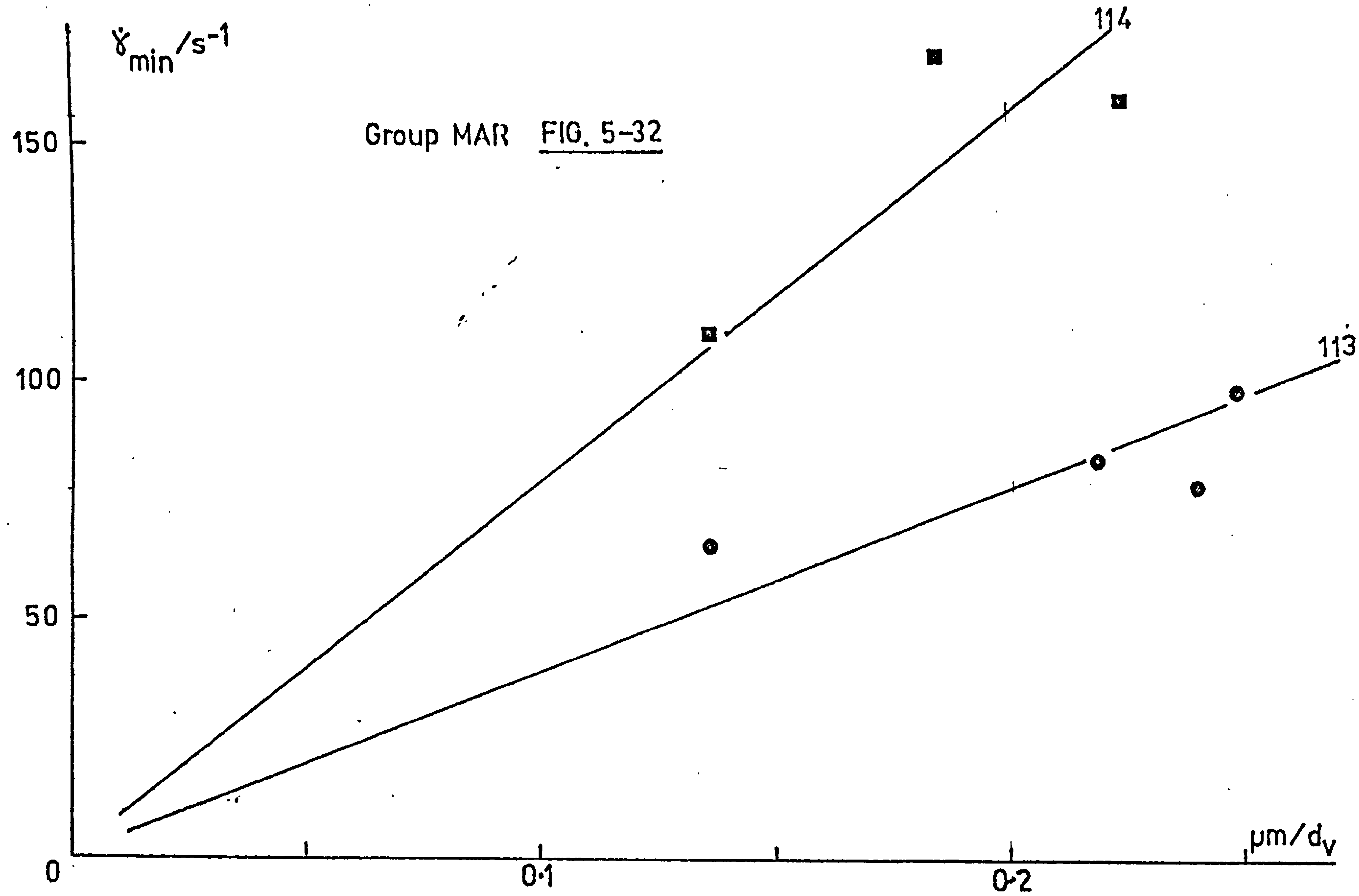

$\dot{\gamma}_{min}/s^{-1}$
Group MAR FIG. 5-32
150
100
50
0
0·1
0·2
μm/d_v
114
113

phenomenon of polyhedral droplets has already been mentioned in Chapter 4; the reasons for their existence have been fully discussed by Kitchener and Mussellwhite [31]. Briefly, they stated that there is a universal van derWaal'sattraction between small bodies such as emulsion droplets. As the droplets grow closer together then if there is an element of elasticity in the surrounding film, thin liquid lamellae can be formed, thus forming polyhedral droplets. However, the presence of a positive disjoining pressure is required for a permanent resistance to the continuing lamellae formation and subsequent coalescence. As the distance between the centres of two droplets distorted by the formation of a thin liquid lamellae between them are closer than if a rigid spherical form were maintained, then the attractive forces between the droplets will be so much higher. Thus the easily deformable droplets in MAR:108 and 113 are held together by stronger attractive forces than if they were rigid spheres, and this accounts for the high values of $\dot{\gamma}_{min}$.

REFERENCES

1. M.L. McGlashan, "Physicochemical Quantities and Units", (The Royal Institute of Chemistry, London, 2nd Edition, 1971)

2. L. Carroll, "Through the Looking Glass", (Mayflower, London, 1969)

3. Report from the Select Committee on Science and Technology, (H.M.S.O., London, 1967-68).

4. J.E. Smith (Ed.), Letters by the Marine Biological Association of the United Kingdom. "Torrey Canyon Pollution on Marine Life", Report by Plymouth Laboratory, (C.U.P. 1968).

5. J.D. Carthy and D.R. Arthur, in "The Chemistry of Crude Oils in Relation to their Spillage on the Sea", edited by R.A. Dean, Field Studies, 1968, 2 (Suppl.), 1.

6. Journal of Institute of Petroleum Symposium, J. Inst. Pet., 1968, 54, 300.

7. S.A. Berridge, M.T. Thew and A.G. Loriston-Clarke, J. Inst. Pet., 1968, 54, 333.

8. "The Torrey Canyon", (H.M.S.O., London, 1967).

9. N. Pilpel, Endeavour, 1968, 27, (100),11.

10. N. Pilpel, Ecologist, 1972 (March), 2, (No. 3), 4.

11. P. Becher, "Emulsions : Theory and Practice", (Reinhold Publishing Corporation, New York, 2nd Edition, 1965).

12. G.D. Parfitt, "Surface and Colloid Chemistry", (Pergamon Press, London, 1966).

13. "The Amateur Scientist", February 1971, page 118.

14. Emulsification Symposium, J.Ind. and Eng. Chem., 1921, 13, 1008.

15. M. Abozeid, Trans. Amer. Inst. Mining Met. Engrs. (Petro.Div.), 1931, 340.

16. H. Fisher, Trans. Amer. Inst. Mining Met. Engrs. (Petro.Div.)., 1931, 359

17. A.S.C. Lawrence and W. Killner, J. Inst.Pet., 1948, 34, 821.

18. H. Hellman and F.-J. Bruns, Tenside, 1970, 7, 11.

19. G.D.M. Mackay, A.Y. McLean, O.J. Betancourt and B.D. Johnson, J. Inst.Pet., 1973, 59. 164.

20. H. Abraham, "Asphalts and Allied Substances" Part I (Van Nostrand, New Jersey, 6th Edition, 1960).

21. A.N. Sachanen, "The Chemical Constituents of Petroleum", (Reinhold, New York, 1945).

22. D.C. Broome, Chapter 23 in "Modern Petroleum Technology", edited by G.D. Hobson and W. Pohl, (Applied Science Publishers, 4th Edition, 1973).

23. H. Abraham, "Asphalts and Allied Substances" Part IV (Van Nostrand, New Jersey, 6th Edition, 1962).

24. S.W. Nicksic and M.J. Jeffries-Harris, J. Inst.Pet., 1968, 54, 107.

25. E.H. Poindexter, J. Colloid Interface Sci., 1972, 38, 412.

26. R.B. Girdler, Paper presented at the Technical Sessions of the Association of Asphalt Paving Technologists, Philadelphia, Pennsylvania, February 15-17, 1965.

27. J.G. Erdman, A.S.T.M. Special Technical Paper 389, Am. Soc. Testing Mat., 1965, 259.

28. J.P. Dickie and T.F. Yen, Analytical Chemistry, 1967, 39, 1847.

29. J.P. Dickie, M.N. Hatter and T.F. Yen, J. Colloid Interface Sci., 1969, 29, 475.

30. J.T. Davis, Volume 2, page 129 of "Recent Progress in Surface Science" edited by J.F. Danielli, K.G.A. Pankhurst and A.C. Riddiford, (Academic Press, New York and London, 1964).

31. J.A. Kitchener and P.R. Mussellwhite, Chapter 2 in "Emulsion Science" edited by P. Sherman, (Academic Press, London and New York, 1968).

32. P. Sherman, Chapter 4 in "Emulsion Science" edited by P. Sherman, (Academic Press, London and New York, 1968).

33. E.S.R. Gopal, Chapter 1 in "Emulsion Science" edited by P. Sherman, (Academic Press, London and New York, 1968).

34. P. Sherman, Chapter 3 in "Emulsion Science" edited by P. Sherman,(Academic Press, London and New York, 1968).

35. M.J. Groves, Ph.D. Thesis, University of Loughborough, 1966.

36. C. Fisher, Particle Size Analysis Conference 1966, The Society for Analytical Chemistry, page 77.

37. M. Barnett and V. Timbrell, Pharm. J., 1962, 189, 379.

38. Demonstrated to the author at a Postgraduate School on Rheology organised by the Chemical Society at the London School of Pharmacy, 9-13 April, 1973.

39. F. Endter and H. Gebauer, Optik, 1956, 13, 97.

40. P. Becher, J. Colloid Sci., 1964, 19, 468.

41. P. Falcon-Uff and K.F. Leverington, Particle Size Analysis Conference 1966, The Society for Analytical Chemistry, page 45.

42. A.M. Neville and J.B. Kennedy, "Basic Statistical Methods for Engineers and Scientists", (Intertext, London, 1964).

43. C.M. Blair, Chem. and Ind., 1960, 538.

44. N. Schwarz and C. Bezemer, Kolloid-z.,1956, 146, 139.

45. G. Herdan, "Small Particle Statistics", (Butterworths, London, 2nd Edition, 1960).

46. J.E. Smith and M.L. Jordan, J. Colloid Sci., 1969, 19, 549.

47. C. Bezemer and N. Schwarz, Kolloid-z.,1956, 146, 145.

48. E.S. Rajagopal, Kolloid-z.,1959, 162, 85.

49. P. Drinker and T. Hatch, "Industrial Dust", (McGraw-Hill, London, 2nd Edition, 1955).

50. N.V. Smirnov and D.E. Brown, (edited) "Tables of the Normal Probability Integral, The Normal Density and its Normalized Derivatives", (Pergamon Press, London, 1965).

51. J.E. Gwyn, E.J. Crosby and W.R. Marshall, Ind.Eng.Chem. (Fund.), 1965, 4, 204.

52. M. Reiner and G.W. Scott-Blair, Chapter 9 in "Rheology - Theory and Applications" Volume 4 edited by F.R. Eirich, (Academic Press, London, 1967).

53. W.H. Bauer and E.A. Collins, Chapter 8 in "Rheology - Theory and Applications" Volume 4 edited by F.R. Eirich, (Academic Press, London, 1967).

54. D.C.-H. Cheng, "The Characterization of Thixotropic Behaviour", (Warren Spring Laboratory, Stevenage, 1971, Report No. LR 157(MH)

55. P.B. Smith, B.P. Research Laboratories, Sunbury-on-Thames, Private Communication.

56. P. Sherman, "Industrial Rheology" (Academic Press, London and New York, 1970).

57. R. Roscoe, in the manual for "Postgraduate School in Rheology", (Chemical Society, London School of Pharmacy, April, 1973).

58. D.J. Shaw, "An Introduction to Colloid and Surface Chemistry", (Butterworths, London, 1st Edition, 1968).

59. S. Wischnitzer, "Introduction to Electron Microscopy", (Pergamon Press, London, 1962).

60. C.E. Hall, J.Appl. Phys., 1950, 21, 61.

61. R.L. Steere, J. Biophys. Biochem. Cytol., 1957, 3, 45.

62. H. Moor, K. Mühlethaler, H. Waldner and A.Frey-Wyssling, J. Biophys. Biochem. Cytol., 1961, 10, 1.

63. H. Moor and K. Mühlethaler, J. Cell Biol., 1963, 17, 609.

64. W.F. Geymeyer, 6th International Conference for Electron Microscopy, (Kyoto, 1966, page 577).

65. L.V. Kolpakov, S.A. Nikitina, A.B. Taubman, V.A. Spiridonova, A.E. Chadlych, N.I. Puchkov and V.M. Lukyanovich, Colloid Journal, 1970, 32, 187.

66. Zs. Pajor, E. Pandula, T. Peres and J. Stark, Fette Seifen Anstrichsmittel, 1968, 70, 182.

67. R. Reed, New Scientist, 21st August, 1969, 43, 377.

68. W. Buchheim, Die Naturwissenschaften, 1970, 57, 41.

69. W. Buchheim, Die Naturwissenschaften, 1970, 57, 672.

70. R.D. Riegelhuth and R.C. Watkins, J. Inst.Pet., 1972, 58, 188.

71. J.H.M. Willison, Ph.D. Thesis, University of Nottingham 1973.

72. M.J. Groves, B. Scarlett and D.C. Freshwater, Particle Size Analysis Conference 1966, The Society for Analytical Chemistry, page 281.

73. D.J. Fluck, A.F. Henson and D. Chapman, J. Ultrastructure Research, 1969, 29, 416.

74. E.J. Perkins, E. Gribbon and J.W.M. Logan, Marine Pollution Bulletin, 1973, 4, 90.

75. M.A. Winterton, Ph.D. Thesis, University of Nottingham, 1974.

76. J.G. Speight, Fuel, 1970, 49, 76.

77. R.B. Williams, "Symposium on Composition of Petroleum Oils, Determination and Evaluation", ASTM STP, 1958, 224, 168.

78. S.A. Knight, Chem. and Ind., 1967, 1920.

79. D.R. Clutter, L. Petrakis, R.L. Stenger and R.K. Jensen, Anal. Chem., 1972, 44, 1395.

80. P. Sherman, Verbal communication, (see reference 38).

81. M. Hediger, "Measurement of Rheological Properties", Contraves Industrial Products Ltd., 1968.

82. L. Bachmann and W.W. Schmitt, Proc.Nat.Acad.Sci. U.S.A., 1971, 68, 2149.

83. J.G. Davy and D. Branton, Science, 1970, 168, 1216.

84. H. Moor, Phil.Trans.Roy.Soc. (Lond.) B, 1971, 261, 121.

85. E.S. Rajagopal, Kolloid-z.,1959, 167, 17.

86. H.H.G. Jellinek, J.Soc.Chem.Ind., 1950, 69, 225.

87. J.A. Davidson and H.S. Haller, J.Colloid Interface Sci., 1974, 47, 459.

88. B. Kunst and H. Mencer, Kolloid-z., 1968, 228, 77.

89. A. Findlay, "Practical Physical Chemistry", (Longmans, London, 8th Edition, 1960).

90. D.D. Eley, J.Polymer Sci., 1946, 1, 535.

91. P. Sherman, Proc. 3rd Intern. Congr. Surface Activity II, 1960, 596.

92. K.J. Lissant, J.Colloid Interface Sci., 1966, 22, 462.

93. W. Albers and J. Th. G.Overbeek, J.Colloid Sci., 1960, 15, 489.

APPENDIX 1. NOMENCLATURE

A	Arithmetic mean of a population.
A'	Rate constant for recombination of droplets.
$\bar{A}$	London - van der Waal's constant.
a	Arithmetic mean of a sample.
a'	Constant of the straight line in the method of least squares.
$\bar{a}$	Mean distance of separation of droplets.
a_1, a_2, a_3	Averages of distribution about the 1st, 2nd and 3rd moments.
B'	Rate constant for disruption of droplets.
b'	Gradient of the straight line in the method of least squares.
C	Constant in Hediger's equation.
c'	Asphaltene concentration.
D	Diameter of droplets in monodispersed emulsion systems.
d_s	Mean surface area diameter.
d_v	Mean volume diameter.
d_{sv}	Mean surface area per unit volume diameter.
d_{vo}	Mean volume diameter after zero stirring time.
d_{vt}	Mean volume diameter after stirring time, t.
$d_{v\infty}$	Mean volume diameter after infinite stirring time.
E	Constant in Eley's expression for viscous heat.
F	Force applied to upper of two parallel plates.
F_o	Probability of size less than x_o, cumulative frequency.
G	Geometric mean diameter.
G'	Torque on spring of viscometer.
g	Probability density of transformed log-normal equation.
g	(subscript) Geometric.
H	Temperature of sample in viscometer.
H_o	Distance separating droplets in residual pairs.

h	Height of sample in viscometer.
i	(subscript) Number of a particular class in an arithmetic series.
j	(subscript) Number of a particular diameter in geometric series.
K	Cylinder constant for viscometer.
K^{I}	Cylinder constant for spring I in Rheotest II.
K^{II}	Cylinder constant for spring II in Rheotest II.
k_o	Rate constant for emulsion formation.
k_d	Rate constant for displacement of detergents by asphaltenes.
L	Area of parallel plates.
l	Distance between parallel plates.
M	Geometric mean diameter (and median) in log-normal distribution.
m	Number of classes in a distribution.
N	Total number of droplets in a sample.
N_t	Number of droplets after infinite stirring time.
n	Number of classes in the 10 - 90% range of the log-normal distribution.
n_i	Number of droplets in a class.
Q	Conversion factor for Zeiss counter readings into microns.
R	General radius of a cone or in a concentric cylinder viscometer.
R_1	Radius of inner cylinder.
R_2	Radius of outer cylinder.
R_o	Radius of cone tip removed.
r	General moment of the log-normal distribution.
S	Total surface area of a sample of N droplets.
S_c	Total surface area per unit volume of continuous phase.
S_d	Total surface area per unit volume of continuous phase of an emulsion with detergent addition.
S_{max}	Total surface area per unit volume of continuous phase after infinite stirring time.

t	Stirring time.
V_c	Total volume of continuous phase around N droplets.
V_d	Total volume of dispersed phase in N droplets.
V_x	Cumulative volume in A.D.E.
v	Velocity of moving parallel plate.
w_i	Probability of a droplet falling in a certain class.
X	Diameter of largest droplet in A.D.E.
x	Droplet diameter.
$\bar{x}$	Independent variable in method of least squares.
x_i	General diameter representing mid-point of class.
x_{n-max}	Modal value of x.
x_o	Upper limit of a diameter class.
x_s	Mean surface diameter obtained from log-normal distribution.
x_{sv}	Mean surface area/unit volume diameter obtained from log-normal distribution.
x_v	Mean volume diameter obtained from log-normal distribution.
Y	Extrapolation point in τ-$\dot{\gamma}$ curve.
y	Frequency function for distribution of logarithms of x.
y'	Frequency function for logarithmic transformation of normal distribution.
y''	Probability density in the normal distribution.
$\bar{y}$	Dependent variable in method of least squares.
Z	Substitution in transformation from log-normal to normal distribution.
$\propto$	Parameter in A.D.E.
α	Scale reading of Rheotest II.
β	Angle between residual droplet pairs and direction of flow.
$\dot{\gamma}$	Rate of shear.
$\dot{\gamma}_{min}$	Critical rate of shear.

η	Newtonian viscosity.
η'	Apparent viscosity.
η_c	Viscosity of continuous phase.
η_i	Viscosity of dispersed phase.
η_{rel}	Relative viscosity (η_∞/η_c)
η_∞	Gradient of linear part of pseudoplastic curve.
θ_c	Celcius temperature.
μ_1', μ_2', μ_3'	1st, 2nd and 3rd moment distributions.
μ'_r	General moment distribution about log-normal transformation.
μ'_{r1}	Moment of true diameter corresponding to μ'_{x1}.
μ'_{x1}	Moment of section diameter.
σ	Arithmetic standard deviation.
σ_g	Geometric standard deviation.
τ	Shearing stress.
ϕ	Volume fraction of dispersed phase.
ψ	Angle between cone and plate.
Ω	Angular velocity in viscometer.
ω	Ratio S_d/S_c.

APPENDIX 2. DROPLET SIZE CALIBRATION

The interval centres (Int.C) for the Carl Zeiss Counter are shown in millimetres for each class in the table below.

Class	Int. C	Class	Int. C	Class	Int. C
1	1.49	17	10·32	33	19·15
2	2·04	18	10·87	34	19·70
3	2·59	19	11·42	35	20·26
4	3·14	20	11·98	36	20·81
5	3·70	21	12·53	37	21·36
6	4·25	22	13·08	38	21·91
7	4·80	23	13·63	39	22·46
8	5·35	24	14·18	40	23·02
9	5·90	25	14·74	41	23·57
10	6·46	26	15·29	42	24·12
11	7·01	27	15·84	43	24·67
12	7·56	28	16·39	44	25·22
13	8·11	29	16·94	45	25·78
14	8·66	30	17·50	46	26·33
15	9·22	31	18·05	47	26·88
16	9·77	32	18·60	48	27·43

The graticule photograph from each film was matched with the counter. If, for example, the light beam of class 28 corresponded to the 10 μm lines, then the scale reading of 16·39 ≡ 10 μm and so 1 μm is equivalent to 1·639 (Q). The scale was then converted to microns by multiplying the reading in each class by 1/Q. Q is recorded for each set of data in Appendix 4. The reduced scale of the counter is one third the size of the readings in the table. Thus Q was multiplied by three when that scale was used.

APPENDIX 3 - PROGRAM PST48

```
'BEGIN'
'REAL'CF,DX,EM,F,PR,Z,Q;
'INTEGER'I;
'BEGIN'
'REAL''ARRAY'D,P,C,A,XM,NTOT,SR,UILXM[1:48];
'FOR'I←1'STEP'1'UNTIL'48'DO''BEGIN'
 SR[I]←READ;  'END';
SHEETS:
NEWLINE(4);
EM←READ;F←READ;PR←READ;Z←READ;Q←READ;
CF←1/Q;
WRITETEXT('('TABLE%%OF%%VALUES%%FOR%%EMULSION')');
PRINT(EM,3,1);
WRITETEXT('('FROM%%DATA%%IN%%FILM')');
PRINT(F,2,0);  PRINT(PR,3,0);
'FOR'I←1'STEP'1'UNTIL'48'DO''BEGIN'
 D[I]←READ;
 'IF'I'EQ'1'THEN'NTOT[I]←D[I]
 'ELSE'NTOT[I]←NTOT[I-1]+D[I];
 XM[I]←SR[I]*CF;
'IF'I=48'THEN'DX←(XM[48]-XM[1])/48;
'END';
 SPACE(4);
WRITETEXT('('NO%%TOTAL%%=')');
PRINT(NTOT[48],4,0);
WRITETEXT('('%%Q%%=')');
PRINT(Q,1,3);
NEWLINE(3);
WRITETEXT('('CLASS%%NO,')');
SPACE(6);
WRITETEXT('('NO%OF%DROPS')');
SPACE(4);
WRITETEXT('('PROP%%P/C')');
SPACE(6);
WRITETEXT('('CUM%NO%P/C')');
SPACE(5);
WRITETEXT('('NORMALISED')');
SPACE(7);
WRITETEXT('('X(MICRONS)')');
SPACE(7);
WRITETEXT('('LOGE%X')');
'COMMENT' X = UPPER INTERVAL LIMIT OF THE CLASS;
 SPACE(6);
WRITETEXT('('S%READING')');
NEWLINE(2);
'FOR'I←1'STEP'1'UNTIL'48'DO''BEGIN'
 SPACE(2);
 PRINT(I,2,0);
 SPACE(10);
 PRINT(D[I],3,0);
 SPACE(7);
 P[I]←(D[I]*100)/NTOT[48];
 PRINT(P[I],2,4);
 SPACE(5);
 'IF'I'EQ'1'THEN'C[I]←P[I]
 'ELSE'C[I]←C[I-1]+P[I];
 PRINT(C[I],3,4);
 SPACE(5);
 A[I]←P[I]/(100*DX);
 PRINT(A[I],1,4);
 SPACE(7);
UILXM[I]←XM[I]+(DX/2);
PRINT(UILXM[I],2,3);
 SPACE(7);
PRINT(LN(UILXM[I]),1,4);
 SPACE(6);
 PRINT(SR[I],2,2);
NEWLINE(1);  'END';
'IF'Z>99'THEN''BEGIN'
 PAPERTHROW;
 'GOTO'SHEETS;
'END';  'END';  'END'
***D
```

PROGRAM LT

```
'BEGIN'
'COMMENT' LINEAR REGRESSION ON X-WHICH IS ASSUMED CORRECT;
'REAL'C,M,XI,VAR,S,T,A,EM,F,PR,Y;
'REAL'SIGX,SIGY,SIGXX,SIGYY,SIGXY;
'REAL'CC,ST,ST2,Z,Q,CF,LVOLD,LSAPUV;
'INTEGER'I,J,K,L,LL,N;
'BEGIN'
'REAL''ARRAY'USR[1:48];
'FOR'K←1'STEP'1'UNTIL'48'DO''BEGIN'
USR[K]←READ;
'END';
POLLY:
EM←READ;F←READ;PR←READ;Z←READ;N←READ;L←READ;
Q←READ;  CF←1/Q;
LL←L+(N-1);
SIGX←SIGY←SIGXX←SIGYY←SIGXY←0;
NEWLINE(4);
WRITETEXT('('FOR%EMULSION%')');
PRINT(EM,3,1);
WRITETEXT('('%%%FILM%NO.')');
PRINT(F,3,0);
PRINT(PR,8,0);
NEWLINE(2);
SPACE(11);
WRITETEXT('('LOGE%X')');
SPACE(5);
WRITETEXT('('Z')');
NEWLINE(2);
'BEGIN'
'REAL''ARRAY'X,Y[L:LL];
'FOR'I←L'STEP'1'UNTIL'LL'DO''BEGIN'
X[I]←LN(CF*USR[I]);
'END';
'FOR'I←L'STEP'1'UNTIL'LL'DO''BEGIN'
 Y[I]←READ;
 SIGX←SIGX+X[I];
 SIGY←SIGY+Y[I];
 SIGXX←SIGXX+(X[I]*X[I]);
 SIGYY←SIGYY+(Y[I]*Y[I]);
 SIGXY←SIGXY+(X[I]*Y[I]);
 SPACE(10);
 PRINT(X[I],1,4);
 PRINT(Y[I],1,4);
 NEWLINE(1);
'IF'I=LL'THEN''BEGIN'
  A←(N*SIGXX)-SIGX↑2;
  M←((N*SIGXY)-(SIGX*SIGY))/A;
  C←((SIGY*SIGXX)-(SIGX*SIGXY))/A;
 S←(N*SIGXX)-(SIGX↑2);
 T←(N*SIGYY)-(SIGY↑2);
'END';'END';
XI←EXP(-C/M);
VAR←1/M;
NEWLINE(4);
WRITETEXT('('GRADIENT%=')');
PRINT(M,2,3);
```

```
SPACE(10);
WRITETEXT('('INTERCEPT%=')');
PRINT(C,2,3);
NEWLINE(2);
WRITETEXT('('XI%=')');
PRINT(XI,2,3);
SPACE(10);
WRITETEXT('('VARIANCE%=')');
PRINT(VAR,2,3);
NEWLINE(2);
WRITETEXT('('GEOMETRIC%STANDARD%DEVIATION%=')');
PRINT(EXP(VAR),2,3);
'END';
NEWLINE(2);
'COMMENT' VALUES TO FIT ONTO BEST LINE;
SPACE(11);
WRITETEXT('('Z')');
SPACE(9);
WRITETEXT('('LOGE%X')');
NEWLINE(2);
Y←-2;
'BEGIN'
'REAL''ARRAY'LOGEX[1:5];
'FOR'J←1'STEP'1'UNTIL'5'DO''BEGIN'
 SPACE(10);
 LOGEX[J]←(Y-C)/M;
 PRINT(Y,1,0);
 SPACE(6);
 PRINT(LOGEX[J],1,3);
 Y←Y+1;
 NEWLINE(1);
'IF'J=3'THEN''BEGIN'
NEWLINE(1);
LVOLD←LOGEX[3]*(1.5*VAR*VAR);
LSAPUV←LOGEX[3]+(2.5*VAR*VAR);
WRITETEXT('('MEAN%VOLUME%DIAMETER%=%')');
PRINT(EXP(LVOLD),2,3);  NEWLINE(2);
WRITETEXT('('MEAN%SURFACE/UNIT-VOLUME%DIAMETER%=%')');
PRINT(EXP(LSAPUV),2,3);  'END';
'END';'END';
'IF'Z>99'THEN''BEGIN'
PAPERTHROW;
'GOTO'PULLY;
'END';'END';'END'
***D
```

COMPILATION REPORT

PROGRAM VMNS

```
'BEGIN'
'COMMENT' VARIOUS MEAN DIAMETERS FROM -EMULSION SCIENCE- P SHERMAN;
'COMMENT'SAME DATA ARRANGEMENT AS PROGRAM PCJDSPST48.;
'REAL'XG,LNXG,XA,XL,XS,XV,XV3,XRV,RXRV,RXRV3,
'REAL'SIGN,SIGNLNX,SIGNX,SIGNX2,SIGNX3,SIGNRX3,XSV,
'REAL'EM,F,PR,Z,CF,Q;
'INTEGER'I;
NEWLINE(5);
'BEGIN'
'REAL''ARRAY'XM,N,SR[1:48];
'FOR'I←1'STEP'1'UNTIL'48'DO''BEGIN'
SR[I]←READ;
'END';
CARD:
EM←READ;F←READ;PR←READ;Z←READ;Q←READ;
CF←1/Q;
SIGN←SIGNLNX←SIGNX←SIGNX2←SIGNX3←SIGNRX3←0;
NEWLINE(4);
SPACE(5);
WRITETEXT('('VARIOUS%%MEAN%%DIAMETERS%%FOR%%EMULSION%%NO.%%')');
PRINT(EM,3,1);
NEWLINE(2);  SPACE(5);
WRITETEXT('('FROM%%DATA%%IN%%FILM')');
PRINT(F,2,0);  PRINT(PR,8,0);
NEWLINE(4);
'FOR'I←1'STEP'1'UNTIL'48'DO''BEGIN'
N[I]←READ;
XM[I]←SR[I]*CF;
SIGN←SIGN+N[I];
SIGNLNX←SIGNLNX+N[I]*LN(XM[I]);
SIGNX←SIGNX+N[I]*XM[I];
SIGNX2←SIGNX2+N[I]*(XM[I]↑2);
SIGNX3←SIGNX3+N[I]*(XM[I]↑3);
SIGNRX3←SIGNRX3+N[I]*(1/(XM[I]↑3));
'IF'I=48'THEN''BEGIN'
LNXG←SIGNLNX/SIGN;
XG←EXP(LNXG);
XA←SIGNX/SIGN;
XL←SIGNX2/SIGNX;
XS←SQRT(SIGNX2/SIGN);
XV3←SIGNX3/SIGN;
XV←EXP(LN(XV3)/3);
RXRV3←SIGNRX3/SIGN;
RXRV←EXP(LN(RXRV3)/3);
XRV←1/RXRV;
XSV←SIGNX3/SIGNX2;
'END';  'END';
NEWLINE(2);  SPACE(5);
WRITETEXT('('GEOMETRIC%%MEAN%%DIAMETER%%')');   SPACE(9);
PRINT(XG,2,4);   NEWLINE(3);   SPACE(5);
WRITETEXT('('ARITHMETIC%%MEAN%%DIAMETER')');   SPACE(9);
PRINT(XA,2,4);   NEWLINE(3);   SPACE(5);
WRITETEXT('('MEAN%%DIAMETER%%LENGTH%%')');   SPACE(9);
PRINT(XL,2,4);   NEWLINE(3);   SPACE(5);
WRITETEXT('('MEAN%%SURFACE%%DIAMETER%%')');   SPACE(9);
PRINT(XS,2,4);   NEWLINE(3);   SPACE(5);
WRITETEXT('('MEAN%%VOLUME%%DIAMETER%%')');   SPACE(9);
PRINT(XV,2,4);   NEWLINE(3);   SPACE(5);
WRITETEXT('('RECIPROCAL%%MEAN%%DIAMETER')');   SPACE(9);
PRINT(XRV,2,4);   NEWLINE(3);   SPACE(5);
WRITETEXT('('MEAN%%VOLUME-SURFACE%%DIAMETER')');   SPACE(5);
PRINT(XSV,2,4);
'IF'Z>99'THEN''BEGIN'
PAPERTHROW;
'GOTO'CARD;
'END';  'END';  'END'
***)
```

APPENDIX 4 - RAW DROPLET SIZE DATA

DATA FOR EMULSIONS	1	14	15	17	21	24	25	26	27	28
STIRRING TIME (SECS)	80	70	70	70	70	60	60	30	10	10
1	0	0	0	14	27	61	180	38	10	15
2	0	0	0	51	83	20	62	20	37	30
3	0	0	0	59	53	27	43	15	44	41
4	0	0	0	76	16	29	48	25	76	43
5	0	3	0	77	12	15	37	28	78	40
6	0	8	1	61	13	15	25	35	66	33
7	1	41	8	43	29	14	16	25	32	31
8	2	80	25	32	17	14	14	33	30	17
9	9	109	63	19	28	12	15	23	30	35
10	19	91	92	16	23	16	9	30	33	23
11	33	63	91	16	22	9	8	13	26	17
12	82	53	81	11	20	10	8	20	16	17
13	190	20	80	12	11	6	5	15	16	10
14	228	17	31	4	14	10	3	16	10	6
15	167	8	24	6	10	2	4	9	9	9
16	117	5	19	1	5	7	9	11	3	7
17	61	3	7	5	6	5	9	15	8	8
18	39	3	8	5	1	5	1	11	6	1
19	26	4	6	1	2	0	3	14	2	4
20	12	0	9	1	3	4	5	11	5	3
21	11	0	6	3	1	4	1	8	1	1
22	3	3	2	0	2	1	3	8	5	1
23	8	1	3	3	1	2	0	11	2	1
24	2	1	2	1	5	4	4	7	1	0
25	6	0	1	2	1	4	6	3	1	1
26	5	0	3	1	0	5	1	1	2	1
27	3	0	1	2	1	3	0	2	4	0
28	5	0	0	0	0	0	1	8	2	0
29	4	0	1	2	0	3	0	5	1	0
30	2	0	0	0	2	2	0	3	0	0
31	2	0	0	1	1	0	0	2	0	1
32	1	0	1	1	0	1	0	1	0	0
33	0	0	1	0	1	2	0	1	0	0
34	1	0	0	1	0	0	0	0	0	0
35	0	0	1	1	0	0	1	0	0	0
36	0	0	0	1	0	0	0	0	0	0
37	0	0	0	0	0	3	0	1	0	0
38	0	0	0	0	0	2	0	1	0	0
39	0	0	0	0	0	1	1	1	0	0
40	1	0	0	0	0	0	0	0	0	0
41	1	0	0	0	0	0	1	0	0	0
42	0	0	0	0	0	0	0	0	0	0
43	0	0	0	0	0	0	0	0	0	0
44	0	0	0	0	0	2	0	0	0	0
45	0	0	0	0	0	0	0	0	0	0
46	0	0	0	0	0	0	0	0	0	0
47	0	0	0	1	0	0	0	0	0	0
48	0	0	0	0	0	1	0	0	0	0
TOTAL	1061	513	567	530	448	325	523	470	596	616
Q	4.692	4.824	4.824	1.639	1.639	0.799	0.799	0.799	0.799	0.799

DATA FOR EMULSIONS	31	32	33	34	35	36	37	38	39	40
STIRRING TIME (SECS)	10	10	10	10	10	5	10	15	30	60
1	0	0	0	22	27	22	42	90	0	0
2	0	0	0	126	164	135	156	162	0	0
3	0	0	0	123	168	94	140	105	0	0
4	3	0	1	42	47	32	67	52	0	0
5	11	1	2	20	30	36	52	16	5	14
6	25	7	16	31	25	51	54	24	21	37
7	65	21	47	22	27	19	21	14	40	76
8	79	32	69	23	21	20	14	14	72	137
9	93	70	83	9	9	14	16	4	78	96
10	76	49	73	10	17	14	12	7	73	59
11	45	46	67	10	12	9	13	4	60	35
12	25	31	40	4	17	9	6	1	40	32
13	11	25	50	10	12	11	7	3	20	17
14	6	16	25	7	10	8	2	0	24	7
15	13	6	21	5	7	2	4	1	10	7
16	6	9	11	5	6	1	5	4	10	4
17	8	5	17	4	4	3	0	0	4	7
18	10	9	13	2	0	3	1	0	5	1
19	10	12	19	1	3	2	0	0	3	4
20	8	9	14	3	3	2	0	0	8	3
21	13	16	25	2	0	0	1	0	6	3
22	17	15	16	0	0	3	0	0	4	4
23	9	7	10	2	0	0	1	0	4	1
24	5	14	7	0	2	1	0	0	5	0
25	6	10	10	0	0	3	0	0	1	0
26	6	4	6	0	1	3	0	0	2	0
27	2	8	9	0	0	3	0	0	2	0
28	1	5	7	0	0	1	0	1	2	0
29	6	1	13	0	1	1	0	0	2	0
30	1	3	4	1	1	0	0	0	0	0
31	4	1	3	0	0	0	0	0	0	1
32	2	3	6	0	0	0	0	0	0	0
33	1	3	11	0	0	0	0	0	2	0
34	3	7	4	0	1	0	0	0	0	0
35	6	4	6	0	0	0	0	0	1	0
36	0	5	7	0	0	0	0	0	1	0
37	3	6	0	0	1	0	0	0	1	0
38	2	4	2	0	0	0	0	0	0	0
39	3	1	3	0	0	0	0	0	0	0
40	2	1	2	0	0	0	0	0	0	0
41	2	1	7	0	0	0	0	0	0	0
42	0	2	2	0	0	0	0	0	0	0
43	1	0	2	0	0	0	0	0	0	0
44	0	0	4	0	0	0	0	0	0	0
45	0	0	0	0	0	0	0	0	0	0
46	0	0	3	0	0	0	0	0	0	0
47	0	0	0	0	0	0	0	0	0	0
48	4	7	10	0	0	0	0	0	0	0
TOTAL	591	470	760	484	563	502	616	502	506	560
Q	4.668	4.668	4.668	1.556	1.556	1.529	1.529	1.529	4.492	4.492

DATA FOR EMULSIONS	41	42	43	44	45	49	50	53	54	56
STIRRING TIME (SECS)	5	10	15	30	60	30	60	15	30	60
1	30	56	65	0	0	114	157	52	82	57
2	92	106	111	0	0	137	154	110	145	147
3	97	87	111	0	0	84	95	90	140	110
4	71	63	54	1	0	37	35	72	61	55
5	45	35	41	5	1	34	44	72	65	50
6	55	31	23	23	14	19	10	49	46	45
7	23	24	17	45	35	13	16	36	29	29
8	21	15	12	60	93	14	12	45	21	25
9	13	13	13	87	83	6	6	39	14	25
10	14	7	7	76	90	8	3	37	13	12
11	18	6	5	78	59	7	1	21	9	7
12	10	5	4	65	36	4	3	22	5	5
13	5	0	0	50	35	4	0	18	3	11
14	4	2	1	26	15	7	1	17	2	5
15	9	2	3	28	16	1	0	4	1	3
16	4	3	1	22	11	0	0	12	3	3
17	0	1	0	29	13	0	2	2	0	0
18	1	0	0	14	10	0	1	4	1	1
19	3	1	0	15	8	0	0	3	1	1
20	3	1	0	12	5	0	0	4	2	1
21	1	0	0	9	4	1	0	3	2	0
22	2	0	0	7	1	0	0	1	1	0
23	5	1	0	10	7	0	0	0	0	1
24	1	0	0	12	3	0	0	0	1	0
25	0	2	1	7	1	0	0	1	0	1
26	0	0	0	5	1	0	0	0	0	0
27	0	0	0	3	0	0	0	1	0	0
28	1	0	0	3	0	0	0	0	0	0
29	1	0	0	3	1	1	0	0	0	1
30	3	0	0	1	0	0	0	1	0	0
31	0	0	0	1	0	0	0	0	0	0
32	0	0	0	1	1	0	0	0	1	0
33	0	0	0	3	0	0	0	0	0	0
34	0	0	0	2	0	0	0	0	1	0
35	0	0	0	1	0	0	0	1	1	0
36	1	0	0	1	0	0	0	0	0	0
37	1	0	0	1	0	0	0	1	0	0
38	0	0	0	3	0	0	0	1	0	0
39	0	0	0	0	0	0	0	0	0	0
40	0	0	0	1	0	0	0	0	0	0
41	1	0	0	1	0	0	0	0	0	0
42	0	0	0	0	0	0	0	0	0	0
43	0	0	0	1	0	0	0	1	0	0
44	0	0	0	0	0	0	0	0	0	1
45	0	0	0	0	0	0	0	0	0	0
46	0	0	0	0	0	0	0	0	0	0
47	0	0	0	0	0	0	0	0	0	0
48	0	0	0	0	0	0	0	0	0	0
TOTAL	538	461	463	712	543	484	546	713	666	602
N	1,529	1,529	1,529	4,587	4,587	1,529	1,529	1,639	1,039	1,039

DROPLET SIZE DATA FOR EMULSION 87

STIRRING TIME (SECS)	5	10	15	35	60
1	58	83	114	0	0
2	104	149	126	0	0
3	44	98	41	0	0
4	31	43	31	1	1
5	67	72	30	4	3
6	43	76	19	12	16
7	25	32	17	35	57
8	26	24	15	65	94
9	19	21	7	65	136
10	16	14	4	77	115
11	12	6	2	59	40
12	6	9	1	36	18
13	4	8	1	27	11
14	5	3	3	15	2
15	2	2	3	10	10
16	1	1	2	13	4
17	1	2	1	11	6
18	2	3	1	10	7
19	4	1	0	16	7
20	4	1	1	18	2
21	2	1	0	10	6
22	1	2	0	11	5
23	2	0	0	13	3
24	0	0	0	6	3
25	2	0	0	2	4
26	3	0	1	6	1
27	3	0	0	6	0
28	0	2	0	2	1
29	2	1	0	4	0
30	1	0	0	4	1
31	1	0	0	2	0
32	1	2	0	4	0
33	2	1	0	2	0
34	0	1	0	2	1
35	0	0	0	3	0
36	0	0	1	1	1
37	1	1	0	0	0
38	1	0	0	0	0
39	0	0	0	1	0
40	0	0	0	0	0
41	0	0	0	0	0
42	0	0	0	0	0
43	0	0	0	0	0
44	0	0	0	0	0
45	0	0	0	0	0
46	0	0	0	0	0
47	0	0	0	0	0
48	0	0	0	0	0
TOTAL	493	659	423	553	560
n	1,529	1,529	1,529	4,587	4,587

DROPLET SIZE DATA FOR EMULSION 88

STIRRING TIME (SECS)	5	10	15	30	60
1	24	19	96	41	55
2	14	22	64	16	21
3	16	28	94	29	30
4	24	37	66	52	52
5	29	55	78	39	44
6	31	46	52	64	60
7	23	59	36	45	37
8	25	44	26	47	29
9	33	52	33	36	35
10	27	31	14	29	27
11	25	27	10	25	19
12	31	23	9	14	23
13	21	24	9	11	12
14	23	13	9	11	20
15	22	13	5	13	11
16	17	8	6	10	10
17	17	11	1	6	9
18	10	3	5	5	4
19	20	14	3	3	5
20	13	10	1	4	3
21	7	5	0	3	0
22	8	7	0	3	2
23	8	4	2	4	1
24	7	4	0	2	0
25	8	5	1	2	0
26	7	4	0	0	1
27	6	0	0	1	1
28	4	0	0	0	0
29	2	1	0	0	0
30	5	2	0	0	0
31	0	3	0	0	0
32	4	3	0	0	0
33	2	1	0	0	0
34	2	0	1	0	0
35	4	1	0	0	0
36	2	1	0	0	0
37	3	1	0	0	0
38	2	0	0	0	0
39	3	0	0	0	0
40	1	0	0	0	0
41	1	0	0	0	0
42	1	0	0	0	0
43	2	1	0	0	0
44	0	0	0	0	0
45	0	1	0	0	0
46	1	0	0	0	0
47	0	0	0	0	0
48	1	0	0	0	0
TOTAL	532	531	621	513	509
n	1,142	1,142	1,142	1,556	1,556

STIRRING TIME (SECS)	DROPLET SIZE DATA FOR EMULSION 91					DROPLET SIZE DATA FOR EMULSION 92			
	5	10	15	30	60	10	15	30	60
1	98	160	67	174	0	56	98	128	0
2	146	132	209	106	0	160	192	239	0
3	41	54	39	44	0	54	70	46	0
4	49	67	33	37	1	43	43	51	2
5	77	68	53	63	4	63	92	64	11
6	59	51	45	23	28	66	93	50	35
7	24	25	25	12	53	48	34	28	99
8	30	30	14	11	141	17	24	15	126
9	24	32	10	7	135	26	18	15	116
10	19	16	9	10	87	26	13	6	85
11	17	20	3	4	33	14	5	5	45
12	8	0	1	1	20	18	7	2	16
13	5	8	1	3	14	7	5	1	6
14	10	6	1	4	3	4	4	0	13
15	10	6	2	1	9	2	4	0	7
16	7	3	1	1	3	4	1	1	12
17	6	4	1	1	8	4	3	0	18
18	4	3	1	0	11	5	1	0	12
19	1	0	0	0	13	2	0	0	16
20	1	4	0	0	22	6	2	0	13
21	0	2	2	0	13	1	2	0	15
22	1	2	0	1	8	2	0	0	14
23	3	0	0	0	10	0	0	0	10
24	2	4	0	0	2	2	0	0	3
25	1	0	0	0	3	1	0	0	6
26	0	2	0	0	0	2	1	0	4
27	2	1	0	0	0	0	0	0	1
28	2	0	1	0	2	2	1	0	1
29	3	1	0	0	2	0	2	0	4
30	1	0	0	0	2	1	1	0	1
31	0	1	0	0	1	0	0	0	1
32	2	0	0	0	0	0	0	0	1
33	1	0	0	0	1	0	1	0	2
34	2	0	0	0	0	1	0	0	1
35	0	1	0	0	0	0	0	0	2
36	1	0	0	0	0	1	0	0	0
37	1	0	0	0	0	0	0	0	0
38	0	0	0	0	0	0	0	0	1
39	0	0	0	0	0	0	0	0	2
40	2	0	0	0	0	0	0	0	0
41	1	0	0	0	0	0	0	0	0
42	0	0	0	0	1	0	0	0	0
43	0	0	0	0	0	0	0	0	0
44	0	0	0	0	0	0	0	0	0
45	0	0	0	0	0	0	0	0	0
46	0	0	0	0	0	0	0	0	0
47	0	0	0	0	0	0	0	0	0
48	0	0	0	0	0	0	0	0	0
TOTAL	656	711	518	503	630	638	715	655	705
Q	1.556	1.556	1.556	1.556	4.668	1.556	1.556	1.556	4.668

STIRRING TIME (SECS)	DROPLET SIZE DATA FOR EMULSION 97					DROPLET SIZE DATA FOR EMULSION 101				
	5	10	15	30	60	5	10	15	30	60
1	92	36	109	0	0	125	125	141	0	0
2	98	32	173	0	0	126	190	173	0	0
3	35	12	68	2	0	36	45	48	0	3
4	47	18	35	10	0	24	39	43	4	5
5	58	8	50	24	1	59	71	71	28	33
6	42	15	46	54	9	36	54	43	72	93
7	19	8	20	93	47	17	32	20	131	108
8	25	8	25	96	112	17	22	12	97	78
9	14	5	21	64	109	16	13	8	75	45
10	22	4	6	42	79	6	9	3	35	28
11	9	2	10	32	34	12	7	3	22	18
12	8	1	5	16	14	10	6	5	21	13
13	11	2	5	15	23	3	6	2	18	11
14	6	2	1	12	6	2	4	2	12	11
15	3	1	2	12	4	3	0	1	14	4
16	4	1	1	9	11	3	3	0	15	6
17	3	0	0	9	6	2	5	3	15	4
18	0	0	2	14	8	3	4	0	15	8
19	2	1	1	20	8	1	1	0	11	7
20	6	0	1	15	6	2	0	0	22	4
21	1	0	1	13	6	1	0	0	10	1
22	5	0	0	14	5	2	0	1	3	4
23	0	1	1	9	6	0	1	0	7	1
24	1	0	0	1	4	1	0	0	2	1
25	1	0	0	2	1	1	0	0	2	1
26	0	0	1	4	1	0	1	0	2	0
27	2	0	0	4	1	0	0	0	1	1
28	1	0	0	3	0	2	0	0	3	0
29	0	0	0	3	0	0	0	0	0	0
30	0	0	0	2	0	1	0	0	1	1
31	2	0	1	2	0	0	0	0	0	1
32	1	0	0	1	0	0	1	0	1	0
33	0	0	0	1	0	0	0	0	1	0
34	1	0	0	2	1	1	0	0	0	0
35	0	0	0	2	0	0	0	0	3	0
36	2	0	0	0	0	0	0	0	0	0
37	0	0	0	2	0	0	0	0	1	0
38	1	0	0	2	0	0	0	0	0	0
39	0	0	0	1	0	0	0	0	0	0
40	0	0	0	1	0	1	0	0	1	0
41	0	0	0	1	0	0	0	0	0	0
42	0	0	0	0	0	0	0	0	1	0
43	0	0	0	0	0	0	0	0	0	0
44	0	0	0	0	0	0	0	0	0	0
45	1	0	0	0	0	1	0	0	1	0
46	0	0	0	0	0	0	0	0	0	0
47	0	0	0	0	0	0	0	0	0	0
48	0	0	0	0	0	0	0	0	1	0
TOTAL	521	157	593	606	502	513	639	576	648	690
Q	1,556	1,474	1,474	4,422	4,472	1,474	1,474	1,474	4,422	4,422

STIRRING TIME (SECS)	DROPLET SIZE DATA FOR EMULSION 102				
	10	15	20	30	60
1	30	105	215	0	0
2	95	172	120	0	0
3	62	66	55	0	3
4	17	29	29	0	7
5	19	40	40	2	21
6	35	29	52	6	61
7	34	17	18	28	67
8	19	15	11	58	78
9	12	8	5	73	80
10	10	7	12	76	62
11	13	6	6	67	32
12	6	8	3	51	27
13	11	1	6	40	7
14	9	3	2	13	8
15	10	3	3	8	4
16	4	5	2	5	2
17	3	0	2	8	1
18	9	0	0	5	3
19	5	2	2	7	3
20	4	0	0	7	13
21	4	2	1	7	2
22	4	0	1	5	4
23	5	0	1	13	5
24	4	0	1	12	5
25	2	1	0	9	3
26	3	0	0	6	8
27	2	1	0	5	1
28	2	0	0	1	0
29	1	0	0	1	4
30	2	0	0	2	0
31	0	0	0	3	0
32	0	0	0	0	0
33	1	0	0	4	1
34	0	1	0	1	0
35	0	0	0	1	0
36	1	0	0	1	1
37	0	0	0	0	1
38	2	0	0	1	0
39	2	0	0	0	0
40	1	0	0	1	0
41	0	0	0	0	0
42	0	0	0	0	1
43	1	0	0	2	0
44	0	0	0	0	0
45	0	0	0	1	0
46	1	0	1	1	0
47	0	0	1	0	0
48	4	0	1	1	0
TOTAL	448	521	565	530	521
Q	1.501	1.501	1.501	4.503	4.503

STIRRING TIME (SECS)	DROPLET SIZE DATA FOR EMULSION 103			
	20	30	45	60
1	56	133	155	66
2	170	184	225	284
3	69	39	39	41
4	24	33	27	19
5	28	46	52	21
6	46	32	27	20
7	38	21	7	8
8	70	19	12	2
9	12	13	5	1
10	19	3	4	3
11	17	4	1	1
12	15	2	0	0
13	8	2	1	0
14	7	2	0	0
15	9	2	0	0
16	9	0	1	0
17	1	1	0	0
18	6	2	0	0
19	6	1	0	0
20	8	1	0	0
21	4	0	0	0
22	5	0	0	0
23	3	0	0	0
24	3	0	1	0
25	4	0	0	0
26	0	0	0	0
27	1	1	0	0
28	2	0	0	0
29	3	0	0	0
30	0	0	0	0
31	0	0	0	0
32	0	0	0	0
33	0	0	0	0
34	1	0	0	0
35	1	0	0	0
36	2	0	0	0
37	0	0	0	0
38	0	0	0	0
39	0	1	0	0
40	1	0	0	0
41	0	0	0	0
42	0	0	0	0
43	0	0	0	0
44	0	0	0	0
45	0	0	0	0
46	1	0	0	0
47	0	0	0	0
48	3	0	0	0
TOTAL	556	542	557	466
Q	1.501	1.501	1.501	1.501

STIRRING TIME (SECS)	DROPLET SIZE DATA FOR EMULSION 104					DROPLET SIZE DATA FOR EMULSION 103				
	15	20	30	45	60	10	15	20	30	60
1	15	10	0	0	0	80	42	105	127	143
2	97	139	0	0	0	125	120	125	108	64
3	127	129	0	0	0	68	51	35	37	49
4	32	23	0	0	0	30	17	31	22	19
5	34	19	0	0	1	42	47	44	32	32
6	54	55	0	0	0	43	49	40	36	47
7	65	51	2	1	3	39	42	17	31	27
8	31	15	5	9	27	22	18	17	19	22
9	26	13	15	36	53	29	18	20	30	19
10	18	18	42	30	100	23	11	12	17	20
11	14	11	94	79	110	13	20	9	13	18
12	10	2	112	75	79	15	12	6	7	16
13	6	4	78	49	30	12	4	8	13	4
14	6	2	36	23	16	9	9	8	9	12
15	5	1	19	17	9	11	4	4	12	4
16	7	1	15	19	3	12	5	6	8	6
17	2	3	12	8	5	5	4	7	6	6
18	3	2	4	1	8	2	5	5	4	7
19	2	1	7	5	4	2	3	2	3	1
20	2	1	12	9	7	1	4	3	3	5
21	0	0	12	8	5	4	0	5	1	3
22	1	2	7	20	11	1	3	4	2	0
23	1	0	26	9	9	2	2	4	4	0
24	2	1	19	19	8	3	2	2	1	2
25	0	0	14	17	2	2	1	2	1	1
26	0	1	12	10	3	1	0	1	3	0
27	0	3	12	7	6	2	2	3	0	1
28	1	0	5	6	0	1	0	1	0	2
29	3	0	3	2	0	3	1	0	0	0
30	0	0	3	2	2	2	0	2	1	1
31	0	0	3	3	0	0	0	0	1	1
32	0	0	8	2	3	1	0	2	0	1
33	1	0	5	4	1	0	0	1	0	0
34	0	0	3	3	4	0	0	0	0	0
35	0	0	2	1	0	0	0	2	0	0
36	0	0	2	2	2	0	1	1	0	0
37	0	0	2	0	0	1	1	0	0	0
38	0	0	1	3	0	1	0	0	0	0
39	0	0	2	2	0	0	0	0	0	0
40	0	0	2	0	0	1	0	0	0	0
41	0	0	2	0	0	0	0	0	0	0
42	0	0	1	0	0	0	0	0	0	0
43	0	0	1	0	0	1	0	0	0	0
44	0	0	2	2	0	0	0	0	0	0
45	1	0	0	1	0	0	0	0	0	0
46	0	0	1	0	0	0	0	0	0	0
47	1	0	0	0	0	0	0	0	0	0
48	0	0	5	0	0	0	0	0	0	0
TOTAL	567	507	608	534	511	608	498	534	551	520
U	1,501	1,501	4,503	4,503	4,503	1,501	1,501	1,501	1,501	1,501

DROPLET SIZE DATA FOR EMULSION 106					
STIRRING TIME (SECS)	10	15	20	30	60
1	63	29	144	136	15
2	123	109	100	40	31
3	73	88	26	12	21
4	39	43	31	16	16
5	31	39	25	14	18
6	25	36	37	16	37
7	10	22	32	20	42
8	14	19	22	14	31
9	9	18	15	19	47
10	8	18	14	20	38
11	5	14	14	13	41
12	11	6	6	11	30
13	9	13	10	15	35
14	3	12	8	17	24
15	4	8	8	21	26
16	3	2	4	14	24
17	6	5	9	22	17
18	5	5	4	10	18
19	4	8	12	21	14
20	6	2	5	12	8
21	3	7	4	9	12
22	2	3	4	8	6
23	5	2	5	8	3
24	1	2	3	11	6
25	1	3	4	7	3
26	5	4	3	9	3
27	2	2	0	7	4
28	6	6	5	3	2
29	3	1	2	5	2
30	4	1	3	8	2
31	0	1	2	7	0
32	2	0	2	5	0
33	0	1	0	3	0
34	1	1	1	3	0
35	0	2	1	7	0
36	2	2	1	2	0
37	3	0	0	8	0
38	0	1	1	1	0
39	1	0	0	1	0
40	1	1	1	5	0
41	0	0	2	1	0
42	1	0	0	1	0
43	1	1	0	1	0
44	1	0	0	0	0
45	0	1	0	1	0
46	0	0	0	1	0
47	1	0	1	1	0
48	3	1	1	1	0
TOTAL	500	539	572	587	576
u	1.501	1.501	1.501	1.501	1.501

DROPLET SIZE DATA FOR EMULSION 107					
STIRRING TIME (SECS)	15	20	30	45	60
1	18	55	81	13	109
2	23	47	60	18	80
3	6	23	15	23	39
4	8	14	11	8	22
5	16	21	10	19	16
6	27	29	19	29	21
7	24	28	19	30	19
8	15	15	18	37	7
9	26	17	21	32	9
10	40	28	27	56	12
11	28	21	17	31	18
12	17	11	18	50	13
13	27	14	21	29	10
14	28	16	20	16	5
15	26	11	12	18	5
16	21	18	14	26	6
17	36	10	17	15	7
18	19	11	13	20	10
19	16	8	18	17	4
20	17	9	11	11	4
21	13	4	12	19	3
22	9	4	9	12	6
23	19	8	10	14	0
24	8	10	12	13	6
25	9	2	7	13	7
26	9	13	9	9	4
27	5	4	9	13	6
28	7	7	9	8	2
29	10	3	16	9	5
30	4	2	14	6	1
31	7	5	9	7	4
32	7	4	6	4	3
33	3	2	5	5	0
34	3	5	7	5	1
35	1	3	5	4	2
36	1	5	12	2	4
37	2	1	3	1	1
38	1	1	5	3	5
39	0	1	3	2	2
40	1	1	6	1	5
41	2	1	5	0	3
42	3	4	0	1	3
43	1	1	4	2	0
44	0	1	4	1	0
45	0	2	0	3	1
46	0	0	3	0	1
47	0	1	0	0	0
48	0	4	7	1	2
TOTAL	563	505	613	614	695
u	1.501	1.501	1.501	1.501	1.501

STIRRING TIME (SECS)	DROPLET SIZE DATA FOR EMULSION 108: 10	15	30	45	60	DROPLET SIZE DATA FOR EMULSION 109: 15	30	45	60
1	3	8	30	16	35	1	4	4	5
2	3	10	33	15	36	0	3	6	5
3	11	15	39	38	37	0	7	8	10
4	16	21	52	38	34	0	13	10	15
5	20	15	51	33	34	1	6	14	20
6	22	23	40	41	37	2	10	16	17
7	39	14	44	43	51	1	1	9	18
8	25	31	42	51	62	2	3	15	17
9	30	15	63	82	77	2	3	10	32
10	32	38	47	50	65	2	3	19	30
11	27	24	50	44	57	3	11	14	38
12	29	34	34	50	36	6	9	26	47
13	30	26	36	28	17	4	11	34	46
14	27	17	35	19	11	1	13	37	38
15	21	24	20	10	7	4	13	37	45
16	15	19	19	6	5	2	19	37	35
17	14	16	7	3	4	4	33	41	23
18	14	13	3	2	0	12	36	27	18
19	10	11	3	1	0	10	38	27	10
20	8	6	2	1	1	11	22	15	7
21	10	8	1	1	0	12	16	12	10
22	3	11	0	0	0	9	22	5	1
23	4	3	0	1	0	21	24	3	2
24	2	2	0	0	0	14	7	2	0
25	2	1	0	0	0	19	4	2	0
26	2	2	0	0	0	10	2	0	3
27	1	0	0	0	0	13	3	1	0
28	1	2	0	0	0	8	0	0	0
29	1	0	0	0	0	10	2	0	0
30	1	0	0	0	0	4	0	0	0
31	0	0	0	0	0	3	0	0	0
32	0	0	0	0	0	8	0	0	0
33	0	0	0	0	0	3	0	0	0
34	0	0	0	0	0	2	0	0	0
35	0	0	0	0	0	2	0	0	0
36	0	0	0	0	0	2	0	0	0
37	0	0	0	0	0	0	0	0	0
38	0	0	0	0	0	0	0	0	0
39	0	0	0	0	0	0	0	0	0
40	0	0	0	0	0	1	0	0	0
41	0	0	0	0	0	0	0	0	0
42	0	0	0	0	0	0	0	0	0
43	0	0	0	0	0	0	0	0	0
44	0	0	0	0	0	0	0	0	0
45	0	0	0	0	0	0	0	0	0
46	0	0	0	0	0	0	0	0	0
47	0	0	0	0	0	0	0	0	0
48	0	0	0	0	0	0	0	0	0
TOTAL	423	409	651	573	696	209	238	431	492
Q	0.558	0.558	0.558	0.558	0.558	0.558	0.558	0.558	0.558

	DROPLET SIZE DATA FOR EMULSION 112					DROPLET SIZE DATA FOR EMULSION 111			
STIRRING TIME (SECS)	10	20	30	45	60	15	30	45	60
1	0	5	12	20	22	0	0	2	3
2	2	11	21	26	21	0	2	2	7
3	13	19	32	29	48	0	1	3	8
4	18	38	40	34	50	0	3	2	5
5	34	33	48	43	48	0	0	4	6
6	31	35	54	56	57	0	6	4	6
7	36	48	58	54	88	1	1	4	11
8	48	40	52	64	69	3	4	2	9
9	48	49	35	61	43	3	6	5	6
10	52	61	48	37	23	3	0	9	17
11	34	46	29	45	22	4	4	8	17
12	41	40	31	15	5	3	6	6	18
13	30	37	26	18	7	6	8	16	18
14	21	27	16	11	1	11	10	12	40
15	25	26	12	6	3	7	11	21	24
16	31	13	11	3	2	9	9	22	41
17	22	11	6	7	0	22	8	14	29
18	16	9	4	1	1	11	9	20	29
19	13	9	1	1	0	18	21	19	30
20	8	2	0	0	2	21	14	12	10
21	4	0	0	0	0	16	12	8	17
22	10	3	0	0	0	11	21	7	8
23	1	2	0	0	0	12	17	5	6
24	8	2	0	0	0	14	15	4	5
25	3	1	0	1	0	8	17	2	1
26	0	0	0	0	0	13	16	3	2
27	2	1	0	0	0	13	7	0	1
28	1	1	0	0	0	5	1	2	1
29	0	0	0	0	0	7	2	0	1
30	1	0	0	0	0	2	4	0	1
31	0	0	0	0	0	0	0	0	0
32	0	0	0	0	0	0	0	0	0
33	0	0	0	0	0	0	1	0	0
34	0	0	0	0	0	2	0	0	0
35	0	0	0	0	0	0	0	0	0
36	0	0	0	0	0	0	0	0	0
37	0	0	0	0	0	0	0	0	0
38	0	0	0	0	0	0	0	0	0
39	0	0	0	0	0	0	0	0	0
40	0	0	0	0	0	0	0	0	0
41	0	0	0	0	0	0	0	0	0
42	0	0	0	0	0	0	0	0	0
43	0	0	0	0	0	0	0	0	0
44	0	0	0	0	0	0	0	0	0
45	0	0	0	0	0	0	0	0	0
46	0	0	0	0	0	0	0	0	0
47	0	0	0	0	0	0	0	0	0
48	0	0	0	0	0	0	0	0	0
TOTAL	553	569	536	532	512	225	236	218	377
Q	0.558	0.558	0.558	0.558	0.558	0.558	0.558	0.558	0.558

	DROPLET SIZE DATA FOR EMULSION 113					DROPLET SIZE DATA FOR EMULSION 114			
STIRRING TIME (SECS)	10	20	30	45	60	10	20	30	60
1	1	12	7	29	36	38	28	51	1
2	3	10	24	24	35	44	49	106	6
3	2	20	17	17	45	62	44	100	13
4	7	18	19	27	43	68	96	104	11
5	11	11	31	23	41	54	81	67	25
6	11	17	21	25	35	40	52	40	20
7	13	9	17	30	46	43	45	29	28
8	14	17	25	28	47	37	28	20	27
9	7	14	19	35	56	33	34	16	30
10	6	13	28	37	52	20	19	11	42
11	14	9	21	47	55	11	12	7	54
12	15	19	26	56	62	11	12	6	46
13	18	7	33	54	52	9	9	0	38
14	19	11	39	47	18	8	5	0	42
15	19	12	41	33	18	6	6	0	32
16	17	22	25	30	12	4	6	1	31
17	10	16	20	17	5	1	1	1	25
18	18	22	24	7	1	1	0	0	16
19	10	14	21	3	0	1	3	1	19
20	12	20	7	1	0	3	1	0	10
21	13	22	3	2	0	1	0	0	18
22	10	22	5	2	0	3	0	0	4
23	9	12	5	0	0	0	0	0	6
24	9	10	2	0	0	2	1	0	8
25	11	5	0	0	0	0	0	0	3
26	7	3	0	1	0	1	0	0	6
27	9	6	0	0	0	1	0	0	6
28	3	1	0	0	0	1	0	0	1
29	3	2	0	0	0	2	0	0	3
30	4	1	0	0	0	0	0	0	4
31	4	3	0	0	0	0	0	0	4
32	2	0	0	0	0	0	0	0	0
33	1	0	0	0	0	0	0	0	3
34	1	0	0	0	0	0	0	0	0
35	1	0	0	0	0	0	0	0	0
36	0	0	0	0	0	0	0	0	2
37	1	0	0	0	0	0	0	0	0
38	0	0	0	0	0	0	0	0	0
39	0	0	0	0	0	0	0	0	0
40	0	0	0	0	0	0	0	0	0
41	0	0	0	0	0	0	0	0	0
42	0	0	0	0	0	0	0	0	0
43	0	0	0	0	0	0	0	0	0
44	0	0	0	0	0	0	0	0	0
45	0	0	0	0	0	0	0	0	0
46	0	0	0	0	0	0	0	0	0
47	0	0	0	0	0	0	0	0	0
48	0	0	0	0	0	0	0	0	0
TOTAL	315	380	480	575	659	514	552	560	584
Q	0.558	0.558	0.558	0.558	0.558	0.703	0.703	0.703	2.108

STIRRING TIME (SECS)	DROPLET SIZE DATA FOR EMULSION 115					DROPLET SIZE DATA FOR EMULSION 116				
	5	10	20	30	60	5	10	20	30	60
1	2	19	5	0	0	103	55	65	26	3
2	44	95	80	0	0	64	66	47	48	20
3	75	78	137	0	0	65	61	42	37	33
4	45	30	53	0	0	68	50	42	60	38
5	30	35	29	0	0	30	32	41	59	38
6	34	48	60	0	0	42	78	28	40	35
7	54	48	60	0	1	36	31	41	28	57
8	49	25	31	0	13	32	33	36	35	43
9	20	19	22	1	26	19	75	42	31	41
10	25	19	18	8	78	20	21	28	32	47
11	38	13	12	35	84	10	14	44	26	37
12	23	12	5	85	80	12	19	19	18	29
13	15	15	7	109	58	10	13	19	12	22
14	12	12	5	78	29	5	5	16	10	13
15	7	9	4	32	22	12	7	15	10	17
16	6	3	2	23	14	5	11	10	10	6
17	3	2	2	13	8	4	6	6	9	5
18	5	2	0	9	7	8	1	7	5	3
19	6	3	1	5	7	8	3	7	1	1
20	3	2	1	12	8	3	4	3	0	1
21	8	1	0	9	23	2	3	3	1	0
22	1	3	0	11	12	2	3	2	3	0
23	6	1	1	9	13	1	1	1	4	0
24	0	3	0	18	10	0	2	0	2	0
25	1	0	0	18	9	2	1	0	0	0
26	1	0	0	17	7	0	2	1	0	0
27	2	1	0	11	7	3	1	1	3	0
28	1	1	0	12	0	1	3	0	0	0
29	1	1	0	13	2	0	0	1	1	0
30	0	1	0	7	0	0	1	0	0	0
31	2	0	0	7	0	0	0	0	0	0
32	0	0	0	1	1	0	0	0	0	0
33	0	1	0	4	0	0	0	0	0	0
34	1	0	0	1	0	1	0	1	0	0
35	0	0	0	2	2	1	1	0	0	0
36	0	0	0	3	0	0	0	0	0	0
37	0	0	0	2	1	0	0	0	0	0
38	0	0	0	0	0	0	0	0	0	0
39	0	0	0	0	0	0	0	0	0	0
40	0	0	0	2	0	1	0	0	0	0
41	0	0	0	1	0	0	0	0	0	0
42	0	0	0	2	0	0	0	0	0	0
43	0	0	0	0	0	0	0	0	0	0
44	0	0	0	1	0	0	0	0	0	0
45	0	0	0	0	0	0	0	0	0	0
46	0	0	0	0	1	0	0	0	0	0
47	0	0	0	0	0	0	0	0	0	0
48	0	0	0	2	1	0	0	0	0	0
TOTAL	520	502	535	563	524	590	503	566	509	487
Q	1.501	1.501	1.501	4.503	4.503	1.115	1.115	1.115	1.115	1.115

DROPLET SIZE DATA FOR EMULSION 117

STIRRING TIME (SECS)	5	10	20	30	60
1	94	155	0	0	0
2	93	107	0	0	0
3	53	53	1	0	0
4	45	61	4	1	8
5	33	28	29	17	27
6	16	11	41	64	71
7	18	22	74	87	111
8	8	13	73	94	83
9	8	12	60	65	70
10	9	5	41	46	48
11	6	8	21	29	16
12	4	5	19	19	14
13	2	2	15	18	11
14	6	3	14	15	9
15	7	3	16	12	9
16	3	1	18	19	4
17	4	1	16	13	9
18	2	0	16	9	7
19	5	0	9	9	0
20	3	0	4	4	1
21	3	0	3	5	0
22	1	0	1	3	1
23	2	0	1	3	0
24	0	0	3	0	0
25	1	0	4	2	0
26	1	1	2	2	0
27	1	1	2	3	0
28	2	0	2	1	0
29	1	0	3	2	1
30	2	0	2	0	1
31	0	0	2	1	0
32	1	1	2	0	0
33	0	1	0	1	0
34	1	0	1	0	0
35	1	0	0	0	0
36	0	0	0	0	0
37	0	0	2	0	0
38	0	0	0	0	0
39	0	0	1	0	0
40	0	0	0	0	0
41	0	0	0	0	0
42	0	0	0	0	0
43	0	0	0	0	0
44	0	0	0	0	0
45	0	0	0	0	0
46	0	0	1	0	0
47	0	0	0	0	0
48	0	0	2	0	0
TOTAL	436	494	505	544	501
Q	1.115	1.115	3.345	3.345	3.345

DROPLET SIZE DATA FOR EMULSION 118

STIRRING TIME (SECS)	10	15	20	30	60
1	8	6	3	0	0
2	68	85	79	0	0
3	137	134	182	0	0
4	73	37	51	0	0
5	38	39	26	0	1
6	49	45	67	0	1
7	67	56	61	1	3
8	31	35	29	2	29
9	33	19	17	6	64
10	23	20	11	26	71
11	19	20	7	60	93
12	14	8	8	76	61
13	9	11	5	62	31
14	9	7	4	42	13
15	11	5	4	12	11
16	6	4	2	11	7
17	5	0	0	5	4
18	5	6	0	3	11
19	6	4	1	5	8
20	3	0	0	5	9
21	0	1	1	10	15
22	2	3	1	4	17
23	0	0	0	10	13
24	4	1	0	7	16
25	1	0	1	15	13
26	1	1	0	23	10
27	1	1	0	22	6
28	4	0	0	18	3
29	0	0	0	13	4
30	2	1	0	7	1
31	0	0	0	4	0
32	2	1	0	5	0
33	0	0	0	2	0
34	1	0	0	4	3
35	0	0	0	7	3
36	0	1	0	1	0
37	0	0	0	3	1
38	0	0	0	2	2
39	0	0	0	1	0
40	0	0	0	3	0
41	1	0	0	0	0
42	1	0	0	0	0
43	1	0	0	2	0
44	0	0	0	0	0
45	0	0	0	1	0
46	1	0	0	1	1
47	0	0	0	0	0
48	0	0	0	0	0
TOTAL	636	551	538	481	525
Q	1.487	1.487	1.487	4.461	4.461

STIRRING TIME (SECS)	DROPLET SIZE DATA FOR EMULSION 119					DROPLET SIZE DATA FOR EMULSION 120				
	15	20	30	45	60	20	25	30	45	60
1	8	19	16	0	0	5	44	45	53	0
2	107	130	192	0	0	81	145	184	204	0
3	64	100	123	0	0	65	77	61	97	0
4	20	31	34	0	0	25	30	19	30	0
5	22	40	45	0	0	26	44	32	37	0
6	63	36	97	2	0	37	58	42	35	0
7	71	61	52	9	1	67	31	32	17	3
8	36	40	22	27	12	27	16	22	15	21
9	20	22	70	52	29	22	12	22	6	47
10	37	23	21	80	81	30	19	16	11	98
11	25	19	17	76	81	16	13	6	2	87
12	19	14	5	30	66	11	4	9	1	58
13	20	15	3	20	22	9	5	4	1	23
14	10	9	5	7	9	8	4	3	1	15
15	9	6	2	10	6	6	5	1	1	4
16	6	6	1	7	5	2	0	1	2	14
17	8	7	2	2	1	5	1	3	1	6
18	8	3	0	5	3	4	1	1	1	2
19	4	0	1	8	4	2	1	0	2	16
20	3	3	1	20	7	3	1	4	0	6
21	5	3	0	18	6	2	0	0	0	12
22	2	1	0	17	5	2	0	1	0	12
23	1	0	1	21	14	2	1	0	0	6
24	1	0	0	23	11	2	2	0	0	9
25	2	0	0	12	8	0	0	0	0	7
26	2	1	0	10	8	1	3	0	0	12
27	2	0	0	11	5	2	0	0	0	7
28	2	1	1	9	4	2	0	0	0	8
29	0	1	0	14	1	1	0	0	0	7
30	0	2	0	4	1	1	0	0	0	7
31	3	1	0	11	0	1	0	0	0	5
32	1	0	0	6	3	1	0	1	0	2
33	0	1	0	3	2	0	0	0	0	1
34	2	0	0	4	0	0	0	0	0	2
35	1	0	0	4	2	0	0	0	0	2
36	1	0	0	3	0	0	0	0	0	3
37	0	0	0	2	0	0	0	0	0	0
38	2	0	0	2	1	0	0	0	0	1
39	1	0	0	1	0	0	0	0	0	1
40	0	0	0	0	0	0	0	0	0	0
41	1	0	0	1	0	0	0	0	0	0
42	2	0	0	2	0	0	0	0	0	0
43	0	0	0	2	0	1	0	0	0	0
44	1	0	0	1	0	0	0	0	0	2
45	0	0	0	1	0	0	0	0	0	0
46	0	0	0	0	0	0	0	0	0	1
47	0	0	0	1	0	1	0	0	0	0
48	0	0	0	1	0	1	0	0	0	0
TOTAL	592	615	663	539	308	473	517	509	517	507
Q	1.487	1.487	1.457	4.461	4.461	1.501	1.501	1.501	1.501	4.503

STIRRING TIME (SECS)	DROPLET SIZE DATA FOR EMULSION 121				
	25	30	40	55	70
1	37	14	77	0	0
2	123	146	161	0	0
3	49	96	74	0	0
4	20	15	23	0	0
5	40	24	48	0	0
6	51	40	43	0	0
7	32	45	16	4	2
8	26	25	12	20	10
9	22	36	13	56	32
10	24	16	11	80	51
11	15	9	7	92	75
12	12	11	5	69	80
13	13	10	2	41	67
14	8	2	5	23	53
15	10	5	1	13	24
16	3	2	0	8	22
17	8	0	1	8	5
18	3	4	2	6	4
19	4	3	0	8	4
20	0	1	1	7	6
21	5	0	0	15	2
22	2	0	1	13	7
23	3	0	0	16	3
24	3	1	0	13	6
25	0	1	1	11	3
26	1	0	0	11	8
27	1	0	0	5	3
28	0	1	0	4	5
29	1	1	0	7	5
30	0	0	0	4	2
31	1	1	0	3	1
32	0	1	0	5	0
33	0	0	0	2	2
34	0	1	0	1	1
35	0	0	0	4	1
36	0	0	0	3	0
37	0	0	0	2	0
38	0	0	0	3	0
39	0	0	0	1	0
40	0	0	0	1	0
41	1	0	0	0	0
42	0	0	0	1	0
43	0	0	0	1	0
44	0	0	0	1	0
45	1	0	0	0	0
46	0	0	0	0	0
47	0	0	0	0	0
48	0	0	0	1	0
TOTAL	519	509	504	563	484
Q	1.501	1.501	1.501	4.503	4.503

STIRRING TIME (SECS)	DROPLET SIZE DATA FOR EMULSION .122				
	30	35	45	60	75
1	3	0	0	0	0
2	67	25	72	0	0
3	150	128	196	0	0
4	63	42	42	0	0
5	31	13	22	0	0
6	54	24	41	0	0
7	71	44	42	0	0
8	47	33	19	3	11
9	34	16	13	12	35
10	27	25	7	43	76
11	23	14	6	79	106
12	15	10	4	89	87
13	12	4	5	64	50
14	8	5	4	38	31
15	6	1	0	20	11
16	7	0	0	10	11
17	1	3	1	4	5
18	4	1	1	10	10
19	4	2	1	2	11
20	3	0	0	4	8
21	1	2	1	5	10
22	0	2	0	5	10
23	2	2	0	9	14
24	1	0	1	11	5
25	2	0	0	8	8
26	0	0	0	14	6
27	0	1	0	16	9
28	1	0	0	13	4
29	1	0	0	3	3
30	0	0	0	7	2
31	0	0	0	5	1
32	0	0	0	1	1
33	0	0	0	2	1
34	2	0	0	1	2
35	1	0	0	3	1
36	0	0	0	3	3
37	0	0	0	2	3
38	0	0	0	1	1
39	0	0	0	0	0
40	0	0	0	1	0
41	0	0	0	1	0
42	0	0	0	0	1
43	0	0	0	0	0
44	0	0	0	0	0
45	0	0	0	0	0
46	0	0	0	0	0
47	0	0	0	0	0
48	0	0	0	1	0
TOTAL	641	397	478	490	537
Q	1.501	1.501	1.501	4.503	4.503

STIRRING TIME (SECS)	DROPLET SIZE DATA FOR EMULSION 123					DROPLET SIZE DATA FOR EMULSION 124				
	10	15	20	40	60	15	20	30	45	60
1	12	2	0	0	0	4	18	27	16	0
2	83	43	34	0	0	78	121	137	129	0
3	100	143	227	0	0	122	145	116	164	0
4	53	84	90	0	0	71	70	50	60	0
5	34	27	21	0	0	37	59	41	40	0
6	44	36	35	0	0	48	60	36	41	1
7	46	61	53	1	0	44	46	41	33	1
8	31	35	37	3	7	34	30	12	9	10
9	26	32	17	13	18	27	26	25	15	23
10	18	26	10	36	77	28	24	14	12	51
11	19	12	6	62	104	20	20	7	6	90
12	17	9	6	81	109	16	15	8	1	100
13	11	8	7	90	83	16	7	10	4	59
14	8	2	2	59	43	10	7	3	1	42
15	7	3	1	36	25	8	3	3	0	29
16	7	1	1	22	16	3	8	4	0	8
17	3	2	0	15	10	6	1	2	0	13
18	5	1	0	7	3	1	8	1	0	7
19	3	3	1	9	9	3	4	1	1	9
20	2	1	0	9	5	2	1	0	0	9
21	2	1	0	10	9	3	3	1	0	11
22	0	3	0	14	17	3	0	0	0	14
23	2	0	1	8	14	5	2	1	0	10
24	3	1	0	20	9	1	2	1	0	6
25	3	1	0	19	9	5	2	0	0	4
26	0	0	1	11	5	2	0	0	0	7
27	1	1	0	8	4	2	0	0	0	7
28	1	1	0	9	0	1	0	0	0	4
29	2	1	0	8	1	1	0	1	0	9
30	1	0	0	6	1	0	0	0	0	6
31	1	0	0	1	0	1	1	0	0	2
32	0	0	0	3	0	0	0	0	0	1
33	0	0	0	0	0	2	0	0	0	2
34	0	0	0	2	1	2	0	0	0	2
35	0	0	0	1	0	0	0	0	0	2
36	0	0	0	4	0	0	0	0	0	1
37	0	0	0	0	0	0	0	0	0	1
38	0	0	0	0	0	0	0	0	0	0
39	0	0	0	0	1	1	0	0	0	0
40	0	0	0	0	0	0	0	0	0	0
41	0	0	0	0	0	0	0	0	0	0
42	0	0	0	0	0	0	0	0	0	0
43	0	0	0	0	0	0	0	0	0	0
44	0	0	0	0	0	0	0	0	0	0
45	0	0	0	0	0	0	0	0	0	0
46	0	0	0	0	0	0	0	0	0	0
47	0	0	0	0	0	0	0	0	0	1
48	0	0	0	1	0	1	0	0	0	1
TOTAL	545	540	550	568	575	608	683	542	532	543
Q	1.501	1.501	1.501	4.503	4.503	1.501	1.501	1.529	1.529	4.587

DROPLET SIZE DATA FOR EMULSION 125

STIRRING TIME (SECS)	20	25	35	45	60
1	26	29	56	0	0
2	129	118	163	0	0
3	111	108	131	0	0
4	59	35	57	0	0
5	32	33	33	0	0
6	32	47	30	1	2
7	36	48	15	11	7
8	29	19	10	18	18
9	13	15	8	41	60
10	11	12	7	65	89
11	13	10	5	66	98
12	6	10	5	53	92
13	10	8	2	40	58
14	5	4	2	27	32
15	2	3	1	20	9
16	10	2	0	11	7
17	7	2	2	10	7
18	6	1	1	10	7
19	0	1	0	12	6
20	2	0	2	11	12
21	1	0	0	9	7
22	5	0	0	10	10
23	4	0	0	9	10
24	2	1	0	11	9
25	3	1	0	12	9
26	0	0	0	5	6
27	0	0	0	7	4
28	0	0	0	8	3
29	2	0	0	3	3
30	0	0	0	8	1
31	1	0	0	3	2
32	0	0	0	3	0
33	1	0	0	6	2
34	2	0	0	1	1
35	0	0	0	2	1
36	0	0	0	2	2
37	0	0	0	2	0
38	0	0	0	2	1
39	0	0	0	2	0
40	0	0	0	1	1
41	0	0	0	1	0
42	0	0	0	1	1
43	0	0	0	0	0
44	0	0	0	0	0
45	0	0	0	0	0
46	0	0	0	0	0
47	0	0	0	0	0
48	0	0	0	0	1
TOTAL	560	507	536	504	578
Q	1.529	1.529	1.529	4.587	4.587

DROPLET SIZE DATA FOR EMULSION 126

STIRRING TIME (SECS)	30	35	45	60	75
1	31	60	35	0	0
2	118	169	167	0	0
3	132	139	124	0	0
4	64	71	46	0	0
5	48	38	36	1	0
6	53	58	38	6	1
7	52	42	31	8	9
8	28	25	18	34	20
9	29	30	16	58	58
10	15	19	12	80	75
11	18	18	7	80	73
12	8	8	0	83	69
13	8	8	4	54	49
14	9	3	0	39	29
15	9	6	1	19	11
16	10	3	1	15	19
17	6	4	1	17	6
18	2	1	0	16	6
19	2	0	0	18	3
20	2	0	0	17	5
21	3	2	0	14	12
22	2	0	1	21	14
23	2	0	1	13	13
24	0	0	0	14	8
25	0	0	0	11	7
26	0	1	0	11	4
27	1	0	0	5	5
28	0	0	0	3	2
29	0	2	0	7	0
30	1	0	0	1	1
31	2	0	0	3	0
32	0	0	0	3	1
33	1	0	0	3	0
34	0	1	0	1	1
35	1	1	0	3	1
36	1	0	0	3	0
37	0	1	0	3	1
38	0	0	0	1	0
39	0	0	0	1	1
40	0	0	0	2	0
41	0	0	0	0	0
42	0	0	0	0	1
43	0	0	0	0	0
44	0	0	0	1	0
45	0	0	0	0	0
46	0	0	0	0	0
47	0	0	0	0	0
48	0	0	0	1	0
TOTAL	658	710	539	670	505
Q	1.529	1.529	1.529	4.587	4.587

STIRRING TIME (SECS)	DROPLET SIZE DATA FOR EMULSION 127				
	35	40	50	60	75
1	18	42	64	0	0
2	113	135	157	0	0
3	143	104	112	0	0
4	41	37	47	0	0
5	28	33	35	0	0
6	43	43	30	2	3
7	41	31	26	5	5
8	15	21	11	33	24
9	27	12	12	47	59
10	19	9	9	61	114
11	7	13	5	60	92
12	10	4	2	45	66
13	3	3	2	39	34
14	1	6	1	23	28
15	0	3	0	17	12
16	0	1	2	14	11
17	2	2	1	8	9
18	4	1	0	6	13
19	1	0	1	9	9
20	1	1	1	9	7
21	0	0	0	7	14
22	2	2	0	16	11
23	0	0	0	18	17
24	1	0	0	10	9
25	1	0	0	11	9
26	0	1	0	13	3
27	1	0	0	15	5
28	0	0	0	13	3
29	0	0	0	4	2
30	1	0	0	8	3
31	1	0	0	6	0
32	0	0	0	3	0
33	0	0	0	6	1
34	0	0	0	2	1
35	0	0	0	4	2
36	0	0	0	1	1
37	0	0	0	2	0
38	0	0	0	4	3
39	1	0	0	8	0
40	0	0	0	0	0
41	0	0	0	2	0
42	0	0	0	0	0
43	0	0	0	2	0
44	0	0	0	1	1
45	0	0	0	1	0
46	1	0	0	0	0
47	0	0	0	1	0
48	0	0	0	2	0
TOTAL	526	504	518	538	571
Q	1.529	1.529	1.529	4.587	4.587

STIRRING TIME (SECS)	DROPLET SIZE DATA FOR EMULSION 128			
	5	10	20	30
1	11	10	16	15
2	67	88	73	79
3	57	85	104	69
4	48	46	45	41
5	28	35	33	28
6	39	42	46	39
7	34	26	32	38
8	21	25	39	34
9	33	27	36	23
10	23	22	29	30
11	24	18	15	18
12	10	16	20	16
13	19	8	8	18
14	13	7	10	15
15	8	14	5	7
16	12	8	6	6
17	6	3	5	9
18	8	2	1	5
19	7	2	1	1
20	6	3	3	2
21	4	2	1	3
22	6	3	1	1
23	2	1	0	1
24	1	2	0	1
25	6	1	0	2
26	3	0	1	1
27	1	0	0	0
28	2	0	0	0
29	1	2	0	0
30	0	1	0	0
31	5	1	0	0
32	6	0	0	0
33	0	0	0	0
34	1	0	0	0
35	1	2	0	0
36	0	0	0	0
37	1	0	0	0
38	2	0	0	0
39	1	0	0	0
40	0	0	0	0
41	0	0	0	0
42	1	0	0	0
43	0	0	0	0
44	0	0	0	0
45	0	0	0	0
46	0	0	0	0
47	0	0	0	0
48	0	0	0	0
TOTAL	527	500	530	500
Q	1.529	1.501	1.501	1.501

	DROPLET SIZE DATA FOR EMULSION 131					DROPLET SIZE DATA FOR EMULSION 132				
STIRRING TIME (SECS)	10	15	25	40	60	20	25	30	40	60
1	113	126	99	0	0	62	57	0	0	0
2	116	156	197	0	0	132	164	0	0	0
3	48	53	63	0	1	51	62	1	0	0
4	62	45	41	0	5	55	47	3	0	0
5	36	36	33	2	36	65	67	8	1	5
6	25	23	23	16	89	33	33	22	21	35
7	25	21	20	46	153	31	25	56	57	84
8	17	13	13	77	172	27	24	76	94	114
9	9	7	10	112	91	17	11	49	95	85
10	13	11	5	73	38	10	9	60	50	42
11	14	6	2	36	24	5	7	26	23	20
12	9	2	2	22	21	2	3	16	16	14
13	9	1	0	12	12	4	2	17	11	13
14	5	5	0	5	13	3	2	11	5	13
15	4	5	1	9	18	4	2	10	12	14
16	7	5	2	8	21	4	1	12	8	16
17	4	0	1	12	9	2	1	16	15	28
18	0	1	1	11	9	2	1	16	23	15
19	1	3	1	13	10	1	2	22	18	24
20	1	0	0	8	5	1	0	11	10	9
21	3	0	0	13	2	0	1	7	12	2
22	4	1	0	5	1	3	0	11	8	4
23	2	1	0	2	2	1	0	10	4	1
24	0	1	0	1	0	0	0	5	7	3
25	0	0	0	2	3	2	1	6	3	2
26	0	0	0	4	0	1	0	8	3	3
27	1	0	0	1	1	0	0	4	2	1
28	0	0	0	2	1	0	0	8	2	2
29	0	0	0	1	0	0	0	5	1	4
30	0	0	0	2	0	0	0	4	3	0
31	0	1	0	0	2	0	0	1	2	2
32	0	0	0	0	0	0	0	6	1	0
33	0	0	0	1	0	0	0	3	3	0
34	0	0	0	0	0	0	0	2	0	1
35	0	0	0	0	1	0	0	1	2	0
36	0	0	0	1	0	0	0	1	0	0
37	0	0	0	2	0	0	0	5	1	0
38	0	0	0	0	0	0	0	1	1	0
39	0	0	0	0	0	0	0	1	0	0
40	0	0	0	0	0	0	0	0	0	0
41	0	0	0	0	0	0	0	1	1	0
42	0	0	0	0	0	0	0	1	0	0
43	0	0	0	0	0	0	0	1	0	0
44	0	0	0	2	0	0	0	0	0	0
45	0	0	0	0	0	0	0	1	1	0
46	0	0	0	0	0	0	0	2	0	0
47	0	0	0	0	0	0	0	0	1	0
48	0	0	0	1	0	1	0	2	1	0
TOTAL	528	519	514	500	740	519	522	509	516	555
Q	1.170	1.170	1.170	3.510	3.510	1.170	1.170	3.510	3.510	3.510

STIRRING TIME (SECS)	DROPLET SIZE DATA FOR EMULSION 133					DROPLET SIZE DATA FOR EMULSION 137				
	25	30	40	60	75	35	40	50	60	75
1	75	192	8	0	0	69	53	87	0	0
2	174	119	110	0	0	141	148	161	0	0
3	60	48	131	0	0	95	91	103	0	0
4	33	41	46	0	0	42	42	34	0	0
5	29	28	24	1	0	38	25	23	2	0
6	11	7	35	8	3	15	30	30	2	5
7	4	9	39	24	6	25	29	29	17	12
8	5	7	27	59	33	18	16	21	36	29
9	1	8	27	57	85	12	9	8	65	77
10	3	7	18	58	91	11	12	7	86	96
11	1	4	12	49	73	9	8	4	70	83
12	0	9	9	45	50	5	8	1	40	71
13	1	2	10	28	26	6	4	1	35	35
14	0	9	2	24	15	4	9	2	34	20
15	1	5	3	16	13	6	5	1	19	13
16	1	4	1	9	13	4	3	0	16	13
17	1	4	2	6	4	2	4	0	8	3
18	3	4	1	5	6	0	1	0	8	9
19	1	4	2	8	10	3	2	0	9	5
20	9	5	2	22	9	4	2	0	9	3
21	5	5	4	8	15	4	1	0	6	7
22	4	2	0	12	15	1	2	2	15	10
23	4	3	1	12	15	3	1	0	10	10
24	2	1	0	13	8	0	3	0	7	9
25	4	1	0	7	9	1	0	0	12	5
26	2	1	1	9	5	2	0	0	8	8
27	4	0	0	5	2	0	0	0	5	6
28	1	1	1	5	2	0	0	0	5	5
29	1	1	0	3	0	0	0	0	4	1
30	0	0	0	4	0	0	0	0	5	7
31	0	0	0	3	1	0	0	0	4	0
32	3	0	0	5	0	0	0	0	2	3
33	0	0	0	1	1	0	1	0	2	1
34	0	0	0	2	0	0	0	0	1	0
35	0	0	0	1	1	0	0	0	0	0
36	0	0	0	1	0	0	0	0	0	1
37	0	0	0	1	0	0	0	0	0	0
38	0	0	0	3	1	1	0	0	3	1
39	0	0	0	0	0	0	0	0	1	0
40	0	0	0	1	0	1	0	0	1	1
41	0	0	0	1	0	0	0	0	0	1
42	0	0	0	0	2	0	0	0	1	0
43	0	0	0	2	0	0	0	0	1	0
44	0	0	0	0	0	0	0	0	1	1
45	0	0	0	1	0	0	0	0	0	1
46	0	0	0	0	0	0	0	0	0	0
47	0	0	0	1	0	0	0	0	0	0
48	0	0	0	2	1	0	0	0	6	1
TOTAL	443	531	515	522	515	522	509	514	555	553
Q	1.170	1.170	1.474	4.422	4.422	1.474	1.474	1.474	4.422	4.422

STIRRING TIME (SECS)	DROPLET SIZE DATA FOR EMULSION 138					DROPLET SIZE DATA FOR EMULSION 143				
	40	45	50	60	75	40	45	50	60	75
1	249	224	190	236	264	39	47	56	0	0
2	79	60	47	59	63	142	146	183	0	0
3	19	16	21	7	6	96	125	131	0	0
4	3	4	3	2	4	54	67	66	0	0
5	2	2	1	2	2	33	41	39	0	5
6	0	0	0	0	0	15	32	31	7	9
7	0	1	0	0	0	23	16	15	20	31
8	0	0	0	0	0	13	19	11	24	34
9	0	0	0	0	1	12	15	13	62	79
10	0	0	0	0	1	9	11	8	80	76
11	0	0	0	0	1	8	5	3	73	54
12	0	0	0	1	0	7	7	2	50	48
13	0	0	0	0	3	3	5	0	33	39
14	0	0	0	2	4	18	2	0	17	19
15	1	0	1	2	18	1	3	0	19	21
16	0	1	2	6	19	4	1	2	13	17
17	1	2	3	12	18	3	1	0	18	16
18	2	6	8	14	38	1	1	0	14	8
19	7	5	18	19	33	4	1	0	9	7
20	8	15	11	16	31	1	1	0	8	6
21	11	25	29	17	21	0	1	0	7	6
22	11	16	23	20	11	0	0	0	6	6
23	20	26	28	21	4	1	0	0	8	5
24	16	20	16	15	4	0	0	0	2	4
25	20	19	22	14	3	1	0	0	3	2
26	16	19	6	14	0	0	0	0	3	2
27	15	10	9	7	0	0	0	0	1	2
28	4	4	7	2	0	0	0	1	4	3
29	8	3	2	1	1	1	0	0	1	1
30	1	0	1	0	1	0	0	0	3	4
31	1	0	0	2	0	0	0	0	3	0
32	1	0	2	0	0	0	0	0	2	0
33	1	1	1	1	0	1	0	0	5	0
34	1	1	1	0	0	0	0	0	2	0
35	0	0	0	0	0	0	0	0	0	1
36	1	0	0	0	0	0	0	0	2	2
37	0	0	1	0	0	0	0	0	0	1
38	0	0	0	0	0	0	0	0	0	0
39	0	0	0	0	0	1	0	0	0	0
40	0	0	0	0	0	0	0	0	0	0
41	0	0	0	0	0	0	0	0	0	0
42	0	0	0	0	0	0	0	0	0	0
43	0	0	0	0	0	0	0	0	0	0
44	0	0	0	0	0	0	0	0	1	0
45	0	0	0	0	0	0	0	0	0	1
46	0	0	0	0	0	0	0	0	0	0
47	0	0	0	0	0	0	0	0	0	1
48	1	0	0	0	0	0	0	0	1	0
TOTAL	499	478	453	492	551	491	547	561	501	510
q	1.087	1.087	1.087	1.087	1.087	1.501	1.501	1.501	4.503	4.503

DATA FOR EMULSIONS	139	140	141	142	144	145	146	148	149
STIRRING TIME (SECS)	60	60	45	45	60	60	60	45	45
1	90	106	130	183	228	327	0	84	0
2	143	96	33	63	136	72	0	116	0
3	129	108	34	55	47	24	0	65	1
4	72	69	37	35	24	0	3	45	6
5	19	27	40	28	11	5	9	38	18
6	6	23	42	30	8	1	38	31	38
7	4	18	35	22	4	0	95	19	63
8	6	16	27	24	7	0	110	15	76
9	8	15	34	14	7	0	96	15	76
10	2	7	23	13	1	0	46	10	52
11	8	5	19	13	4	0	26	9	28
12	1	5	12	6	1	0	17	7	27
13	0	6	12	1	5	0	12	6	20
14	1	6	8	4	4	0	6	2	12
15	0	3	5	5	2	2	9	3	9
16	0	3	2	7	3	2	21	1	15
17	0	4	5	5	4	1	12	3	10
18	0	7	1	3	4	5	10	2	11
19	0	2	0	1	4	1	5	3	11
20	1	2	1	0	5	7	5	1	7
21	0	3	1	1	1	5	5	5	2
22	1	5	0	1	1	0	3	3	3
23	1	2	0	2	0	0	1	2	1
24	0	3	0	0	1	7	4	2	2
25	0	1	0	0	1	0	0	2	3
26	0	1	0	0	0	3	0	1	1
27	1	3	0	0	1	6	0	1	1
28	1	1	0	1	0	1	2	4	2
29	1	4	0	0	1	0	1	2	2
30	1	4	0	1	0	0	1	1	0
31	1	1	0	0	1	1	1	1	2
32	6	1	0	0	0	0	0	1	1
33	6	4	0	1	0	1	1	2	0
34	6	3	0	0	0	1	1	0	4
35	2	1	0	0	0	0	0	0	0
36	7	1	0	0	1	0	0	1	0
37	5	1	0	0	0	0	1	0	0
38	6	3	0	0	0	0	0	0	0
39	4	2	0	0	0	0	0	0	0
40	3	1	0	0	0	0	0	0	0
41	2	2	0	0	0	0	0	0	0
42	1	1	0	0	0	0	0	0	0
43	1	0	0	0	0	0	0	0	1
44	0	0	0	0	0	0	0	0	0
45	0	2	0	0	0	1	0	0	0
46	4	0	0	0	0	0	0	0	0
47	1	0	0	0	0	0	0	0	0
48	2	1	0	0	0	0	0	0	1
TOTAL	553	579	500	500	517	517	541	500	500
H	2.108	2.108	0.703	0.703	1.081	1.037	3.761	1.225	3.675

DATA FOR EMULSIONS	150	151	152	156	156	147	147	147	147
STIRRING TIME (SECS)	60	60	60	15	30	5	10	20	30
1	0	7	27	19	15	92	103	36	69
2	54	100	102	66	78	103	123	33	82
3	123	170	141	69	69	62	50	32	37
4	130	100	90	34	33	36	51	32	23
5	74	46	39	25	27	33	37	43	30
6	49	27	29	56	38	19	32	30	17
7	37	23	29	45	40	22	30	26	21
8	39	12	17	46	35	18	30	22	15
9	28	10	20	17	32	19	17	32	14
10	21	3	16	26	25	11	19	27	15
11	15	5	6	16	17	5	16	30	16
12	11	1	10	11	20	7	13	26	14
13	10	0	2	11	23	4	7	18	12
14	3	1	3	17	9	6	3	15	8
15	2	1	2	9	8	2	3	10	7
16	4	0	1	9	7	2	3	11	6
17	0	0	1	8	9	2	5	8	8
18	1	0	0	6	5	0	7	12	8
19	1	0	1	7	7	1	3	7	8
20	1	1	0	2	2	3	0	3	8
21	0	0	1	2	1	1	1	2	7
22	3	0	0	5	0	4	1	3	8
23	0	0	0	0	1	0	2	4	1
24	0	0	2	1	0	0	2	3	5
25	1	0	1	1	3	1	0	3	6
26	0	0	0	1	2	1	0	1	4
27	0	0	0	1	0	1	0	5	2
28	0	0	0	0	0	0	0	1	1
29	0	0	1	2	1	0	0	0	2
30	0	0	1	2	0	0	1	1	5
31	0	0	0	0	1	0	0	0	2
32	0	0	0	1	0	2	1	1	1
33	0	0	0	0	0	0	0	0	3
34	0	0	1	0	0	0	0	0	0
35	0	0	0	1	0	0	0	0	0
36	0	0	0	0	0	1	0	1	0
37	0	0	0	0	0	0	0	1	0
38	0	0	0	0	0	0	1	0	0
39	0	0	0	0	0	0	0	0	2
40	0	0	0	0	0	0	0	0	0
41	0	0	0	0	0	1	0	0	0
42	0	0	0	0	0	0	0	0	0
43	0	0	0	0	0	0	0	0	0
44	0	0	0	0	0	0	0	0	0
45	0	0	0	0	0	0	0	0	0
46	0	0	0	0	0	0	0	0	0
47	0	0	0	0	0	0	0	0	0
48	0	0	0	0	0	0	0	0	0
TOTAL	607	507	543	516	508	459	543	479	467
Q	1.639	1.639	1.639	1.501	1.501	1.087	1.087	1.225	1.225

DATA FOR EMULSIONS	115	115	117	118	118	119	119	120	120
AGEING TIME (DAYS)	7	14	14	5	7	5	7	5	7
1	0	0	0	0	0	0	0	0	0
2	0	0	0	0	0	0	0	0	0
3	0	0	0	0	0	0	0	0	0
4	0	0	0	0	0	0	0	0	0
5	0	0	0	0	1	0	0	0	0
6	0	0	31	0	6	0	0	0	1
7	0	1	54	8	21	1	1	2	4
8	3	2	72	18	42	9	10	12	26
9	14	25	74	43	77	22	37	67	47
10	33	31	82	55	97	55	60	72	81
11	83	72	65	76	63	70	109	66	90
12	106	82	40	54	47	101	99	61	91
13	74	64	35	63	43	73	52	47	62
14	60	67	31	35	20	45	29	34	32
15	24	46	20	28	13	19	17	21	20
16	16	36	14	15	10	15	15	8	13
17	13	24	10	12	12	10	8	13	13
18	5	20	6	8	12	13	9	8	8
19	3	14	5	17	8	6	10	10	9
20	2	13	2	12	6	5	5	12	11
21	4	13	4	10	12	5	5	14	9
22	3	10	5	11	11	5	8	10	9
23	10	7	3	15	13	12	14	16	14
24	7	6	1	10	16	5	8	20	14
25	7	2	2	6	8	7	7	9	7
26	5	7	2	5	3	9	3	6	5
27	4	4	3	6	1	4	7	6	6
28	7	3	0	2	1	4	5	5	4
29	0	7	2	7	2	6	5	5	8
30	2	4	1	5	1	1	3	3	1
31	0	1	0	4	1	1	0	2	0
32	0	0	0	3	3	3	1	3	1
33	1	2	0	1	0	3	1	2	0
34	0	1	1	2	1	0	0	4	3
35	1	0	0	1	0	1	2	2	3
36	1	0	0	1	0	1	3	1	2
37	0	1	0	1	0	1	0	0	1
38	1	0	0	1	0	0	1	1	3
39	0	2	0	0	0	0	1	2	1
40	0	0	0	0	0	0	0	0	0
41	0	0	0	0	0	0	0	1	1
42	0	0	0	1	0	0	0	0	0
43	0	0	0	2	0	0	0	0	1
44	0	1	0	0	0	0	0	0	0
45	0	0	0	1	0	0	0	0	0
46	0	0	0	0	0	0	0	0	0
47	0	0	0	0	0	0	0	0	0
48	0	0	0	0	0	0	0	2	0
TOTAL	489	568	583	539	551	521	535	527	599
Q	4.503	4.587	4.587	4.503	4.587	4.503	4.587	4.503	4.587

DATA FOR EMULSIONS	121	121	122	122	123	124	125	126	127
AGEING TIME (DAYS)	5	7	5	7	1	1	1	1	1
1	0	0	0	0	0	0	0	0	0
2	0	0	0	0	0	0	0	0	0
3	0	0	0	0	0	0	0	0	0
4	0	0	0	0	0	0	0	0	0
5	0	1	0	0	0	0	1	0	0
6	0	6	1	0	5	2	9	4	0
7	1	23	4	0	28	17	24	13	1
8	8	44	33	0	62	37	53	22	3
9	18	68	68	5	93	50	86	73	12
10	44	85	104	27	93	67	88	62	42
11	87	51	87	63	73	85	78	77	56
12	86	35	60	103	46	54	44	63	63
13	68	23	50	107	18	40	26	49	63
14	32	21	27	92	19	30	12	29	32
15	21	7	12	49	11	18	15	18	23
16	14	9	8	22	7	14	12	12	11
17	4	13	3	15	3	10	8	6	7
18	7	13	5	11	6	10	6	6	4
19	6	12	7	12	6	9	7	4	3
20	11	9	3	6	7	11	12	7	5
21	13	5	3	5	6	15	16	4	9
22	13	7	5	3	7	10	8	14	4
23	17	10	9	6	5	17	6	7	8
24	6	8	7	4	7	10	9	9	3
25	8	4	5	6	3	19	3	8	10
26	9	4	6	1	6	10	4	9	3
27	7	4	2	2	4	4	6	7	8
28	5	3	4	2	2	7	3	5	6
29	3	6	1	3	1	2	1	3	4
30	2	4	2	2	0	2	0	4	2
31	5	3	2	1	1	1	2	4	1
32	2	1	1	1	1	2	0	3	1
33	3	0	1	1	0	2	0	2	5
34	3	1	0	0	3	5	0	3	1
35	0	1	1	0	1	1	2	1	2
36	1	0	0	0	0	3	1	2	2
37	0	0	1	0	0	0	0	0	1
38	1	1	0	0	0	1	1	0	0
39	0	1	0	0	0	0	0	1	0
40	0	0	0	0	0	0	0	1	0
41	0	1	0	0	0	1	0	2	3
42	0	0	0	0	0	1	0	0	0
43	0	1	0	0	0	1	0	0	0
44	0	1	0	0	0	0	1	1	0
45	0	0	0	0	0	0	0	0	0
46	0	0	0	0	0	0	0	1	0
47	0	1	0	0	0	0	0	0	0
48	1	1	0	0	0	1	0	1	0
TOTAL	506	508	522	549	524	560	544	557	398
Q	4.503	4.587	4.587	4.587	4.587	4.587	4.587	4.587	4.587

DATA FOR EMULSIONS	127	133	139	140	1	202	203	204
AGEING TIME (DAYS)	7	8	3	3	4 YEARS	0	0	0
1	27	0	209	193	0	0	4	61
2	45	0	123	114	0	0	67	155
3	69	0	51	60	0	5	92	85
4	91	0	22	21	0	10	60	22
5	55	5	10	13	6	50	13	32
6	58	9	11	11	11	146	17	37
7	33	17	5	10	22	238	8	23
8	19	36	4	6	55	185	16	12
9	16	61	3	4	70	238	4	10
10	8	65	1	2	85	172	6	11
11	13	57	0	2	67	97	8	6
12	16	35	2	1	51	37	4	12
13	9	42	0	1	40	43	4	6
14	15	32	0	2	28	40	2	3
15	12	22	0	2	18	31	0	2
16	8	22	0	0	12	13	2	1
17	7	14	1	3	5	17	1	4
18	7	9	0	2	4	18	4	2
19	7	16	0	4	3	12	3	3
20	4	6	0	2	5	4	1	3
21	4	4	2	3	0	3	1	0
22	2	4	0	2	2	7	0	0
23	4	6	2	0	6	7	0	1
24	0	4	1	0	4	4	1	1
25	2	3	1	0	5	3	0	1
26	3	5	3	1	0	10	0	3
27	4	19	1	0	1	5	0	1
28	3	1	4	0	0	4	0	2
29	0	7	1	1	2	2	0	1
30	0	3	2	0	2	4	0	0
31	0	5	2	0	1	3	0	1
32	0	1	2	0	0	3	3	0
33	2	1	0	0	1	4	0	0
34	1	1	0	0	0	3	0	0
35	0	1	0	0	0	0	0	0
36	0	2	1	0	0	0	0	1
37	1	3	0	0	0	1	1	0
38	0	2	0	0	1	2	2	0
39	0	1	1	0	0	0	1	0
40	0	0	0	1	0	1	0	0
41	0	0	0	0	0	2	0	0
42	0	0	2	0	0	1	0	0
43	0	0	0	0	0	0	0	0
44	0	0	0	0	0	1	0	0
45	0	0	0	0	0	1	0	0
46	0	0	0	0	0	0	0	0
47	0	0	0	0	0	0	0	0
48	0	2	0	0	0	2	0	0
TOTAL	554	512	467	461	500	1429	325	504
G	4,587	4,917	1,225	1,223	4,917	4,824	1,639	1,556